



UNIVERSITA' DEGLI STUDI DI PADOVA

SEDE AMMINISTRATIVA: UNIVERSITA' DEGLI STUDI DI PADOVA

DIPARTIMENTO DI SCIENZE CHIMICHE

SCUOLA DI DOTTORATO IN SCIENZE MOLECOLARI

INDIRIZZO: SCIENZE CHIMICHE

CICLO XXI

*C*₃ AND *pseudo-C*₃ TITANA AND VANADATRANES: STEREOSELECTIVE SELF-ASSEMBLY AND OXYGEN TRANSFER REACTIONS

Coordinatore: Prof. Maurizio Casarin

Supervisore: Prof. Giulia Marina Licini

Dottoranda: Marta Pontini

31 Gennaio 2009

alla mia famiglia

Contents

Chapter 1 – General introduction	1
1.1 Introduction	2
1.2 C₃-Symmetric Ligands	4
1.3 Tris-phenolamines: C₃-Symmetric ligands for coordination chemistry	7
1.3.1 Group (IV) complexes	8
1.3.2 Group (V) complexes	13
1.3.3 Group (VI) complexes	15
1.3.4 Iron and late transition metal complexes	15
1.3.5 Group XI, XII and XIII complexes	16
1.4 Amine tri-phenolate complexes: catalytic activity	18
1.5 Aim of the thesis	22
Chapter 2 – Oxovanadatrane complexes as functional and structural models of Haloperoxidases	25
2.1 Introduction	14
2.1.1 Reactivity and selectivity of sulfoxidations catalyzed by VHPOs	31
2.1.2 Functional and structural models of VHPOs	32
2.2 V(V)amine tri-phenolate complexes: synthesis and structural study	35
2.3 V(V)amine tri-phenolate complexes : catalytic activity	38
2.3.1 Oxidation of sulfides to the corresponding sulfoxides	39
2.3.2 Oxidation of halides	42
2.4 Conclusions	44
2.5 Experimental	44
Chapter 3 – Stereoselective self-assembly of C₃-titanatranes	49
3.1 Introduction	50
3.1.1 Ti(IV) amine triphenolate complexes	50
3.2 Self-assembly of C₃-titanatranes	52
3.2.1 Stability of the μ -oxo complex	57
3.2.2 Reactivity of the μ -oxo complex	59
3.3 Ti(IV) μ-oxo complexes as multifunctional platforms	61
3.3.1 Achiral <i>tris</i> -(<i>o</i> -phenyl-phenol) amines via Suzuki coupling	63
3.3.2 Coordination chemistry of ligands 17a-e with Ti(V)	68
3.4 Enantiopure titanatrane with propeller like chirality	74
3.5 Coordination chemistry of 1a with Zr(IV) e Hf(IV)	78
3.6 Conclusions	80
3.7 Experimental	80
Chapter 4 – Enantiopure pseudo-C₃ titanatranes	101
4.1 Introduction	102

4.1.1 Enantiopure amine triphenolate ligands	103
4.1.2 Chiral 1,3- Aminophenols	104
4.1.3 Synthesis of 1-(2'-alkoxyaryl)-alkylamine	105
4.2 Synthetic strategy based on the aminophenol building block	107
4.2.1 1-(2-(benzyloxy)-3-bromo-5-methylphenyl)ethanamine: synthesis	108
4.2.1.1 Synthesis of the racemic aminoalcohol and classical resolution	108
4.2.1.2 Stereoselective synthesis	111
4.2.1.3 Kinetic enzymatic resolution	113
4.3 Chiral amine tri-phenolate ligands: synthesis and coordination chemistry with Ti(IV)	116
4.4 Selective synthesis of mixed μ-oxo complexes	120
4.5 Conclusions	121
4.6 Experimental	122
Summary	135
Riassunto	137

Chapter 1

General introduction

1.1 Introduction

Symmetry, chirality, and their combinations are to be found in many creations of Nature and in some greatest achievements of mankind. From a beautiful flower to Da Vinci's 'Vetruvian man', expression of these concepts provides continuing inspiration and example to artists and scientists alike.

The principles of symmetry have inspired and directed the design of molecules for many years.¹ While two-fold symmetry rotational symmetry has been successfully employed in a large number of chiral ligands and catalysts,² there is still comparatively little known about the efficiency of systems of higher rotational symmetry in this and other areas. C_3 -Symmetry in particular, which is aesthetically pleasing in both a natural and synthetic contest, has several potential uses in chemical endeavours. For this reason there is an ongoing interest in the application of C_3 -symmetric molecules in areas as diverse as stereoselective catalysis,³ molecular recognition⁴ and material science.⁵

Actually, ligand symmetry together with the chelate effect are two main factors that chemists have to bear in mind when facing the design of novel systems: in the area of stereoselective catalysis, considerable recent work focuses on complexes of transition elements with highly symmetric polydentate chiral ligands,⁶ since incorporation of molecular symmetry into ligands and catalysts is a guiding principles behind their design, as the reduction of the number of possible intermediates or transition states is thought to simplify their mode of action and its interpretation.

For example, it has been postulated that C_3 -symmetric ligands, that are chiral and tripodal, should be highly effective in catalytic reactions involving octahedral metal complexes:⁷ only tridentate C_3 -symmetric ligands in octahedral geometries render the three open coordination sites homotopic, that is stereochemically identical (A=B=C, Figure 1, b) and this equivalence reduces the number of possible transition states to one.⁸ On the other hand, such a ligand may yield an unfavourable situation in a square-planar geometry (Figure 1, c), the same as a bidentate C_2 ligand would yield in an octahedral arrangement (Figure 1, d, e).

The small number of complexes or intermediates facilitates the rationalism of the system under investigation, since one has to deal with few species in solution. The higher the symmetry degree of the ligand, the greater the simplification one can achieve.

¹ See, for example: Noyori, R. *Asymmetric Catalysis in Organic Synthesis*, Wiley, New York, **1994**.

² See, for example: Tang, W.; Zhang, X. *Chem. Rev.* **2003**, *103*, 3029.

³ See, for examples: (a) Foltz, C.; Stecker, B.; Guido, M.; Bellemin-Laponnaz, S.; Wadepohl, H.; Gade, L. *Chem. Eur. J.* **2007**, *13*, 9912. (b) Bellemin-Laponnaz, S.; Gade, L. *Angew. Chem.* **2002**, *114*, 3623. (c) Bringmann, G.; Pfeifer, R.-M.; Rummey, C.; Hartner, K.; Breuning, M. *J. Org. Chem.* **2003**, *68*, 6859.

⁴ Moberg, C. *Angew. Chem. Int. Ed.* **2006**, *45*, 4721.

⁵ See, for examples: van Gestel, J.; Palmanas, A.R.A.; Titulaer, B.; Vekemans, J. A.J.M.; Meijer, E. W. *J. Am. Chem. Soc.* **2005**, *127*, 5490.

⁶ (a) Moberg, C. *Angew. Chem. Int. Ed.* **1998**, *37*, 228. (b) Gibson, S. E.; Castaldi, M. P. *Chem Comm.* **2006**, 3045.

⁷ (a) Burk, M.J.; Harlow, R. L. *Angew. Chem.* **1990**, *102*, 1511. (b) Burk, M.J.; Harlow, R.L. *Angew. Chem. Int. Ed. Engl.* **1990**, *27*, 1462.

⁸ Keyes, M. C.; Tolman, W.B. in *Adv. Catal.* **1997**, *2*, 189.

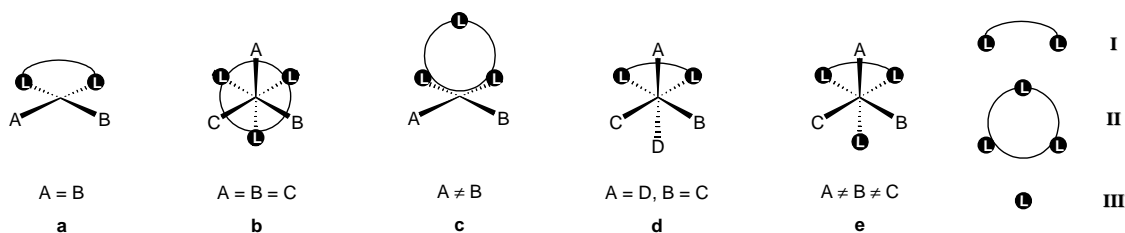


Figure 1. Relationship between empty coordination sites (A-D) in complexes with C_2 -symmetric, bidentate (I) and C_3 -symmetric tridentate (II) ligands, in various complex geometries. III: achiral, monodentate ligand.

A more detailed analysis of situations arising from the coordination of polydentate ligands having high rotational symmetry to a metal centre, is represented in Figure 2: the most common complex geometries, such as square-planar, tetrahedral, square-pyramidal, trigonal-bipyramidal and octahedral, have been considered, corresponding to complexes of metal ions having coordination numbers equal to 4, 5 and 6.^{6a}

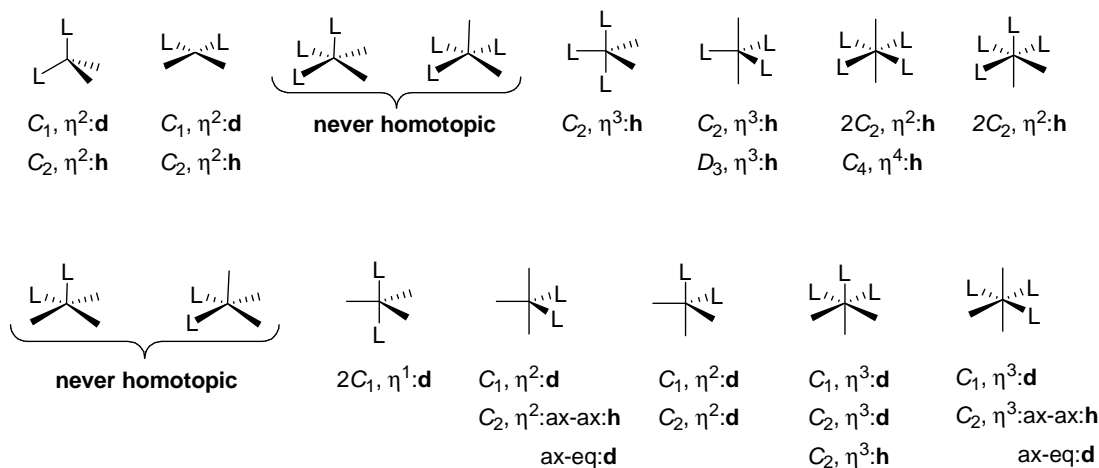


Figure 2. Relationship between coordination sites in chiral complexes containing ligands of different denticities (η^n) and rotational symmetries (C_n). h= homotopic, d= distereotopic, ax= axial and eq= equatorial sites.

By carefully analyzing the structures reported on Figure 2, it follows that homotopic coordination sites may be encountered with:

- Square-planar tetrahedral complexes, containing bidentate C_2 -symmetric ligands.
- Octahedral complexes, containing two bidentate C_2 ligands or one C_3 -symmetric ligand.
- Trigonal-pybiramidal complexes, containing a bidentate C_3 -symmetric ligand or a tridentate D_3 -symmetric ligand.

Although in the present discussion only the situations leading to the equivalence of all the open coordination sites of the complex, i.e. to obtain a maximum simplification, have been considered, also arrangements in which only two (or three) of many free sites are made homotopic, are advantageous as they also imply a reduction of reaction paths. It is worth to point out that considerations made so far might be not fully applicable in the case of

fluxional species, or if the complex undergoes dynamic equilibria or in case a fast ligand exchange occurs.⁶

In the area of chiral molecular recognition,⁴ particularly important for biological functions, asymmetric synthesis and chiral separation, the role of threefold rotational symmetry is to simplify the possible modes of coordination, thus requiring an increased matching of the binding groups on the receptor and the target molecule that enhances the probability of discrimination. From Nature itself, examples of uses of C_3 -symmetry can be found: signalling through receptors of the tumor necrosis factor receptor superfamily relies strongly on the formation of C_3 -symmetric complexes.⁹ However, symmetry is not itself a property that determines the ability of a C_3 -symmetric receptor to recognize a chiral guest, but it reduces the number of different complexes obtained from a receptor and a substrate. At the basis of the process of chiral recognition, in fact, there is a combination of attractive and repulsive interactions, the former including hydrogen bonds, ion-dipole and dipole-dipole interactions, π stacking, and hydrophobic interactions, but using C_3 -symmetric ligands, the host-guest complexes give rise to three identical situations, that is, only one complex (Figure 3). Thereby frequently resulting in more efficient discrimination of the enantiomeric guest. This factor may, but does not necessarily have to, lead to improved selectivities.^{4,10}

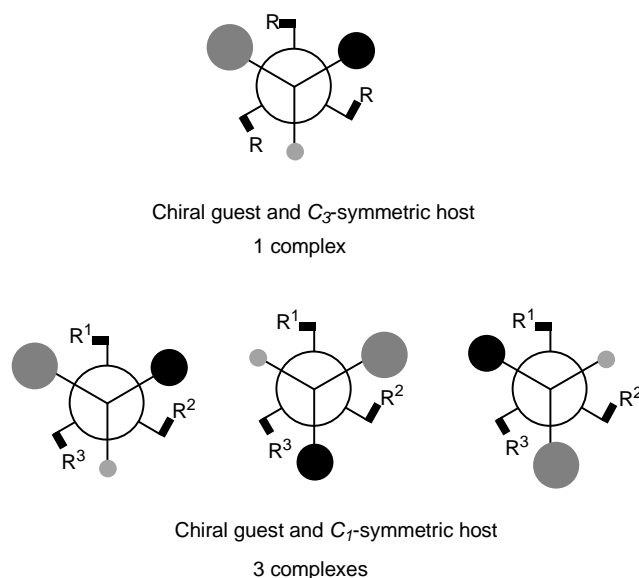


Figure 3. C_3 -symmetry reduces the number of different complexes as compared to C_1 and C_2 -symmetry.

Thus the benefits coming from the use of highly symmetric species should be taken into account in the design of novel ligands, catalytic systems and receptors.

1.2 C_3 -Symmetric Ligands

Polydentate ligands give robust complexes and are modular. Furthermore, when they are highly symmetric, they facilitate the study of the coordination chemistry and reactivity

⁹ Bodmer, J.-L.; Schneider, P; Tschopp, J. *Trends Biochem. Sci.* **2002**, 27, 19.

¹⁰ Gibson, S. E.; Castaldi, M. P. *Angew. Chem. Int. Ed.* **2006**, 45, 4718.

reducing the number of possible species. In transition metal coordination chemistry, ligands are used to control the environment of the metal. In particular, the possibility to modulate the electronic properties and the steric volume around the metal is essential to control its catalytic behaviour and coordination modes. If this control has to be exerted under catalytic conditions, robust and stable complexes are vital.

Chiral and achiral polydentate C_3 -ligands of podand (A-C) or macrocyclic (D) topologies have been studied for the coordination of transition metals and main group elements (Figure 4).

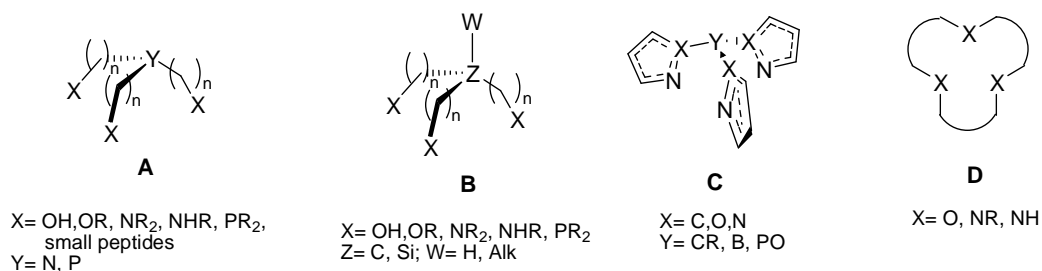


Figure 4. General structures of polydentate C_3 -symmetric ligand with podand (A-C) or macrocyclic (D) topology.

Several class of ligands on which strong anionic donors ($X= OH, NHR$) are combined with neutral donating functions ($Y= N, P$) as well as with non donating atoms ($Z= C, Si$) have been prepared.¹¹ Both these ligand topologies are all suitable for early transition metals or main group elements in high oxidation state. On the other hand, ligands bearing neutral donors in all binding sites (such as C) are suitable for less acidic late transition metals.

Coordination of A-D type ligands to metal ions affords highly robust chelate complexes (chelate effect): in many cases such complexes are also highly symmetric when assuming octahedral or trigonal-bipyramidal geometries. Some examples of chiral tri- or tetradentate C_3 -symmetric ligands that have been successfully employed with main group elements or transition metals in asymmetric catalysis or molecular recognition are listed in Figure 5.

¹¹ (a) Burk, M.J.; Feaster, J. E.; Harlow, R.L. *Tetrahedron: Asymmetry* **1991**, 2, 569. (b) Aldofsson, H.; Wärnmark, K.; Moberg, C. *J. Chem. Soc. Chem. Commun.* **1992**, 1054. (c) Aldofsson, H.; Nordström, K.; Wärnmark, K.; Moberg, C. *Tetrahedron: Asymmetry* **1996**, 7, 1967. (d) Tokar, C.J.; Kottler, P.B.; Tolman, W.B. *Organometallics* **1992**, 11, 2737. (e) Kawasaki, K.; Tsumura, S.; Katsuki, T. *Synlett* **1995**, 1245.

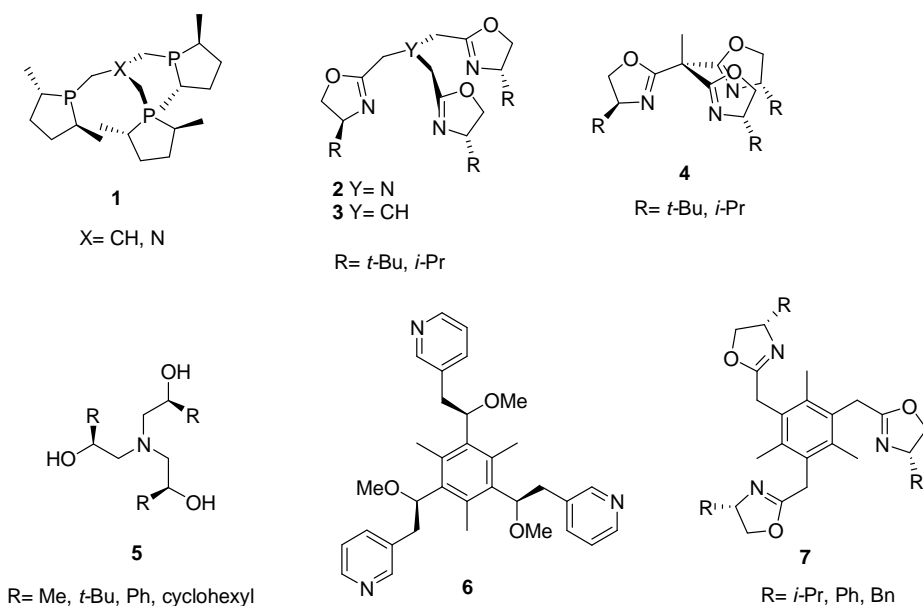


Figure 5. Miscellaneous C_3 -symmetric ligand successfully applied in metal catalyzed stereoselective reactions.

Rh(I)/triphosphanes **1** have been employed in the catalytic hydrogenation of non-symmetric olefins yielding e.e.'s up to 98%.^{11a} Other interesting applications are the olefin epoxidations catalyzed by Mn(II)/1,4,7-triazacyclononane (**D**, Figure 4, X=NR) (ee \leq 56%), asymmetric allylic oxidation of cycloalkenes catalyzed by Cu(I) or Cu(II) complexes of *tris*(oxazoline) **2** or **3** (up to 88% ee for **2** and up to 81% for **3**).^{11e} *Tris*(oxazoline) **4**¹² has been used in asymmetric Cu(I) catalyzed cyclopropanation of styrene affording the corresponding cyclopropanes with 70% ee,^{12b} in the stereospecific polymerization of α -olefins catalyzed by organolanthanide complexes, obtaining polyolefins with M_w/M_n values between 1.58 and 2.08, isotacticities of 80-95%.^{12c,d} Desymmetrization of meso-epoxides by direct addition of trialkylsilyl azides (ee \leq 93%)¹³ and trialkylsilyl halides (ee \leq 95%),¹⁴ catalyzed by Zr(IV)/(*S,S,S*)-triisopropanolamine (**5**, R= Me)¹⁵ or asymmetric sulfoxidations mediated by Ti(IV) or Zr(IV) triisopropanolamine **5**¹⁶ (ee up to 91%)¹⁷ are all concrete applications. Moreover, new chiral molecules such as *tris*(pyridine) ligand **6** open new possibility in ruthenium chemistry.¹⁸

¹² (a) Gade, L.; Bellemin-Lapponnaz, S.; *Chem. Eur. J.* **2008**, *14*, 4142. (b) Bellemin-Lapponnaz, S.; Gade, L. *Angew. Chem. Int. Ed.* **2002**, *41*, 3473. (c) Lukešová, L.; Ward, B. D.; Bellemin-Lapponnaz, S.; Wadepohl, H.; Gade, L. *Organomet.* **2007**, *26*, 4652. (d) Lukešová, L.; Ward, B. D.; Bellemin-Lapponnaz, S.; Wadepohl, H.; Gade, L. *Dalton Trans.* **2007**, 920.

¹³ Nugent, W. A. *J. Am. Chem. Soc.* **1992**, *114*, 2768.

¹⁴ Nugent, W. A. *J. Am. Chem. Soc.* **1998**, *120*, 7139.

¹⁵ Grassi, m.; Di Silvestro, G.; Farina, M. *Tetrahedron* **1985**, *41*, 177.

¹⁶ Nugent, W. A.; Harlow, R. L.; *J. Am. Chem. Soc.* **1994**, *116*, 6142.

¹⁷ (a) Di Furia, F.; Licini, G.; Modena, G.; Motterle, R.; Nugent, W. A. *J. Org. Chem.* **1996**, 5175. (b) Nugent, W. A.; Licini, G.; Bonchio, M.; Bortolini, O.; Finn, M. G.; McClelland, B. W. *Pure & App. Chem.* **1998**, *70*, 1041. (c) Licini, G.; Bonchio, M.; Modena, G.; Nugent, W. A. *Pure & App. Chem.* **1999**, *71*, 463. (d) Bonchio, M.; Di Furia, F.; Licini, G.; Mantovani, S.; Modena, G.; Nugent, W. A. *J. Org. Chem.* **1999**, *64*, 1326. (e) Buonomenna, M. G.; Drioli, E.; Bertocello, R.; Milanese, L.; Prins, L. J.; Scrimin, P.; Licini, G. *J. Catal.* **2006**, *238*, 221.

¹⁸ Castaldi, M. P.; Gibson, S. E.; Rudd, M.; White, A. J. P. *Chem. Eur. J.* **2006**, *12*, 238.

On the other hand, the first example of chiral recognition, in C_3 -symmetric environment, has been developed by Ahn, who discovered that C_3 -benzene-based *tris*(oxazoline) receptors **7** selectively coordinate α -chiral primary ammonium ions.^{19,20}

1.3 Tris-phenolamines: C_3 -Symmetric ligands for coordination chemistry

In the last decade a significant number of reports relate on the complexation behaviour of tris-phenolamines (TPA, LH_3) with a wide variety of early transition metals (d^0 , d^5) and main group elements (d^{10}). Late transition metal complexes have been described, but are still rare.

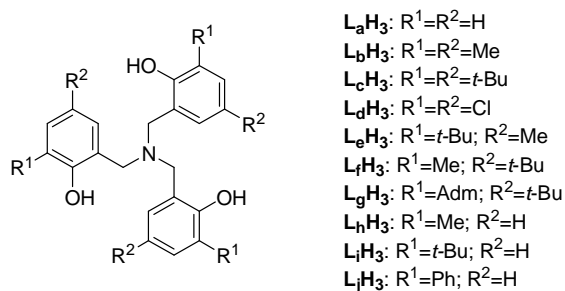


Figure 6

The highly modular nature of the phenol moieties, associated to the threefold symmetry and tetradentate nature of the system, allow to obtain a large family of complexes: *tris*-phenolamines are able to provide three anionic binding sites, the oxygen atoms, for the coordination of the metal, plus a neutral nitrogen donor in bridgehead position, which participates in the coordination of the metal centre, generating a highly stable structure, thanks also to the chelate effect. Only few exceptions have been reported, for P(III) and Ni(II) complexes, in which the *tris*-phenolamine binds in a bidentate and tridentate fashion, respectively.

The donor interaction of the nitrogen with the metal increases electron density on the latter. Although the electron density on the metal element increases, it causes a polarization of all the bonds, resulting in bond lengthening and therefore in a net increase in Lewis acidity.²¹

Importantly, steric and electronic factors can have a significant and important role in the stability and catalytic activity of the complex. As an example, *ortho* groups to the phenol oxygen (R), upon complexation with the metal ions, are in close proximity to the metal center and can therefore be used as control element. On the other side, *para* groups (R'), can modify the electronic properties of the ligand without affecting the steric demand of the system (Figure 6).

¹⁹ (a) Kim, S.-G.; Kim, K.-H.; Jung, J.; Shin, S. K.; Ahn, K.H. *J. Am. Chem. Soc.* **2002**, *124*, 591. (b) Kim, S.-G.; Kim, K.-H.; Kim, Y. K.; Shin, S. K.; Ahn, K.H. *J. Am. Chem. Soc.* **2003**, *125*, 13819. (c) Kim, J.; Kim, S.-G.; Seong, K. R.; Ahn, K.H. *J. Org. Chem.* **2005**, *70*, 7227.

²⁰ For additional applications, see: Gibson, S. E.; Castaldi, M. P. *Angew. Chem. Int. Ed.* **2006**, *45*, 2.

²¹ (a) Denmark, S. E.; Beutner, G.L.; Wynn, T.; Eastgate, M. D. *J. Am. Chem. Soc.* **2005**, *127*, 3774. (b) Gordon, M. S.; Carroll, M. T.; Davis, L.P.; Burggraf, L. w. *J. Phys. Chem.* **1990**, *94*, 8125.

For most of these complexes detailed crystallographic and in solution studies are available. This large amount of data arises from the high stability of amine triphenolate complexes, for which the chelate effect coming from the polydentate TPA ligand is a direct responsible. In the vast majority of examples, mononuclear complexes displaying a 1:1 ligand/metal ratio are obtained. The trigonal bipyramidal (TBP) and octahedral (OCT) geometries predominate whereas tetracoordinate complexes with trigonal monopyramidal (TMP) geometry are unusual (Figure 7).

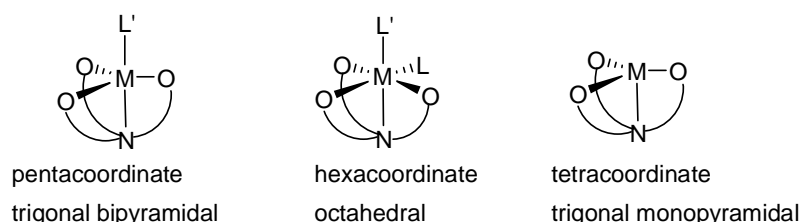
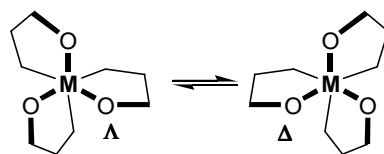


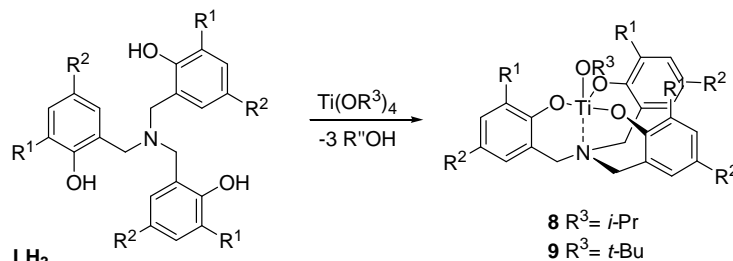
Figure 7

Amine triphenolate metal complexes are characterised by a propeller-like arrangement of the ligand around the metal when viewed along the metal-nitrogen axis. As a consequence, C_3 -symmetric TBP complexes are obtained in the two helical arrangements, Δ/Λ or P/M , which interconvert at room temperature yielding a racemic mixture of enantiomeric complexes (Figure 8).

Figure 8. Clockwise (Δ) and counter-clockwise (Λ) enantiomeric conformations of TPA complexes

1.3.1 Group (IV) complexes

Group (IV) amine triphenolate complexes, and in particular titanium complexes, are the most extensively studied. These complexes are usually prepared by transesterification of the corresponding tetraalkoxide $M(OR'')_4$ species, in which R'' is *iso*-propoxide or *tert*-butoxide. Group (IV) complexes display mainly a pentacoordinate trigonal bipyramidal (TBP) geometry (Scheme 1).



Scheme 1. Synthesis of Ti(IV) amine triphenolate complexes

The first amine triphenolate Ti(IV) complex was reported by Kol and coworkers in 2001.²² The X-ray crystal structure was solved for complex **8c** which bears *tert*-butyl substituents in *ortho* and *para* positions and an apical *iso*-propoxy (Figure 9).

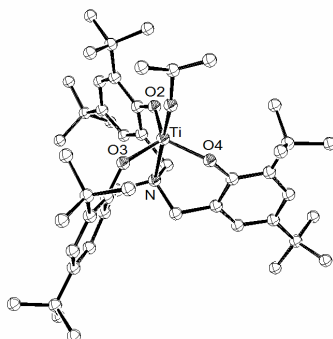
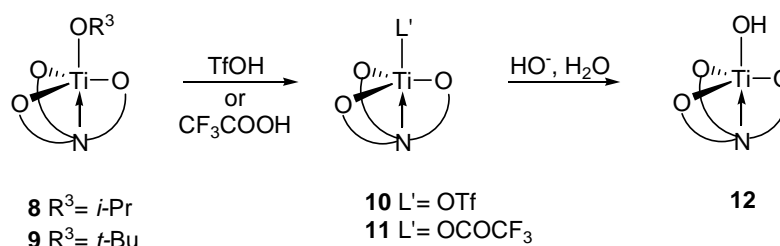


Figure 9. Molecular structure of $L_cTi(O-iPr)$ **8c**, ($R=R'=t-Bu$)²²

A distorted TBP geometry was found in which the titanium lays 0.24 Å above the plane formed by the three phenolate oxygen atoms. The TPA ligand adopts a propeller-like conformation around the metal and both enantiomers are present in the crystal. The *t*-Bu substituents in *ortho* position form a pocket around the metal and this steric bulk protects the monomeric complex from aggregation and it confers a high stability to the complex. Indeed, whereas complex **8c** is air and moisture tolerant, a similar monomeric complex bearing *ortho,para* methyl substituents **8b** ($R=R'=Me$) results to be less stable and aggregates in the presence of moisture to give dinuclear species.^{22,23}

The apical alkoxide ligand in this metal complexes can be easily exchanged with more acidic ligands; for example reaction with trifluoroacetic acid gives rise to the corresponding $LTiOCOCF_3$ complex **11c**,²⁴ whereas reaction with triflic acid affords **10c**²⁵ (Scheme 2).



Scheme 2. Apical ligand exchange reactions in Ti(IV) TPA complexes

X-Ray and ¹H NMR data indicate that the complexes remain monomeric and structurally similar to the precursor.

²² Kol, M.; Shamis, M.; Goldberg, Z.; Goldschmidt, Z.; Alfi, S.; Hayut-Salant, E. *Inorg. Chem. Commun.* **2001**, *4*, 177.

²³ Nielson, A. J.; Shen, C.; Waters, J.M. *Polyhedron* **2006**, *25*, 2039.

²⁴ Ugrinova, V.; Ellis, G. A.; Brown, N. S. *Chem. Comm.* **2004**, 468.

²⁵ Bull, S. D.; Davidson, M. G.; Johnson, A. L.; Robinson, D.; Mahon, M. F. *Chem. Comm.* **2003**, 1750.

Interestingly, complexes bearing a trifluoroacetate apical ligand are able to afford an unusually stable LTiOH complex **12** by reaction with basic water, a reactivity that was not observed for the complexes bearing apical alkoxide groups.²⁴

In these complexes a similar influence of the π -donating ability of the apical ligand in structure is observed. When the apical *Oi*-Pr group is substituted by a poorer π -donor as Cl or OTf, the Ti-Cl or Ti-OTf bonds are significantly longer than the equivalent one in the alkoxide complex, reflecting a weaker π -donation to the titanium atom. To compensate this electron deficiency, the metal atom is constricted to interact stronger with both the phenolate oxygen atoms and the nitrogen from the tertiary amine so a shortening in the Ti-O and Ti-N lengths is observed, 0.029 and 0.118 Å respectively for Cl²³ (Table 1, entries 1 and 2) and 0.053 and 0.089 Å for OTf²⁵ (Table 1, entries 5 and 6). This phenomena has also been observed in other metal complexes and, for example, it has been extensively studied by Holmes and coworkers in Si(IV) amine triphenolate complexes (see below).²⁶

Table 1. Selected bonds and angles of TBP Ti(IV) amine triphenolate complexes

Entry	R	R'	L'	d (Ti-O) ^a (Å)	d (Ti-N) (Å)	d (Ti-L') ^b (Å)	N-Ti-L' ^b (deg)
1 ²²	<i>t</i> -Bu	<i>t</i> -Bu	O- <i>i</i> -Pr	1.841 (6)	2.334 (5)	1.778 (4)	179.3 (2)
2 ²³	"	"	Cl	1.812 (2)	2.216 (2)	2.3074 (7)	179.51 (5)
3 ²⁴	"	"	OMe	1.851 (2)	2.308 (2)	1.7880 (13)	178.69 (6)
4 ²⁴	"	"	OH	1.834 (3)	2.364 (2)	1.810 (2)	179.15 (8)
5 ²⁵	Me	Me	O- <i>i</i> -Pr	1.853 (2)	2.305 (2)	1.774 (2)	179.70 (8)
6 ²⁵	"	"	OTf	1.800 (2)	2.216 (2)	2.002 (2)	177.25 (8)
7 ²⁸	"	"	ArO ^c	1.830 (2)	2.306 (2)	1.834 (2)	174.89 (8)
8 ²⁷	Adamantyl	<i>t</i> -Bu	Cl	1.812 (9)	2.251 (9)	2.310 (1)	178.45 (6)
9 ²⁷	"	"	OTf	1.809 (2)	2.172 (3)	2.031 (2)	173.5 (1)

^a Average of the three Ti-O_{phenolate} distances. ^b L' = atom of the apical ligand directly bounded to the Ti(IV) ion. ^c Ar = 2,6-di-*iso*-propylphenyl

Complexes **10g** (L_iTiOTf) and **13g** (L_iTiCl), bearing ligands with bulky adamantyl (Adm) groups in *ortho* position have also been described (Table 1, entries 8 and 9).²⁷ The X-ray crystal structures of these complexes are similar to the chloride and triflate titanium complexes previously reported.

A Ti(IV) tetrahydroborate complex has been also reported. In this case the tetrahydroborate unit occupies the apical position bounding the metal in a η^3 fashion.²⁸

So far only Ti(IV) complexes of TBP geometry have been discussed, but complexes where titanium can accommodate an extra ligand moving to a hexacoordinated, octahedral geometry have been also described.^{23,29} Brown *et al.* have reported a series of octahedral complexes obtained by reaction of **9c** with more acidic bidentate ligands as acetylacetonato (acac) (Figure 10).

²⁶ Chandrasekaran, A.; Day, R. O.; Holmes, R. R. *J. Am. Chem. Soc.* **2000**, *122*, 1066.

²⁷ Cortes, S. A.; Muñoz Hernández, M. A.; Nakai, H.; Castro-Rodriguez, I.; Meyer, K.; Fout, A. R.; Miller, D. L.; Huffman, J. C.; Mindiola, D. J. *Inorg. Chem. Commun.* **2005**, *8*, 903.

²⁸ Johnson, A. L.; Davidson, M. G.; Mahon, M. F. *J. Chem. Soc. Dalton Trans.* **2007**, 5405.

²⁹ Fortner, K. C.; Bigi, J. P.; Brown, S. N. *Inorg. Chem.* **2005**, *44*, 2803.

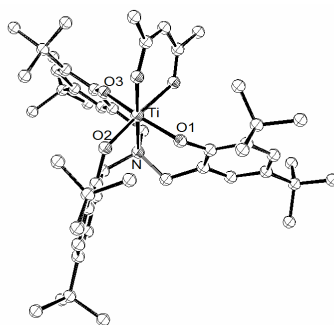


Figure 10. Molecular structure of $L_cTi(acac)$ ²⁹

In the OCT complexes the bidentate ligand occupies an axial position (*trans* to the nitrogen from the tertiary amine) and an equatorial position (*trans* to one of the phenolate oxygens of the tripodal ligand). The OCT complexes have C_1 symmetry and the amine triphenolate ligand retains the propeller-like conformation around the metal (Figure 10).

This ability to coordinate bidentate ligands makes possible the activation of alkyl hydroperoxides and hydrogen peroxide to form peroxy complexes that are active in oxygen transfer reactions.³⁰

As mentioned before, already in the preliminary studies by Kol *et al.*, a significative different thermodynamic stability for titanium alkoxo complexes bearing peripheral substituents of different steric size has been observed.²² This so called “*ortho* effect” arises from the steric size and electronic nature of the *ortho* peripheral substituents of the ligand. These substituents determinate the steric hindrance around the metal, and so, the binding mode and the stability of the complex.

Peripheral substituents influence strongly the complexes stability towards nucleophiles. This is well illustrated by the response of complexes bearing different *ortho* substituents to moisture (Figure 11). Complexes bearing bulky *ortho* *t*-Bu substituents are stable to moisture, even in the presence of excess of water no exchange of the apical ligand nor degradation of the complex are observed.^{22,24,30} On the other hand, complexes bearing small substituents, as Me or H, tend to form aggregates after exposure to moisture.^{22,23,30a}

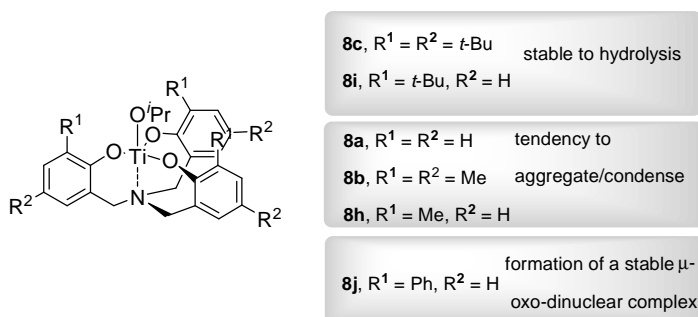


Figure 11

³⁰ (a) Mba, M; Prins, L. J.; Licini, G. *Org. Lett.* **2007**, *9*, 21. (b) Zonta, C.; Cazzola, E.; Mba, M.; Licini, G. *Adv. Synth. Catal.* **2008**, *350*, 2503.

The lack of reactivity of complexes bearing bulky substituents versus water is extremely unusual, as titanium alkoxides are well known to readily react with water. This behaviour has been studied more in detail by Brown *et al.*²⁴ The authors were able to obtain the hydroxo complex **12c** only by hydrolysis of the trifluoroacetate **11c**, which did not further condense as expected, but remained stable in solution (Scheme 2). The corresponding μ -oxo dimer **14c** ($L_cTi-O-TiL_c$) was obtained only in the solid state after concentration of solutions of **12c**. The crystal structure of **14c** shows a bent μ -oxo bridge (155.54° (9)) and Ti-O distances of 1.825 (15) Å (Figure 12). The complex is stable in the solid state under anhydrous conditions but the oxo-bridge is easily cleaved in solution. The instability of the oxo-bridge is steric in origin as the *t*-Bu substituents are forced to close contact in the dinuclear complex. On the other hand, Ti(IV) amine triphenolate complexes, bearing smaller substituents in *ortho* position, form polynuclear species in presence of water. This property was first observed by Kol *et al.* for complex **8b** (R=R'=Me) and the polynuclear species was tentatively identified as a μ -oxo-**14b** ($L_bTi-O-TiL_b$).²² This has been recently confirmed by X-ray analysis.²³

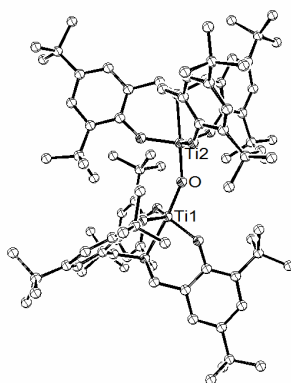


Figure 12. Molecular structure of μ -oxo complex **14c**²⁴

Table 2. Selected bonds and angles of oxo-bridged dinuclear Ti(IV) complexes **14** from TPA L_bH_3 and L_cH_3 .

Complex	R	R'	d (Ti-O) ^a	d (Ti-N) (Å)	d (Ti-O _{central}) (Å)	N-Ti-O _{central} (deg)	Ti-O-Ti (deg)
1 ²⁴ 14c	<i>t</i> -Bu	<i>t</i> -Bu	1.844 (2)	2.275 (2)	1.8250 (15)	174.19 (7)	155.54 (9)
			1.847 (2)	2.289 (2)	1.8254 (15)	178.15 (7)	
2 ²³ 14b	Me	Me	1.8382 (18)	2.379 (2)	1.8076 (17)	179.41 (8)	147.48 (11)
			1.8346 (19)	2.388 (2)	1.8219 (17)	178.52 (8)	

^a Average of the three Ti-O_{phenolate} distances. ^b The μ -oxo bridge is located on a crystallographic centre of inversion leading to a perfectly linear Ti-O-Ti bond angle.

The structure of **14b** is quite similar to the complex **14c** bearing *t*-Bu substituents (Figure 12), but now the Ti-O-Ti bond angle is smaller (Table 2, entries 1 and 2), probably due to the less severe interactions among the *ortho* methyl substituents.

As in the case of Ti(IV), Zr(IV) and Hf(IV) amine triphenolate complexes can be obtained by transesterification reaction with a metal tetraalkoxide.

Only a single example of Hf(IV) complexes has been reported. The X-ray crystal structure of the complex bearing bulky ortho,para *tert*-butyl substituents has been resolved showing a monomeric pentacoordinate TBP complex with C_3 symmetry.³¹

Reaction of $Zr(Oi-Pr)_4$ with ligand L_cH_3 bearing bulky *t*-butyl peripheral substituents gave a TBP monomeric complex.³² On the other hand, reaction with less hindered ligands like L_bH_3 ($R=R'=Me$) led to the formation of the C_3 -symmetric zwitterionic complex **15b**, with a Zr(IV): L_bH_3 ratio 1:2, in which the metal adopts a distorted octahedral geometry (Figure 13).^{33,34,35}

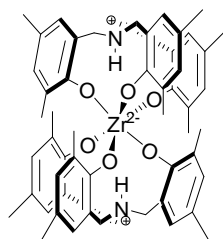


Figure 13³³

The coordination of two trianionic ligands to the zirconium atom affords a dianionic metal centre. The charge is compensated by the protonation of both nitrogen atoms. These hydrogens are trapped in a cage-like arrangement and the distances to each one of the phenolate oxygen atoms (2.21 (3), 2.29 (2) and 2.15 (3) Å) are indicative of the presence of a N-H...O hydrogen bond. The formation of the zwitterionic structure originates mainly from two different factors: *i.* zirconium has the right size to accommodate the NH...O motifs, without incurring in repulsive NH-M interactions; *ii.* the decreased steric size of the peripheral substituents allows the approaching of two ligand molecules to the metal.

1.3.2 Group (V) complexes

In group V complexes, the hexacoordinate, octahedral geometry predominates; only vanadium is reported to give TBP structures, even though, as in the case of Ti(IV), it can also adopt octahedral geometries to accommodate an extra ligand. The most important difference to respect group IV complexes is that the amine triphenolate ligand does not adopt a propeller-like arrangement around the metal in the octahedral geometry. Reaction of L_bH_3 and L_cH_3 with $VCl_3 \cdot THF$ led to the formation of C_3 -symmetric TBP species in which a THF molecule occupies the apical position.³⁶ When $V(O)(OR)_3$ are used as metal precursors, TBP geometries are observed as well, in which the axial position *trans* to the nitrogen of the tripod

³¹ Chmura, A. J.; Davidson, M. G.; Frankis, C. J.; Jones, M. D.; Lunn, M. D *Chem. Commun.* **2008**, 1293.

³² Gendler, S.; Segal, S.; Goldberg, I.; Goldschmidt, Z.; Kol, M. *Inorg. Chem.* **2006**, *45*, 4783.

³³ Davidson, M. G.; Doherty, C. L.; Johnson, A.L.; Mahon, M. F. *Chem. Commun.* **2003**, 1832.

³⁴ Nielson, A. J.; Shen, C.; Waters, J. M. *Crystal Str. Commun.* **2003**, m494.

³⁵ Chartres, J. D.; Dahir, A.; Tasker, P. A.; White, F. J. *Inorg. Chem. Commun.* **2007**, *10*, 1154.

³⁶ Groysman, S.; Goldberg, I.; Goldschmidt, Z.; Kol, M. *Inorg. Chem.* **2005**, *44*, 5073.

product. In order to obtain the dichloro complex, the authors had to synthesize the diamido complex. However, even if dimethylamino groups are more readily replaced than alkoxides, large excess of TMSCl was necessary to replace both monodentate ligands.

1.3.3 Group (VI) complexes

Among the group VI metals only tungsten and molybdenum TPA complexes have been described.

Reaction of L_bH_3 ($R=R'=Me$) with $MoO_2(acac)_2$ led to formation of a hexacoordinate octahedral complex.⁴² The presence of two oxo moieties results in an anionic charge of the metal that is balanced by protonation of the nitrogen of a second TPA molecule that acts as cation.

Neutral octahedral complexes are obtained by reaction of TPA ligands with $MoO_2Cl_2(dmf)_2$ ($dmf=$ dimethylformamide) or $MoO_2(OCH_2CH_2OH)_2$ (complex 174c, Figure 15).⁴³ Ligand exchange reactions with high-boiling point alcohols and with TMSCl are possible. All the structures possess C_1 -symmetry, meaning that the tripodal ligand wraps around the metal in a propeller-like conformation.

TPA tungsten complexes have been obtained from $W(OCH_2CH_2O)_3$ or $W(O)Cl_4$.⁴⁴ They present similar structural characteristics to molybdenum complexes, though, in cases of important steric clash, loss of the propeller-like arrangement is observed.

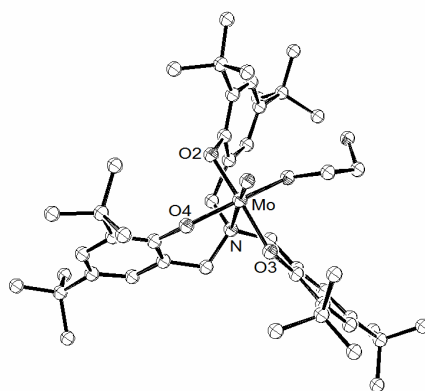


Figure 15. Molecular structure of $L_cMo(O)(OCH_2CH_2OH)$ complex 17c.⁴⁴

1.3.4 Iron and late transition metal complexes

The report of Koch *et al.* on Fe(III) complexes is the only example for TPA iron complexes.⁴⁵ Complexes have been obtained by reaction of L_aH_3 or L_bH_3 with $FeCl_3$, but four-coordinate complexes could not be isolated. Instead pentacoordinate TBP structures were obtained where the apical position is occupied by a solvent molecule or 1-methylimidazole. The

⁴² Lehtonen, A.; Kessler, V. G. *Inorg. Chem. Comm.* **2004**, 7, 691

⁴³ Lehtonen, A.; Sillanpää, R. *Polyhedron* **2007**, 26, 5293.

⁴⁴ Lehtonen, A.; Sillanpää, R. *Organometallics* **2005**, 24, 2795.

⁴⁵ Hwang, J.; Govindaswamy, K.; Koch, S. A. *Chem. Comm.* **1998**, 1667.

structure displays all the features discussed before for Ti(IV) complexes and, in the same way, Fe(III) is able to accommodate an extra ligand adopting an octahedral geometry.

Itoh *et al.* described a Ni(II) complex obtained by reaction of L_cH_3 with NiCl₂ in the presence of 1,2,3,3-tetramethylguanidine (TMG). The resulting complex (L_cH)Ni(II)(TMG) has a four-coordinate distorted square planar geometry in which the TPA acts as a tridentate ligand binding the metal with two phenolate oxygens and the tertiary amine nitrogen.⁴⁶

1.3.5 Group XI, XII and XIII complexes

Verkade and coworkers have studied the different binding modes for Al(III) complexes with TPA bearing peripheral substituents of different steric size. They observed that reaction of AlMe₃ with TPA ligands bearing peripheral methyl substituents, L_bH_3 , led to formation of a dimer in which two alumatrane units with TBP geometry are linked by two interactions between the Al from one monomer and one oxygen phenolate from the other.⁴⁷ However, when the TPA ligand bears bulky *t*-butyl substituents, L_eH_3 , (R=*t*-Bu, R'=Me) a monomeric proalumatrane **18e** with TMP geometry was isolated in which the steric hindrance around the vacant site protects it from dimerization (Figure 16).⁴⁸

Reaction of these complexes with equimolar amounts of water resulted in the formation of water-coordinated complexes, in which the water molecule occupies the axial position *trans* to the nitrogen. Also in this case the steric size of the *t*-Bu substituents enhances the stability towards hydrolysis of the Al-O_{phenoxide} bonds. A large variety of Al(III) complexes has been obtained starting from the Al(III) dimer bearing L_bH_3 (R=R'=Me) ligands using different nucleophiles.^{47,49}

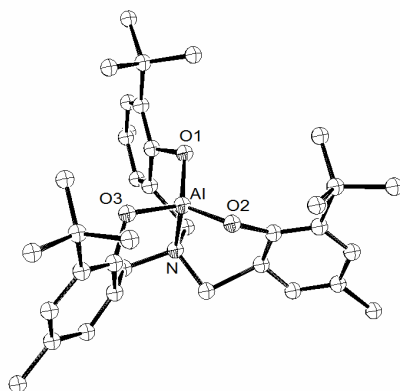


Figure 16. Molecular structure of $L_eAl(III)$ complex **18e**⁴⁸

Ga(III) and In(III) complexes of TPA obtained through reaction with [PPh₄][GaCl₄] and InCl₃, respectively, in the presence of 1-methylimidazole have been reported by Martell,

⁴⁶ Nagataky, T.; Itoh, S. *Chem. Lett.* **2007**, 36, 748.

⁴⁷ Su, W.; Kim, Y.; Ellern, A.; Guzei, I. A.; Verkade, J. G. *J. Am. Chem. Soc.* **2006**, 128, 13727.

⁴⁸ Su, W.; Kobayashi, J.; Ellern, A.; Kawashima, T.; Verkade, J. G. *Inorg. Chem.* **2007**, 46, 7953.

⁴⁹ For more examples, see: Kim, Y.; Verkade, J. G. *Inorg. Chem.* **2003**, 42, 4804.

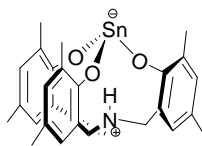
Koch *et al.*⁵⁰ No four-coordinate complex with TBP geometry was obtained in any case: Ga(III) coordinates with a TBP geometry bearing an extra 1-methylimidazol ligand, while the larger In(III) gave an octahedral complex.⁵¹

An important feature observed in group XI complexes is that the metal centre is situated below the plane defined by the three phenolate oxygens.

Among the group XII metals, Holmes and coworkers have reported several Si(IV) amine triphenolate complexes, all of them displaying distorted TBP geometry. Special attention has been given to the effects of the electronegativity of the apical ligand in the structure of the complex.^{26,51,52} As expected, an increment of electronegativity causes a shortening in the Si-N bond length and the shorter this bond the more the structure resembles an ideal TBP geometry. Interestingly, the highly electronegative apical ligand CCl₃ afforded the shortest Si-N bond length (2.025 Å in a range going from 2.838 to 2.025 Å) and a rigid structure that does not racemize.

A Ge(IV) complex L_bGe(OiPr)(HOiPr) was recently reported by Davidson *et al.* displaying the typical TBP geometry.⁵²

Reaction of Sn[N(SiMe₃)₂] with L_bH₃ allowed the isolation of the tricoordinate pyramidal Sn(II) complex **181b** (Figure 17). The negative charge created on the metal is balanced by protonation of the nitrogen.²⁵



181b

Figure 17

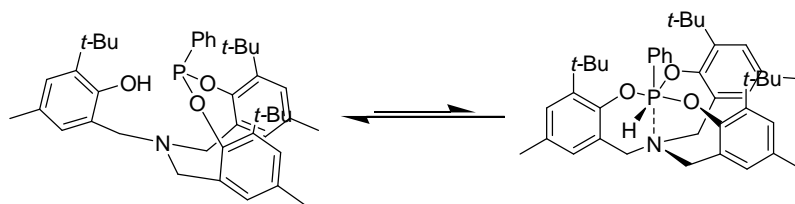
Phosphorus complexes have been also studied by Holmes and coworkers, among the group XIII elements. Phosphorous tends to form complexes in which the TPA ligand binds in a bidentate fashion with only two phenolate oxygens.⁵³ Also complexes in which one arm has been lost via N-C bond cleavage (R₂PN(ArCH₂)₂) are common. Phosphatranes, in which the TPA binds in a tetradentate fashion, can be obtained only in low yields. On the other hand, tricoordinated and hexacoordinated species have been found to be in equilibrium in solution (Scheme 3).^{53b}

⁵⁰ Motekaitis, R. J.; Martell, A. E.; Koch, S. A.; Hwang, J. W.; Quarless, D. A.; Welch, M. J. *Inorg. Chem.* **1998**, *37*, 5902.

⁵¹ (a) Timosheva, N. V.; Chandrasekaran, A.; Day, R. O.; Holmes, R. R. *Organometallics* **2000**, *19*, 5614. (b) Timosheva, N. V.; Chandrasekaran, A.; Day, R. O.; Holmes, R. R. *Organometallics* **2001**, *20*, 2331.

⁵² Chmura, A. J.; Chuck, C. J.; Davidson, M. G.; Jones, M. D.; Lunn, M. D.; Bull, S. D.; Mahon, M. F. *Angew. Chem. Int. Ed. Engl.* **2007**, *46*, 2280.

⁵³ (a) Chandrasekaran, A.; Day, R. O.; Holmes, R. R. *Inorg. Chem.* **2000**, *39*, 5683. (b) Timosheva, N. V.; Chandrasekaran, A.; Day, R. O.; Holmes, R. R. *J. Am. Chem. Soc.* **2002**, *124*, 7035. (c) Timosheva, N. V.; Chandrasekaran, A.; Holmes, R. R. *Inorg. Chem.* **2004**, *43*, 7403.



Scheme 3. Equilibrium in solution between tricoordinate and hexacoordinate phosphorus complexes of TPA

Parkin *et al.* have reported that reaction of $\text{Sb}(\text{OEt})_3$ with L_cH_3 ($\text{R}=\text{R}'=t\text{-Bu}$) and recrystallization from DMSO led to the isolation of a $\text{L}_c\text{Sb}(\text{DMSO})$ complex⁵⁴ in which the antimonium complex has a five coordinate square pyramidal geometry with one DMSO molecule occupying an equatorial position *trans* to one phenolate oxygen, and the lone pair occupying the axial position. Antimonium is also able to adopt an octahedral geometry as demonstrated by the isolation of L_cSbBr_2 .⁵⁴

A four-coordinate bismuth complex was isolated by Davidson, Wilson *et al.*: its X-ray crystal structure shows that the phenolate oxygens are disposed in a T form.⁵⁵ In the same report a TMP five-coordinate Bi(III) complex from L_bH_3 ($\text{R}=\text{R}'=\text{Me}$) was obtained but it resulted to be stable only in the solid state. However, increasing the steric size of the substituents (from Me to *t*-Bu) led to the isolation of a stable toluene adduct in which two C_3 symmetric monomeric units associate via a toluene bridge into a bis(bismuth)toluene inverted sandwich.

1.4 Amine *tri*-phenolate complexes: catalytic activity

While a substantial number of publications regarding the synthesis and coordination chemistry of *tris*-phenolate amino ligands are available, studies dealing with their catalytic activities have been only recently reported.

These studies are mainly related with the amine triphenolate complexes Lewis Acid properties and consequently, to the capability of the tetradentate TPA ligands to stabilize the active site under turnover conditions, in particular in polymerization and oxygen transfer processes. Lewis Acids based on d^0 metal compounds (*e.g.* $\text{Ti}(i\text{-OPr})_4$) are widely used in synthetic organic chemistry.⁵⁶ However, Lewis Acids are very often air and moisture sensitive. For these reasons to prepare Lewis Acids complexes displaying high catalytic activity and, at the same time, good stability on time and on handling, is an important task. Amine *tri*-phenolate complexes, due to their high-stability, are good candidates for successful application in Lewis Acid catalysis.

Polymerizations. Group (IV) TPA complexes [$\text{Ti}(\text{IV})$, $\text{Zr}(\text{IV})$ and $\text{Hf}(\text{IV})$] have been found to be effective catalysts in ring opening polymerization (ROP) of lactide.^{31,32,57}

⁵⁴ Kelly, B. V.; Weintrob, E. C.; Buccella, D.; Tanski, J. M.; Parkin, G. *Inorg. Chem. Commun.* **2007**, 10, 699.

⁵⁵ Turner, L. E.; Davidson, M. G.; Jones, M. D.; Ott, H.; Schulz, V. S.; Wilson, P. J. *Inorg. Chem.* **2006**, 45, 6123.

⁵⁶ *Lewis Acids in Organic Synthesis* Ed. Hisashi Yamamoto 2000, Wiley-VCH.

⁵⁷ Kim, Y.; Jnaneshwara, G.K., Verkade, J. G. *Inorg. Chem.* **2003**, 42, 1437.

ROP of cyclic esters like lactide is of large interest due to the biodegradability of poly lactide (PLA) and the availability of lactide from renewable resources (corn, beets and dairy products).⁵⁸

Bulk polymerization of *rac*-lactide (130°C, [lactide]/[catalyst]=300) affords PLA with different level of stereoselection depending on the metal present in the catalyst (Table 3).

Table 3. Bulk polymerization of *rac*-[lactide] catalyzed by L_cMOiPr/OtBu complexes (M= Ti(IV), Zr(IV), Hf(IV), Ge(IV)).

Entry	M	Time, h	Yields, %	M _n ^b	PDI ^c	Pr ^d	Ref
1	Ti	0.5	50	37100	1.38	0.50	31
2 ^e	Ti	14	24	43400	1.44	nd	57
4	Zr	0.1	78	32300	1.22	0.96	31
6	Hf	0.5	95	71150	1.19	0.88	31
7 ^f	Ge	24	85	35700	1.15	0.79	52

^a Reaction conditions: 130° C, [lactide]/[M]=300, no solvent. ^b Number average molecular weight. ^c Polydispersity index (PDI=M_w/M_n). ^d Probability of heterotactic enchainment. ^e Data referring to L_cTiOiPr (R=*t*-Bu, R'=Me). ^f Data referring to L_bGeOiPr catalyst (R=R'=Me).

The polymerization occurs via a coordination-insertion mechanism initiated by alkoxo groups. Stereoselectivity of the polymerization strongly depends on the metal ion nature: Zr(IV), followed by Hf(IV), affords the PLA with high reactivity and high heterotacticity (Table 4, entries 4 and 6). More detailed investigation on Zr(IV) complexes speciation in solution (CDCl₃) confirmed the living nature of the polymerization with first order kinetics in the monomer. ROP on *rac*- and (*S,S*)-LA showed that the first process, yielding to heterotactic PLA, is seven time faster than the second one, affording isotactic PLA. Factors governing the stereoselectivity of the processes are still not fully understood.³¹

A similar Ge(IV) complex, bearing methyl groups on the aromatic rings revealed to be also an effective single-site initiator for lactide ROP: under comparable reaction conditions highly heterotactic PLA was obtained (Pr=0.78-0.82) even if the system is less reactive than the Hf(IV) and Zr(IV) ones (Table 4, entry 7).⁵²

Oxidations. The activation of peroxides by metal complexes has been the focus of intense research efforts because of its relevance to biochemical processes, as well as the applications of this chemistry in industrial oxidation processes.⁵⁹ In fact the direct and selective oxidation of nucleophiles like heteroatoms (sulfur, nitrogen, phosphorous) or double bonds affords valuable derivatives and building blocks for fine chemistry.⁶⁰ In most of the cases the activation of peroxides can be regarded as Lewis Acid catalysis in which the mechanism of

⁵⁸ Williams, C. K.; Hillmyer, M.A. *Polym. Rev.* **2008**, *48*, 1.

⁵⁹ (a) "Organic Peroxides" Ed. W. Ando, 1992 John Wiley & Sons. (b) "Metal Catalyzed Oxidations of Organic Compounds" Eds. R. A. Sheldon, J. K. Kochi 1981 Academic Press.

⁶⁰ Blaser, H.-U.; Pugin, B.; Spindler, F. *J. Mol. Catal. A: Chem.* **2005**, *231*, 1.

activation starts with the coordination of the peroxide to the metal and it follows with the electrophilic oxygen transfer via a η^2 metalloperoxo intermediate.⁶¹

The *in situ* prepared Ti(IV) complexes **8a**, **8h**, and **8i** have been resulted to be effective homogeneous catalysts in the oxidation of sulfides and secondary amines using hydrogen peroxide as primary oxidant.³⁰ In particular, **8i** (R=*t*-Bu, R'=H) afforded the best performances being air and moisture tolerant and stable and active even in the presence of a large excess of water.

In sulfoxidations, catalyst **8i** efficiently activates hydrogen peroxide affording the sulfoxides in high yields and chemoselectivities, catalyst loading down to 0.01 %, TOF up to 1700 h⁻¹ and TONs up to 8000. The system has been effectively applied to a series of sulfides (Table 4).^{30a}

Table 4. Oxidation of sulfides by aqueous H₂O₂ catalysed by **8i**.^a

$$\text{R}^1\text{-S-R}^2 \xrightarrow[\text{CH}_3\text{OH, 28}^\circ\text{C}]{\text{H}_2\text{O}_2, \mathbf{8i}} \text{R}^1\text{-S(=O)-R}^2 + \text{R}^1\text{-SO}_2\text{-R}^2$$

Entry	R ¹	R ²	conv. (%) ^b	SO:SO ₂ ^{cc}	Yield (%) ^d
1	Ph	Me	96	98:2	92
2	<i>p</i> -Tol	<i>n</i> -Bu	97	95:5	89
3	Ph	Bu	95	93:7	84
4	<i>n</i> -Bu	<i>n</i> -Bu	91	93:7	83
5	<i>p</i> -MeO-C ₆ H ₄	Me	94	94:6	86
	<i>p</i> -NO ₂ -C ₆ H ₄	Me	77	85:15	61

^a Reactions carried out at 28° C with a 1:1 molar ratio of substrate/aq H₂O₂ 1% catalyst on 0.5 mmol scale. ^b Determined by ¹H NMR (CD₃OD, 300 MHz) and quantitative GC analysis on the crude reaction mixture after total oxidant consumption (iodometric test). ^c Sulfoxide:sulfone ratio measured at the end of the reaction. ^d Isolated yields in sulfoxide based on the substrate, after radical chromatography.

Oxidation of secondary amines to the corresponding nitrones have also been explored.^{30b,62} Also in this case excellent results in term of reactivity and selectivity were obtained. Reactions carried out in methanol afforded nitrones in good yields, up to 99%, catalyst **8i** loading down to 0.01 %, TOFs up to 11000 h⁻¹ and TONs up to 8000. A range of substrates have been effectively oxidized in good yields and chemoselectivities, demonstrating the versatility of the catalyst (Table 5).

⁶¹ For Ti (IV), see: Bonchio, M.; Calloni, S.; Di Furia, F.; Licini, G.; Modena, G.; Moro, S.; Nugent, W. A. *J. Am. Chem. Soc.* **1997**, *119*, 6935. For V (V), see: Schneider, C. J.; Penner-Hahn, J. E.; Pecoraro, V. L. *J. Am. Chem. Soc.* **2008**, *130*, 2712.

⁶² For a related reaction, see: Forcato, M.; Nugent, W. A.; Licini, G. *Tetrahedron Lett.* **2003**, *44*, 49.

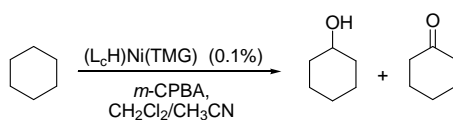
Table 5. Oxidation of secondary amines to nitrones by aqueous H₂O₂ (70%) catalyzed by **8i** (5%) at 60°C.^a

	Substrate	Product	Time (h)	Yields ^b (%)
1			2.0	92
2			3.5	97
3			45.0	73
4			45.0	92
5			0.5	99
6			3.0	76

^a Reaction conditions: amine = 1.0 M; amine: H₂O₂: **8i** = 1:4:0.05, 60°C. ^b Based on the substrate, determined via ¹H NMR.

Dealing with V(V) amine *tri*-phenolate complexes, Goldschmidt, Kol and others firstly reported on their catalytic activity in oxidation reaction.³⁶ They described preliminary results on the capability of these system in the oxidation of styrene. Employing 5% mol of vanadium(V) complexes L_bVO, L_dVO (R=R'=Me or R=R'=Cl) in a benzene solution of styrene/t-BuOOH, styrene oxide was obtained. The rate of oxidation was slow (4-5 turnover per day) and additional products formed along the reaction. Similar complexes have been prepared also in this research group: their characterization and reactivity will be the described in *Chapter 2* of this Thesis.³⁷

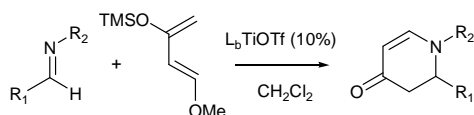
(L_cH)Ni(TM_G) has been found to be able to activate *m*-chloroperbenzoic acid in the hydroxylation of cyclohexane (Scheme 4).⁴⁶

**Scheme 4.** Oxidation of cyclohexane by *m*-CPBA catalyzed by (L_cH)Ni(TM_G)

Reactions carried out in $\text{CH}_2\text{Cl}_2/\text{MeCN}$ at room temperature, 0.1% of catalyst, gave cyclohexanol in moderate yields (30% after 2 hs) but with a significantly high alcohol/ketone ratio (A/K= 65).

Other Lewis acid catalysis. Bull and Davidson first examined the catalytic activity of different substituted TPA-Ti(IV) complexes.²⁵ Complex **8b**, ($\text{R}=\text{R}'=\text{Me}$) is monomeric and air stable. However, **8b** showed a poor catalytic activity as Lewis Acid. This reduced activity, compared with other titanium alkoxides and phenolates, arise from *N* donation of the TPA ligand. In order to increase the reactivity, the complex with the more labile apical triflate, arising from the reaction of **8b** with Me_3SiOTf , has been prepared. The triflate complex L_bTiOTf **10b** showed enhanced catalytic activity, in particular for a series aza-Diels-Alder reactions (Table 6).

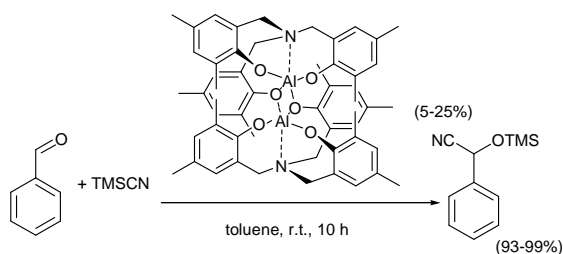
Table 6. Diels-Alder reaction between imines and Danishefsky's diene catalyzed by L_bTiOTf **10b**.^a



Entry	R ¹	R ²	Time/min	Yield ^a (%)
1	Ph	Bn	45	73
2	2-Npth	Bn	40	71
3	3,5-(MeO) ₂ C ₆ H ₃	Bn	70	60
4	Cyc	Bn	45	56
5	Ph	<i>i</i> -Pr	60	72
6	Ph	3,4-(MeO) ₂ C ₆ H ₃	80	62

a. All yields for chromatographically pure compounds.

Complex **8b** have also been used for the activation of borohydrides in the reduction of acetophenone,²⁸ while aluminium complexes showed to be powerful Lewis Acid catalysts as well, extensively used in organic synthesis.⁵⁶ Mononuclear alumatrane complexes, prepared by Verkade *et al.*, are able to form a stable adduct with benzaldehyde coordinated in the apical position.⁴⁷ The coordinated benzaldehyde reacts readily with one equivalent of trimethylsilyl cyanide. Similarly the dimeric complex $(\text{L}_b)_2\text{Al}_2$ promotes the reaction when it is present in catalytic quantities (Scheme 5).



Scheme 5. Trimethylsilyl cyanation of benzaldehyde catalyzed by L_{b2}Al_2 .

1.5 Aim of the thesis

The work described in this thesis has been dealing with the amine triphenolate ligands, their use in catalysis and for building up functional structures with controlled geometries. In

particular their synthesis, coordination chemistry towards Ti(V) and V(V) and catalytic performances on oxygen transfer reactions have been investigated.

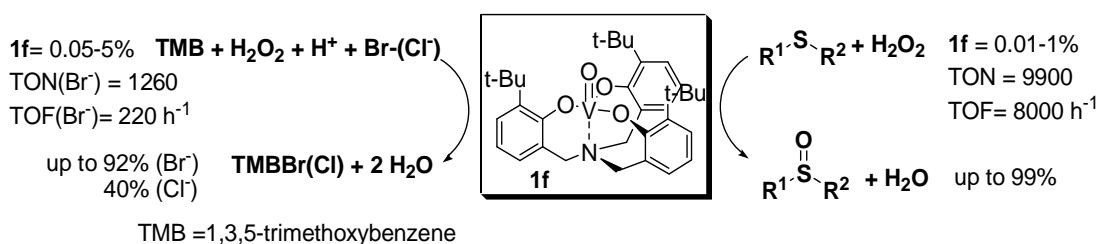
In this respect, *Chapter 2* describes the synthesis and the structural characterization of V(V) complexes with C_3 -symmetric *tris*-phenol amines as structural and functional models of vanadium haloperoxidases (VHPOs). Catalytic application of such V(V)/amine triphenolate complexes in the oxidation of sulfides and halides will be discussed and the optimization of the catalytic system will be presented.

Chapter 3 discloses the particular coordination behaviour of *tris*-(2-hydroxy-3-phenylbenzyl)amine with Ti(IV) metal centre: a completely stereoselective self-assembly process is at the basis of the formation of a highly stable, inert dinuclear S_6 -symmetric μ -oxo complex. In this contest, a new efficient method for the synthesis of *ortho*-aryl functionalized *tris*-arylphenol amines will be reported, using a Suzuki coupling reaction as main strategic step, together with new examples of dinuclear μ -oxo complexes possessing peripheral anchoring sites, ready to be exploited for the construction of stable and spatially ordered new materials.

Finally, *Chapter 4* is dedicated to the preparation of chiral, enantiopure *tris*-(*ortho*-arylphenol)amines ligands and to study the synthesis and properties of the corresponding titanatrane complexes.

Chapter 2

Oxovanadatrane complexes as functional and structural models of haloperoxidases



The coordination chemistry and catalytic activity of C₃-symmetric triphenolate amino complexes have been investigated. In this context, V(V)-oxo triphenolate amino complex **1** has been synthesized: it possesses a TBP geometry which emulates the one found in Vanadium haloperoxidases (VHPOs). Here we will show that V(V)-complex **1f** bearing *tert*-butyl peripheral substituents is a structural and functional model of VHPOs. The complex catalyzes efficiently sulfoxidations at rt using hydrogen peroxide as terminal oxidant yielding the corresponding sulfoxides in quantitative yields and high selectivities (catalyst loading down to 0.01%, TONs up to 9900, TOF up to 8000 h⁻¹) as well as chlorination and bromination of trimethoxybenzene (catalyst loading down to 0.05%, TONs up to 1260, TOF up to 220 h⁻¹).

This Chapter has been published:

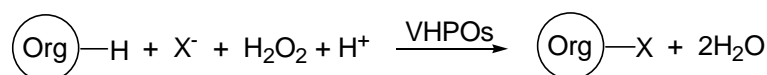
Mba, M.; Pontini, M.; Lovat, S.; Zonta, C.; Bernardinelli, G.; Kündig, E. P.; Licini, G. *Inorg. Chem.* **2008**, *47*, 8616.

2.1 Introduction

The growing interest in vanadium chemistry has been inspired by the discovery of its bioinorganic functions. For example, the vanadium-dependent nitrogenase enzyme features vanadium in medium oxidation states of V(II)-V(IV), postulated to bind and reduce dinitrogen. Vanadium dependent haloperoxidases feature vanadium in its highest oxidation state. The five-coordinated V(V) centre possesses a trigonal bipyramidal geometry in the resting state, being surrounded by three equatorial oxygen donors, an axial oxygen and nitrogen donors.¹

Relying on these structural motifs, model compounds are being designed mimicking the coordination sphere in the active-site of vanadium-dependent enzymes, especially haloperoxidases. Several V(V) complexes emulating the coordination sphere of the metal in these enzymes have appeared in literature as structural and functional models for Vanadium haloperoxidases.^{2,3}

Vanadium haloperoxidase (VHPOs), first discovered in marine seaweed *Ascophyllum nodosum* in 1984,⁴ are vanadium-dependent enzymes able to oxidize halides to the corresponding 'X⁺' species in the presence of hydrogen peroxide leading to halogenation of suitable substrates.⁵ The global process could be written as follow:



Scheme 1

It has been shown that VHPOs catalyze also the oxidation of different organic substrates, i.e. sulfides to sulfoxides, phosphine to phosphinoxides.⁶

The nomenclature for the haloperoxidases has traditionally been based on the most electronegative halide which can be oxidized by hydrogen peroxide catalyzed by the enzyme. Thus chloroperoxidase catalyzes the oxidation of chloride, bromide and iodide;

¹ (a) Messerschmidt, A.; Wever, R. *Proc. Natl. Acad. Sci. U.S.A.* **1996**, *93*, 392. (b) Messerschmidt, A.; Wever, R. *Biol. Chem.* **1997**, *378*, 309.

² (a) de La Rose, R.; Clague, M. J.; Butler, A. *J. Am. Chem. Soc.* **1992**, *114*, 760. (b) Clague, M. J.; Keder, N. L.; Butler, A. *Inorg. Chem.* **1993**, *32*, 4754. (c) Colpas, G. J.; Hamstra, B. J.; Kampf, J. W.; Pecoraro, V. L. *J. Am. Chem. Soc.* **1996**, *118*, 3469. (d) Conte, V.; Bortolini, O.; Carraro, M.; Moro, S. *J. Inorg. Biochem.* **2000**, *80*, 41. (e) Nica, S.; Pohlmann, A.; Plass, W. *Eur. J. Inorg. Chem.* **2005**, 2032. (f) Schneider, C. J. Penner-Hahn, J. E.; Pecoraro, V. L. *J. Am. Chem. Soc.* **2008**, *130*, 2712.

³ (a) Smith, T. S.; Pecoraro, V. L. *Inorg. Chem.* **2002**, *41*, 6754. (b) Santoni, G.; Licini, G.; Rehder, D. *Chem. Eur. J.* **2003**, *9*, 4700. (c) Rehder, D.; Santoni, G.; Licini, G.; Shulzke, C.; Meier, B. *Coord. Chem. Rev.* **2003**, *237*, 53. (d) Wikete, C.; Wu, P.; Zampella, G.; De Gioia, L.; Licini, G.; Rehder, D. *Inorg. Chem.* **2007**, *46*, 196.

⁴ Vilter, H. *Phytochemistry* **1984**, *23*, 1387.

⁵ (a) Butler, A. *Coord. Chem. Rev.* **1999**, *187*, 17. (b) Butler, A.; Carter, J.; Simpson, M. In *Handbook on Metalloproteins*; Bertini, I., Sigel, A., Sigel, H., Eds.; Marcel Dekker Inc.: New York, Basel, 2001; pp 153-179.

⁶ (a) Andersson, M. A.; Willetts, A.; Allenmark, S. G. *J. Org. Chem.* **1997**, *62*, 8455. (b) Dembitsky, V. M. *Tetrahedron* **2003**, *59*, 4701.

bromoperoxidase catalyzes the oxidation of bromide and iodide, while iodoperoxidase catalyzes the oxidation of only iodide.

Since now VHPOs have been isolated from a number of marine algae and also from some lichens⁷ and fungi⁸.

Halogens are abundant constitutive elements of the biosphere particularly in marine environment. Marine water is approximately 0.5 M in chloride, 1mM in bromide and 1 μ M in iodide. Consequently, it is not surprising that marine organisms have developed means to incorporate halogens into their metabolites. Many of these natural halogenated compounds are involved in biological functions, such as chemical defence or as regulatory hormones. In many cases these compounds are also of pharmacological interest due to their biological activities, including antifungal, antineoplastic, antiviral, antiinflammatory.⁹

A wide range of marine natural organohalogens is generated thanks to these enzymes: starting from volatile halohydrocarbons, such as bromoform, dibromomethane, methyl iodide, bromo- and chloroanisoles,¹⁰ and including also phenolic derivatives such as aeroplysinin-1, an antimicrobial metabolite from sponges (see Figure 1, a),¹¹ or 14-debromoprearaplysinin, from the marine sponge *Druinella purpurea* (Figure 1, b),¹² both of them probably originating from tyrosine.

Numerous chiral chlorinated and brominated terpenoids have also been isolated, including solenoide E (Figure 1, d),¹³ an antiinflammatory and antiviral diterpene, isolated from a gorgonian. Other brominated and chlorinated indoles are also known, e.g. 5-bromo-*N,N*-dimethyltryptamine (Figure 1, c)¹⁴ from a marine sponge.

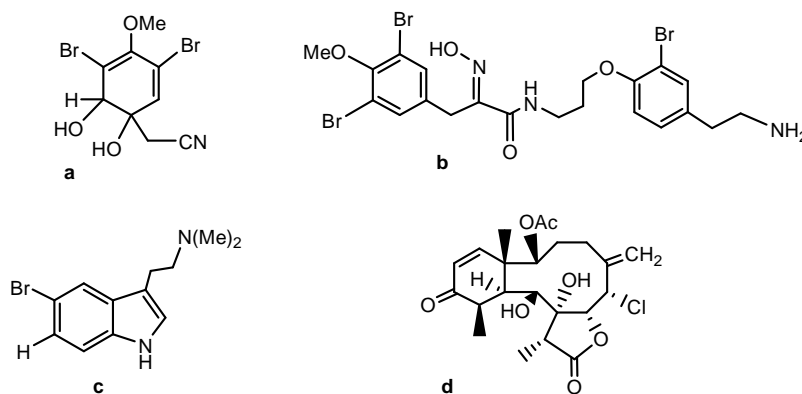


Figure 1. Examples of halogen containing, marine, natural products with important biological activities

⁷ Plat, H.; Krenn, E.; Wever, R., *Biochemical Journal* **1987**, 248, 277.

⁸ van Schijndel, J. W. P. M.; Vollenbroek, E. G. M.; Wever, R. *Biochimica et Biophysica Acta* **1993**, 1161, 249.

⁹ (a) Neidleman, S. L.; Geigert, J. L.; Biohalogenation; Ellis Horwood Ltd. Press: New York, 1986. (b) Butler, A.; Walker, J. V. *Chem. Rev.* 1993, 93, 1937.

¹⁰ (a) McConnell, O. J.; Fenical, W. *Tetrahedron Lett.* **1977**, 48, 4159. (b) Gschwend, P. M.; MacFarlane, J. K.; Newman, K. A. *Science* **1985**, 227, 1033.

¹¹ Nieder, M.; Hager, L. *J Natl. Prod.* **1990**, 53, 757.

¹² James, M.D.; Kunze, H.B.; Faulkner, D.J. *J. Natl. Prod.* **1991**, 54, 1137.

¹³ Groweiss, A.; Look, S.; Fenical, W. *J. Org. Chem.* **1988**, 53, 2401.

¹⁴ Djura, P.; Stierle, D.B.; Faulkner, D.J.; Arnold, E.; Clardy, J. *J. Org. Chem.* **1980**, 45, 1435.

VHPOs are particularly stable enzymes: they are capable of withstanding temperatures up to 70°C and remain completely functional in the presence of several organic solvents. Moreover they are not susceptible toward oxidative inactivation.

VHPOs are composed of one or more subunits of around 60-70 KDa and have only one bounded vanadium atom for each subunit. Determination of the crystal structure of this enzyme revealed a molecule with an overall cylindrical shape measuring about 80 × 50 Å. The secondary structure is mainly α -helical with two four-helix bundles as main structural motifs (Figure 2).

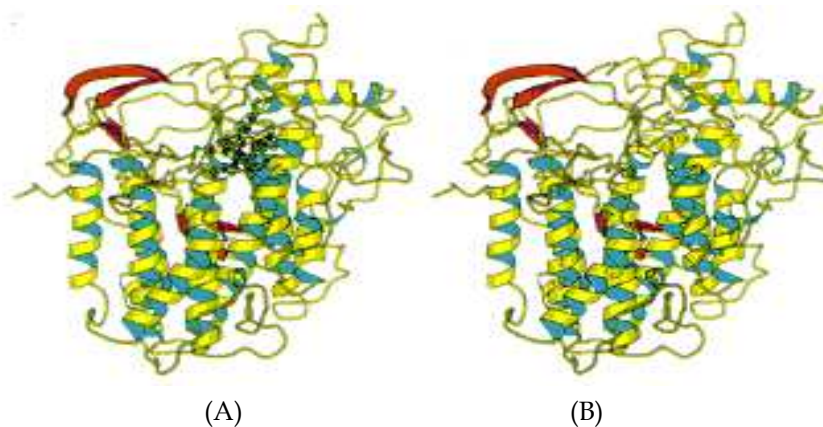


Figure 2. Ribbon-type representation of the CPO molecule.^{1a} (A) Molecule plus vanadium binding site. (B) Molecule without metal site

The active site of the enzyme is located on top of the second four-helix bundle and one channel allows the entrance of hydrogen peroxide, X⁻ and a possible organic substrate.^{1,15,16} In one side the channel is composed of hydrophobic residues, while the other side is mainly hydrophilic.¹ Insights into structural features of the inorganic cofactor and its environment were obtained by X-ray diffraction of the VCPO from pathogenic fungus *Curvularia inaequalis*.¹ In the native state the vanadium ion is characterized by a trigonal bipyramidal geometry, where three oxygen atoms belong to the equatorial plane and one oxygen occupies an axial position. The other apical ligand is His496, which links the metal ion to the protein, whereas Lys353, Arg360, His404, and Arg490 are involved in hydrogen bonds with the oxygen atoms of the cofactor (Figure 3).

¹⁵ Almeida, M.; Filipe, S.; Humanes, M.; Maia, M. F.; Melo, R.; Severino, N.; Da Silva, J. A. L.; Frausto da Silva, J. J. R.; Wever, R. *Phytochemistry* **2001**, 57, 633.

¹⁶ Tschirret-Guth, R.A.; Butler, A. *J. Am. Chem. Soc.* **1994**, 116, 411.

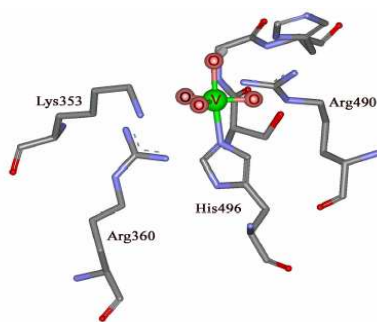


Figure 3. Structure of the active site of the vanadium haloperoxidase from *Curvularia inaequalis*

In the peroxo derivative of the enzyme, the peroxide is bound side-on to the vanadium centre in a η^2 -fashion and the cofactor is characterized by a strongly distorted tetragonal pyramidal geometry, with two oxygen atom type and one peroxo atom in the equatorial plane, while His496 and the other peroxo atom occupy axial positions (Figure 4).

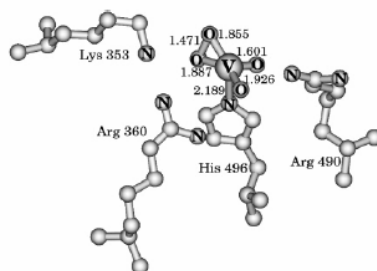


Figure 4. Structure of the peroxo form of the active site of the vanadium haloperoxidase from *Curvularia inaequalis*

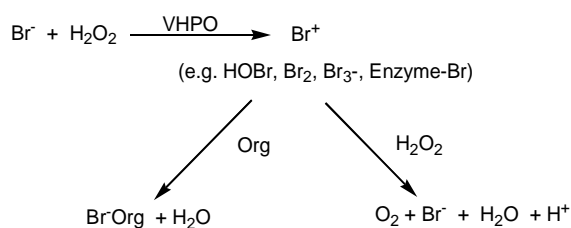
The VHPOs require one equivalent of vanadium for activity.¹⁷ The vanadium centre does not appear to undergo redox cycling during turnover and is proposed to function as a Lewis acid: the role of the metal is to serve as a strong Lewis acid in the activation of the primary oxidant hydrogen peroxide.

VHPOs catalyze peroxidative halogenation reactions and the halide-assisted disproportionation of hydrogen peroxide.¹⁸ In the first step, the enzyme catalyzes the oxidation of halides by hydrogen peroxide, producing an intermediate which is a two-electron-oxidized X^+ halogen species; for bromide hypobromous acid, bromine, tribromide, or an enzyme-bound "bromonium ion equivalent," are all consistent with the *in vitro* reactivity of the enzyme.

In the second step, the oxidized intermediate can halogenate appropriate organic substrates or react, in the absence of a suitable organic substrate, with another equivalent of hydrogen peroxide, forming dioxygen and consequently acting as catalase, as depicted in Scheme 2 for bromide.

¹⁷ de Boer, E.; van Kooyk, Y.; Tromp, M.; Wever, R. *Biochim. Biophys. Acta* **1986**, 869, 48.

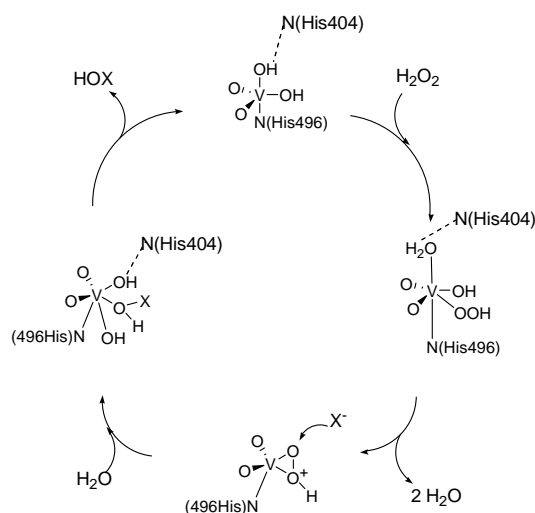
¹⁸ Everett, R. R.; Butler, A. *Inorg Chem.* **1989**, 28, 393.



Scheme 2. Summary of the general reactivity of VHPOs with bromide

A general consensus currently exists for the mechanism for VHPOs, which is a “ping-pong” mechanism: hydrogen peroxide coordinates to the vanadium centre, forming the peroxovanadate active specie. The rate-determining step in the catalytic cycle is the nucleophilic attack of the halide on the protonated protein-peroxide complex, generating a X^+ species, which immediately reacts with the organic substrates and halogenates them. This step will generate singlet oxygen in the absence of RHI, and has been investigated in detail with Cl⁻, Br⁻, I⁻.

The apical hydroxyl group of the enzyme is hydrogen bonded to a histidine residue (His404) in a protein environment. This hydrogen bond makes the OH group more nucleophilic. When a peroxide molecule approaches the active site, the OH unit is protonated and HOO⁻ is generated. The weakly ligated water molecule dissociates from vanadium ion and a side-on bound peroxide intermediate is formed after the departure of another water molecule. Subsequently attack of a chloride ion at a peroxo oxygen and the uptake of a proton from a surrounding water molecule leads to the generation of hypochlorous acid (HOCl) and restoration of the native state (Scheme 3).



Scheme 3. Proposed catalytic mechanism of VHPOs

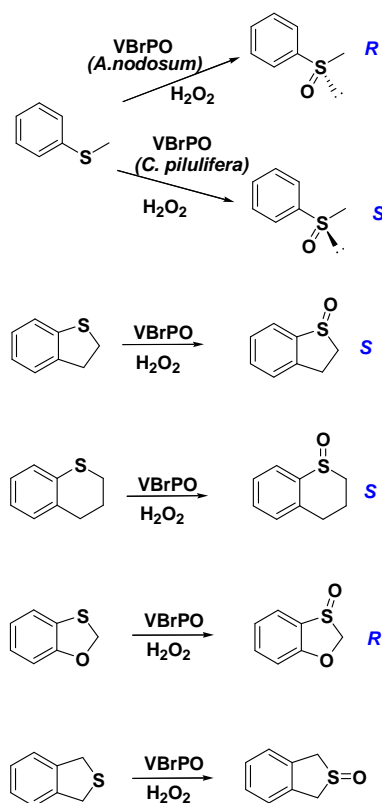
According to the literature, the oxygen transfer involves the attack of the substrate on the deprotonate peroxo oxygen: before the nucleophilic attack of the substrate the peroxo moiety is protonated to hydroperoxo and Lys353 seems to polarize the peroxidic bond.¹ Besides, the oxidation reaction towards halides increases in velocity adding acids and the spectroscopic data are consistent with the protonation of one or more sites of the peroxidic species.

2.1.1 Reactivity and selectivity of sulfoxidations catalyzed by VHPOs

Every nucleophilic organic compound, which can gain access to the VHPOs active site and which have a oxidation potential lower than the reduction potential of hydrogen peroxide, could be oxidized theoretically. The formation of the mono-hydroperoxo complex, that is the protonation of one peroxy-oxygen of the active specie, is particularly important for the enzymatic reactivity. The positive charge in fact creates the right site for a nucleophilic attack of a substrate which will be oxidized.

VHPOs are able to catalyze stereoselective sulfoxidations.^{19,20} Depending on the substrate, up to 91% e.e. could be achieved. Moreover, different enzymes may produce opposite enantiomers, starting from the same substrate. As a example, the enzymes obtained respectively from *Ascophillum nodosum* and from *Corallina pilulifera* activate the hydrogen peroxide in the oxidation of thioanisole, affording the corresponding sulfoxide with high yields and selectivities, exceeding 95% enantiomeric excess of (*R*)-enantiomer for the first enzyme, and 55% e.e. of (*S*)-enantiomer, for the second one (Scheme 4).²⁰ Instead the chloroperoxidase doesn't oxidize in an enantioselective manner, yielding the racemic sulfide.

VBrPO, extracted from the marine algae *Corallina officinalis*, resulted a particularly efficient catalyst in the oxidation of cyclic sulfides (Scheme 4).

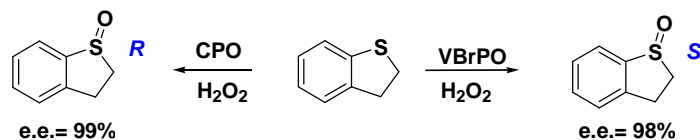


Scheme 4

¹⁹ (a) Andersson, M. A.; Willetts, A.; Allenmark, S. G. *J. Org. Chem.* **1997**, *62*, 8455. (b) Dembitsky, V. M. *Tetrahedron* **2003**, *59*, 4701.

²⁰ ten Brink, H.B.; Schoemaker, H.E.; Wever, R. *Eur. J. Biochem.* **2001**, *268*, 132.

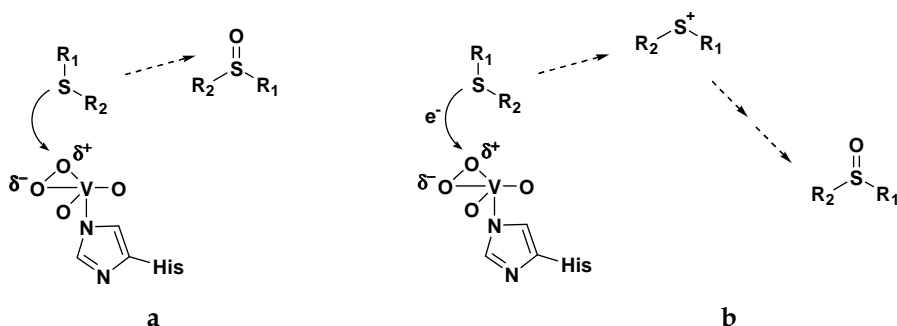
Complementary stereoselective sulfoxidation by means of different haloperoxidases can be reached using a heme-containing chloroperoxidase from marine fungus *Caldariomyces fumago*, and VBrPO from *Corallina officinalis*: using hydrogen peroxide as the oxygen source the enzymes catalyze the oxidation of 2,3-dihydrobenzothiophene with excellent and opposite enantioselectivity, as shown in Scheme 5.²⁰



Scheme 5

The enzymatic mechanism of oxidation seems to be the same of the one operating in the halogenation: a two-electrons transfer mechanism.²¹

With VBrPO from *A. nodosum* there is the direct transfer of oxygen from the vanadium bound peroxide to the sulfide, in a selective manner, strongly suggesting that the aromatic sulfide binds in the active site near the activate oxygen with relatively low affinity (a, Scheme 6). For CPO the sulfide is oxidized by a one-electron transfer step by the peroxo-intermediate of the enzyme, forming a positively charged sulphur radical, which migrates from the enzyme and is subsequently converted to the product via subsequent chemical steps (b, Scheme 6).



Scheme 6. Schematic models for the sulfoxidation mechanism of the VBrPO from *A. nodosum* (a) and CPO from *C. fumago* (b).

2.1.2 Functional and structural models of VHPOs

A variety of vanadium compounds have been studied as functional models for V-haloperoxidases to get a better understanding of the working mechanism of the vanadium haloperoxidase enzyme and the role of vanadium and then to utilize them as efficient catalyst in oxidation reactions.²² These complexes are reactive, towards the oxidation of sulfides and halides, in analogy with the VHPOs.²³

²¹ Ligtenbarg, A. G. J.; Hage, R.; Feringa, B. L. *Coord. Chem. Rev.* **2003**, 89.

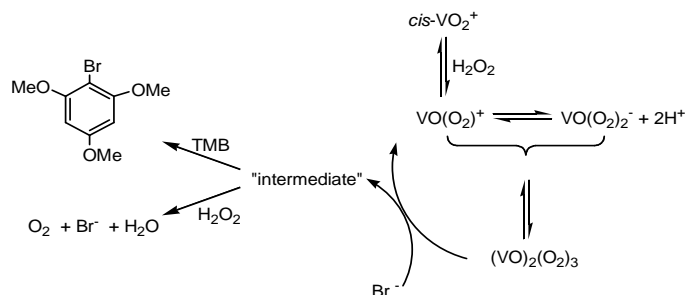
²² Butler, A. in: Reedijk, J.; Bouwman, E. (Eds.) *Bioinorganic Catalysis*, 2nd ed (Chapter 5), Marcel Dekker, New York, 1999,

²³ Bolm, C. *Coord. Chem. Rev.* **2003**, 245.

The role of the ligands in the VHPs models is crucial: in fact in the absence of ligands, which stabilize the monomeric complex, vanadium establishes a series of oligomeric and protonating equilibria, depending on his concentration and on the acidic conditions.

The first reported functional mimic of VBrPO is *cis*-dioxovanadium(V) [VO_2^+] in acidic aqueous solution.^{2a} *Cis*-dioxovanadium(V) is shown to catalyse the bromination of 1,3,5-trimethoxybenzene (TMB) as well as the bromide-mediated disproportionation of hydrogen peroxide (Scheme 7). In a first step, hydrogen peroxide gives red oxoperoxo [$\text{VO}(\text{O}_2)^+$] and yellow oxodiperoxo [$\text{VO}(\text{O}_2)_2^-$] complexes. The ratio between the two species depends on the hydrogen peroxide concentration and pH. In a second step these species combine, yielding dioxotriperoxodivanadium(V) [$(\text{VO})_2(\text{O}_2)_3$], which is considered to be the actual oxidant. Contrary to natural haloperoxidases, it functions only at low pH (2 or less), because at lower acid concentrations the amount of monoperoxovanadate is insufficient for dimerisation to occur to the actual oxidant.

Another difference with the enzyme is the low rate of catalysis indicating the importance of the protein environment around the active site.



The identification of the dimeric specie as the active one is due to kinetic measurements: the halide oxidation depends on metal complex according to a second order law. The maximum velocity is observed at low pH and at a concentration of hydrogen peroxide in which the $[(\text{VO})_2(\text{O}_2)_3]$ concentration is at his highest value, that is when the concentrations of $[\text{VO}(\text{O}_2)^+]$ and $[\text{VO}(\text{O}_2)_2^-]$ are equal.

Consequently, if simple ions are already able to catalyze the same oxidation reactions of the natural enzyme, multidentate ligands will be able to modulate reactivity and selectivity of the metal complexes.

In recent years several vanadium complexes of multidentate ligands containing O and N donor sites were tested for catalysis in oxidation reactions.

Ligands that yield active functional model systems for VBrPO include Schiff base ligands derived from salicylideneamino acid, such as *N*-(2-hydroxyphenyl)salicyl imine or *N*-(2-carboxyphenyl)salicyl imine. When the vanadium(V) peroxo adduct becomes too much stabilized by the donating properties of the ligand, as for instance observed for pyridine-2,6-dicarboxylic acid (H_2 -dipic), oxidation of bromide is not observed.

Due to the harsh reaction environment (low pH, H_2O_2), in some cases the complexes are not stable under turnover conditions: for example the corresponding vanadium(V)

compounds of carboxyphenylsalicylideneamine (CPS)VO(OEt)(EtOH) (Figure 5) dissociate from the metal ion in the presence of acid and hydrogen peroxide.

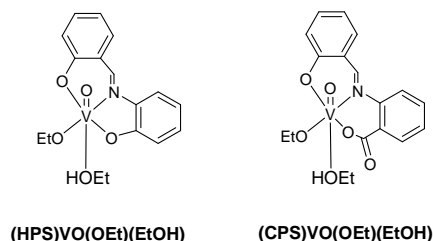


Figure 5. Mononuclear complexes (HPS)VO(OEt)(EtOH) and (CPS)VO(OEt)(EtOH) derived from ligands *N*-(2-hydroxyphenyl)salicylideneamine and *N*-(2-carboxyphenyl)salicylideneamine respectively.

A VBrPO mimic that has been well studied is the oxovanadium(V) complex of hydroxyphenyl-salicylideneamine (HPS)VO(OEt)(EtOH) (Figure 5). The complex in solution forms different species in rapid equilibrium and one of them is the active species (HPS)VO(OH). Upon addition of H₂O₂ a single oxoperoxovanadium(V) complex (HPS)VO(O₂)⁻ is formed. Subsequently addition of bromide affords one turnover towards a two-electron oxidised form (e.g. HOBr, Br₂, Br₃⁻, or V-OBr), which, in presence of trimethoxybenzene, yields one equivalent of the brominated product 2-bromo-1,3,5-trimethoxy-benzene (BrTMB).

The structural models known to date mimic the oxygen-rich coordination environment of the metal and the binding of histidine, in the presence of oxo groups, phenolate and alkoxides moieties and one nitrogen donor unit. Different ligands have been employed to obtain monomeric V(V) complexes and they have been tested in the activation of hydrogen peroxide (Figure 6).^{2,3}

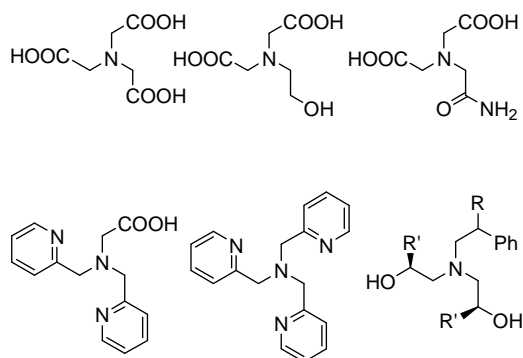
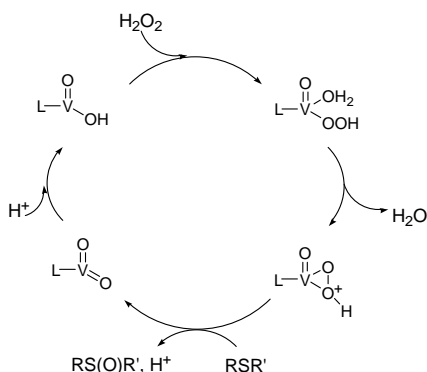


Figure 6. Ligands whose V(V) complexes have been tested for catalysis of bromide or sulfide oxidation.

For each ligand the monomeric complex is obtained using a 1:1 ratio vanadium precursor/ligand. Addition of hydrogen peroxide affords a new monomeric metal peroxidic species, effective in halide oxidations and sulfoxidations.

The nucleophile sulfide attacks the electrophilic oxygen of the peroxy moiety, with the subsequent heterolytic break of the O-O bond (Scheme 8). Consequently, the peroxy complex is an electrophilic oxidant.



Scheme 8. Mechanism of sulfoxidations catalyzed by V(V) mono-peroxy-complexes with a tetradentate ligand.

2.2 V(V)amine tri-phenolate complexes: synthesis and structural study

Concerning vanadium chemistry with amine tri-phenolate ligands, only one study has been reported, showing V(V)oxo complexes formation via reaction between the ligand precursor and VO(Oi-Pr)₃.²⁴ The family of tetradentate amine tri-phenolate ligands strongly binds to the metal and enables “fine tuning” of the complex structure, seeming to provide a “natural environment” for vanadium. We could obtain similar complexes (**1d-f**) and we tested their ability to catalyze the oxidation of sulfides and halides with hydrogen peroxide.²⁵

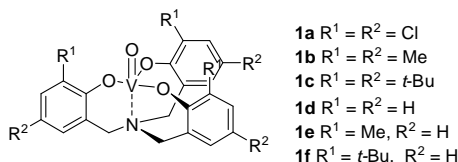


Figure 7. C₃-symmetric V(V) amine triphenolate complexes.

Reaction of tris-phenolamines²⁶ with VO(Oi-Pr)₃ in dry THF under nitrogen yielded complexes **1d-f** as deep red crystalline solids in high yields (92-94%). The observed complexation behaviour is in complete accordance with the structurally similar complexes **1a-c** described in literature, which contain additional *para* substituents on the phenolic moiety.²⁴

Complexes **1e** and **1f** (R¹= Me and *t*-Bu, respectively) show highly symmetric ¹H NMR spectra, in agreement with the formation of single C₃-symmetric, mononuclear species, with a single ⁵¹V NMR signal (-381.9 ppm and -389.1 ppm, CDCl₃, respectively), whereas complex

²⁴ Groysman, S.; Goldberg, I.; Goldschmidt, Z.; Kol, M. *Inorg. Chem.* **2005**, *44*, 5073.

²⁵ Mba, M.; Pontini, M.; Lovat, S.; Zonta, C.; Bernardinelli, G.; Kündig, E. P.; Licini, G. *Inorg. Chem.* **2008**, *47*, 8616.

²⁶ Prins, L. J.; Mba, M.; Kolarović, A.; Licini, G. *Tetrahedron Lett.* **2006**, *47*, 2735.

1d shows a complicate, non-symmetric ^1H NMR spectrum and two different signals in ^{51}V NMR (-396.8 and -428.8 ppm, CDCl_3) indicative of the presence of aggregates or a mixture of species in solution (Table 1).

Table 1. ^{51}V NMR Chemical shift values (ppm) for **1d-f** complexes, in CDCl_3 as solvent.

Complex	δ (ppm) in CDCl_3
$\text{VO}(\text{O}i\text{-Pr})_3$	-625.8
1d	-396.83 , -428.78
1e	-381.90
1f	-389.07

For example, the ^1H NMR spectra of the oxovanadatrane complex **1f** and the corresponding ligand show the maintenance of the high symmetry of the ligand into the complex. The enantiomeric benzylic protons of the ligand become diastereotopic in the complex, resulting as two broad singlets (Figure 8).

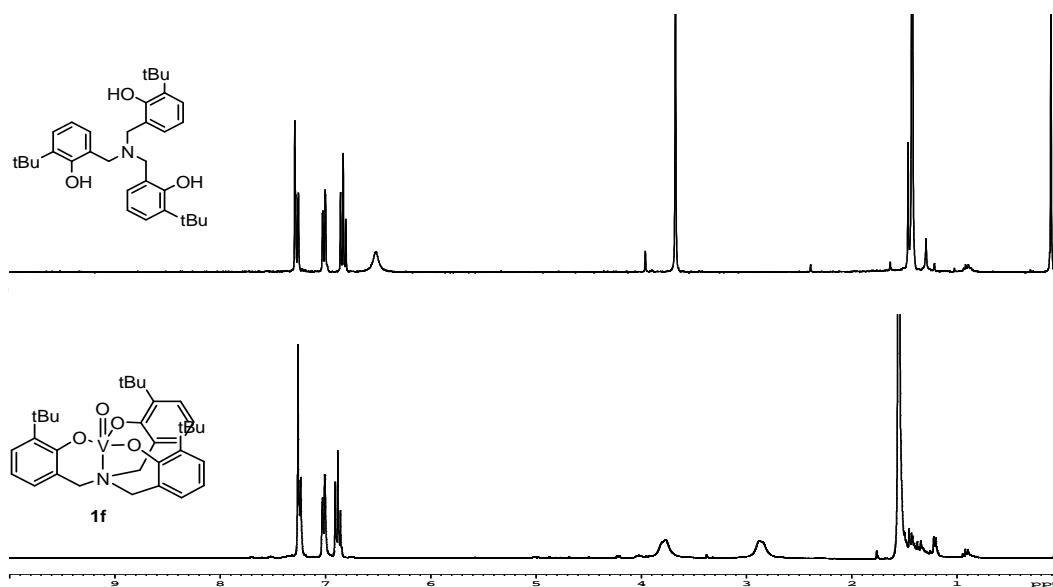


Figure 8. ^1H NMR spectra (300 MHz, CDCl_3) respectively of **1f** ($\text{R}^1 = t\text{-Bu}$) and its corresponding free ligand.

At lower temperatures these methylene signals consistently resolve in a clear AB system, due to the slowing down of the racemization process between the to propeller-like chiral enantiomers (Δ - Λ) (Figure 9 and Figure 10).

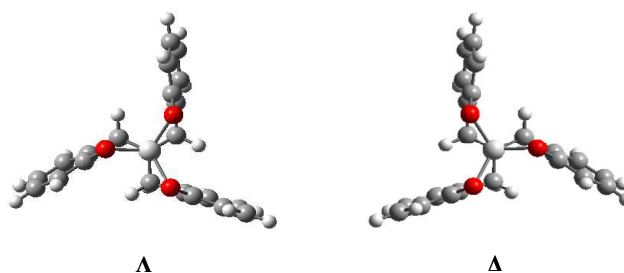


Figure 9. Clockwise (Δ) and counter-clockwise (Λ) enantiomeric conformations of amine tri-phenolate complexes.

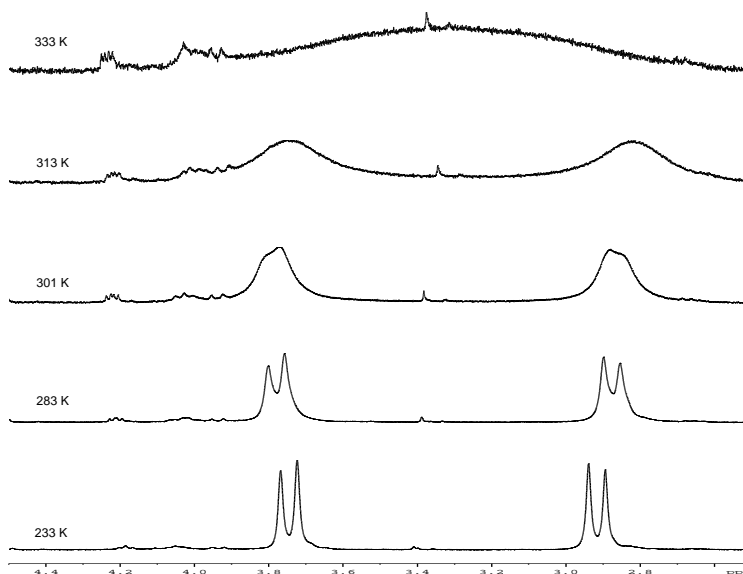


Figure 10. VT NMR experiment of **1f** in CDCl_3 (233- 333 K).

The X-ray structure of complex **1f**, crystallized from dichloromethane/hexane, is consistent with what we observe in solution, by NMR spectroscopy, and it is structurally analogous to the reported X-ray structures of complexes **1a-c**.

The solid-state structure reveals a monomeric pentacoordinate complex, which adopts a trigonal bipyramidal geometry (TBP), with the oxo function occupying the axial position, *trans* to the central nitrogen. The V centre is positioned slightly above the phenolate oxygens plane, pointing towards the oxo function. The V-N bond is weak, being effected by the *trans* effect of a strong π -donor oxo ligand (Figure 11).¹

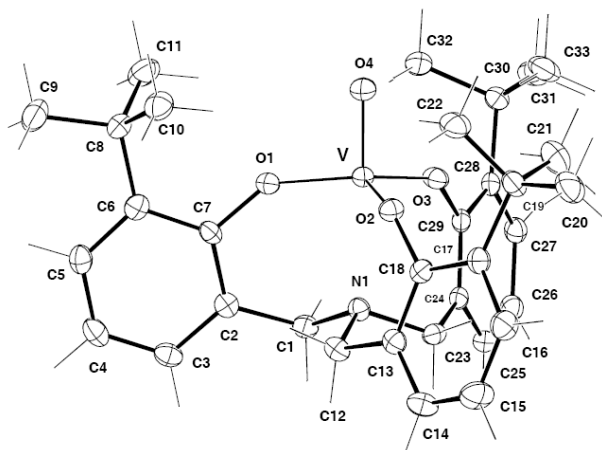


Figure 11. X-ray structure of **1f**, recorded at 150 K.

Table 2. Selected bond lengths (Å) and angles (degrees) for crystal structure of **1f**, with reference to atom labelling reported in Figure 10. See experimental part for details on crystal data and structure refinement.

Bond Lengths, Å			
V-O1	1.809(1)		
V-O2	1.807(1)		
V-O3	1.807(1)		
V-O4	1.604(1)		
V-N1	2.416(2)		

Angles, degrees			
O1-V-O2	122.50(6)	O1-V-O3	117.42(6)
O1-V-O4	97.75(6)	O1-V-N1	81.36(6)
O2-V-O3	114.18(6)	O2-V-O4	97.68(7)
O2-V-N1	81.16(6)	O3-V-O4	98.98(7)
O3-V-N1	83.22(6)	O4-V-N1	177.79(6)

The coordination environment of vanadium in these structures mimicks, to a large extent, the coordination environment of the metal centre in vanadate-dependent HPOs. In fact both structures have a trigonal bipyramidal geometry and in both cases the ligand set around the metal is [O₄N], with the amine (imine in the enzyme) ligand occupying an axial position. In the amine triphenolate complexes the oxo function occupies the second axial position, whereas in the active site of the enzyme this position is occupied by a hydroxo or an aqua ligand.

2.3 V(V)amine tri-phenolate complexes: catalytic activity

The use of multidentate amine triphenolate ligands for complexation of the metal affords a great advantage due to the high stability of the metal complexes, which allows low catalyst concentrations without the loss of catalyst integrity. Second, a nearly occupation of all coordination sites of the metal by a single ligand reduces the chances of formation of multimeric and often undefined metal-species under catalytic conditions.

In this contest the reactivity of complexes **1d-f** as functional models of VHPOs was examined in the sulfides and halides oxidation.

2.3.1 Oxidation of sulfides to the corresponding sulfoxides

Although the oxidation of sulfides by vanadium complexes is not new,^{27,28,29,30} the exact mechanism by which it is accomplished is still a subject of study.

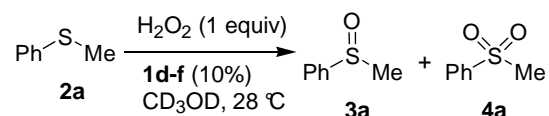
The active species in the process is a V(V) complex associated with and/or generated by hydrogen peroxide or an organic hydroperoxide. There are two possible mechanisms of sulfide oxidation, an electrophilic route^{26a} and a radical one.^{25d} The first one is more prevalent and proceeds via nucleophilic attack by sulfide on a coordinated peroxide.^{31,32}

To study the catalytic activity of **1d-f** in sulfoxidation reactions, we used hydrogen peroxide as terminal oxidant.

The use of hydrogen peroxide is highly advantageous, since it is non-toxic, inexpensive and yields water as the only side product.

To work under homogeneous conditions and follow the reaction course via ¹H-NMR, sulfide oxidations were performed in methanol-*d*₄ using a 10% catalyst loading and a 1:1 ratio of thioanisole **2a** and H₂O₂ (35% in water) (Table 3).

Table 3. Oxidation of **2a** by aqueous H₂O₂ (35%) catalyzed by **1d-f**.^a



Entry	Catalyst	Time(min) ^b	Yields (%) ^c	3a:4a ^c
1	1d	720	7	>99:1
2	1e	10	89	99:1
3	1f	10	99	99:1
4	--	720	3	>99:1

^aReaction conditions: [**2a**]₀=[H₂O₂]₀=0.09 M, 10% catalyst CD₃OD, 28 °C. ^bTime required for complete oxidant consumption. ^cDetermined on the oxidant by ¹H NMR (CD₃OD, 300 MHz), DCE as internal standard, and quantitative GC analysis on the crude reaction mixture after complete oxidant consumption (iodometric test).

²⁷ (a) Nakajima, K.; Kojima, M.; Fujita, J. *Chem. Lett.* **1986**, 1483. (b) Nakajima, K.; Kojima, M.; Toriumi, K.; Saito, K.; Fujita, J. *Bull. Chem. Soc. Jpn.* **1989**, 62, 760. (c) Nakajima, K.; Kojima, K.; Kojima, M.; Fujita, J. *Bull. Chem. Soc. Jpn.* **1990**, 63, 2620. (d) Ballistreri, F.P.; Tomaselli, G.A.; Toscano, R.M.; Conte, V.; Di Furia, F. *J. Am. Chem. Soc.* **1991**, 113, 6209. (e) Vetter, A.H.; Berkessel, A. *Tetrahedron Lett.* **1998**, 39, 1741.

²⁸ (a) Bortolini, O.; Di Furia, F.; Modena, G. *J. Mol. Catal.* **1982**, 16, 61. (b) Di Furia, F.; Modena, G.; Seraglia, R. *Synthesis* **1984**, 325.

²⁹ Bolm, C.; Bienewald, F. *Angew. Chem. Int. Ed. Engl.* **1995**, 34, 2640.

³⁰ Drago, C.; Caggiano, L.; Jackson, R.F.W. *Angew. Chem. Int. Ed.* **2005**, 44, 7221.

³¹ Butler, A.; Clague, M.J.; Meister, G.E. *Chem. Rev.* **1994**, 94, 625.

³² (a) Di Furia, F.; Modena, G. *Rev Chem. Intermed.* **1985**, 6, 51. (b) Di Furia, F.; Modena, G. *Pure Appl. Chem.* **1982**, 54, 1853.

We were pleased to find that, in the presence of the mononuclear complexes **1e-f**, sulfide **2a** was oxidized to the corresponding sulfoxide **3a** in high yields, with almost complete sulfoxide/sulfone selectivity and in very short reaction times (10 min) (Table 3, entries 1 and 2). In contrast, complex **1d** (R¹=H) gave very low conversions and only after extended reaction times (7%, 12 h). While the reaction performed without V(V) catalyst afforded even lower conversions.

Because complex **1f** revealed to be the most active and efficient catalyst and, in addition, does not require to be handled under inert atmosphere, our studies were continued testing only the catalytic performances of complex **1f**.

Substrate/Catalyst Ratio. Catalyst loading is an aspect of major importance for catalytic systems, since it determines the cost of the process. Results reported in Table 4 show the effect of increasing the substrate/catalyst ratio on the oxidation of thioanisole **2a** with hydrogen peroxide.

Using V(V)-amino triphenolate complex **1f** as catalyst, 10:1 and 100:1 and 1000:1 ratios were used. Substrate concentrations were varied from 0.1 to 1 M (Table 4, entries 1-2, catalyst loading 1% and 0.1%, respectively). Fast reactions with high yields were obtained in all cases. Catalyst concentration was further decreased (0.001 M- 0.0001 M), using a constant substrate concentration ([**2a**]₀ = 1.0 M) (Table 4, entries 2-4).

Table 4. Oxidation of thioanisole **2a** by aqueous H₂O₂ (35%) catalyzed by **1f**. Effect of concentration and catalyst loading.^a

#	[2a] ₀ (M)	1f (%)	<i>t</i> _{1/2} (min) ^b	yields (%) ^c	3a:4a ^c	time (min) ^d	TON	TOF (h ⁻¹) ^e
1	0.1	1	6	97	96:4	25	97	240
2	1.0	0.1	24	98	98:2	80	980	1330
3	1.0 ^f	0.1	6	98	97:3	20	980	8000
4	1.0	0.01	265	97	97:3	850	9700	1790
5	1.0 ^f	0.01	110	99	98:2	255	9900	2667

^aReactions conditions: **2a**:H₂O₂ =1:1, 28 °C, CD₃OD,. ^bTime for 50% decrease of [H₂O₂]₀..

^cDetermined on the oxidant by ¹H NMR (CD₃OD, 300 MHz) in the presence of DCE as internal standard and quantitative GC analysis on the crude reaction mixture after total oxidant consumption (iodometric test). ^dTime required for total oxidant consumption.

^eDetermined at 20% conv.. ^fReactions performed with H₂O₂ (70%).

In particular, using 0.1% catalyst and 70% aqueous H₂O₂ comparable yields and reaction times of the reaction performed with 1% catalyst could be achieved with remarkable TOF (8000 h⁻¹) (Table 2, entry 3).

The catalyst loading was then further decreased to 0.01% without affecting the efficiency of system but simply slowing down the reactions (Table 2, entries 4-5). Also in this case the use of more concentrated H₂O₂ increases the system performances: the reaction is complete in less than 5 hours, with 9900 TON and still significative TOF (2667 h⁻¹).

The system reported here is more efficient than the vanadium-dependent bromoperoxidases, which present TONs of 450-520 in 20 hours.⁶ Moreover, to the best of our knowledge, the **1f**/H₂O₂ system seems to be the most active VHPOs model so far reported, as far as TONs (9900 in 4 h) and TOFs (up to 8000) are concerned.^{3a}

Scope of the reaction. The general scope of the V(V)-based catalytic system has been examined. A series of alkyl aryl, and dialkyl sulfides was oxidized and optimized conditions were used: [**2a-g**]₀=[H₂O₂]₀=0.5 M, 0.1% of catalyst, working on a preparative scale (8 mmol).

Table 5. Oxidation of sulfides **2a-g** by aqueous hydrogen peroxide (35%) catalyzed by **1f** (0.1%).^a

$$\begin{array}{c}
 \text{R}^1\text{-S-R}^2 \\
 \mathbf{2a-g}
 \end{array}
 \xrightarrow[\text{CH}_3\text{OH, 28 }^\circ\text{C}]{\text{H}_2\text{O}_2 \text{ (1 equiv)}}
 \begin{array}{c}
 \text{O} \\
 \parallel \\
 \text{R}^1\text{-S-R}^2 \\
 \mathbf{3a-g}
 \end{array}
 +
 \begin{array}{c}
 \text{O} \quad \text{O} \\
 \diagdown \quad / \\
 \text{R}^1\text{-S-R}^2 \\
 \mathbf{4a-g}
 \end{array}$$

Entry	Sub.	R ¹	R ²	Yields (%) ^b	3:4	Time (min) ^c
1	2a	Ph	Me	98 (98)	99:1	120
2	2b	<i>p</i> -Tol	Me	>99 (99)	99:1	120
3	2c	<i>p</i> -Tol	<i>n</i> -Bu	96 (94)	> 99:1	120
4	2d	Ph	Bn	>99 (99)	> 99:1	90
5	2e	<i>n</i> -Bu	<i>n</i> -Bu	99 (91)	> 99:1	60
6	2f	<i>p</i> -MeO-C ₆ H ₄	Me	98 (94)	> 99:1	100
7	2g	<i>p</i> -NO ₂ -C ₆ H ₄	Me	98 (70)	97:3	240

^aReaction conditions: [**2a-g**]₀:[H₂O₂]₀=0.5M, **1f** 0.1%, 28 °C, MeOH ^bDetermined by quantitative GC analysis on the crude reaction mixture after total oxidant consumption (iodometric test). Isolated yields are given in brackets. ^cTime required for total oxidant consumption.

In analogy with what observed previously for **2a**, in all cases the oxidation with H₂O₂ afforded the corresponding sulfoxides in short reaction times (1-4 h), quantitative yields, also in isolated products, and very high selectivity for the sulfoxide formation. Dialkyl sulfides were oxidized faster than the corresponding aryl alkyl ones (Table 5, entries 4 and 5), being methyl-*p*-nitrophenyl sulfide **2g** the less reactive substrate (Table 5, entry 7).

All these results are consistent with the occurrence of an electrophilic oxygen transfer process and prove the generality and applicability of the method also on preparative scale.

Investigation of the Active Species. The solution behaviour of **1f** under turn over conditions has been explored via ⁵¹V NMR spectroscopy. A CD₃OD solution of **1f** (Figure 12, spectrum 1) showed a singlet at δ = -396.2 ppm. The stepwise addition of up to 3 equivalent of hydrogen peroxide afforded a new species (δ = -649.3 ppm, Figure 12, spectra 2-5) in the range expected for diperoxovanadium complexes^{3a,33} associated with colour change of the solution from red to light yellow. The addition of an excess of sulfide **2a** gave complete

³³ (a) Conte, V.; Di Furia, F.; Moro, S. *J. Mol. Catal. A* **1997**, *11*, 93. (b) Slebonick, C.; Pecoraro, V. L. *Inorg. Chimica Acta* **1998**, *283*, 37.

oxidation to the sulfoxide **3a**, restoring of catalyst **1f** ($\delta = -400.6$ ppm, Figure 12, spectrum 6) and solution turned blue. The upfield chemical shift and the change of colour originate from the presence of sulfoxide **3a**, as proved by independent addition of **3a** to the original catalyst solution. A similar behaviour could be detected in the ^1H NMR spectra: *t*-Bu protons signal moved from 1.52 to 1.31 ppm to go back to 1.52 ppm after **2a** oxidation (Figure 13).

Consequently the catalyst is stable under oxidative reaction conditions, allowing the recycle of the catalyst and high turn over numbers.

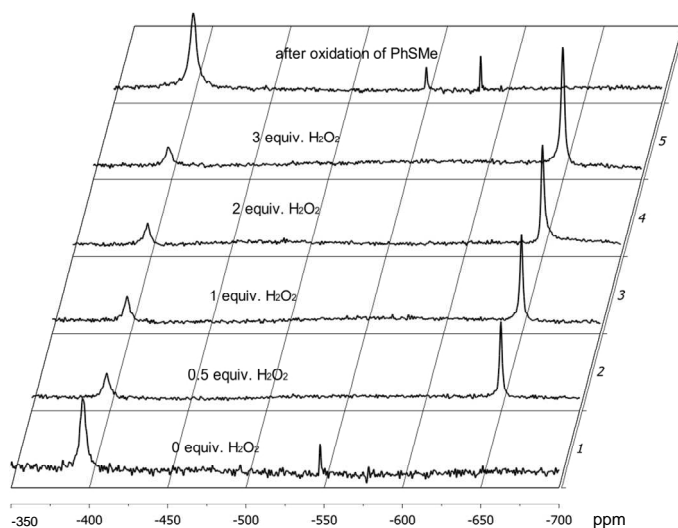


Figure 12. ^{51}V NMR (300 MHz, CD_3OD) of complex **1f**. Effect of the addition of 35% hydrogen peroxide (spectra 1-5). Spectra after addition of thioanisole and consumption of the oxidant (iodometric test) (spectrum 6).

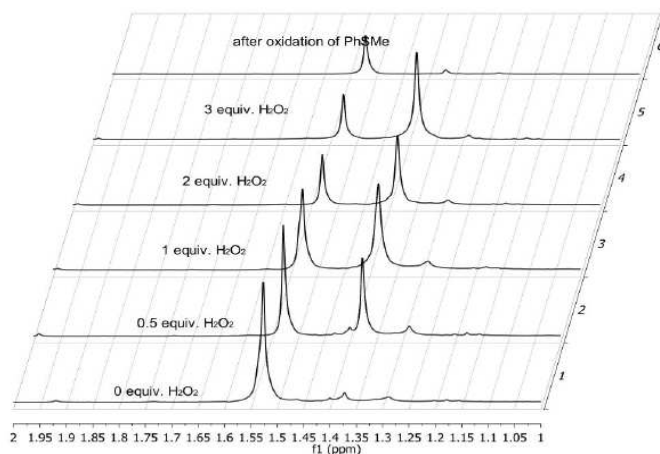


Figure 13. ^1H NMR (300 MHz, CD_3OD) of complex **1f** in the region from 2.0 to 1.0 ppm. Effect of the addition of 35% hydrogen peroxide (spectra 2-5) and subsequent thioanisole **2a** (3 equiv) addition (spectrum 6).

2.3.2 Oxidation of halides

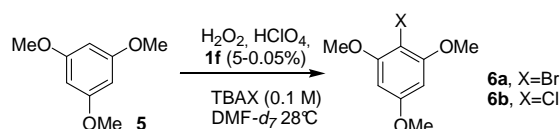
The activity of complex **1f** was tested also in halides oxidation. Reactions were performed with tetrabutylammonium bromide (TBAB) and tetrabutylammonium chloride (TBAC) as halogen sources in presence of 1,3,5-trimethoxybenzene **5** as substrate for halogenation.^{2a,b}

Under the reaction conditions described by Butler *et al.*^{2a,b} ($[1f]_0 = 1$ mM, $[H_2O_2]_0 = 8$ mM, $[TBAB]_0 = 100$ mM, $[5]_0 = 20$ mM, $[HClO_4]_0 = 3$ mM in *N,N*-dimethylformamide, DMF) the bromination proceeds almost instantaneously to the mono brominated product **6a**. Yields slightly exceed 100%, based on the limiting reagent that, in this case, is the acid, (Table 6, entry 1). Working in absence of acid afforded only 2.5% of **6a**, consistently with the expected stoichiometry of the reaction that requires also one equivalent of acid (Table 6, entry 2).^{2a,b}

Increasing both H_2O_2 and acid up to a $5:H_2O_2:HClO_4=1:1:1$ ratio gave **6a** in 87% yield, which could be further increased up to 92% working in the presence of a 2-fold excess of H_2O_2 (Table 6, entries 3 and 4).

In order to test the catalyticity of the system, the catalyst amount was decreased to 0.5% and 0.05%: **6a** was obtained in high yields (87%) with TON=173 in the first case (Table 6, entry 7) and 63% yield with a TON up to 1260 in the second one (Table 6, entry 8).

Table 6. **6a** or **6b** formation as a function of $[H^+]$, $[H_2O_2]$, and V catalysts (**1f** or $VO(acac)_2$).^a



#	X	1f (%)	$[H_2O_2]_0$ (mM)	$[H^+]_0$ (mM)	$[6a,b]$ (mM)	$t_{1/2}^b$ (min)	Yield ^c (%)	TON
1	Br	5	8	3	3.3	< 5	110	3.3
2	Br	5	40	-	0.5	--		0.5
3	Br	5	20	20	17.3	17	87	17
4	Br	5	40	20	18.4	6	92	18
5	Br ^d	5	40	20	10.7	250	54	11
6	Br	--	20	20	2.2	--	11 ^e	--
7	Br	0.5	20	20	17.3	33	87	173
8	Br	0.05	20	20	12.6	1440	63	1260
9	Br ^d	0.05	20	20	6.0	>5000	30	600
10	Cl	5	8	3	1.2	--	40 ^e	1.2
11	Cl	5	40	20	1.1	--	5 ^e	1.1

^a Reaction conditions: $DMF-d_7$, 28 °C using $[5]_0=20$ mM, $[TBAX]_0=0.1$ M, X=Br or Cl. ^bTime for a 50% decrease of $[H_2O_2]_0$. ^cBased on the limiting agent $HClO_4$ and determined by 1H NMR (DCE as internal standard) on the crude reaction mixture after total oxidant consumption (iodometric test). ^d $VO(acac)_2$ has been used as catalyst. ^eAfter 2 days.

In order to prove catalyst **1f** stability under turnover conditions analogous reactions were performed with $VO(acac)_2$ (5% and 0.05%): in both cases slower reaction and lower conversions into products were obtained (54% *vs* 92% using 5% of catalyst and 30% *vs* 63% using 0.05%, Table 6 entries 4, 5, 8 and 9). Reaction performed without catalyst afforded **6a** in low yields (11%) after much longer reaction time (Table 6, entry 6).

Reactions were also carried out in presence of Cl^- ions. Slow chlorination of **5** could be achieved (**1f**=5%) obtaining **6b** in 40% yields after 2 days (Table 4, entry 10). Increasing acid and oxidant to a $5:H_2O_2:HClO_4=1:2:1$ ratio (Table 6, entry 11) did not increase the system

performances: similar substrate conversions were obtained (1.1 mM) indicating that the system cannot perform more than one catalytic cycle. Cl⁻ oxidation can be observed in these reaction conditions because of the partial protonation of the active vanadium peroxo complex even in the presence of a large excess of chloride ions.^{3c}

2.4 Conclusions

In the present work the V(V)-catalytic oxidation of sulfides and halides using hydrogen peroxide as primary oxidant has been described and investigated in detail. Mononuclear C₃-symmetric V(V) amine triphenolate complex **1f** is particularly stable and proved to be highly efficient catalyst for these oxidations and it can be defined as a structural and also a functional model for VHPOs.

The complex adopts a trigonal bipyramidal geometry (TBP) and the coordination environment of vanadium is characterized by an oxo group, phenolate moieties and one nitrogen donor unit.

Sufoxidations proceed in high yields, without oxidant decomposition, with catalyst loading down to 0.015, TONs up to 9900 and TOFs up to 8000 h⁻¹: the system **1f**/H₂O₂ reported here seems to be the most active VHPOs model so far reported, as far as TONs (9900 in 4 h) and TOFs (up to 8000) are concerned. Moreover, bromide oxidation can be performed efficiently, leading to the halogenation of **5** and confirming that this complex can emulate the reactivity of VHPOs.

2.5 Experimental

General remarks

All chemicals and dry solvent have been purchased from Aldrich or Fluka and used as provided, without further purifications. 70 % aqueous hydrogen peroxide was purchased from Ausimont. 70 % aqueous HClO₄ was purchased from Erba. Triphenolamines were synthesized as previously reported.³⁴

Flash chromatographies have been performed with Macherey-Nagel silica gel 60 (0.04-0.063 mm, 230-400 mesh). The NMR spectra have been recorded on a Bruker AC 250 (¹H: 250.13 MHz; ¹³C: 62.9 MHz) or a Bruker AV 300 (¹H: 300.13 MHz; ¹³C: 75.5 MHz) spectrometer. Chemical shift (δ) have been reported in parts per million (ppm) relative to the residual undeuterated solvent as an internal reference (CDCl₃: 7.26 ppm for ¹H NMR and 77.0 ppm for ¹³C NMR; CD₃OD: 4.84 ppm for ¹H NMR and 49.05 ppm for ¹³C NMR). The following abbreviations have been used to explain the multiplicities: s = singlet, d = doublet, t = triplet, dd = double doublet, m = multiplet, br = broad. ¹³C NMR spectra have been recorded with complete proton decoupling. ⁵¹V NMR spectra have been recorded at 301K with 10000 scans at 78.28 MHz with a broadband probe, using VO(O₂) picolinate (5 · 10⁻³ M, water, pH = 1) as external standard. Analytical gas chromatography analysis has been carried out on a Shimadzu GC-2010 gas chromatograph with a FID detector and a capillary column EQUITY™-5 using decane as internal standard. Injector temperature has been 250

³⁴ For the synthetic procedure of the ligands and their characterizations see Prins, L. J.; Mba, M.; Kolarović, A.; Licini, G. *Tetrahedron Letters* **2006**, *47*, 2735.

°C, detector temperature has been 280 °C and the carrier gas has been He (1 mL/min) with a HP-5MS column. APCI-MS spectra have been obtained on a LC/MS Agilent series 1100 spectrometer in positive mode, by direct flow injection using methanol as mobile phase, with ESI-ion trap mass detector. High-resolution mass spectra have been obtained with ESI-TOF Mariner™ Biospectrometry™ Workstation of Applied Biosystem by flow injection analysis; exact mass measurements have been obtained by external calibration with two appropriate lock mass compounds.

IR spectra have been recorded on a Nicolet 5700 FT-IR, with range 4000-400 cm⁻¹ and resolution 4 cm⁻¹, using KBr pellets.

Melting points are uncorrected and have been determined with a Leitz-Laboroux 12.

All oxygen or moisture sensitive compounds have been handled under controlled atmosphere (nitrogen) in a glovebox Mbraun MB 200MOD, equipped with a MB 150 G-I recycling system. V(V) complexes were always prepared, handled and stored in glovebox, with exception of complex **1f** which could be handled in open air.

General procedure for preparation of oxovanadatrane complexes

Complexes **1d-f** were prepared in glovebox by slowly addition of a solution of VO(Oi-Pr)₃ (0.615 mmol) in dry THF (1 mL) to a solution of the corresponding ligand³² (0.610 mmol) in dry THF (5 mL). An immediate change in colour of the solution was observed (from colourless to dark-red). The solution was stirred for 1 hr at rt and then the solvent was evaporated under vacuum leading to a dark-red solid, which was repeatedly washed with small volumes of hexane and dried in vacuum. Yield: 92- 94%.

VO/tris-(2-hydroxy-benzyl) amine (**1d**)

¹H-NMR (300 MHz, CDCl₃): δ 3.61 (12H, *bs*), 7.08-6.80 (12H, *m*), 7.47-7.08 (13H, *m*), 7.82 (1H, *d*, *J* = 8.4 Hz). ⁵¹V-NMR (78.28 MHz, CDCl₃): δ -396.83, -428.78. IR (KBr, cm⁻¹): 754, 960, 1072, 1119, 1265, 1457, 1726, 2957.

VO/ tris-(2-hydroxy-3-methylbenzyl) amine (**1e**)

¹H-NMR (300 MHz, CDCl₃): δ 2.45 (9H, *s*), 2.90 (3H, *bs*), 3.77 (3H, *bs*), 6.97 (3H, *d*, *J* = 7.1 Hz), 7.10 (3H, *d*, *J* = 7.1 Hz). ¹³C-NMR (50 MHz, CDCl₃): δ 16.8 (CH₃), 57.62 (CH₂), 123.4 (CH), 124.8 (C), 125.7 (CH), 127.6 (CH), 129.7 (CH), 167.2 (C). ⁵¹V-NMR (78.28 MHz, CDCl₃): δ -381.9, (78.28 MHz, CD₃OD): δ -387.9. IR (KBr, cm⁻¹): 776, 890, 960, 1079, 1231, 1461, 2923, 3058. Anal. Calcd. for C₂₄H₂₄NO₄V: C 65.39, H 5.48, N 3.17. Found: C 65.02, H 5.52, N 3.08.

VO/tris-(2-hydroxy-3-tert-butylbenzyl) amine (**1f**)

¹H-NMR (300 MHz, CDCl₃): δ 1.53 (27H, *s*), 2.87 (3H, *bs*), 3.77 (3H, *bs*), 6.89 (3H, *t*, *J* = 7.5 Hz), 7.03 (3H, *d*, *J* = 7.3 Hz), 7.24 (3H, *d*, *J* = 7.3 Hz). ¹³C-NMR (50 MHz, CDCl₃): δ 29.9 (CH₃), 35.3 (C), 57.6 (CH₂), 123.3 (CH), 125.7 (CH), 126.8 (C), 128.1 (CH), 136.5 (C), 143.9 (C). ⁵¹V-NMR (78.28 MHz, CDCl₃): δ -389.07, (78.28 MHz, CD₃OD): δ -396.2. IR (KBr, cm⁻¹): 752, 891, 945, 1080, 1188, 1236, 1426, 2952, 3081. APCI-MS: 568.25 [M + H]⁺, calc. 568.26. Anal. Calcd. for C₃₃H₄₂NO₄V: C 69.83, H 7.46, N 2.47. Found: C 69.38, H 7.51, N 2.35.

X-ray crystallographic data collection and structure refinement for 1f

In order to obtain crystals suitable of crystallographic analysis, in a screw capped vial 30 mg of **1f** were dissolved in 2.0 mL of dichloromethane and 5.0 mL of hexane were layered on the top of the solution. After standing for a week, dark red crystals of **1f** were collected.

Crystallographic parameters are given in Table 7.

Table 7. Crystallographic experimental details for **1f**.

Empirical Formula	C ₃₃ H ₄₂ NO ₄ V
Formula Weight	567.7 g/mol
Crystal System	Triclinic
Space Group	P $\bar{1}$
Unit Cell Dimensions: lengths, Å	$a = 8.8248(6)$, $b = 9.8319(7)$, $c = 17.6222(12)$
angles, deg	$\alpha = 93.345(8)$, $\beta = 90.242(8)$, $\gamma = 92.825(8)^\circ$.
Volume, Å ³	1524.5(18)
Z	2
Density d_x , g·cm ⁻³	1.237
Absorption Coefficient μ , mm ⁻¹	0.360
Crystal Size, mm ³	0.128 x 0.205 x 0.234
Temperature	150 K
Scanning mode	ϕ -scan
Mo _{Kα} radiation: λ (Å)	0.71073
ϕ min, max	0- 300.3 (°)
Index Ranges	-10 < h < 10 ; -12 < k < 12 ; -21 < l < 21
Angular range	4.3° < 2θ < 51.2°
Reflections Measured at 150 K	16203
Unique reflections	5554 (R _{int} = 0.039)
Reflections with $ F_o > 3\sigma(F_o)$	3997
Refinement Method	Full-matrix least-squares based on F using weights of $1/[\sigma^2(F_o) + 0.00015(F_o^2)]$
Resolution	Direct methods (SIR97)
Minimized function	$\Sigma (\omega (F_o - F_c)^2)$
Function of weight	$\omega = 1/[\sigma^2(F_o) + 0.00015(F_o^2)]$
Goodness-of-fit (S)	1.30 (1)
Final R Indices [$I > 2\sigma(I)$]	R = 0.034, $\omega R = 0.032$
Largest Diff. Peaks and Holes, eÅ ⁻³	0.88 and -0.63

General procedure for monitoring thioanisole 2a oxidation catalyzed by 1d-f using aqueous H₂O₂ as oxidant (Table 3).

A screw-cap NMR tube was charged with a solution of complex **1d-f** (0.0054 mmol) in CDCl₃, solvent was removed under vacuum and then CD₃OD, the internal standard (1,2-dichloroethane, DCE), 35% aqueous H₂O₂ (0.0540 mmol) and thioanisole (0.0540 mmol) were added, to a final volume of 0.6 mL. Concentrations of sulfide **2a**, sulfoxide **3a** and sulfone **4a** were determined by integration of the methyl group signals: Ph-S-Me (2.4 ppm), Ph-SO-Me (2.8 ppm) and Ph-SO₂-Me (3.1 ppm) in respect of the internal standard, DCE (3.78 ppm).

General procedure for monitoring thioanisole 2a oxidation catalyzed by 1f using aqueous H₂O₂ as oxidant (Table 4).

A screw-cap NMR tube was charged with a solution of the complex **1f** in CDCl₃, solvent was removed under vacuum and then CD₃OD followed by the internal standard (1,2-dichloroethane), aqueous H₂O₂ (35% or 70% in water as indicated in Table 4) and thioanisole **2a** were added to a final volume of 0.6 mL, with final concentrations as reported in Table 4. The monitoring of the concentration of sulfide, sulfoxide and sulfone was made by integration of the methyl group signals: Ph-S-Me (2.4 ppm), Ph-SO-Me (2.8 ppm) and Ph-SO₂-Me (3.1 ppm). Final yields were determined by ¹H-NMR after complete H₂O₂ consumption (iodometric test) in respect of the internal standard DCE (3.78 ppm).

General procedure for sulfoxidation reactions catalyzed by 1f using aqueous H₂O₂ as oxidant (Table 5).

To a solution of the corresponding thioethers **2a-g** (0.8 mmol) and catalyst **1f** (0.008 mmol) in MeOH, was added 35% aqueous H₂O₂ (0.8 mmol), to a final volume of 1.6 mL. The reaction mixture was stirred at rt until all oxidant consumption (iodometric test). The reaction mixture was washed with 5% sodium metabisulfite aqueous solution, the layers were separated and the aqueous one extracted with chloroform. The organic layers were washed with brine, dried over MgSO₄ and the solvent was removed under reduced pressure. The crude was purified by column chromatography on silica gel (petroleum ether/ ethyl acetate 1:1) obtaining the products with isolated yields reported on Table 5. Ratios sulfoxide:sulfone were determined by quantitative GC analysis and by ¹H NMR (CDCl₃, 300 MHz). Yields were determined by quantitative GC analysis. The sulfoxides **3a-g** and sulfones **4a-g** ¹H NMR spectra match those already reported in the literature.³⁵

Procedure for the monitoring of the effect of the addition of 35% hydrogen peroxide to complex 1f.

A screw cap NMR tube was charged with a solution of complex **1f** (0.003 mmol) in CDCl₃. The solvent was removed under vacuum and then CD₃OD (0.5 mL) was added. Increasing amount of 35% aqueous H₂O₂ were added corresponding to 0.5, 1, 2 or 3 equivalents as indicated in Figure 11 and 12, recording the corresponding ¹H- and ⁵¹V-NMR. After 3 equivalents of thioanisole were added and after total oxidant consumption (iodometric test), ¹H- and ⁵¹V-NMR spectra were recorded.

General procedure for monitoring the bromination and chlorination reactions catalyzed by 1f using aqueous H₂O₂ as oxidant (Table 6)

A screw-cap NMR tube was charged with a solution of the complex **1f** in DMF-*d*₇ (0.0006 mmol), 1,3,5-trimethoxybenzene (0.012 mmol), TBABr or TBACl (0.06 mmol) and DCE as internal standard. An appropriate volume of 35% aqueous H₂O₂ and 70% aqueous HClO₄

³⁵ (a) Brunel, J.M.; Diter, P.; Duetsch, M.; Kagan, H. B. *J Org. Chem.* **1995**, *60*, 8086. (b) Rebiere, F.; Samuel, O.; Ricard, L.; Kagan, H. B. *J. Org. Chem.* **1991**, *56*, 5991. (c) Pitchen, P.; Dunach, E.; Dshmuikh, M. N.; Kagan, H. B. *J Am. Chem. Soc.* **1984**, *106*, 8188.

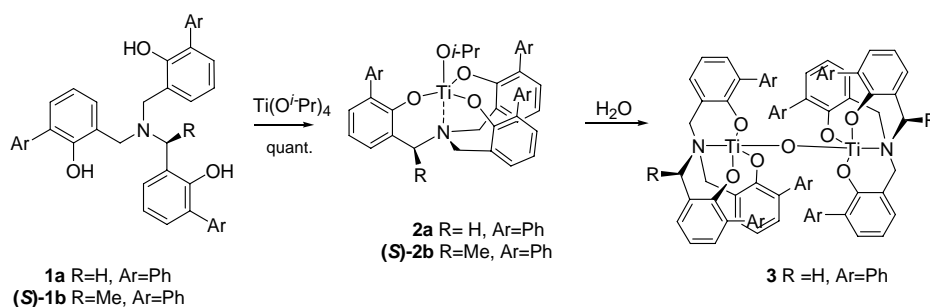
were added, as reported in Table 6, to a final volume of 0.6 mL. reactions were performed at rt and monitored via $^1\text{H-NMR}$ (concentrations of TMB and halogenated product were detected by integration of the aromatic CH: **5** (6.11 ppm), BrTMB **6a** (6.38 ppm) and ClTMB **6b** (6.40 ppm). Final yields were determined by $^1\text{H-NMR}$ after complete H_2O_2 consumption (iodometric test) in respect of the internal standard DCE (3.78 ppm). Mono halogenation of the substrate has been confirmed via $^1\text{H-NMR}$ and GC-MS analysis that match those already reported in the literature.³⁶

³⁶ For compound **6a**: de La Rosa, R; Claque, M.J.; Butler, A. *J. Am. Chem. Soc.* **1992**, *114*, 760. Mondal, M.; Vedavati, G. Puranik, V.G.; Argade, N. P. *J. Org. Chem.* **2006**, *71*, 4992.

For compound **6b**: Masao, H.; Shigetaka, Y.; Hirohuki, M.; Takashi, M. *Can. J. Chem.* **1997**, *75*, 1905.

Chapter 3

Stereoselective self-assembly of C₃-titanatranes



The mononuclear Ti(IV) amine triphenolate complex **2a**, obtained by reaction of *tris*-(2-hydroxy-3-phenylbenzyl)amine **1a** with Ti(O^{*i*}-Pr)₄ and bearing phenyl *ortho*-substituents, have been found to afford quantitatively and spontaneously the corresponding μ-oxo dinuclear complex only as a heterochiral S₆-symmetric diastereoisomer **3**. On the other hand an analogous chiral, enantiopure complex (*S*)-**2b** maintains its mononuclear structure even in the presence of a water excess. Thus, a new efficient method for the synthesis of *ortho*-aryl functionalized *tris*-phenolamines **1** has been developed using Suzuki coupling reaction as the main strategic step: the introduction of new functionalities in the *meta* position of the peripheral phenyls permits, after complexation with Ti(O^{*i*}-Pr)₄, to obtain dinuclear μ-oxo complexes, which possess anchoring sites ready to be exploited for the construction of stable and spatially ordered structures.

Part of this Chapter has been published:

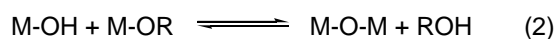
Bernardinelli, G.; Seidel, T. M.; Kündig, E. P.; Prins, L.J.; Kolarovic, A.; Mba, M.; Pontini, M.; Licini, G. *Dalton Trans.* **2007**, 1573.

3.1 Introduction

Early transition metals of tripodal trianionic ligands of type $[X_3N]^{3-}$ have been drawing particular attention: while $[N_3N]^{3-}$ triamido-amine ligands afford well-defined mononuclear complexes,^{1,2} the less shielded $[O_3N]^{3-}$ trialkoxo-amine ligands often suffer from complicating formation of polynuclear species.³

The hydrolysis of metal alkoxides is a ubiquitous reaction of tripodal titanium complexes and forms the basis for the sol-gel route of metal oxide synthesis.

In general, the hydrolytic process is believed to involve the initial hydrolysis of the metal alkoxide to form an intermediate metal hydroxide (Scheme 1, eqn. 1) which subsequently condenses with further metal alkoxide or hydroxide to built up μ -oxo bridges (Scheme 2, eqn. 2).⁴ While discrete well-defined metal hydroxides complexes are not common, a number have been studied with the respect to their formation by hydrolysis of metal alkoxides. In all cases thus far described, the hydrolysis equilibrium of eqn. (1) is either thermoneutral or favourable.^{5,6}



Scheme 1

Very few reports of sol-gel processes involve the use of titanium(IV) aryloxides, even though such molecular complexes are widely used as catalysts in organic chemistry or as building blocks in supramolecular chemistry.^{7,8,9}

For titanium(IV) based alkoxides, hydrolytic self-assembly is generally an uncontrolled pathway.¹⁰ Using modular and polydentate ligands this process can be tuned, also by taking advantage of the chelate effect.

3.1.1 Ti(IV) amine triphenolate complexes

Earlier reports on Ti(IV) tripodal amine triphenolate complexes, based on NMR data and supported by X-ray crystallography, evidenced the fact that they are present in solution and at the solid state as a racemic mixture of Δ and Λ mononuclear complexes, resulting from a

¹ Schrock, R.R. *Acc. Chem. Res.* **1997**, 30, 9.

² Gade, L. H. *Chem. Commun.* **2000**, 173.

³ Verkade, J.G. *Acc. Chem. Res.* **1993**, 26, 483.

⁴ Lyvage, J.; Henry, M., Sanchez, C. *Prog. Solid State Chem.* **1988**, 18, 4668.

⁵ Bergquist, C.; Storrie, H.; Koutcher, L., Bridgewater, B. M.; Friesner, R.A.; Perkin, G. *J. Am. Chem. Soc.* **2000**, 122, 12651.

⁶ Blanchard, J., In, M.; Schaudel, B.; Sanchez, C. *Eur. J. Inorg. Chem.* **1988**, 8, 1115.

⁷ Gigant, K.; Rammal, K.; Henry, M. *J. Am. Chem. Soc.* **2001**, 123, 11632.

⁸ Rammal, A.; Brisach, F.; Henry, M. *J. Am. Chem. Soc.* **2001**, 123, 5612.

⁹ Senouci, A.; Yaakoub, M.; Huguenard, C.; Henry, M. *J. Mater. Chem.* **2004**, 14, 3215.

¹⁰ Babcock, M.; Klemperer, W.G. *Inorg. Chem.* **1989**, 28, 2003.

helical wrapping of the ligand around the metal ion, with racemization barriers (ΔG^\ddagger) in the range of 65.7- 74.4 KJ mol⁻¹ (Figure 1).^{11,12}

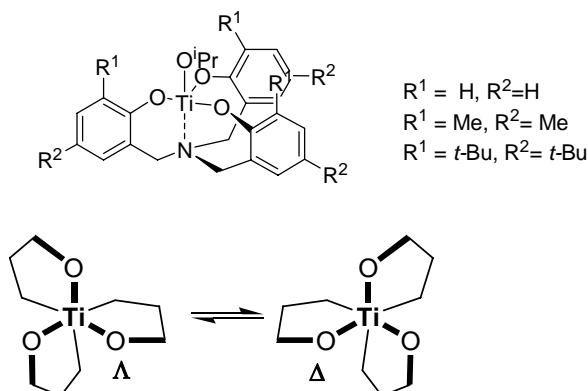


Figure 1

These reports also demonstrated that the stability of Ti(IV) complexes in solution strongly depends on the steric size of the peripheral substituents. Complexes bearing small *ortho* substituents ($R^1 = \text{H}, \text{Me}$) tend to give aggregates like μ -oxo and *bis* μ -oxo complexes in the presence of traces of water.^{9,13} In contrast, mononuclear complexes bearing bulky groups like *t*-butyl are highly stable and resistant to hydrolysis.

The lack of hydrolytic reactivity of complexes bearing bulky substituents is extremely unusual as titanium alkoxide are well known to react violently with water. This process of hydrolysis gives an initial LTiOH species that successively condensates to the corresponding μ -oxo dimer (Scheme 1).⁴

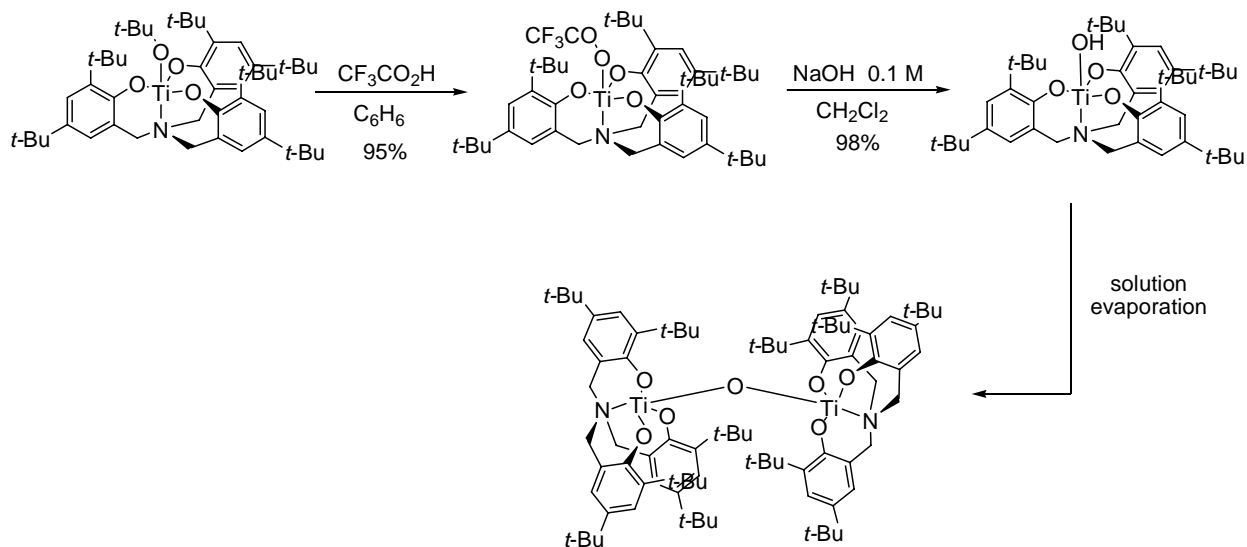
Besides, for the complex bearing *t*-butyl groups neither the apical *iso*-propoxide nor the phenolates oxygen groups form bridges to another metal atom. This implies that the *iso*-propoxide groups are well shielded within a cavity formed by these tripodal ligands, as confirmed by the shorter C(*i*-Pr)-O-Ti bond (1.778 Å) compared to the lengths of the other Ti-O bonds of the phenolate oxygens (1.825- 1.866 Å), which indicates a strong π -interaction and by the slightly distorted trigonal bipyramidal geometry around the titanium with the metal lying above the plane defined by the three oxygen atoms of the phenolate rings.¹¹ Furthermore, the corresponding μ -oxo complex cannot be obtained by direct hydrolysis of the alkoxide, which is moisture stable, but only via evaporation to dryness of a solution of the corresponding Ti(IV)-hydroxy complex, obtained after apical group exchange with a more acidic one and subsequent basic work up (Scheme 2). Ti(IV)-hydroxy complex undergoes condensation to form μ -oxo complex if its solution is evaporated, where the process is driven by the low solubility of the dimeric complex. A bent μ -oxo bridge (155.53°) was determined in the crystal structure and Ti-O_{central} distances of 1.825 Å. Moreover, the μ -

¹¹ Kol, M.; Shamis, M; Goldberg, I.; Goldschmidt, Z.; Alfi, S.; Hayut-Salant, E. *Inorg. Chem. Commun.* **2001**, *4*, 177.

¹² Moberg, C. *Angew. Chem. Int. Ed. Engl.* **1998**, *37*, 248.

¹³ Nielson, A. J.; Shen, C.; Waters, J. M. *Polyhedron* **2006**, 2039.

oxo bridge was not stable and easily cleaved in the presence of traces of water.^{14,15} The stability of the complex towards hydrolysis is of steric origin as the *t*-Bu substituents are forced to close contact in the dimer.

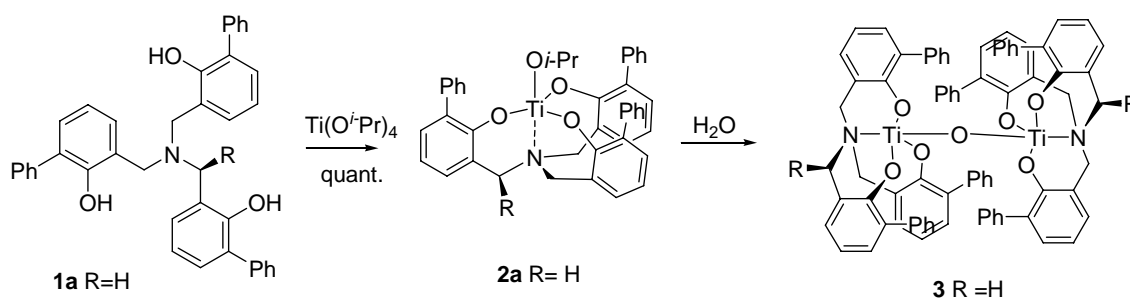


Scheme 2

3.2. Self-assembly of C₃-titanatranes

In this context, a particular behaviour towards hydrolysis has been observed for titanatrane **2a**, obtained from *in situ* complexation of one equivalent of titanium precursor Ti(O^{*i*}-Pr)₄ with *tris*-(2-hydroxy-3-phenylbenzyl)amine ligand **1a** bearing bulky phenyl substituents in *ortho* positions.

Complex **2a** spontaneously forms a highly stable μ -oxo dinuclear complex **3** in the presence of only traces of water, showing the labile nature of the apical *iso*-propoxide ligand in this case (Scheme 3).



Scheme 3

The new compound **3** owns rather different structural characteristics compared to the analogue μ -oxo group discussed before: a linear Ti-O-Ti bond with the peripheral phenyl

¹⁴ Kim, Y.; Verkade, J. G. *Organometallics* **2002**, 21, 2395.

¹⁵ Ugrinova, V.; Ellis, G.A.; Brown, S. N. *Chem. Commun.* **2004**, 468.

groups intercalating and disposed in a propeller like fashion shielding the Ti-O-Ti core and with the two chiral titanatrane groups having opposite configuration (Δ and Λ). More in detail, reaction of **1a** with one equivalent of Ti(O*i*-Pr)₄ in CDCl₃ yields the corresponding mononuclear, C₃ symmetric Ti (IV) complex **2a**. The ¹H NMR spectrum shows a single set of signals and the six methylene protons appear in a single broad singlet at 3.62 ppm. This is in agreement with an average C_{3v} symmetric complex in which the two enantiomeric conformations are in fast interconversion at room temperature. However, upon standing in solution, complex **2a** readily transforms into a new, highly symmetric species and over the time the precipitation of a yellow solid out of the solution, corresponding to the μ -oxo dimer **3**, was observed. The spontaneous formation of the new species is quantitative in a few hours.

Dimer **3** is highly insoluble in most organic solvents, which probably is the driving force of the process, and it is air and moisture tolerant. No reversion to monomeric complexes was observed even in presence of large excess of water.

The ¹H NMR spectra of **3** shows a single set of signals with releasing of *i*-PrOH, originating from the apical iso-propoxy ligand (Figure 2).

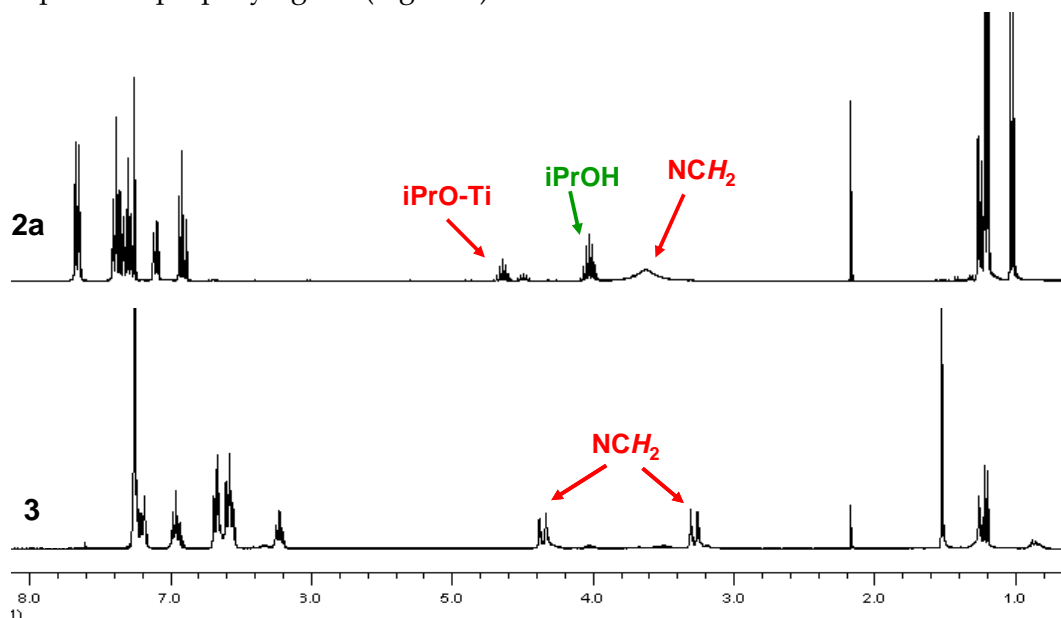


Figure 2. ¹H NMR (300 MHz, CDCl₃) spectra of complex **2a** and the μ -oxo complex **3**

Interestingly, the methylene protons of the new species appear as an AB system with resonances at 4.36 and 3.28 ppm respectively, pointing to a rigid structure and indicating that the racemization rate of the titanatrane moiety in the new species now is much slower. Actually, high temperature VT NMR experiments (300 MHz, toluene-*d*₈) didn't let to any change in the ¹H NMR spectra and no appearance of another diastereomeric species has been detected when heating up to 100 °C: this observation is consistent with the hypothesis that the formation of the μ -oxo dimer has suppressed the racemization process. An additional experiment was performed: a solution of the μ -oxo **3** in toluene was refluxed for 1h, then the ¹H NMR spectra was recorded but no changes were observed, as a prove of the high stability of complex **3**. The fact that even at 100 °C the methylene signals of **3** remain an AB system

indicates that the new complex is much more stable towards racemization than the mononuclear complex **2**. On the other hand, the five protons of the peripheral phenyl rings give only three signals, even at much lower temperature (even at $-90\text{ }^{\circ}\text{C}$), pointing to a dynamic process that renders equivalent the protons. Most likely the six phenyl rings should move at the same time in a process which implies just the oscillation of the ring. (Figure 3).

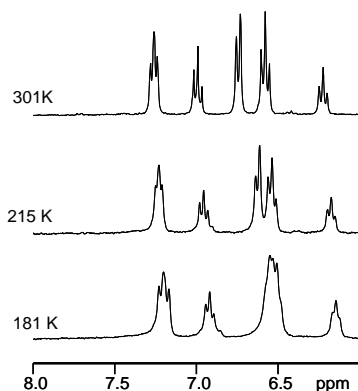


Figure 3

ESI-MS experiments ($1\mu\text{M}$, acetonitrile, HCOOH 0,1%, as mobile phase) confer the dinuclear nature of complex **3** also in solution. Even more not only **3** is stable under ESI experimental conditions but it is the only species detectable in the spectrum. It is present as H^+ ($m/z = 1233$), Na^+ ($m/z = 1255$) and K^+ adduct ($m/z = 1271$). No other species were detected (Figure 4A) and the isotopic distributions were in complete agreement with the calculated ones (Figure 4B).

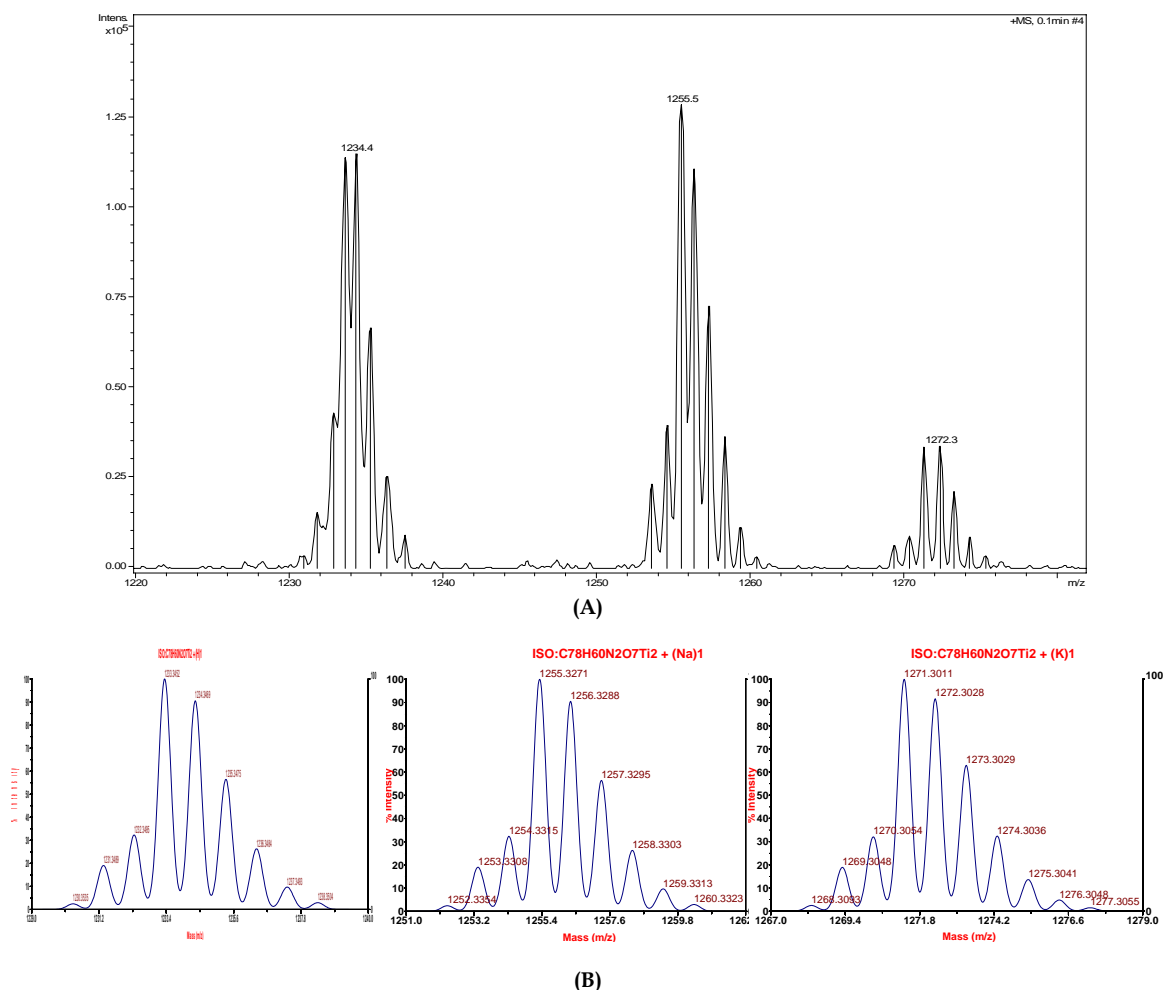


Figure 4. ESI-MS of complex **3**, FIA positive analysis, solution 10⁻⁷M CH₃CN. (A) Zoom in the region from $m/z=1220$ -1280. (B) Calculated isotopic distributions for [M+H]⁺, [M+Na]⁺, and [M+K]⁺.

The synthesis of the complex in a mixture of CHCl₃/C₆H₆ allowed us to obtain crystals suitable for X-ray analysis (Figure 5). The crystal structure of **3** confirms the formation of a dinuclear Ti(IV) complex with a linear μ -oxo bridge linking two titanatranes units of opposite stereochemistry. The μ -oxo bridge is located on a crystallographic centre of inversion leading to a perfectly linear Ti-O-Ti bond angle. This contrasts with the bent bridge found in a corresponding μ -oxo complex with *t*-Butyl as *ortho* and *para* substituents.⁸ The distance Ti-O_{central} (1.7978(7) Å) is in the range observed in other similar complexes^{16,17} but it is shorter than the one found in complexes bearing a bent bridge (1.8251 and 1.8256 Å).⁸ Both titanium atoms show a trigonal bipyramidal geometry with Ti-N bonds of 2.331(3) Å (Table 1).

¹⁶ (a) Olmstead, M. M.; Power, P. P.; Viggiano, M. J. *Am. Chem. Soc.* **1983**, *105*, 2927. (b) Kuhn, N.; Kratz, T.; Blaser, D.; Boese, R. *Inorg. Chim. Acta* **1995**, *238*, 179. (c) Kayal, A.; Ducruet, F.; Lee, S. N. *Inorg. Chem.* **2000**, *39*, 3696. (d) Lam, T. C. H.; Chan, E. Y. Y.; Mak, W.-L.; Lo, S.M.L.; Williams, I. D.; Wong, W.-T.; Leung, W.-H. *Inorg. Chem.* **2003**, *42*, 1842.

¹⁷ (a) Rao, M. L. N.; Houjou, H.; Hiratani, K. *Chem. Commun.* **2002**, 420. (b) Levason, W.; Popham, M. C.; Reid, G.; Webster, M. *Dalton Trans.* **2003**, 291. (c) DiMauro, E. F.; Mamai, A.; Kozłowski, M. C. *Organometallics* **2003**, *22*, 850.

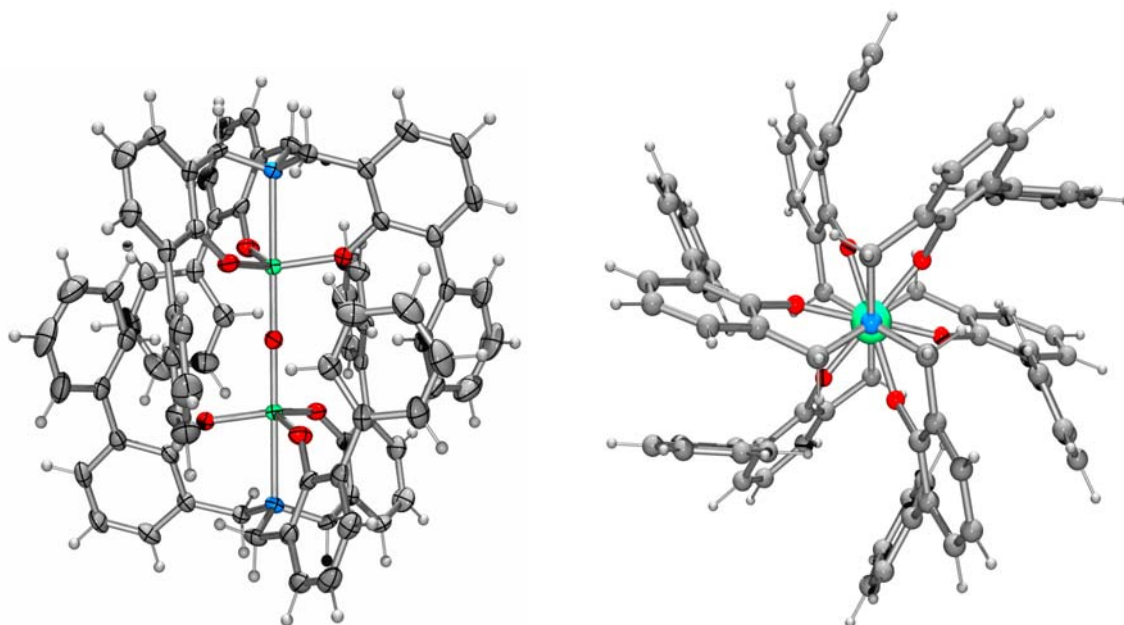


Figure 5. Left: ORTEP view of **3**. Ellipsoids are represented at 40% probability level. The central O atom is located on a centre of inversion. Selected bond distances [\AA] and angle [$^\circ$]: $\text{Ti-O}_{\text{central}} = 1.7978(7)$, $\text{Ti-N} = 2.331(3)$, $\text{Ti-O-Ti} = 180.0$. Disordered solvent molecules are omitted for clarity. Right: View along the N-Ti-O-Ti-N axis.

The peripheral phenyl rings from the two ligands intercalate around the μ -oxo bridge: each internal *ortho* proton points toward the π -cloud of the next ring, belonging to the other titanatrane moiety. The perpendicular distances between H_{ortho} and the centre of the phenyl ring are 2.74 \AA or 2.78 \AA which suggests participation of CH- π interactions in the stabilisation of the complex.¹⁸ This structural characteristic is reflected also in solution since the ^1H NMR spectrum of **3** exhibits significant up field shifts for the signals from the protons of the peripheral phenyls (ca. 1 ppm), especially proton in *ortho*, when compared with the monomeric complex. Interestingly, only three sets of signals are present for the *ortho*, *meta* and *para* protons, with relative intensities in a 2:2:1 ratio, thus indicating fast rotation of the phenyl rings on the NMR time scale (Figure 2).

¹⁸ (a) Nishio, M.; Hirota, M.; Umezawa, Y. *The CH/ π interaction*; Wiley-VCH: New York, **1998**. (b) Tsuzuki, S.; Honda, K.; Uchamaru, T.; Mikami, M.; Fujii, A. *J. Phys. Chem. A* **2006**, *110*, 10163.

Table 1. Selected bond lengths (Å) and angles(degrees) for crystal structures of **3**. See experimental part for details on crystal data and structure refinement.

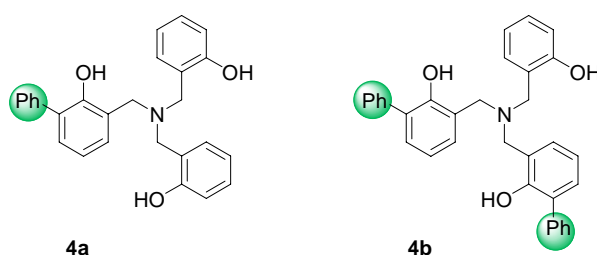
Bond Lengths (Å)			
Ti-O1	1.816(3)		
Ti-O2	1.818(3)		
Ti-O3	1.818(3)		
Ti-O4 _{central}	1.7978(7)		
Ti-N	2.331(3)		

Angles, degrees			
O1-Ti-O2	118.4(2)	O1-Ti-O3	118.5(2)
O1-Ti-O4 _{central}	98.73(9)	O1-Ti-N	81.7(1)
O2-Ti-O3	116.9(2)	O2-Ti-O4 _{central}	98.35(9)
O2-Ti-N	81.6(1)	O3-Ti-O4 _{central}	97.73(8)
O3-Ti-N	81.9(1)	O4 _{central} -Ti-N	179.5(1)

The ligands keep the propeller like conformation around the metal as in the monomeric complexes but remarkably, starting from a racemic complex in which the two enantiomers are present, Δ and Λ , only one of the three possible dimers is obtained, thus dimer **3** is an heterochiral dimer (Δ - Λ) formed by two enantiomeric tripodal Ti(IV) complexes. No traces of the diastereomeric homochiral complexes (Δ - Δ and Λ - Λ) are present in the ¹H NMR spectrum.

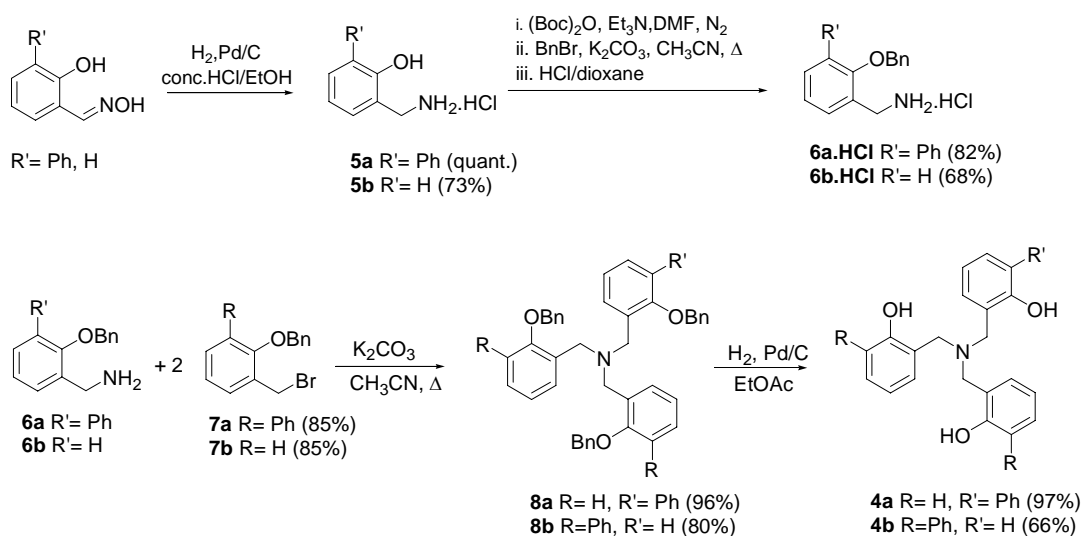
3.2.1 Stability of the μ -oxo complex

In order to investigate in more detail the spontaneous and easy formation of the μ -oxo complex **3** and its high stability in time towards hydrolysis, we decided to synthesize two new *tris*-phenolamines **4** bearing only one or two *ortho*-phenyl substituents (Figure 6), with the purpose to observe the contributions of secondary interactions on the stability of the dimer **3** and the importance of shielding of Ti-O-Ti bond.

**Figure 6**

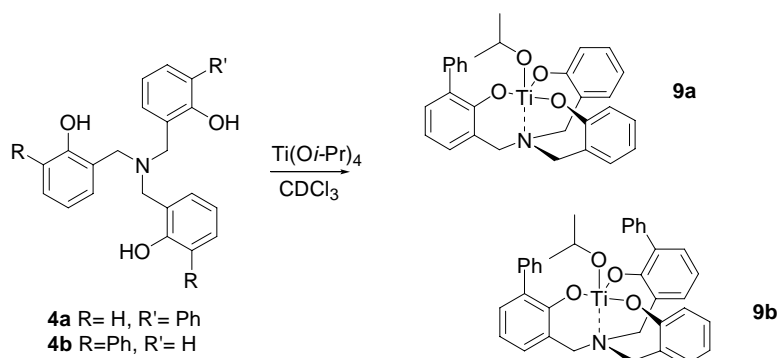
Accordingly, synthesis and characterization of ligands **4a-b** and the subsequent study of complexation with Ti(Oi-Pr)₄ were undertaken.

After three passages of protection of amine **5** as *N*-Boc derivative, protection of the phenol as benzyl ether and removal of Boc-protective group, amine **6.HCl** was obtained in good yields. Amino phenol **6.HCl** were used to prepare the *tris*-phenolamines **4a-b** via a nucleophilic substitution with benzyl bromide derivative **8a** (or **8b**) followed by hydrogenolysis. All steps were obtained with good yields. (Scheme 4).



Scheme 4

The coordination chemistry of amino triphenols **4a-b** with $\text{Ti}(\text{O}i\text{-Pr})_4$ was explored via ^1H NMR. In analogy with what we observed in the other cases, mononuclear pseudo- C_3 -symmetric complexes **9a-b** were obtained quantitatively (Scheme 5).



Scheme 5

Due to the lack of C_3 -symmetry, ^1H NMR spectra are more complicated. However, in both cases, the six methylene protons furnished a single, broad singlet consistent with the occurrence of a fast racemization on the NMR time scale of the titanatrane chiral monomers (Figure 7).

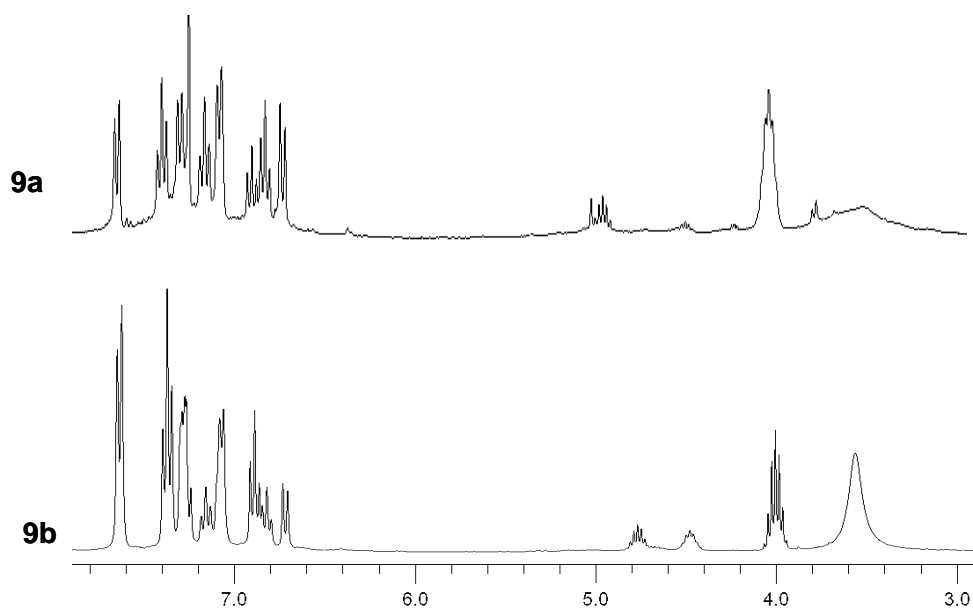


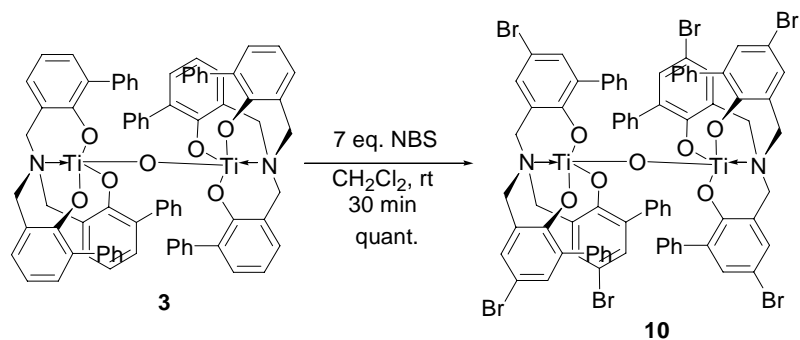
Figure 7. ¹H NMR (300 MHz, CDCl₃) spectra of **9a** and **9b**

In both cases no spontaneous formation of dinuclear μ -oxo species was detected: complexes resulted stable in solution over the time, even after addition of excess of water. Moreover, monomers are highly stable in a wide range of temperatures (-40° to +50° C). VT-NMR experiments revealed the maintenance of a single set of signals for each complex, as also confirmed by 2D-¹H-NMR COSY experiments. ESI-MS analysis (acetonitrile or methanol plus 0.1% formic acid as mobile phase) showed the presence of only mononuclear complexes, even in the case of wet samples. Apical ligand exchange has been observed due to the ESI-MS conditions: the protonated trifluoroacetate ([LTi-HCOO + H]⁺ *m/z* 502.3 for **9a**, 578.3 for **9b**) or methoxy derivatives ([LTi-OMe + H]⁺ *m/z* 488.2 for **9a** and 564.1 for **9b**) were detected.

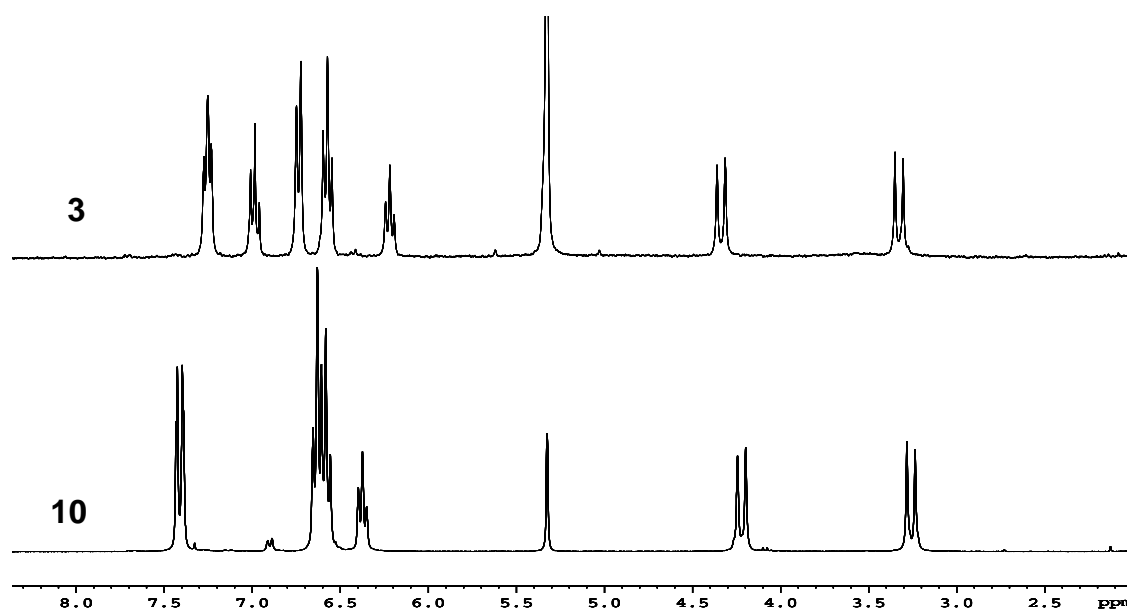
All these experiments indicate the fundamental importance of the three phenyl *ortho*-substituents for the formation of the dinuclear μ -oxo complex **3**. Our hypothesis is that the six peripheral phenyl groups in the dimer **3** shield the Ti-O-Ti bond and do not allow further hydrolysis or the reaction of other nucleophiles for restoring the mononuclear complexes. It seems also that their intercalation around the μ -oxo bridge is stabilized by CH- π interactions.

3.2.2 Reactivity of the μ -oxo complex

Reaction of dimer **3** with 7 equivalents of NBS in anhydrous dichloromethane affords quantitatively the hexa-bromo-derivative **10** (Scheme 6). ¹H NMR spectrum of complex **10** is highly symmetric showing a single set of signals for the six arms of the ligands, indicative for the complete hexa-bromination of *para* positions. (Figure 8).



Scheme 6

Figure 8. ¹H-NMR (300 MHz, CD₂Cl₂) of **3** and **10**

The X-ray analysis on crystals obtained from a solution of **10** in dichloromethane at 150 K could be solved revealing that, also in this case, the central oxygen lies on the inversion centre of the complex which is characterized by a S_6 symmetry (Figure 9). The distance Ti-O_{central} (1.811(1) Å) is longer than the one found in complexes **3**. Both titanium atoms maintain the trigonal bipyramidal geometry with Ti-N bonds of 2.383(5) Å.

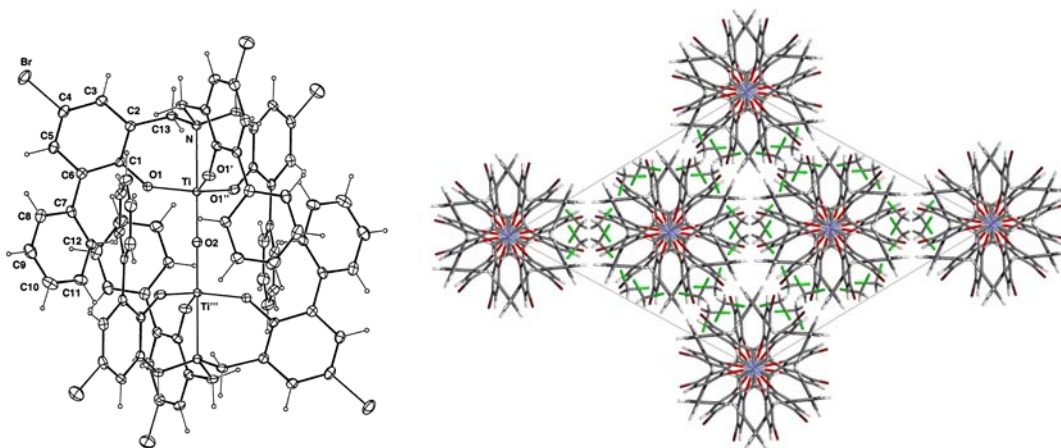


Figure 9. Left: ORTEP view of **10**. Ellipsoids are represented at 40% probability level. The central O atom is located on a centre of inversion. Selected bond distances [Å] and angle [°]: Ti-O_{central} = 1.811 (1), Ti-N = 2.383 (5), Br-C4 = 1.898 (3). Ti-O-Ti = 180.0. Right: The cell unit, with dichloromethane molecules in green and complexes disposed along the Ti-O-Ti axes.

Reaction of **3** with NIS or HNO₃/H₂SO₄ or under Friedel-Crafts conditions did not provide the desired product but only higher molecular weight compounds, probably due to secondary polymerization processes. Further preliminary attempts to further functionalization of **10** using different Suzuki conditions or through Br-Li exchange followed by reaction with an electrophile did not work, so far.

3.3 Ti(IV) μ -oxo complexes as multifunctional platforms

The capacity of amine triphenolate titanatrane complex **2a**, bearing phenyl substituents, to assemble spontaneously affording ordered and stable structures could be exploited to build up supramolecular systems¹⁹ and molecular scaffolds for further applications even in material sciences. The dimeric Ti(IV) μ -oxo complex could be selectively functionalized in its periphery in order to be used as platform with multiple functions disposed in a controlled way into space (Figure 10): a poly-functional platform is a molecule or particle, possessing regularly distributed anchoring sites, which can be used for the formation of new bonds with other molecules for building up more complex systems.

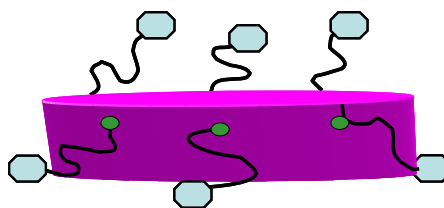


Figure 10

¹⁹ (a) Lehn, J.-M. *Supramolecular Chemistry*, VCH, Weinheim, **1995**. (b) Steed, J. W.; Atwood, J. L. *Supramolecular Chemistry*, Wiley, Chichester, **2000**. (c) Albrecht, M. *Chem. Eur. J.* **2000**, *6*, 3485. (d) Rammal, A.; Brisach, F.; Henry, M. *J. Am. Chem. Soc.* **2001**, *123*, 5612. (e) Albrecht, M.; Mirtschin, S.; de Groot, M.; Janser, I.; Runsink, J.; Raabe, G.; Kogej, M.; Schalley, C. A. *J. Am. Chem. Soc.* **2005**, *127*, 10371. (f) Matsumoto, K.; Sawada, Y.; Saito, B.; Sakai, K.; Katsuki, T. *Angew. Chem. Int. Ed. Engl.* **2005**, *44*, 4935.

The μ -oxo complex **3** is a good candidate for this purpose because it is inert, stable to further hydrolysis, and it self-organizes. A precise control of molecular arrangement at supramolecular level is essential to obtain well-defined nanoscopic architectures, with precise forms and new functionalities. In our case the construction of suitable *tris*-phenolamines should be the key element for the self-organized construction of more complex platforms. Self-assembly of suitably programmed building blocks is ubiquitous in nature and often occurs on several hierarchical levels simultaneously, in order to generate functional systems. At the basis of this process there are the concepts of molecular recognition, which represents the selective interaction at least two components in a self-process, and self-organization, that is related to systems capable of spontaneously generating a well-defined (functional) supramolecular architecture from its complementary components under a given set of conditions.

For example, the shell-forming protein building blocks of the tobacco mosaic virus need to fold into the correct tertiary protein structure before they can be organized around a templating RNA strand. All these processes are mediated by non covalent forces which guide the formation of secondary structure elements on the lowest hierarchy level. These form the tertiary structure on the next level which displays the necessary building sites for the assembly of the virus from a total of 2131 building blocks to occur as programmed on the highest level. Other examples for hierarchical self-assembly are multi-enzyme complexes, the formation of cell membranes with all the receptors and ion channels, or the functional entities embedded into them, or molecular motors such as ATP synthase.

For generation of high degree of complexity, as it is found in nature's functional molecules, different non covalent interactions are required, while aggregation can only develop limited complexity.

Self-assembly is thus an efficient strategy to create complexity and, at the same time, function in nature and moreover makes the programming of individual components more challenging for the synthetic chemist.

The use of the μ -oxo complex as structural platform requires the introduction of suitable functional groups in the periphery of the molecule, without compromising the self-assembling process, that can be further transformed efficiently and in high yields.

The dinuclear complex **3** has twelve potential anchoring sites. Six sites correspond to the *para* positions of the phenolate group of the ligands (Figure 11). These positions can be functionalized for example with *N*-bromosuccinimide affording the hexa-bromine derivative as shown before, or using suitable *para* substituted phenols as starting materials.

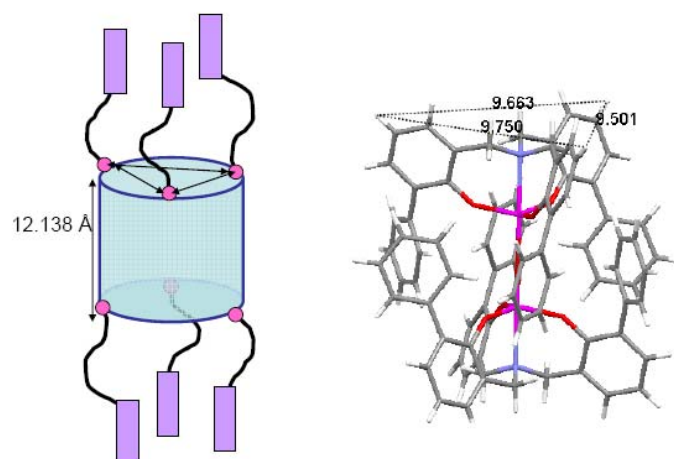


Figure 11. Anchoring sites for the formation of linear structures. Distances calculated for the μ -oxo complex.

The other six sites potentially anchoring sites are the *meta* positions of the peripheral *ortho* phenyl moieties, affording six-tip star structure (Figure 12).

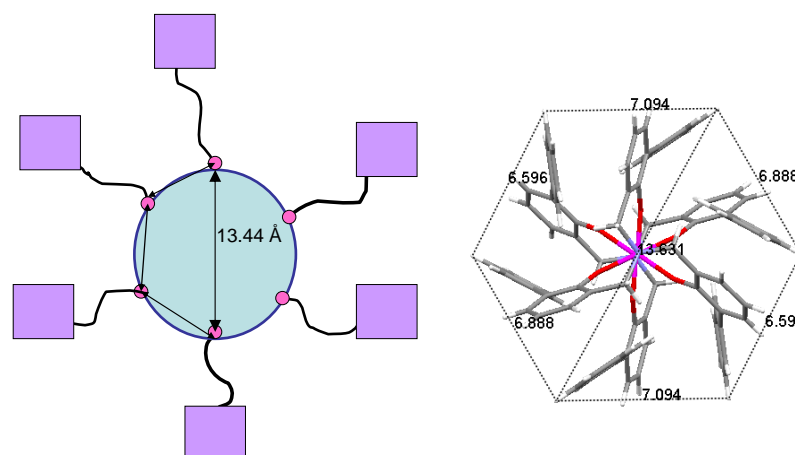


Figure 12. Anchoring sites in the periphery for the construction of star structure. Distances calculated for the μ -oxo compound.

In order to achieve these results a more general synthesis of amine tri-phenolate ligands is necessary, yielding a common intermediate that can be further functionalized, depending on the desired application.

3.3.1 Achiral *tris*-(*o*-phenyl-phenol) amines via Suzuki coupling

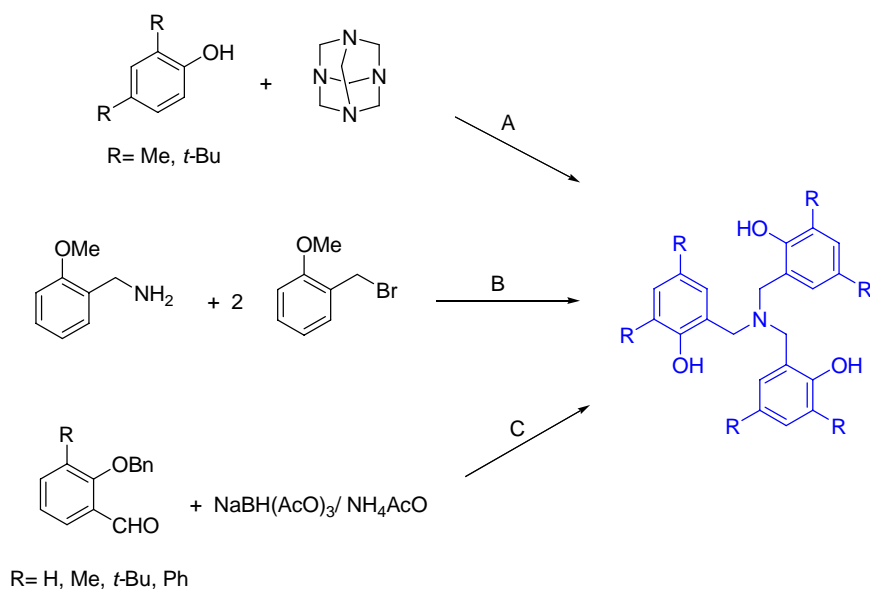
The synthesis of tri-phenol amines is reported to be performed via three different procedures in literature: one step Mannich reaction of *ortho,para*-disubstituted phenols with hexamethylenetetramine²⁰ (Scheme 7, A), alkylation of 2-methoxybenzylamine with two equivalents of 2-methoxybenzylbromide²¹ (Scheme 7, B) or reductive amination, starting

²⁰ Chandrasekaran, A.; Day, R. O.; Holmes, R. R. *J. Am. Chem. Soc.* **2000**, 122, 1066.

²¹ Hwang, J.; Govindaswamy, K.; Koch, S. A. *Chem. Commun.* **1998**, 1667.

from an *ortho*-functionalized salicylic aldehyde protected at the OH as benzyl ether²² (Scheme 7, C).

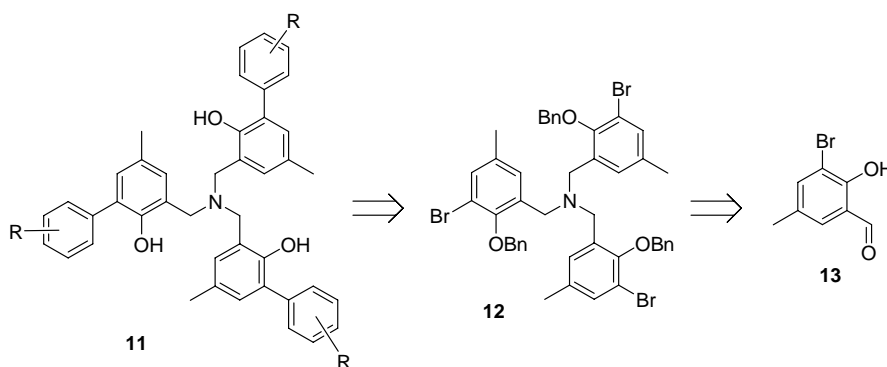
The first synthetic path can be applied only to *para*-substituted phenols and affords the products in 40-70% yields after rather long reaction times (two weeks) and harsh reaction conditions, while the second requires two different phenolic reagents and protection of the OH functions as methylethers. It has been applied to the synthesis of the unsubstituted compounds affording the product, after removal of the protecting groups with AlCl₃ in 56% overall yields. The third synthetic approach, based on reductive amination as the main step, has been developed in this research group and permits to prepare a series of *ortho*-substituted tri-phenol amines, using NH₄AcO as nitrogen source and NaBH(AcO)₃ as reducing agent. The advantages of this synthetic procedure are related to the simple and mild reaction conditions, short reaction times, satisfactory chemical yields, efficient purifications and on an easy access to a variety of highly pure *ortho*-substituted derivatives. This strategy has been also applied for the preparation of ligand **1a**.



Scheme 7

²² Prins, L.J.; Mba, M. B.; Kolarović, A.; Licini, G. *Tetrahedron Lett.* **2006**, *47*, 2735.

In order to study the effect of substitution in the aromatic rings on the Ti(IV) μ -oxo complex formation, the introduction of substituents in the peripheral aryl moiety resulted necessary and consequently a new synthetic strategy to easily tune the steric and electronic properties of the aryl group in *ortho* position has been developed. Taking advantage of the three fold reductive amine approach developed by our group, the *ortho*-bromo salicylic aldehyde derivative **13** was used as starting material obtaining the *tri*-bromo intermediate **12**. In this way different aryl substituents could be introduced at the end of the synthesis through Suzuki-Miyaura coupling, without requiring optimization of the whole synthesis for each derivative (Scheme 8).

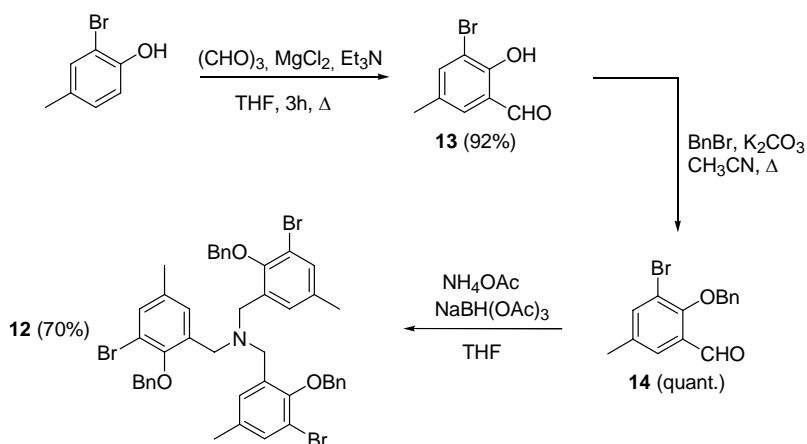


Scheme 8

The use of Suzuki-Miyaura coupling has many advantages. Boronic acids are readily available, nontoxic and air- and water-stable: a large variety of boronic acids is also commercially available and this facilitate the building up of a wide family of ligands. Reactions occur under mild conditions and are amenable to a variety of reaction conditions, including the use of aqueous solvents and substrate supports. The inorganic boron byproducts can be easily removed after completion of the reaction. Moreover the coupling proceeds with high regio- and stereoselectivity and it is little affected by steric hindrance. It does not affect other functional groups in the molecule and can be used in one-pot strategies.

Furthermore the starting material **13** has a *para*-methyl group, which renders increases the solubility of the final ligands and the corresponding complexes. At the same time the methyl substitution could permit further insertion of functionalities.

More in detail, the *tri*-bromo *tris*-phenolamine derivative has been prepared in the protected *O*-benzylated form **12** (Scheme 9).

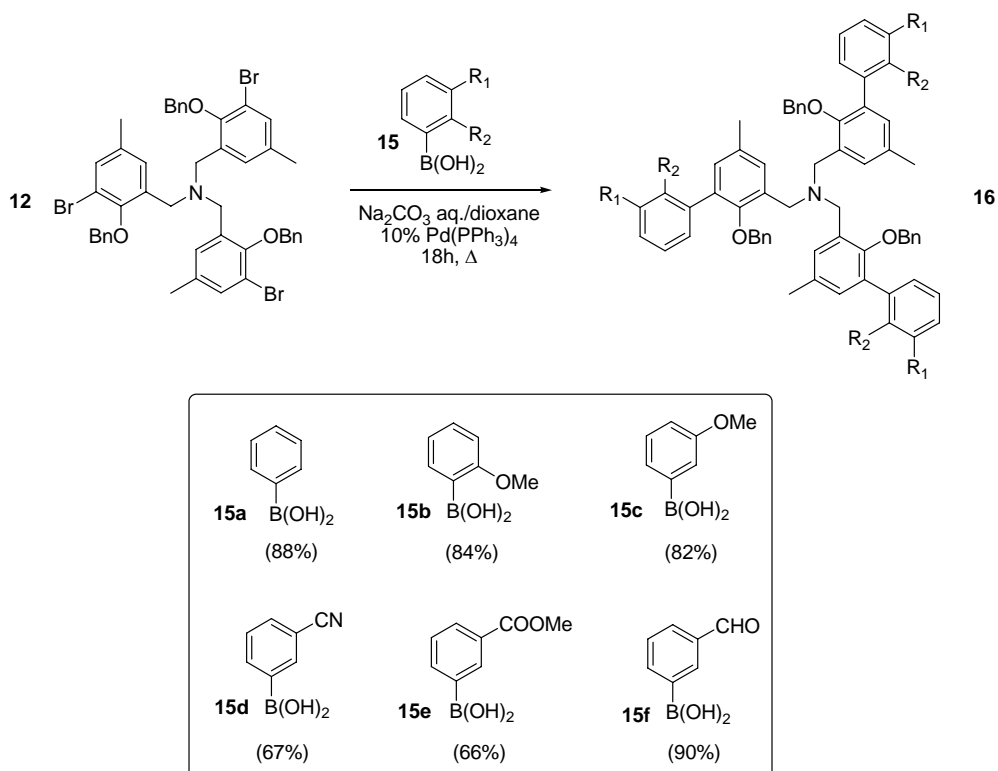


Scheme 9

The commercially available 2-bromo-4-methyl-phenol has been selectively formylated in the *ortho* position thus affording aldehyde **14**, after being protected at the alcoholic function as benzyl ether. The use of a benzyl moiety as protecting group for the phenolic OH allows an easy and efficacious purification of the intermediates via chromatography or crystallization. Moreover all attempts to use different, smaller protective groups failed: protection with methyl ether resulted non practicable, since the removal of the protective group was not general and complete for all the ligands reported in this chapter, even using different reagents and reaction conditions: AlCl_3 /toluene at r.t., BBr_3 / CH_2Cl_2 -78°C , or 0°C or r.t., BCl_3 / CH_2Cl_2 -78°C or AlCl_3 /toluene under reflux. Because of the scarcely successful results, *O*-benzyl protecting groups were used in all the synthesis reported in the following section.

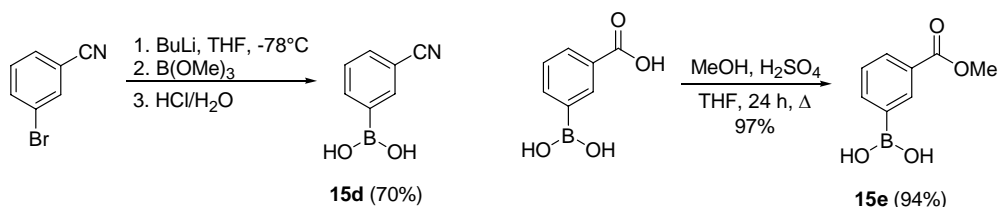
Tris-phenolamine **12** was obtained in 70% yields in isolated product via three fold reductive amination, using aldehyde **14** as substrate, NH_4AcO as nitrogen source and $\text{NaBH}(\text{AcO})_3$ as reducing agent.

Suzuki-Miyaura coupling reaction between ligand **12** and phenyl boronic acid **15a** to give the final ligand **16a** was studied in mode detail in order to optimize the reaction conditions (Scheme 10). Different palladium source and bases were tested finding that the most standard conditions are the best one ($\text{Pd}(\text{PPh}_3)_4$, Na_2CO_3 aq., dioxane). Complete conversion into the product was obtained using a two fold excess of equivalents of boronic acid. Suzuki-Miyaura coupling was monitored via ESI-MS due to the difficult differentiation among the partially coupled products, via TLC or NMR techniques.



Scheme 10

Boronic acids **15d** and **15e** were synthesized respectively via bromine-lithium exchange, anion capture using B(OMe)₃ and subsequent acidic hydrolysis for **15d** and via esterification of 3-(dihydroxyboryl)benzoic acid, affording **15e** (Scheme 11).

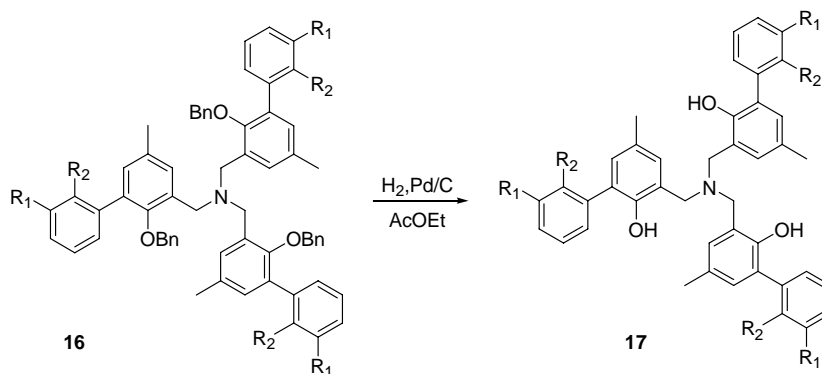


Scheme 11

Suzuki couplings were obtained in good to high yields after chromatographic purification (66-90%). Only in the case of **15e** the Suzuki coupling reaction conditions were modified in order to avoid the parallel hydrolysis of the methylester groups. Instead of dioxane a toluene/methanol 3:1 mixture was used, yielding the final cross-coupling product **16e**, without traces of hydrolysis.²³

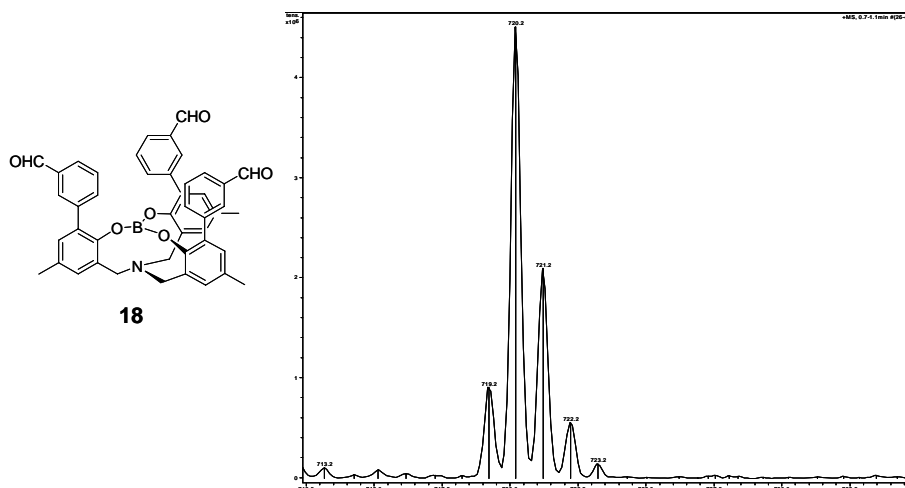
Deprotection of *O*-benzyl groups was performed on systems **16a-e** via hydrogenolysis (H₂/Pd/C) obtaining the pure **17a-e** in good yields (82- 89%) (Scheme 12).

²³ (a) Nicolau, K.C. ; Evans, R. M. ; Roecker, A.; Hughes, R.; Downes, M.; Pfefferkorn, J. A. *Org. Biomol. Chem.* **2003**, *1*, 908. (b) Adamski-Werner, S. L.; Palaninathan, S. K.; Sacchetti, J. C.; Kelly, J. W. *J. Med. Chem.* **2004**, *47*, 355.



Scheme 12

For compound **16f**, BnO-hydrogenolysis could not be applied due to the presence of aldehydic groups. Different procedures were exploited, in particular the use of BCl_3 as Lewis acid.²⁴ The reaction with BCl_3 (3.6 equiv. for aldehydic function), in the presence of an excess of pentamethylbenzene, lead to the complete deprotection of the three O-benzylic groups in half a hour. Pentamethylbenzene resulted necessary since it works as scavenger for the benzylic cation, that is generated during the reaction, and in this way it drives the reaction to completion. Unfortunately, even if the yield was almost quantitative (98%), the product was obtained as the highly symmetric, mononuclear boratrane **18**, as clearly shown by the MS spectra reported in Figure 13. Complex **18** resulted to be air stable and resistant to hydrolytic acidic conditions.

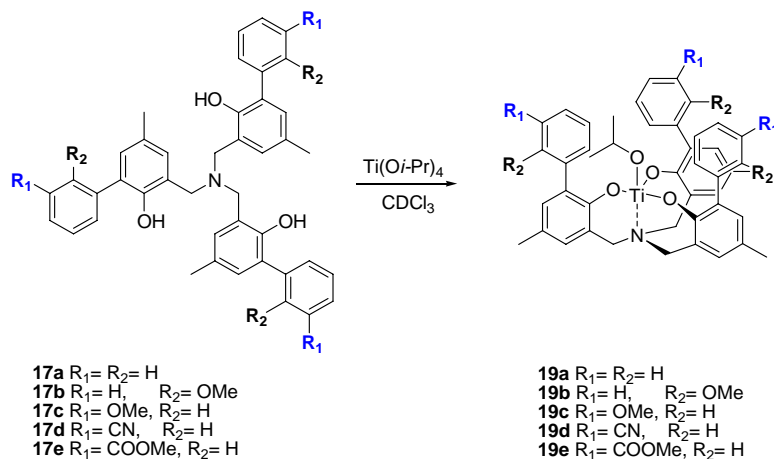
Figure 13. ESI-MS analysis of complex **18**, $[\text{M}+\text{Na}]^+$ ($m/z = 720.3$)

3.3.2 Coordination chemistry of ligands **17a-e** with Ti(V)

C_3 -symmetric tris-phenolamines **17a-e** tightly bind Ti(IV) ion displacing three equivalents of *iso*-propoxide ligand from $\text{Ti}(\text{O}i\text{-Pr})_4$ and forming complexes **19**, by reaction with one equivalent of $\text{Ti}(\text{O}i\text{-Pr})_4$ in CDCl_3 solution at room temperature (Scheme 13). The fourth

²⁴ Okano, K.; Okuyama, K.; Fukuyama, T.; Tokuyama, H. *Synlett* **2008**, *13*, 1977.

alkoxide ligand, coming from the metal precursor, occupies the apical position in the trigonal-bipyramidal geometry of the complexes. Upon addition of the titanium precursor to the ligand solution, an immediate change in solution's colour is observed, from colourless to yellow, indicating the formation of the new Ti(IV) complexes.



Scheme 13

For all titanatranes complexes **19**, ¹H NMR spectra were consistent with the quantitative formation of the single, highly-symmetric mononuclear complex, without any traces of the free ligands. A new signal correspondent to the apical *iso*-propoxide appeared at about 4.50 ppm (heptet, 1H), whereas signals of the three equivalents of free *iso*-propanol were found at ca 4.02 ppm (heptet, 3H) and 1.20 ppm (doublet, 18H).

Initially the complexation behaviour of **17a-c** was studied in detail: in each case the highly symmetric mononuclear complex was obtained at room temperature just after mixing the reagents, as confirmed by the single set of ¹H NMR signals of the reaction mixture and their integration's values.

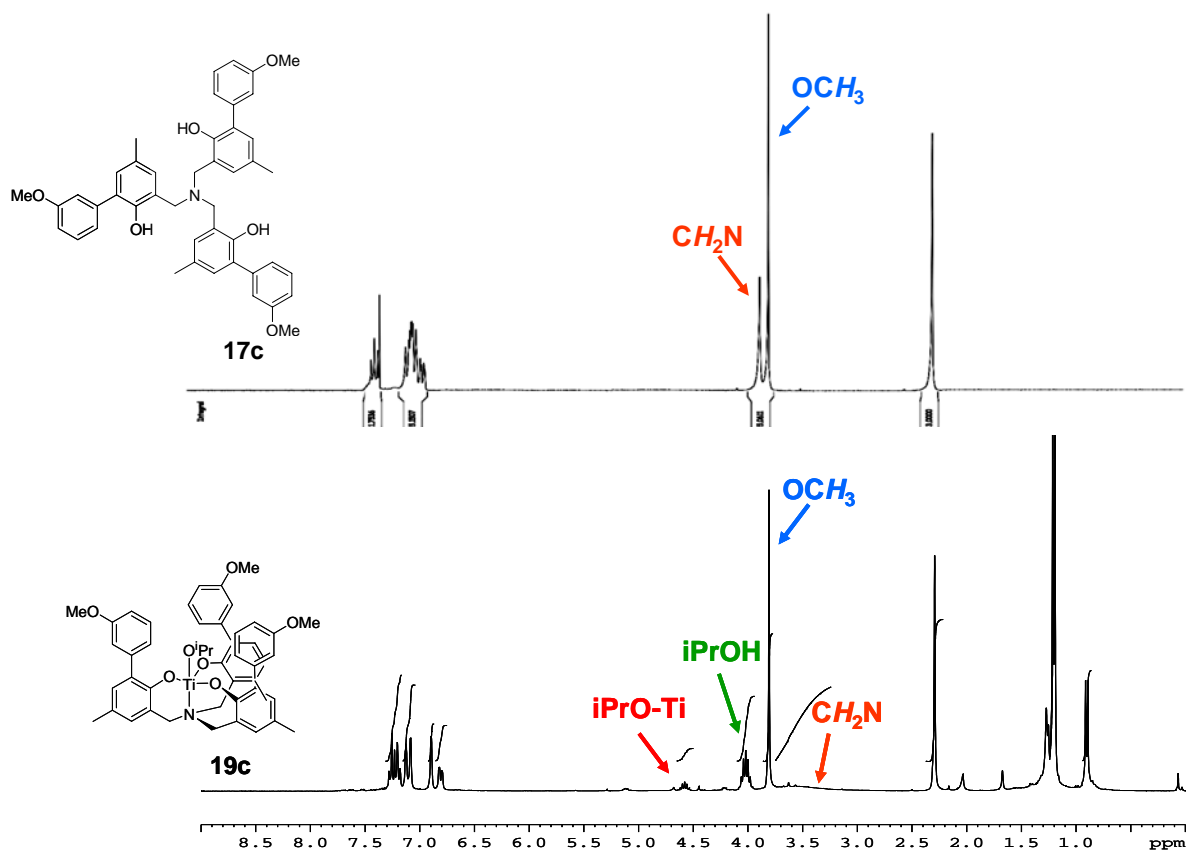


Figure 14. ¹H-NMR spectra of ligand **17c** and the corresponding mononuclear Ti(IV) complex **19c**.

Interestingly, spectrum of complex **19b** shows the diastereotopic benzylic protons as two doublets at 2.92 and 4.14 ppm (Figure 15), while complexes **19a** and **19c** show a single broad singlet, characteristic of a much faster interconversion of the two enantiomeric complexes (Figure 14).

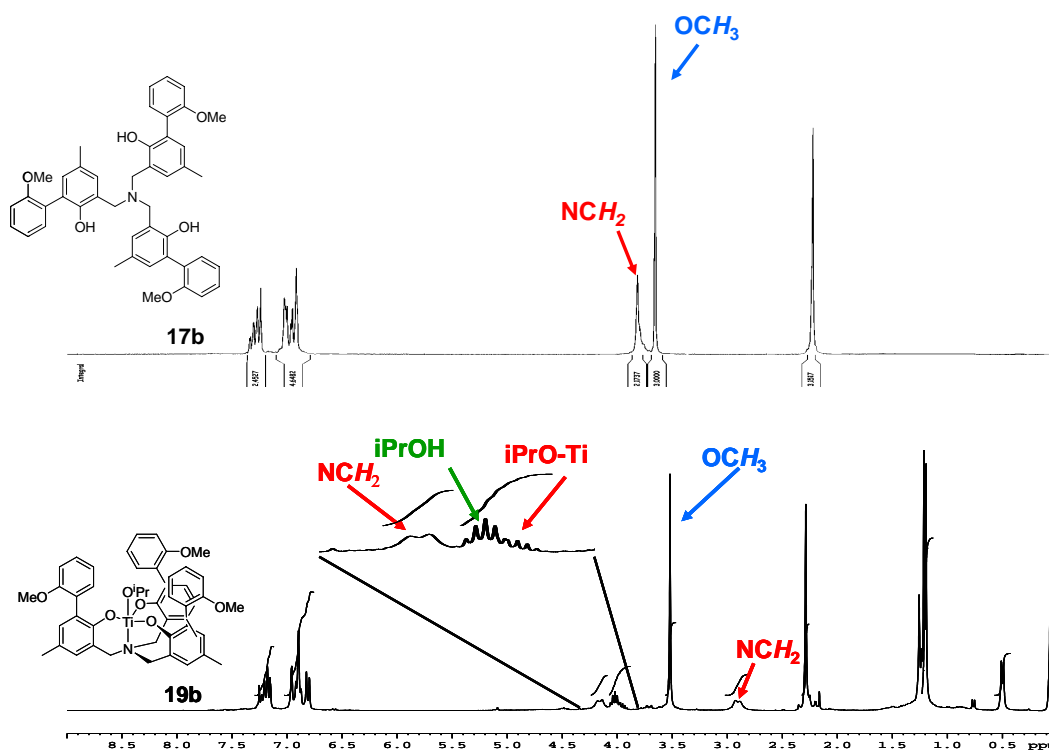


Figure 15. ¹H-NMR spectra respectively of ligand **17b** and the corresponding Ti(IV) complex **19b**.

After addition of water complex **19a** quickly evolved to a new species, the μ -oxo complex **20a**, that, thanks to the *para*-methyl groups, is more soluble than **3** and does not precipitate out of the solution (Figure 16). As evidenced by the green rectangle in Figure 16, the shielding signals for protons of peripheral phenyls indicate the actual CH- π interactions between the aromatic substituents of the two titanatranes units: such aromatic protons are upfielded as a consequence of the diamagnetic ring current. Moreover, the two doublets of the benzylic protons possess a coupling constant of 13.7 Hz, pointing out the formation of a rigid structure, in which the interconversion process between the two helical enantiomers is blocked.

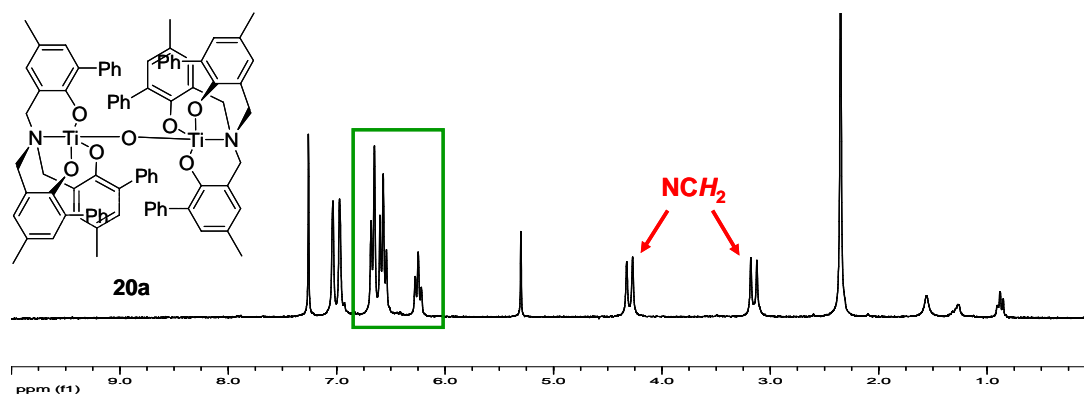


Figure 16. ¹H-NMR spectrum of μ -oxo complex **20a**, with the de-shielded protons of the peripheral substituents in the green rectangle.

The behaviour of complexes **19b-c** in the presence of water resulted rather different, despite of the more hindrance originating from the presence of the MeO groups on *ortho* aryl groups.

Complex **19b** did not form spontaneously the dinuclear μ -oxo complex, not even after addition of excess of water: the only change that was observed was the exchange of the apical *i*-PrO ligand to yield the hydroxo complex. This new species appears stable in solution at room temperature, over the time. On the contrary, complex **19c**, after addition of water, evolved rapidly and in a quantitative way to the μ -oxo complex **20c** (Figure 17).

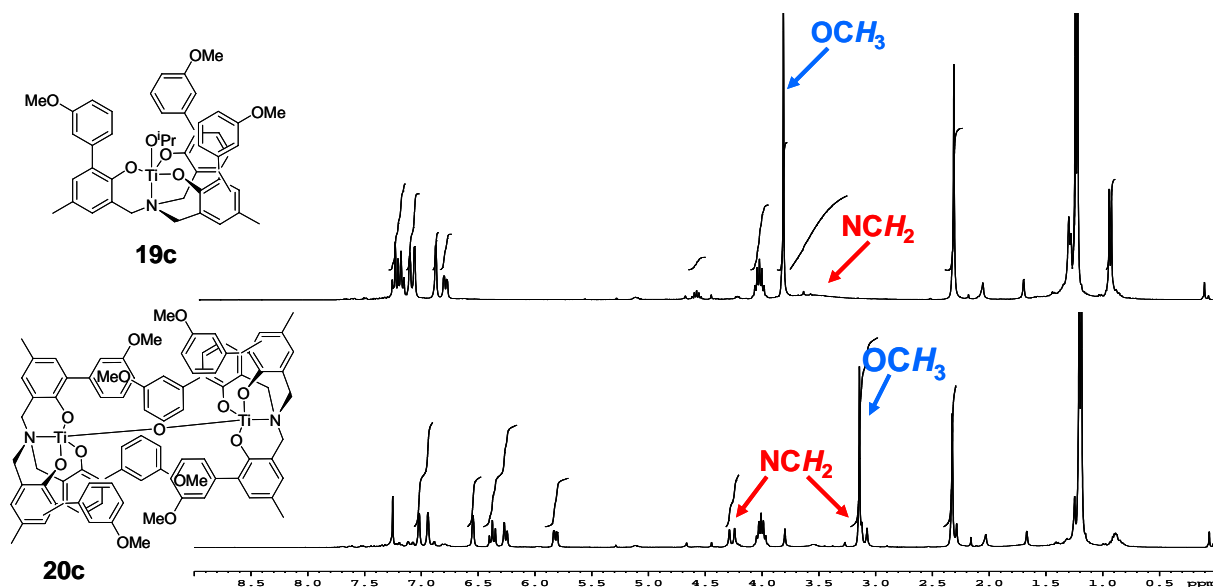


Figure 17. ^1H -NMR spectra respectively of the Ti(IV) mononuclear complex **19c** and the corresponding μ -oxo complex **20c**.

Thus, we can conclude that the introduction of substituents in the aromatic rings of the system can be an additional element of control in the formation of the μ -oxo complexes: i.) the presence of *p*-groups on the phenol rings allows the μ -oxo complex formation, the process is slightly slowed down but the compound solubility is increased. ii.) *ortho*-methoxy groups on the peripheral aromatic do not allow the μ -oxo complex formation, yielding, spontaneously, to stable Ti-hydroxo complexes while iii.) *m*-substituents ring allow the μ -oxo complex formation and slow down the dimerization process (extra water addition is required).

Consequently, differently functionalized μ -oxo complexes for building up platforms must have extra functional groups in *meta* position on the peripheral aromatic ring, such as **17d** (*m*-CN) and **17e** (*m*-COOMe)

The complexation behaviour of **17d** and **17e** was similar to **17c**, with the formation of monomeric complexes **19d-e**, both characterized by a fast interconversion between the two helical enantiomers. These complexes remain stable in solution for days, but, upon water addition, a clear transformation into the corresponding μ -oxo complexes **20d-e** can be observed. While the formation of **20d** is quantitative and clean, as confirmed by NMR and ESI-MS analysis (Figure 18), dimer **20e** is obtained together with the contemporary formation

of oligomeric species. However, after crystallization from diethyl ether, complex **20e** can be isolated as a pure solid.

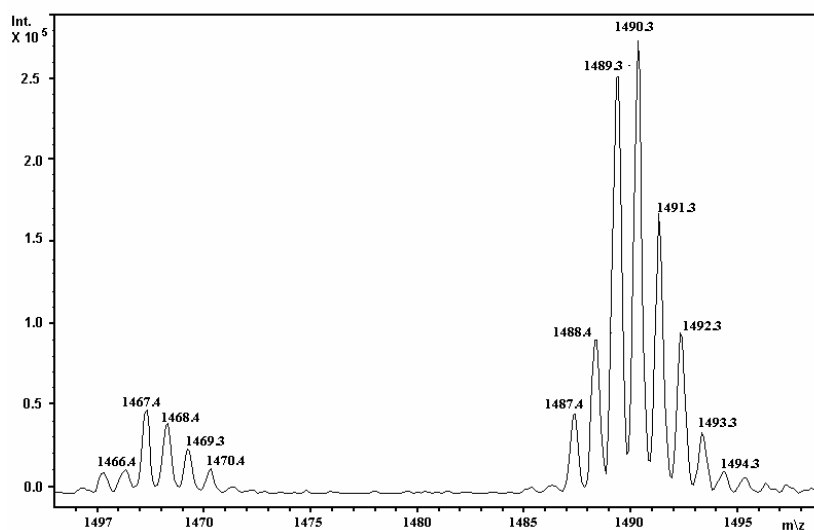


Figure 18. ESI-MS of **20d**, showing its isotopic distribution for $[M+H]^+$ and $[M+Na]^+$

The high symmetry of these species is maintained in the dinuclear complexes since a single set of signals for each type of proton is present in the ^1H NMR. π shielding of the aromatic protons pointing inside the complex has been evidenced: as example the meta proton of the peripheral aromatic ring, which appears as a triplet at 7.41 ppm in **19e** resonates at 6.37 ppm in **20e** (Figure 19).

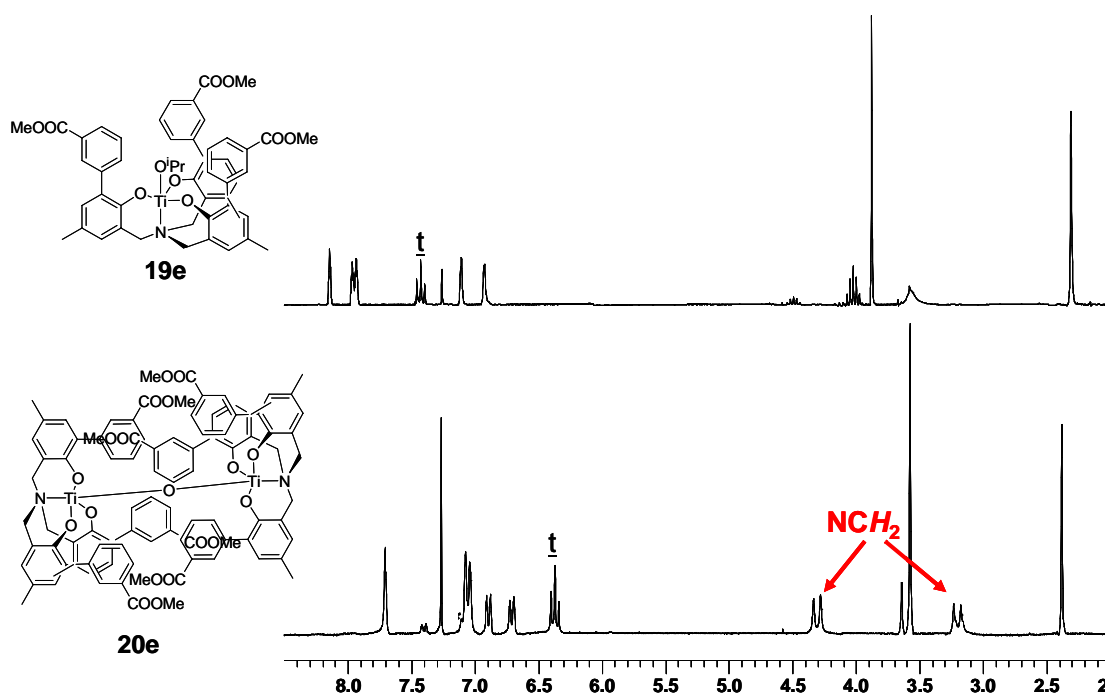
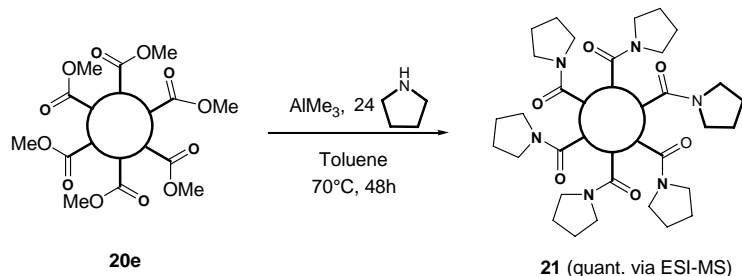


Figure 19. ^1H -NMR spectra of the Ti(IV) monomeric complex **19e** and the corresponding μ -oxo complex **20e**.

In this contest a first proof of the effective possibility of further functionalize the dimers has been obtained with complex **20e** through aminolysis reaction, using pyrrolidine and the Lewis acid AlMe_3 as catalyst (Scheme 14).²⁵ The reaction has been monitored via ESI-MS: the complete conversion to the hexa-functionalized product **21** ($m/z=1990$ $[\text{M}+\text{H}]^+$, 1923 $[\text{M}+\text{Na}]^+$, 1939 $[\text{M}+\text{K}]^+$) was evident after 48h. Consequently μ -oxo complexes can be effectively exploited as stable platforms for the construction of functional materials.

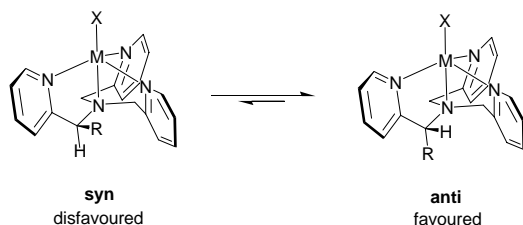


Scheme 14

3.4 Enantiopure titanatrane with propeller like chirality

As previously discussed, an efficient chiral self-discrimination, or heterorecognition, process has been hypothesized for the formation of the heterochiral dimer **3**. In order to establish whether or not the formation of the μ -oxo complex **3** implies a stereo-self-discrimination process or simply the formation of the most stable diastereomeric species, the investigation on the behaviour of an analogous, enantiomerically pure complex becomes fundamental. In order to achieve this goal, the complete control of ligand helicity in the amine triphenolate complex is required.

The control of the direction of the propeller-like twist could be achieved through the introduction of a single stereocentre (a methyl) on one of the arms of the tripodal ligand, in analogy what was reported by Canary and coworkers on comparable systems. According to their studies, the helicity of $\text{Zn}(\text{II})$ and $\text{Cu}(\text{II})$ tripodal complexes of tris(pyridylmethyl)amino ligands can be controlled by the introduction of a single stereogenic centre in one of the benzylic positions, proposing that the *alpha* methyl group would adopt a pseudo axial position and the preferred diastereoisomer should have the methyl group in *anti* position with respect to the proximal phenyl moiety to avoid *syn*-pentane-like interactions (Scheme 15).^{26,27}



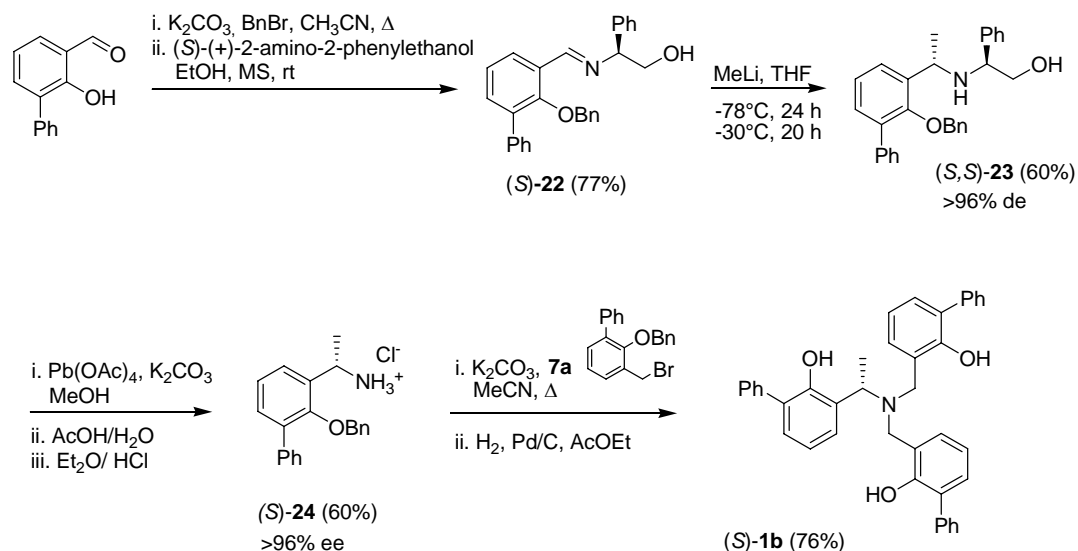
Scheme 15

²⁵ Basha, A.; Lipton, M.; Weinreb, S. M. *Tetrahedron Lett.* **1977**, *48*, 4174.

²⁶ (a) Canary, J.W.; Allen, C.S.; Castagnetto, J. M.; Wang, Y. *J. Am. Chem. Soc.* **1995**, *117*, 8484. (b) Chiu, Y.-H.; dos Santos, O.; Canary, J.- W. *Tetrahedron* **1999**, 12069.

²⁷ Dai, Z.; Zhu, X.; Canary, J. W. *Chirality* **2005**, *17*, 227.

One may speculate that this observation in 5-membered metallacycles could also hold for 6-membered metallacycles present in an enantiomerically pure Ti(IV) amine triphenolate complex **2b**. The synthesis of ligand (*S*)-**24** was undertaken to confirm or refute this hypothesis and was obtained through reaction of enantiopure amine with two equivalent of the corresponding bromo-benzyl derivative **7a** (Scheme 16).



Scheme 16

Amine (*S*)-**24** was obtained through diastereoselective alkylation of an imine: conversion of 2-hydroxybiphenyl-3-carbaldehyde to its benzylether and imine formation with 2-phenylglycinol afforded (*S*)-**22**. Methyl lithium addition gave, albeit in low yield, the diastereoisomerically highly enriched (*S,S*)-**23** which was converted to the primary amine (*S*)-**24** via Pb(OAc)₄ oxidation followed by hydrolysis.²⁸ Reaction of (*S*)-**24** with two equivalents of 2-benzyloxy-3-bromomethyl-biphenyl, followed by hydrogenolysis of the benzyl groups gave ligand (*S*)-**1b** (Scheme 16).

Ligand (*S*)-**1b** cleanly reacts with Ti(Oi-Pr)₄ in dry CHCl₃ yielding the pseudo-C₃ symmetric complex (*S*)-**2b**. The ¹H NMR spectrum in CDCl₃ shows the quantitative formation of a single mononuclear Ti(IV) complex. Due to the loss of C₃-symmetry of the system, the ¹H NMR spectrum of complex (*S*)-**2b** is more complex than **2a**, but it shows a single set of signals for each of the diastereotopic benzylic protons (Figure 20).

²⁸ (a) Bernardinelli, G.; Fernandez, D.; Gosmini, R.; Meier, P.; Ripa, P. A.; Schupfer, P.; Treptow, B.; Kündig, E. P. *Chirality* **2000**, *12*, 529. (b) Kündig, E. P.; Botuha, C.; Lemerrier, G.; Romanens, P.; Saudan, L.; Thibault, S. *Helv. Chim. Acta* **2004**, *87*, 561.

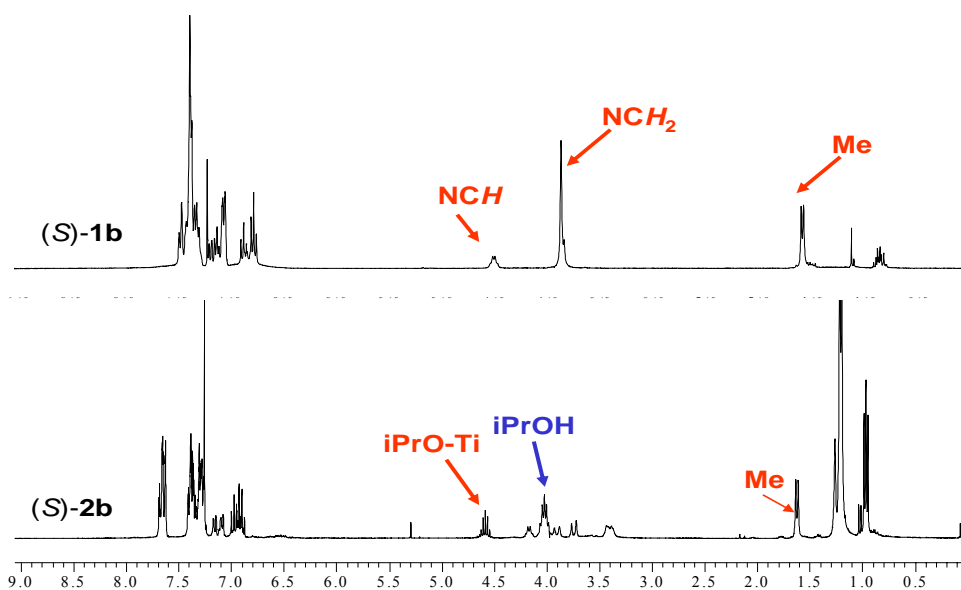


Figure 20. $^1\text{H-NMR}$ (300 MHz, CDCl_3) spectra of ligand (*S*)-**1b** and complex (*S*)-**2b**.

VT NMR experiments from -40° up to 60°C gave no indication of the presence of any other diastereomeric species, confirming that the remote stereogenic centre can completely control the helicity of the titanatrane complex.

Circular dichroism spectrum of Ti(IV) complex (*S*)-**2b** show significantly enhanced signals compared with the one of free chiral ligand (*S*)-**1b** (Figure 21).

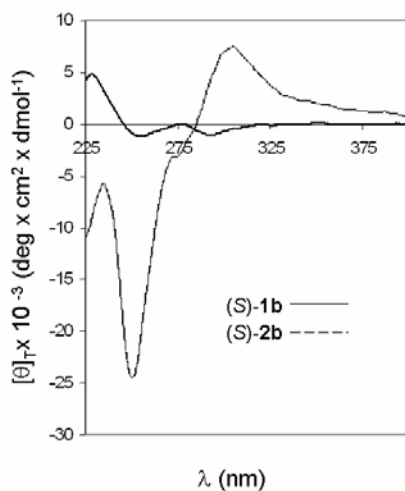


Figure 21. Circular dichroism spectra (CH_2Cl_2) for ligand (*S*)-**1b** and complex (*S*)-**2b**.

These data are consistent with the presence of a propeller like conformation for the mononuclear complex (*S*)-**2b**.

On the basis of Canary's results and calculations, the preferred diastereoisomer should have the methyl group in *anti* position with respect to the proximal phenyl moiety, being favoured by the absence of *syn*-pentane-like interactions, and this should generate a Δ (right-handed) propeller-like twist.²⁶

The X-ray crystal structure of a similar enantiopure chiral complex, bearing *ortho* and *para* *tert*-butyl substituents, reported by Bull, Davidson *et al.* confirms that the introduction of an *R* stereocentre conduce to the formation of the predicted counter-clockwise helix: a left-handed propeller like twist, thus a (*R*, Λ)-complex (Figure 22).²⁹

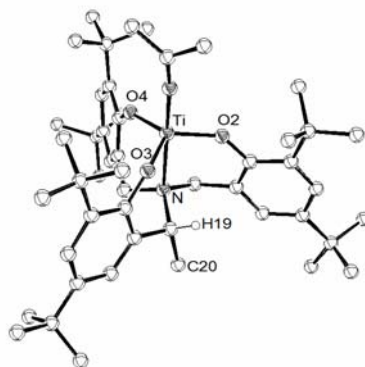
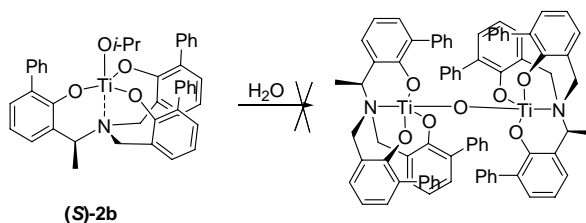


Figure 22. Molecular structure of Ti(IV) (*R*, Λ)-complex, reported by Bull, Davison *et al.*²⁹

Exposure of complex (*S*)-**2b** to moisture or treatment with D₂O in dioxane didn't let to the formation of the corresponding dinuclear μ -oxo complex: only the displacement of the apical ligand by OH could be detected (Scheme 17). Forcing the reaction conditions (heating or long reaction times) let only decomposition of the system. ESI-MS analysis did not show the formation of any other μ -oxo species in solution, even after long reaction times.



Scheme 17

The behaviour of the enantiopure complex (*S*)-**2b** confirms that the self-assembly process is indeed a highly stereoselective process between two enantiomeric structures. (*S*)-**2b** maintains its mononuclear structure and does not form the corresponding μ -oxo complex, not even in the presence of large amounts of water and under much harsher reaction conditions.

A more detailed study on the process of stereoselective self-discrimination will be presented in the following *Chapter 4*.

²⁹ Axe, P.; Bull, S. D.; Davidson, M. G.; Gilfillan, C. J.; Jones, M. D.; Robinson, D. E. J. E.; Turner, L. E.; Mitchell, W. L. *Org. Lett.* **2007**, *9*, 223.

3.5 Coordination chemistry of **1a** with Zr(IV) e Hf(IV)

In order to better understand the potentialities of the Ti(IV) μ -oxo systems, the study on the complexation behaviour of *tris*-(2-hydroxy-3-phenylbenzyl)amine ligand **1a** with other metal centres has been undertaken. In particular Zr(IV) and Hf(IV) have been chosen as metals of interest because they belong to the same group as Ti(IV) and are highly oxophilic. In analogy with Ti(IV), Zr(IV) and Hf(IV) amine triphenolate complexes have been obtained by transesterification reaction with a suitable metal tetraalkoxide.^{30,31}

Only a single example of Hf(IV) amine triphenolate complexes has been reported in the literature. The X-ray crystal structure of the complex bearing bulky *ortho,para tert*-butyl substituents has been resolved showing a monomeric pentacoordinate trigonal bipyramidal complex with C_3 -symmetry (Figure 22).³⁰

The reaction of $Zr(Oi-Pr)_4$ with the same ligand gave a monomeric complex with a trigonal bipyramidal geometry.^{31a} On the other hand, reaction with less bulky ligands, like methyl groups, led to the formation of the C_3 symmetric zwitterionic complex **25** with a Zr(IV): ligand ratio 1: 2, in which the metal ion adopts a distorted octahedral geometry (Figure 22).³¹

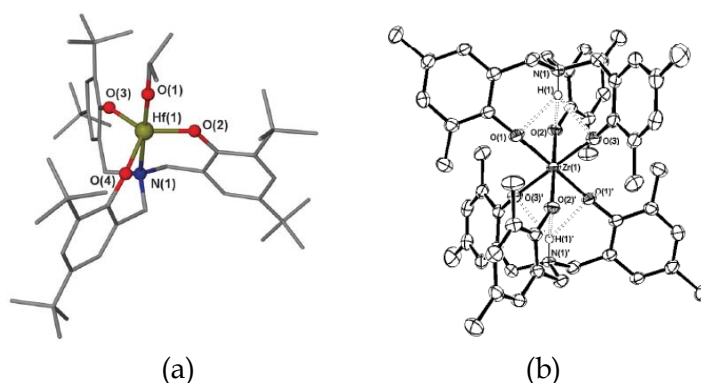


Figure 22. Molecular structure of (a) Hf(IV) pentacoordinate TBP complex. (b) Zwitterionic Zr(IV) complex **25**.

The coordination of two trianionic ligands to the zirconium atom affords a dianionic metal centre. The charge is compensated by the protonation of both nitrogen atoms. These hydrogens are trapped in a cage-like arrangement and the distances to each one of the phenolate oxygen atoms (2.21 (3), 2.29 (2) and 2.15 (3) Å) are indicative of the presence of a N-H \cdots O hydrogen bond. The formation of the zwitterionic structure originates mainly from two different factors: i.) zirconium has the right size to accommodate the NH \cdots O motifs, without incurring in repulsive NH-M interactions and ii.) the decreased steric size of the peripheral substituents allows the approaching of two ligand molecules to the metal.

On the bases of all these pieces of information, the coordination chemistry of Zr(IV) and Hf(IV) with *tris*-(2-hydroxy-3-phenylbenzyl)amine **1a** have been investigated. For both metal atoms the *tetra*-butoxide metal precursor has been used.

³⁰ Chmura, A. J.; Davidson, M. G.; Frankis, C. J.; Jones, M. D.; Lunn, M. D. *Chem. Comm.* **2008**, 1293.

³¹ (a) Davidson, M. G.; Doherty, C. L.; Johnson, A. L.; Mahon, M. F. *Chem. Commun.* **2003**, 1832. (b) Nielson, A. J.; Shen, C.; Waters, J. M. *Crystal Str. Commun.* **2003**, m494. (c) Chartres, J. D.; Dahir, A.; Tasker, P. A.; White, F. J. *Inorg. Chem. Commun.* **2007**, 10, 1154.

The reaction of Zr(O^tBu)₄ and **1a** 1:1 in dichloromethane, led to the formation of the corresponding mononuclear complex **26**, together with other species, probably aggregates (Figure 23, spectrum a). Addition of water (D₂O) afforded a much simplified spectrum where the only signals relative to a mononuclear, highly symmetric Zr(IV) complex **26** are present. (Figure 23, spectrum b). The spontaneous evolution of this complex leads to the formation of complicate aggregates.

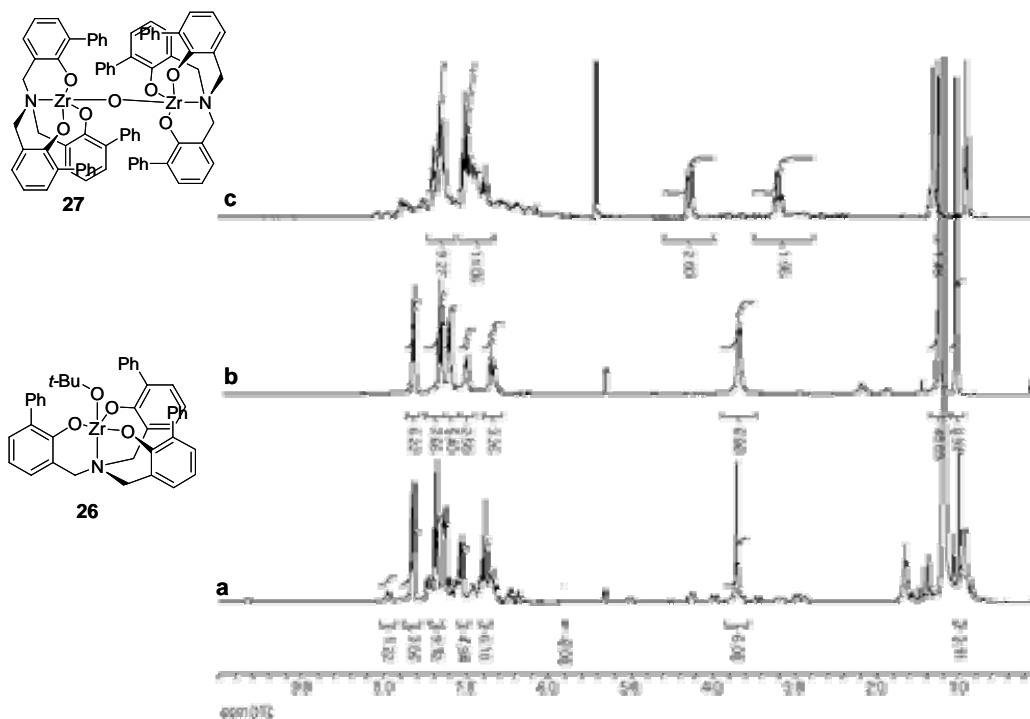


Figure 23. ¹H NMR (300 MHz, CD₂Cl₂) spectra of Zr(IV) complexes, obtained from reaction between Zr(O^tBu)₄ and **1a** 1:1 in CD₂Cl₂: (a) complex **26** after mixing the reagents; (b) complex **26** after D₂O addition; (c) complex **27**, obtained after solvent evaporation and successive dissolution in CD₂Cl₂.

On the contrary, after removing under vacuum the wet solvent and dissolving the white solid obtained, the spectrum of a new, highly symmetric species was obtained: (Figure 23, c). The ¹H MNR seems to be consistent with the formation of a μ-oxo complex **27**. However, no up field shifts of the peripheral aromatic protons are present, probably due to the longer Zr-O bonds. Further evidences of the formation of this complex could not be obtained so far: ESI-MS and APCI-MS experiments did not show the presence of the μ-oxo complex in solution, since the system is not stable under that conditions (only signal of the free ligand could be detected), neither crystals suitable for diffractometric analysis could be obtained.

The Hf(IV) complex formation, performed with the same procedure reported for the Zr(IV) complex, gave the mononuclear highly stable species **28**. (Figure 24). However, addition of water caused an immediate decomposition to complex aggregates.

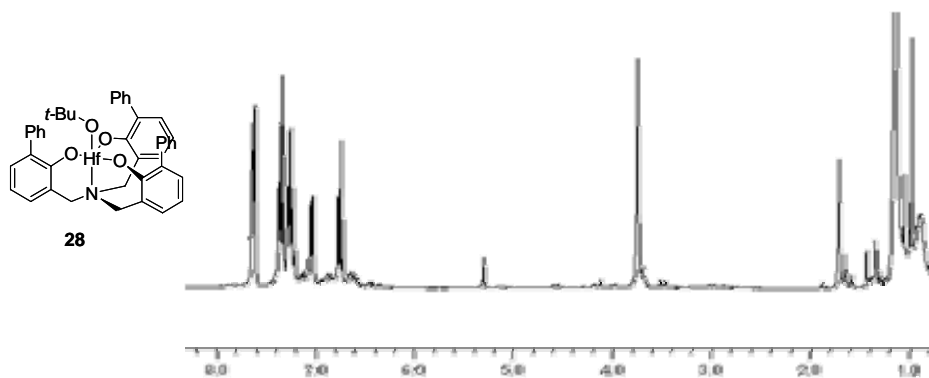


Figure 24. ^1H NMR (300 MHz, CD_2Cl_2) spectrum of Hf(IV) complex 28

3.6 Conclusions

Amine tri-phenolate complexes, bearing three phenyl *ortho* substituents, have been found to easily dimerize in the presence of traces of water, affording the corresponding dinuclear μ -oxo complexes. These highly symmetric complexes are stable to further hydrolysis and do not form the original mononuclear complexes even in the presence of excess of alcohols. Studies on the origin of the high stability of these species pointed out that the presence of the three peripheral phenyl groups (six in the complex) are crucial for the complexes stability, probably due to Ti-O-Ti bonds shielding.

Set up of a new synthetic procedure for the synthesis of different aryl derivatives (through the introduction of the aryl group in the last step via Suzuki coupling on the tri-bromo triphenolamine 12) allowed the synthesis of a series of new ligands with different functionalities in the periphery. Coordination chemistry studies with Ti(IV) showed that the dimerization process is still possible, even if it is slowed down, in the presence of methyl groups in *para* substituted phenols and *meta* substituted aryl rings on the *ortho* position. Derivatives with methoxy, cyano and methyl esters have been obtained: in the latter case the μ -oxo complex could be further functionalized to a hexa amide in the presence of excess of pyrrolidine and AlMe_3 . Furthermore, μ -oxo complex 3 could be quantitatively converted into the corresponding hexa-bromo derivative by simple reaction with NBS. These results, taken all together, indicate that the dinuclear Ti μ -oxo complexes could be used as stable and versatile multifunctional platforms, and future studies will move in this direction.

3.7 Experimental

General remarks

Dry solvents were purchased from Fluka. Where 'degassed' solvents or solutions are noted, degassing was carried out by three freeze-pump-thaw cycles. Chemicals were purchased from Aldrich, Fluka or Acros and used without further purification.

If not mentioned separately all reactions were carried out under nitrogen and the glassware was oven-dried prior to use. Molecular sieves (3 Å and 4 Å) were heated (160 °C) under vacuum (0.4 mbar) for 16 h. Flash chromatography (FC) was performed as described

in literature³² using Macherey-Nagel silica gel 60 (0.04-0.063 mm, 230-400 mesh). T.l.c. analyses: Macherey-nagel POLYGRAM[®] SIL G/UV₂₅₄; detection by UV/VIS, ninhydrin or blueshift solution as the visualizing agent or by treatment with Ce-Mo-staining reagent made from Ce(SO₄)₂ (4.0 g), H₃PMo₁₂O₄₀ (8.0 g) and H₂SO₄ (80.0 g) in 320 ml water.

Optical rotations were measured on a Perkin-Elmer 241 polarimeter, 1 dm cell, c in g/100ml. IR spectra have been recorded on a Nicolet 5700 FT-IR, with range 4000-400 cm⁻¹ and resolution 4 cm⁻¹. ¹H and ¹³C{¹H} NMR spectra (referenced to tetramethylsilane or residual solvent peak) were recorded at 301 K on Bruker AC-250, 300, 400 or 500 MHz instruments. The following abbreviations have been used to explain the multiplicities: s = singlet, d = doublet, t = triplet, dd = double doublet, m = multiplet, br = broad. MS: EI (70 eV) VG7070, m/z in amu. ¹³C NMR spectra have been recorded with complete proton decoupling. Analytical gas chromatography with a mass spectroscopy (GC-MS) has been carried out on an Agilent 6850 Series spectrometer equipped with a split mode capillary injector and electron impact mass detector. Injector temperature has been 250 °C, detector temperature has been 280 °C and the carrier gas has been He (1 mL/min) with a HP-5MS column. Melting points are uncorrected and have been determined with a Leitz-Laboroux 12. ESI-MS experiments of complexes were performed in a ESI-TOF Mariner[™] Biospectrometry[™] Workstation of Applied Biosystems by flow injection analysis using acetonitrile or methanol/formic acid 0.1% as mobile phase; in all cases, isotope patterns were in agreement with values calculated from the molecular formulas. All titanatrane complexes were prepared under nitrogen atmosphere in a MBraun MB 200MOD glove-box, equipped with a MB 150 G-I gas recycling system (nitrogen working pressure: 6 bar). Oxygen and water levels inside the box were real-time monitored by MBraun oxygen and moisture analyzers.

2-Benzyloxy-biphenyl-3-carbaldehyde

A mixture of K₂CO₃ (69.5 mmol, 9.6 g), 2-hydroxybiphenyl-3-carbaldehyde (16.0 mmol, 3.17 g) and benzyl bromide (17.8 mmol, 2.12 mL) in dry CH₃CN (285 mL) was refluxed for 18 h. The mixture was filtered through Celite washed with ethyl acetate and the filtrate was concentrated under reduced pressure. The resulting yellow oil was purified by flash chromatography using petroleum ether/ethyl acetate 10:1 as eluant. The final product was obtained as a white solid (2.04 g, 7.1 mmol, 87%).

Mp: 99 – 101°C. IR (KBr) ν (cm⁻¹): 695, 743, 769, 803, 868, 918, 963, 1026, 1072, 1173, 1205, 1220, 1245, 1274, 1298, 1373, 1433, 1453, 1497, 1573, 1583, 1683, 1804, 1878, 1901, 1953, 2878, 3032, 3061, 3344. ¹H-NMR: (500 MHz, CDCl₃) δ 4.56 (2H, s), 7.06– 7.09 (2H, m), 7.27– 7.32 (4H, m), 7.42– 7.51 (3H, m), 7.64– 7.66 (3H, m), 7.84 (1H, dd, J = 7.8, 1.8 Hz), 10.35 (1H, s). ¹³C{¹H}-NMR: (125 MHz, CDCl₃) δ 77.1 (CH₂), 124.7 (CH), 127.4 (CH), 127.9 (CH), 128.49 (CH), 128.53 (2xCH), 128.6 (2xCH), 128.7 (2xCH), 129.2 (2xCH); 130.2 (C), 135.5 (C), 136.4 (C), 137.2 (C), 137.3 (CH), 159.2 (C), 190.3 (CH). MS (ESI): 306.3 [M + NH₄]⁺. HR-MS (ESI): calcd for C₂₀H₁₇O₂: 303.1254; found 303.1251.

³² Stille, C. W. *J. Org. Chem.* **1978**, *43*, 2953.

Tris-(2-benzyloxy-3-phenylbenzyl)amine

2-Benzyloxy-biphenyl-3-carbaldehyde (24.9 mmol, 7.18 g) was weighed in a round bottom flask, then dry THF (56 mL) and ammonium acetate (8.3 mmol, 639 mg) were added under N₂. After 40 min under stirring, sodium triacetoxo borohydride (37.4 mmol, 7.93 g) was added and the mixture was stirred for 48 h at room temperature (TLC petroleum ether/AcOEt 9:1) and then evaporated to dryness. The residue was dissolved in AcOEt (100mL) and washed with KOH_{aq} 15% (2 x 25 mL) and brine (2 x 25 mL). Drying over MgSO₄ and evaporation of the solvent gave the crude product that was further purified by crystallization in CHCl₃/hexane, affording the final product as a white solid (50%).

Mp: 120-122 °C. IR (KBr) ν (cm⁻¹): 697, 764, 1070, 1202, 1429, 1455, 2927, 3030, 3060. ¹H-NMR: (250 MHz, CDCl₃) δ 3.84 (6H, s), 4.36 (6H, s), 7.03-7.00 (2H, m), 7.32- 7.18 (5H, m), 7.46-7.37 (3H, m), 7.65- 7.62 (2H, m), 7.82 (1H, d, J = 6.4 Hz). ¹³C{¹H}-NMR: (62.9 MHz, CDCl₃) δ 52.9 (3xCH₂), 75.0 (3xCH₂), 124.6 (3xCH), 127.3 (3xCH), 128.0 (3xCH), 128.3 (6xCH), 128.4 (6xCH), 128.5 (6xCH), 129.5 (3xCH), 129.6 (6xCH), 133.8 (3xC), 135.4 (3xC), 137.1(3xC), 139.0 (3xC), 154.7 (3xC). MS (ESI): 834.4 [M + H]⁺. HR-MS (ESI): calcd for C₆₀H₅₂NO₃: 834.3947; found 834.3949.

Tris-(2-hydroxy-3-phenylbenzyl)amine (1a)

Tri-(2-benzyloxy-3-phenylbenzyl)amine (4.14 mmol, 3.45g) was dissolved in degassed AcOEt (0.5 N) and catalytic amount of 10% Pd/C was added under nitrogen. Next, a H₂-atmosphere (1 atm) was applied and the reaction was stirred for 3.5 h at room temperature. The reaction mixture was filtered over Celite, dried over Na₂SO₄ and evaporated to dryness, yielding the final product **1a** as a white solid (95%).

1a: Mp: 157.7-158.5 °C. IR (KBr) ν (cm⁻¹): 693, 751, 1063, 1087, 1191, 1230, 1431, 1460, 1591, 1611, 2828, 3028, 3058, 3293 (broad, OH). ¹H-NMR: (300 MHz, CDCl₃) δ 3.89 (6H, s), 6.88 (3H, m), 7.16 (6H, m), 7.49-7.32 (15H, m). ¹³C{¹H}-NMR: (62.9 MHz, CDCl₃) δ 55.9(3xCH₂), 120.1 (3xCH), 123.5 (3xC), 127.6 (3xCH), 128.8 (3xC), 128.9 (6xCH), 129.5 (6xCH), 130.0 (3xCH), 130.4 (3xCH), 137.7 (3xC), 152.5 (3xC). MS (ESI): 564.7 [M + H]⁺. HR-MS (ESI): calcd for C₃₉H₃₄NO₃: 564.2538; found 564.2536.

2-hydroxy-biphenyl-3-carbaldehyde oxime

To a solution in methanol (5 mL) of 2-hydroxybiphenyl-3-carbaldehyde (4.72 g, 23.81 mmol), a solution of hydroxylamine hydrochloride (3.31 g, 47.63 mmol) in water (46 mL) was added and the reaction mixture was stirred at room temperature for 15 h. Then the reaction mixture was evaporated and the residue dissolved in CH₂Cl₂ (30 mL) and washed with water (30 mL). The aqueous phase was extracted with CH₂Cl₂ (3 x 30 mL), dried over Na₂SO₄ and concentrated to give the product as a yellowish solid (4.16g, 82%).

¹H-NMR: (250 MHz, CDCl₃) δ 5.50 (1H, s), 7.21 (1H, t, J = 7.7 Hz), 7.49- 7.85 (7H, m), 8.52 (1H, s).

3-(aminomethyl)biphenyl-2-ol hydrochloride (5a)

2-hydroxybiphenyl-3-carbaldehyde oxime (9.38 mmol, 2.0 g) was dissolved in EtOH (100 mL), followed by 10% Pd/C (0.20 g) and HCl_{aq} conc. (9.4 mL) in N₂-atmosphere. A H₂-atmosphere (1 atm) was applied and the reaction was stirred for 4 h at room temperature. The mixture was filtered through a pad of Celite and concentrated. Toluene (100 mL) was added and evaporated under reduced pressure. Compound **5a** was isolated in quantitative yield (2.21 g) as a white solid.

5a: Mp: 157- 159° C. IR (KBr) ν (cm⁻¹): 705, 757, 779, 1104, 1207, 1229, 1440, 1458, 1474, 1523, 1614, 2636, 2922, 2955, 3329. ¹H-NMR: (250 MHz, CD₃OD) δ 4.18 (2H, s), 7.01 (1H, t, *J* = 7.8 Hz), 7.26 (2H, t, *J* = 7.8, 1.4 Hz), 7.49- 7.32 (5H, *m*). ¹³C{¹H}-NMR: (62.9 MHz, CD₃OD) δ 41.1 (CH₂), 122.0 (CH), 122.8 (C), 128.9 (CH), 130.1 (2xCH), 130.5 (2xCH), 131.1 (CH), 131.7 (C), 133.4 (CH), 139.1 (C), 153.6 (C). MS (ESI): 200.3 [M + H]⁺. HR-MS (ESI): calcd for C₁₃H₁₄NO: 200.1075; found 200.1077.

2-(aminomethyl)phenol hydrochloride (5b)

2-hydroxybenzaldehyde oxime (11.1 mmol, 1.52g) was dissolved in EtOH (120 mL), followed by 10% Pd/C (0.25 g) and HCl_{aq} conc. (8 mL) in N₂-atmosphere. A H₂-atmosphere (1 atm) was applied and the reaction was stirred for 4 h at room temperature. The mixture was filtered through a pad of Celite and concentrated. Toluene (100 mL) was added and evaporated under reduced pressure. Compound **5b** was isolated as a white solid (1.30 g, 73%).

5b: ¹H-NMR: (250 MHz, CD₃OD) δ 4.08 (2H, s), 6.82- 6.90 (2H, *m*), 7.21- 7.27 (2H, *m*). MS (ESI): 124.1 [M + H]⁺.

(2-(benzyloxy)biphenyl-3-yl)methanamine hydrochloride (6a.HCl)

Amine chloroidrate **5a** (8.48 mmol, 2.0 g) was dissolved in DMF (20 mL) and then Et₃N (17.00 mmol, 2.35 mL) and Di-*tert*-butyl dicarbonate (Boc₂O, 9.33mmol, 2.036 g) were added. The reaction mixture was stirred under nitrogen for 7 h and then diluted with half-saturated brine (20 mL). The layers were separated and the aqueous one was extracted with dichlorometane (3 x 40 mL). The organic phase was dried over Na₂SO₄ and concentrated. The (2-Hydroxy-biphenyl-3-ylmethyl)-carbamic acid tert-butyl ester Boc-**5a** was isolated as a yellow oil in a quantitative yield and used directly in the next step.

Boc-**5a** (8.48 mmol, 2.536 g) was dissolved in dry acetonitrile (17 mL); benzyl bromide (9.75 mmol, 1.16 mL) and K₂CO₃ (33.93 mmol, 4.69 g) were added. The resulted suspension was refluxed for 15 h under nitrogen. Then the mixture was filtered over Celite and concentrated. The residue was taken up with AcOEt (20 mL), washed with diluted brine (20 mL) and dried over Na₂SO₄ and then concentrated to dryness. The product (2-Benzyloxy-biphenyl-3-ylmethyl)-carbamic acid tert-butyl ester was obtained as a pale yellow oil in quantitative yield and it was used directly in the next step.

(2-Benzyloxy-biphenyl-3-ylmethyl)-carbamic acid tert-butyl ester (4.89 mmol, 1.9 g) was dissolved in 4M HCl/dioxane (88 mL) and the mixture was stirred for 10 minutes at room

temperature. The residue was dissolved in water (150 mL) and extracted with AcOEt (3 x 50 mL). The organic phase was dried over Na₂SO₄ and then evaporated under reduced pressure, affording compound **6a.HCl** as a white solid (1.30 g, 82%).

6a.HCl: Mp: 173-175° C. IR (KBr) ν (cm⁻¹): 697, 761, 915, 963, 1072, 1207, 1263, 1373, 1434, 1454, 1498, 1528, 1601, 1623, 2637, 2820, 2898, 2950, 3024. ¹H-NMR: (250 MHz, CD₃OD) δ 3.96 (2H, s), 4.49 (2H, s), 7.11- 7.68 (13H, m). ¹³C{¹H}-NMR: (62.9 MHz, CD₃OD) δ 40.4 (CH₂), 76.5 (CH₂), 126.2 (CH), 128.7 (C), 129.1 (CH), 129.6 (2xCH), 129.7 (CH), 129.9 (2xCH), 130.0 (2xCH), 130.3 (2xCH), 130.7 (CH), 134.0 (CH), 137.2 (C), 137.9 (C), 139.5 (C), 156.0 (C). MS (ESI): 290.1 [M + H]⁺. HR-MS (ESI): calcd for C₂₀H₂₀NO: 290.1544; found 290.1546.

(2-(benzyloxy)phenyl)methanamine hydrochloride (**6b**)

Compound **5b** (3.0 mmol, 479 mg) was weighed in a double necked round bottom flask, then dry DMF (7 mL), Et₃N (6.0 mmol, 843 μ L) and Di-*tert*-butyl dicarbonate (Boc₂O, 3.3 mmol, 720 mg) were added under nitrogen. The mixture was stirred for 2 h at room temperature. Half-saturated brine (10 mL) was added and the aqueous layer was extracted with CH₂Cl₂ (3 x 20 mL). The organic phase was dried over Na₂SO₄ and concentrated, affording the crude product Boc-**5b** as a pale-yellow oil, which was directly used in the next step.

The (2-Hydroxy-benzyl)-carbamic acid tert-butyl ester Boc-**5b** (3.0 mmol, 669 mg) was dissolved in CH₃CN (6 mL), K₂CO₃ (12.0 mmol, 1.66 g) and benzyl bromide (3.3 mmol, 393 μ L) were added under nitrogen. The reaction mixture was refluxed for 18 h, then let to cool down to room temperature, filtered over Celite to remove the salts and concentrated under reduced pressure. The residue was dissolved in CHCl₃ (30 mL) and washed with NH₄Cl_{aq}. sat. (2 x 15 mL), dried over Na₂SO₄ and concentrated to dryness, yielding quantitatively the (2-Benzyloxy-benzyl)-carbamic acid tert-butyl ester product as a yellow oil, solidifying on standing, which was used directly in the last step.

The (2-Benzyloxy-benzyl)-carbamic acid tert-butyl ester (3.0 mmol, 939 mg) was dissolved in 4M HCl/dioxane (54 mL) and stirred for 10 minutes at room temperature, then concentrated under vacuum and the residue was dissolved in toluene and repeatedly concentrated. Crystallization in hot dioxane/toluene afforded the final product **6b.HCl** as small white needles (508 mg, 68%).

6b.HCl: Mp: 167- 169° C. ¹H-NMR: (250 MHz,) δ 7.52-7.34 (7H, m), 7.16 (1H, m), 7.02 (1H, m), 5.24 (2H, s), 4.16 (2H, s). ¹³C{¹H}-NMR: (62.9 MHz, CD₃OD) δ 40.1 (CH₂), 71.3 (CH₂), 113.6 (CH), 122.2 (CH), 122.6 (C), 128.7 (2xCH) , 129.1(CH) , 129.7 (CH), 131.8 (CH), 132.1 (CH), 138.2 (C), 158.2 (C). MS (ESI): 214.1 [M + H]⁺. HR-MS (ESI): calcd for C₁₄H₁₆NO: 214.1231; found 214.1233.

1-(2-Benzyloxybiphenyl-3-yl)-methanol

2-Benzyloxy-biphenyl-3-carbaldehyde (1.73 mmol, 500 mg) was dissolved in ethanol (10 mL) and NaBH₄ (2.08 mmol, 78.7 mg) was added. The resulting mixture was stirred at room temperature for 2.5 h (TLC AcOEt/petroleum ether 1:4), concentrated to dryness, taken in

Et₂O (20 mL) and washed with NaOH_{aq} 10% (20 mL). The layers were separated and the aqueous one extracted with Et₂O (2 x 20 mL). The combined organic phases were washed with brine (2 x 20 mL), dried over MgSO₄ and concentrated to dryness. 1-(2-Benzyloxybiphenyl-3-yl)-methanol was obtained as a white solid in 93% yield and was used without further purifications.

Mp: 69 -70 °C. IR (KBr) ν (cm⁻¹): 696, 749, 766, 804, 982, 1004, 1204, 1433, 1454, 2884, 2940, 3028, 3052, 3509. ¹H-NMR: (250 MHz, CDCl₃) δ 4.55 (2H, s), 4.78 (2H, s), 7.20– 7.55 (11H, *m*), 7.74 (2 H, *d*, *J* = 7.2 Hz). ¹³C{¹H}- NMR: (62.9 MHz, CDCl₃) δ 62.1 (CH₂), 75.4 (CH₂), 124.8 (CH), 127.6 (CH), 128.5 (CH), 128.6 (CH), 128.7 (2xCH), 128.8 (CH), 129.4 (CH), 131.1 (CH), 135.0 (C), 135.4 (C), 136.9 (C), 138.6 (C), 154.5 (C). MS (ESI): 291.1 [M + H]⁺, 313.2 [M + Na]⁺, 329.1 [M + K]⁺. HRMS (ESI): calcd for C₂₀H₁₉O₂: 291.1380; found 291.1383.

2-(benzyloxy)-3-(bromomethyl)biphenyl (7a)

To a solution of alcohol 1-(2-Benzyloxybiphenyl-3-yl)-methanol (1.03 mmol, 300 mg) in dry toluene (5 mL), at 0 °C and under N₂ atmosphere, was added dropwise a solution of PBr₃ (1.13 mmol, 110 μ L) in dry toluene (2 mL). The mixture was stirred at 0 °C for 20 minutes, then allowed to warm to room temperature and stirred for another 30 minutes. The solution was diluted with ice water (5 mL) and stirred vigorously for 3 minutes; then diluted with CHCl₃. The organic phase was separated, washed with brine (10 mL), dried over MgSO₄ and concentrated. Column chromatography of the crude product, using petroleum ether/AcOEt 9:1 as eluant, afforded compound **7a** as a white solid (85 %).

7a: Mp: 84-85 °C. IR (KBr) ν (cm⁻¹): 695, 766, 913, 976, 1066, 1072, 1219, 1375, 1454, 2880, 2951, 3027, 3050, 3430. ¹H-NMR: (250 MHz, CDCl₃) δ 4.55 (2H, s) 4.63 (2H, s), 7.16– 7.45 (11H, *m*), 7.62 (2H, *d*, *J* = 6.9 Hz). ¹³C{¹H}-NMR: (75 MHz, CDCl₃) δ 27.5 (CH₂), 73.5 (CH₂), 123.5 (CH), 126.4 (CH), 127.0 (CH), 127.2 (CH), 127.3 (CH), 127.4 (CH), 128.0 (CH), 129.3 (CH), 130.8 (CH), 130.9 (C), 134.6 (C), 135.5 (C), 137.0 (C), 153.3 (C). MS (ESI): 353.1 [M + H]⁺. HR-MS (ESI): calcd for C₂₀H₁₈OBr: 353.0536; found 353.0538.

(2-(benzyloxy)phenyl)methanol

2-Benzyloxy-carbaldehyde (14.14 mmol, 3.0 g) was dissolved in 2-propanol (50 mL) and NaBH₄ (21.21 mmol, 800 mg) was added. The resulting mixture was stirred at room temperature for 3 h (TLC AcOEt/petroleum ether 1:9) and then concentrated to dryness, taken in Et₂O (100 mL) and washed with NaOH_{aq} 10% (75 mL). The layers were separated and the aqueous one extracted with Et₂O (2 x 10 mL). The combined organic phases were washed with brine (2 x 50 mL), dried over MgSO₄ and concentrated to dryness. 1-(2-Benzyloxyphenyl)-methanol was obtained as a colourless oil (2.78 g, 92%) that was used without further purifications.

IR (KBr) ν (cm⁻¹): 696, 750, 758, 804, 982, 1004, 1204, 1222, 1436, 1454, 2866, 2940, 3028, 3050, 3510. ¹H-NMR: (250 MHz, CDCl₃) δ 4.74 (2H, s), 5.13 (2H, s), 7.00– 6.95 (2H, *m*), 7.41- 7.25 (7 H, *m*). ¹³C{¹H}- NMR: (62.9 MHz, CDCl₃) δ 62.3 (CH₂), 70.2 (CH₂), 111.8 (CH), 121.2 (CH), 127.5 (2xCH), 128.3 (CH), 128.9 (2xCH), 129.0 (CH), 129.1 (CH), 129.6 (C), 136.9 (C), 156.7 (C). MS (ESI): 215.1 [M + H]⁺. HR-MS (ESI): calcd for C₁₄H₁₅O₂: 215.1072; found 215.1074.

1-(benzyloxy)-2-(bromomethyl)benzene (7b)

To a solution of alcohol (2-(benzyloxy)phenyl)methanol (12.13 mmol, 2.6 g) in dry toluene (60 mL), at 0 °C and under N₂ atmosphere, was added dropwise a solution of PBr₃ (13.34 mmol, 1.29 mL) in dry toluene (11 mL). The mixture was stirred on ice-bath for 20 minutes and then at room temperature for another 30 minutes. The solution was diluted with ice water (60 mL) and toluene (30 mL) and stirred vigorously for 3 minutes. The organic phase was separated, washed with brine (30 mL), dried over MgSO₄ and concentrated. Column chromatography of the crude product, using petroleum ether/AcOEt 9:1 as eluant, afforded compound **7b** as a white solid (85 %).

7b: Mp: 82-84 °C. IR (KBr) ν (cm⁻¹): 696, 751, 1025, 1048, 1095, 1194, 1222, 1251, 1452, 1492, 1601, 2866, 3032, 3064. ¹H-NMR: (250 MHz, CDCl₃) δ 4.63 (2H, s), 5.17 (2H, s), 6.94– 6.91 (2H, m), 7.41– 7.28 (5H, m), 7.52– 7.49 (2H, m). ¹³C{¹H}-NMR: (75 MHz, CDCl₃) δ 29.3 (CH₂), 70.2 (CH₂), 112.5 (CH), 121.2 (CH), 126.7 (C), 127.3 (2xCH), 128.1 (CH), 128.8 (2xCH), 130.4 (CH), 131.2 (CH), 137.0 (C), 156.7 (C). MS (ESI): 277.1 [M + H]⁺. HR-MS (ESI): calcd for C₁₄H₁₄OBr: 277.0228; found 276.02230.

[Bis-(2-benzyloxybenzyl)]-(2-benzyloxy-3-phenylbenzyl)amine (8a)

Compound **7b** (3.77 mmol, 1.04 g), amine **6a** (1.71 mmol, 558 mg) and K₂CO₃ (8.55 mmol, 1.18 g) were dissolved in dry CH₃CN (18 mL) under nitrogen and refluxed for 44 hours (TLC AcOEt/petroleum ether 1:9). After cooling down to room temperature, the mixture was filtered over Celite and concentrated. The residue was dissolved in CHCl₃ (120 mL) and washed with diluted brine (50 mL). The aqueous phase was re-extracted with CHCl₃ (2 x 50 mL). The organic layers were dried over Na₂SO₄ and concentrated. The recovered yellow oil (1.246 g, 96%) was used directly in the next step.

8a: IR (KBr) ν (cm⁻¹): 696, 734, 753, 795, 858, 910, 1026, 1079, 1097, 1237, 1288, 1372, 1430, 1452, 1498, 1587, 1601, 2247, 2864, 2929, 3032, 3063. ¹H-NMR: (250 MHz, CDCl₃) δ 3.85 (6H, s), 4.37 (2H, s), 5.06 (4H, s), 6.88– 7.05 (6H, m), 7.15– 7.48 (20H, m), 7.62 (2H, d, *J* = 8.3, 1.8 Hz), 7.80 (2H, d, *J* = 7.8, 1.4 Hz), 7.86 (2H, d, *J* = 7.4, 1.4 Hz). ¹³C{¹H}-NMR: (62.9 MHz, CDCl₃) δ 52.6 (2xCH₂), 52.9 (CH₂), 70.0 (2xCH₂), 74.8 (CH₂), 111.6 (2xCH), 121.0 (2xCH), 124.6 (CH), 127.2 (CH), 127.3 (5xCH), 127.5 (CH), 127.9 (2xCH), 128.0 (CH), 128.3 (2xCH), 128.4 (CH), 128.5 (2xCH), 128.6 (5xCH), 128.7 (C), 128.9 (CH), 129.4 (CH), 129.49 (2xCH), 129.51 (2xCH), 134.2 (C), 135.2 (C), 137.2 (2xC), 137.5 (2xC), 139.0 (C), 154.5 (C), 156.9 (2xC). MS (ESI): 758.4 [M + H]⁺. HR-MS (ESI): calcd for C₄₈H₄₄NO₃: 682.3321; found 682.3323.

(2-benzyloxybenzyl)-[bis-(2-benzyloxy-3-phenylbenzyl)]-amine (8b)

The starting 1-(2-Benzyloxybiphenyl-3-yl)-methanol **7a** (1.9 mmol, 671 mg), amine **6b** (0.86 mmol, 184 mg) and K₂CO₃ (4.32 mmol, 596 mg) were suspended in dry CH₃CN (9 mL) under N₂-atmosphere and refluxed for 45 h (TLC AcOEt/petroleum ether 1:9). The mixture was diluted with AcOEt, filtered and concentrated. The residue was dissolved in CHCl₃ (60 mL) and washed with diluted brine (25 mL). The aqueous layer re-extracted with CHCl₃ (2 x 25 mL) and the combined organic phase was dried over Na₂SO₄ and concentrated. Column

chromatography on silica gel of the crude dark brown oil (733 mg), using AcOEt/petroleum ether 1:9 and 0.1 % Et₃N as eluant, afforded the product **8b** as a yellow oil (522 mg, 80%).

8b: IR (KBr) ν (cm⁻¹): 697, 735, 765, 798, 864, 910, 1018, 1079, 1102, 1203, 1259, 1368, 1429, 1452, 1498, 1587, 1600, 2248, 2865, 2909, 3031, 3062. ¹H-NMR: (250 MHz, CDCl₃) δ 3.80 (6H, s), 4.33 (4H, s), 5.06 (2H, s), 6.89- 7.02 (6H, m), 7.13-7.45 (22H, m), 7.60 (4H, m), 7.72 (1H, d, *J* = 7.4 Hz), 7.81 (2H, d, *J* = 7.4 Hz). ¹³C{¹H}-NMR: (62.9 MHz, CDCl₃) δ 52.8 (CH₂), 52.9 (2xCH₂), 70.1 (CH₂), 75.0 (2xCH₂), 111.8 (CH), 121.1 (CH), 124.6 (2xCH), 127.3 (CH), 127.4 (2xCH), 127.7 (CH), 127.9 (CH), 128.1 (2xCH), 128.4 (5xCH), 128.4 (4xCH), 128.5 (C), 128.6 (5xCH), 128.7 (2xCH), 129.0 (2xCH), 129.3 (CH), 129.6 (4xCH), 129.7 (CH), 134.0 (2xC), 135.3 (2xC), 137.2 (2xC), 137.5 (C), 139.0 (2xC), 154.6 (2xC). MS (ESI): 758.4 [M + H]⁺. HR-MS (ESI): calcd for C₅₄H₄₈NO₃: 758.3634; found 758.3636.

[Bis-(2-hydroxybenzyl)]-(2-hydroxy-3-phenylbenzyl)amine (**4a**)

Compound **8a** (1.65 mmol, 1.246 g) was dissolved in AcOEt (80 mL) and 10% Pd/C (125 mg) was added under nitrogen. A H₂-atmosphere was applied and the reaction mixture was stirred 8 h at room temperature, till the conversion, monitored by ¹H-NMR, was complete. The mixture was filtered through a pad of Celite and concentrated, resulting in isolation of a light brown oil. Radial chromatography of the crude product on silica gel, using petroleum ether (b.p. 40-60 °C)/ethyl acetate 8:2 and 0.1% Et₃N as eluant, afforded **4a** as a light brownish solid (660 mg, 97%).

4a: Mp: 173-175°C. IR (KBr) ν (cm⁻¹): 700, 755, 1039, 1087, 1236, 1372, 1432, 1460, 1489, 1592, 2814, 3056, 3386. ¹H-NMR: (250 MHz, CDCl₃) δ 3.77 (6H, s), 6.77- 7.34 (16H, s). ¹³C{¹H}-NMR: (62.9 MHz, CD₃OD) δ 56.0 (CH₂), 56.7 (2xCH₂), 116.5 (2xCH), 119.9 (2xCH), 120.3 (CH), 122.4 (C), 122.9 (C), 127.5 (CH), 128.8 (2xCH), 129.3 (C), 129.5 (2xCH), 129.6 (2xCH), 130.5 (CH), 130.7 (CH), 131.0 (2xCH), 137.3 (C), 152.1 (C), 156.1 (2xC). MS (ESI): 412.2 [M + H]⁺. HR-MS (ESI): calcd for C₂₇H₂₆NO₃: 412.1912; found 412.1914.

(2-hydroxybenzyl)-[bis-(2-hydroxy-3-phenylbenzyl)]-amine (**4b**)

Amine **8b** (0.508 mmol, 385 mg) was dissolved in AcOEt (24 mL) and 10% Pd/C (77 mg) was added under N₂-atmosphere. The mixture was stirred under H₂-atmosphere (1 atm) and the conversion was monitored by ¹H NMR. After 3.5 h the solution was filtered through a pad of Celite and concentrated, resulting in isolation of yellow oil (260 mg). The compound was crystallized from CHCl₃/hexane, resulting in small white crystals (164 mg, 66%).

4b: Mp: 154-156°C. IR (KBr) ν (cm⁻¹): 699, 754, 788, 829, 961, 1067, 1218, 1373, 1432, 1461, 1498, 1590, 2817, 3031, 3051, 3344. ¹H-NMR: (250 MHz, CDCl₃) δ 3.81 (6H, s), 6.80 (2H, t, *J* = 7.8 Hz), 6.89 (2H, t, *J* = 7.8 Hz), 7.08- 7.17 (6H, m), 7.35- 7.44 (10H, m). ¹³C{¹H}-NMR: (62.9 MHz, CDCl₃) δ 55.7 (2xCH₂), 57.0 (CH₂), 116.5 (CH), 120.0 (CH), 120.4 (2xCH), 122.9 (C), 123.6 (2xC), 127.8 (2xCH), 128.9 (C), 129.2 (4xCH), 129.3 (CH), 129.5 (4xCH), 130.2 (2xCH), 130.5 (CH), 130.8 (2xCH), 137.4 (C), 152.1 (2xC), 156.3 (C). MS (ESI): 488.2 [M + H]⁺. HR-MS (ESI): calcd for C₃₄H₃₀NO₃: 488.2225; found 488.2227.

***In situ* synthesis of mononuclear titanatranes (2a) and (9a-b)**

Complexes were prepared in glovebox by mixing homogeneous solutions of the corresponding ligands (0.10 M) and Ti(O*i*-Pr)₄ (0.18 M) in dry CDCl₃ in a 1:1 ratio to a final concentration 0.01 M of the complex. Bright yellow solutions were obtained which were used without further purifications and without removing the three equivalents of *i*-PrOH released from the metal precursor. In all cases resonances relative to free *iso*-propanol released in the reaction were present in the NMR spectra: ¹H-NMR (300 MHz, CDCl₃): 4.04 (1H, *hept*, *J* = 6.1 Hz), 1.22 (6H, *d*, *J* = 6.1 Hz). ¹³C-NMR (75 MHz, CDCl₃): δ 64.5 (CH), 25.1 (CH₃).

Ti(IV)/1a Complex (2a): ¹H NMR: (300 MHz, CDCl₃) δ 1.02 (6H, *d*, *J* = 6.0 Hz), 3.62 (6H, *bs*), 4.64 (1H, *hept*, *J* = 6.0 Hz), 6.91 (3H, *m*), 7.10 (3H, *m*), 7.25–7.41 (12H, *m*), 7.64–7.68 (6H, *m*).

Ti(IV)/4a Complex (9a): ¹H NMR: (300 MHz, CDCl₃) δ 1.34 (6H, *d*, *J* = 6.0 Hz), 3.50 (6H, *bs*), 4.97 (1H, *hept*, *J* = 6.0 Hz), 6.74 (2H, *d*, *J* = 8.0 Hz), 6.86–6.81 (2H, *m*), 6.93–6.88 (1H, *m*), 7.09 (3H, *m*), 7.15 (2H, *t*, *J* = 7.6 Hz), 7.32–7.29 (2H, *m*), 7.43–7.38 (2H, *m*), 7.66 (2H, *d*, *J* = 7.7 Hz).

Ti(IV)/4b Complex (9b): ¹H NMR: (300 MHz, CDCl₃) δ 1.27 (6H, *d*, *J* = 6.0 Hz), 3.58 (6H, *bs*), 4.78 (1H, *hept*, *J* = 6.0 Hz), 6.74 (2H, *d*, *J* = 8.0 Hz), 6.93–6.81 (3H, *m*), 7.11–7.08 (3H, *m*), 7.18 (3H, *t*, *J* = 7.6 Hz), 7.32–7.31–7.26 (4H, *m*), 7.41–7.36 (4H, *m*), 7.65 (4H, *d*, *J* = 7.6 Hz). ¹³C{¹H}-NMR: (75 MHz, CDCl₃) δ 24.6, 24.7, 60.0, 62.5, 77.58, 116.4, 117.7, 118.0, 124.7, 125.7, 125.9, 127.2, 127.3, 128.0, 128.5, 128.6, 129.0, 129.04, 138.9, 159.1, 160.8.

Synthesis of Ti(IV) μ-oxo complex (3)

In the case of titanatrane complex **2a** (R=H) addition of water allows the complete formation of complex **3**, which crystallizes out of the solution. Filtration and washing with cold benzene allows the recovery of complex **3** as a yellow crystalline compound (87%).

3: Mp > 300 °C. IR (KBr) ν (cm⁻¹): 3433, 3054, 2882, 1585, 1455, 1424, 1269, 1240, 1065, 874, 753, 694. ¹H NMR: (300 MHz, CDCl₃) δ 3.28 (6H, *d*, *J* = 13.9 Hz), 4.36 (6H, *d*, *J* = 13.9 Hz), 6.23 (6H, *t*, *J* = 7.3 Hz), 6.58 (12H, *t*, *J* = 7.4 Hz), 6.68 (12H, *d*, *J* = 7.4 Hz), 6.96 (6H, *t*, *J* = 7.4 Hz), 7.19 – 7.26 (12H, *m*). ¹³C{¹H}-NMR: (75 MHz, DMSO-*d*₇) δ 60.8 (6xCH₂), 118.6 (6xC), 126.5 (6xCH), 127.0 (6xCH), 127.1(6xCH), 127.8 (12xCH), 129.2 (12xCH), 129.4 (6xC), 129.8 (6xCH), 139.4 (6xC), 160.0 (6xC). MS (ESI): 1233. 4 [M + H]⁺; 1255. 5 [M + Na]⁺; 1271.3 [M + K]⁺. HRMS: calcd for C₇₈H₆₁N₂O₇Ti₂: 1233;3451 found 1233.3454.

Crystal Data for 3: {O[(Ti N (C₁₃H₁₀O)₃]₂} (C₆H₆)₂ (CHCl₃)_{0.6}, *M* = 1461.0, monoclinic, space group *P*2₁/*n*, *a* = 13.2828(8), *b* = 15.6644(7), *c* = 18.5844(12) Å, β = 105.269(7)°, *V* = 3730.3(4) Å³, *Z* = 2, *T* = 200 K, μ = 0.34 mm⁻¹, *D*_c = 1.301 g.cm⁻³, λ(MoKα) = 0.71073 Å, 27925 measured reflections, 7259 unique (*R*_{int} = 0.084) from which 3203 with |*F*_o| > 4σ(*F*_o). The structure was solved by direct methods (SIR-97) and refined by full matrix least-square (XTAL 3.2) on *F*. *R* = 0.046, ω*R* = 0.043, GOF = 1.35(2)

Synthesis of Ti(IV) μ-oxo complex (10)

Complex **3** (1.599 mmol, 1.97 g) was weighed in a double necked round bottom flask and then dry CH₂Cl₂ (20 mL) was added under nitrogen. To the resulting suspension, *N*-bromosuccinimide (9.916 mmol, 1.76 g) was added in one pot and the mixture was stirred for half an hour at room temperature, till the suspension became dark green. The mixture

was washed with H₂SO₄ aq 10% and extracted with dichloromethane (3x20 mL). The organic layers were dried over Na₂SO₄ and concentrated, affording a yellow-brown solid **10**.

10: Mp > 300 °C. IR (KBr) ν (cm⁻¹): 3435, 3054, 1635, 1456, 1436, 1429, 1268, 1236, 1114, 875, 779, 767, 742, 715, 695, 638, 596. ¹H NMR: (250 MHz, CDCl₃) δ 3.21 (6H, *d*, *J* = 14.0 Hz), 4.23 (6H, *d*, *J* = 14.0 Hz), 6.36- 6.38 (6H, *m*), 6.58- 6.56 (24H, *m*), 7.32 (6H, *d*, *J* = 2.2 Hz), 7.38 (6H, *d*, *J* = 2.2 Hz). MS (ESI): 1729.1 [M + Na]⁺; 1744.8 [M + K]⁺. HR-MS (ESI): calcd for C₇₈H₅₄Br₆N₂NaO₇Ti₂: 1728.7826; found 1728.7828.

Crystal Data for 10: O[TiN(C₁₃H₉BrO)₃]₂ (CH₂Cl₂)₆, *M* = 2216.2, trigonal, space group *R* $\bar{3}c$. Unit Cells Dimensions, lengths *a* = 22.9789 (12), *b* = 22.9789 (12), *c* = 28.4726 (16) Å, angles α = β = 90°, γ = 120°. Volume *V* = 13020.2(12) Å³, *Z* = 6, *T* = 150 K, Absorption coefficient μ = 3.370 mm⁻¹. Density d_x = 1.696 g·cm⁻³. λ (MoK α) = 0.7107 Å, 41601 measured reflections, 2834 unique (*R*_{int} = 0.085) from which 1496 with $|F_o| > 4\sigma(F_o)$. The structure was solved by direct methods (SIR-97) and refined by full matrix least-square (XTAL 3.2) on *F*. *R* = 0.029, ωR = 0.027, GOF = 1.04(2).

3-bromo-2-hydroxy-5-methylbenzaldehyde (**13**)

To a solution of 2-bromo-4-methylphenol (82.71 mmol, 10 mL) in dry THF (165 mL) under N₂ atmosphere, TEA (165.42 mmol, 23.1 mL) and MgCl₂ (124.06 mmol, 11.8 g) were added. The resulting mixture was stirred for 40 min at room temperature and then paraformaldehyde was added (413.6 mmol, 12.4 g). The reaction mixture was thermostated at 90 °C, left under reflux for 4 h and then cooled to room temperature. Then it was filtered over Celite washing with AcOEt (150 mL) and finally washed with HCl 1 M (150 mL). The organic phase was separated, washed with brine (2 x 100 mL), dried over MgSO₄ and concentrated in vacuum to give a pale brown solid **13** (16.4 g, 92%).

13: Mp: 56- 57 °C. IR (KBr) ν (cm⁻¹): 1009, 1043, 1150, 1191, 1242, 1276, 1300, 1377, 1413, 1457, 1650, 2846. ¹H-NMR: (250 MHz, CDCl₃) δ 2.34 (3H, *s*), 7.32 (1H, *d*, *J* = 1.4 Hz), 7.61 (1H, *d*, *J* = 1.4 Hz), 9.81 (1H, *s*), 11.39 (1H, *s*). ¹³C{¹H}-NMR: (62.9 MHz, CDCl₃) δ 20.2 (CH₃), 110.9 (C), 130.0 (C), 130.8 (C), 133.1 (CH), 140.9 (CH), 156.1 (C), 196.2 (CHO). GC-MS: 214 (100, M⁺), 196 (8), 185 (5), 168 (7), 157 (3), 106 (13), 77 (34), 51 (14).

2-Benzyloxy-3-bromo-5-methylbenzaldehyde (**14**)

A mixture of 3-bromo-2-hydroxy-5-methylbenzaldehyde **13** (76.1 mmol, 16.4 g), K₂CO₃ (305 mmol, 42 g), and benzyl bromide (87.5 mmol, 10.41 mL) in CH₃CN (152 mL) was refluxed for 18 h. The mixture was filtered through a pad of Celite washed with ethyl acetate and the filtrate was concentrated under reduced pressure. The resulting pale yellow oil was diluted in CHCl₃ (100 mL) and washed with HCl 1M (2 x 100 mL) and brine (2 x 100 mL). The organic layer was dried over MgSO₄ and the solvents were removed in vacuum. The crude product was washed with hexane, obtaining compound **14** in quantitative yield as a white solid.

14: Mp: 56- 57 °C. IR (NaCl) ν (cm⁻¹): 1003, 1107, 1228, 1257, 1370, 1459, 1497, 1598, 1693, 2738, 2852, 2888, 2950, 3032, 3068. ¹H-NMR: (250 MHz, CDCl₃) δ 2.30 (3H, s), 5.04 (2H, s), 7.18– 7.46 (5H, *m*), 7.52 (1H, *d*, *J* = 1.0 Hz), 7.62 (1H, *d*, *J* = 1.0 Hz), 10.03 (1H, s). ¹³C{¹H}-NMR: (62.9 MHz, CDCl₃) δ 20.7 (CH₃), 77.9 (CH₂), 118.2 (C), 128.0 (CH), 129.0 (2×CH), 129.05 (2×CH), 129.1 (CH), 131.1 (C), 135.5 (C), 136.2 (C), 140.2 (CH), 156.4 (C), 189.4 (CHO). GC-MS: 304 (2, M⁺), 277 (8), 213 (5), 91 (100). Anal. Calcd. for C₁₅H₁₃BrO₂: C 59.04, H 4.29. Found: C 59.04, H 4.11.

Tris-(2-benzyloxy-3-bromo-5-methyl-benzyl)amine (12)

Substrate 2-Benzyloxy-3-bromo-5-methylbenzaldehyde **14** (65.5 mmol, 20 g) was weighed in a double necked round bottom flask, then dry THF (198 mL) and ammonium acetate (21.5 mmol, 1.66 g) were added under N₂. After 40 min under stirring, sodium triacetoxy borohydride (96.8 mmol, 20.5 g) was added and the mixture was stirred for 48 h at room temperature (TLC petroleum ether/AcOEt 7:3) and then evaporated to dryness. The residue was dissolved in Et₂O (100mL) and washed with KOH_{aq} 15% (2 x 100 mL) and brine (2 x 100 mL). Drying over MgSO₄ and evaporation of the solvent gave the crude product that was further purified by crystallization in CHCl₃/EtOH 8:11, affording the final product **12** as a white solid (70%).

12: Mp: 163–164 °C. IR (NaCl) ν (cm⁻¹): 1127, 1221, 1270, 1370, 1453, 1497, 2867, 2921, 3030, 3063. ¹H-NMR: (250 MHz, CDCl₃) δ 2.23 (9H, s), 3.55 (6H, s), 4.79 (6H, s), 7.24– 7.39 (21H, *m*). ¹³C{¹H}-NMR: (62.9 MHz, CDCl₃) δ 20.9 (3×CH₃), 52.5 (3×CH₂), 75.4(3×CH₂), 117.4 (3×C), 128.3 (3×CH), 128.4 (6×CH), 128.6 (3×CH), 130.1 (3×CH), 132.6 (3×CH), 134.3 (3×C), 135.4 (3×C), 137.0 (3×C), 151.9 (3×C). MS (ESI): 884.7 [M + H]⁺. HR-MS (ESI): calcd for C₄₅H₄₃Br₃NO₃: 884.07726; found 884.07728.

3-cyanophenyl boronic acid (15d)

Substrate 3-bromobenzonitrile (13.87 mmol, 2.52 g) was weighed in a double necked round bottom flask, then dry THF (70 mL) was added under N₂, followed by triisopropylborate (38.82 mmol, 9 mL). The solution was cooled down to -78 °C and then butyl lithium (15.25 mmol, 9.5 mL, 1.6 M in hexane) was added dropwise. After 45 min at -78 °C, the solution was warmed up to room temperature and magnetically stirred for 1 h. It was washed with 2N HCl (40 mL) and the resulting suspension was stirred for 12, then extracted with Et₂O (3×40 mL). The combined organic phases were dried over MgSO₄ and the solvents evaporated under vacuum, obtaining a solid which was further washed with CH₂Cl₂ and filtered to give product **15d** as a white solid (70%).

15d: ¹H-NMR: (250 MHz, CDCl₃) δ 7.39 (1H, *t*, *J* = 8.0 Hz), 7.61 (1H, *d*, *J* = 7.7 Hz), 7.75 (1H, *d*, *J* = 8.0 Hz), 7.79 (1H, s).

3-(methoxycarbonyl)phenyl boronic acid (15e)

H₂SO₄ (7 mL) was added to a solution of substrate 3-(dihydroxyboryl)benzoic acid (7.79 mmol, 1.29 g) in methanol (70 mL) and the reaction mixture was refluxed for 24 h. After

cooling down to room temperature, the solution was washed with NaHCO₃ till pH= 7. The aqueous phase was extracted with AcOEt (3×125 mL) and the combined organic phases were dried over Na₂SO₄ and concentrated to dryness, affording product **15e** as a white solid (94%).

15e: ¹H-NMR: (250 MHz, CDCl₃) δ 3.89 (3H, s), 7.45 (1H, bs), 7.82- 8.03 (2H, m), 8.25- 8.41 (1H, m).

General procedure for the synthesis of Tris-(2-benzyloxy-3-aryl-5-methyl-benzyl)amine (16):

Substrate **12** (2.8 mmol, 2.5 g) and boronic acid **15** (16.9 mmol) were added to a Schlenk tube under nitrogen. The Schlenk tube was evacuated and then refilled with nitrogen. Degassed dioxane (31 mL), degassed Na₂CO_{3(aq)} 2M (40 mL) and finally the palladium source Pd(PPh₃)₄ (0.28 mmol, 323 mg) were added to the Schlenk tube. The reaction was stirred at 100°C for 15 h. At the conclusion of the reaction, which was checked by ESI-MS, the reaction mixture was cooled down to room temperature, filtered over Celite and then concentrated under vacuum. The residue was diluted with CH₂Cl₂ (50 mL), washed with NaOH 1M (2 x 50 mL) and NaCl_{aq} sat. (2 x 50 mL) for ligands **16 a-e**; for ligand **16f** the solution was washed only with water (3 x 50 mL). The organic phase was dried over Na₂SO₄, concentrated and the residue purified by column chromatography on silica gel, affording compound **16**.

16a: white solid. yield: 88%. Mp: 120-122 °C. IR (KBr) ν (cm⁻¹): 695, 735, 980, 1207, 1360, 1374, 1457, 1464, 1496, 2862, 2912, 3031, 3060, 3447. ¹H-NMR: (250 MHz, CDCl₃) δ 2.37 (9H, s), 3.80 (6H, s), 4.29 (6H, s), 6.94 (6H, d, J = 7.8 Hz), 7.07- 7.15 (9H, m), 7.32- 7.40 (9H, m), 7.56 (12H, t, J = 7.8 Hz). ¹³C{¹H}-NMR: (62.9 MHz, CDCl₃) δ 21.1 (3×CH₃), 52.7 (3×CH₂), 75.2 (3×CH₂), 127.2 (3×CH), 128.0 (3×CH), 128.3 (12×CH), 128.6 (6×CH), 129.6 (6×CH), 130.0 (3×CH), 130. (3×CH), 133.4 (3×C), 133.7 (3×C), 135.1 (3×C), 137.3 (3×C), 139.2 (3×C), 152.6 (3×C). MS (ESI): 876.6 [M + H]⁺. HR-MS (ESI): calcd for C₆₃H₅₈NO₃: 876.44167; found 876.44169.

16b: white solid. yield: 84%. Mp: 165-167 °C. IR (NaCl) ν (cm⁻¹): 1160, 1184, 1215, 1228, 1265, 1270, 1288, 1362, 1457, 1468, 1510, 1631. ¹H-NMR: (250 MHz, CDCl₃) δ 2.34 (9H, s), 3.69 (9H, s), 3.79 (6H, s), 4.34 (6H, s), 6.83 (6H, dd, J = 7.8, 1.5 Hz), 6.89- 7.46 (24H, m), 7.57 (3H, d, J = 2.4 Hz). MS (ESI): 966.4 [M + H]⁺. HR-MS (ESI): calcd for C₆₆H₆₄NO₆: 966.47336; found 966.47338.

16c: white solid. yield: 82%. Mp: 168-169 °C. IR (NaCl) ν (cm⁻¹): 1154, 1205, 1225, 1265, 1284, 1360, 1456, 1464, 1506, 1630. ¹H-NMR: (250 MHz, CDCl₃) δ 2.36 (9H, s), 3.71 (9H, s), 3.80 (6H, s), 4.33 (6H, s), 6.83- 7.25 (30H, m), 7.57 (3H, s). ¹³C{¹H}-NMR: (62.9 MHz, CDCl₃) 21.3 (3×CH₃), 52.8 (3×CH₂), 55.4 (3×CH₃), 75.2 (3×CH₂), 113.4 (3×CH), 114.6 (3×C), 122.0 (3×C), 127.9 (3×C), 128.4 (6×CH), 128.6 (6×CH), 129.3 (3×CH), 130.0 (3×C), 130.2 (3×C), 133.4 (3×CH), 133.7 (3×CH), 134.9 (3×CH), 137.3 (3×CH), 140.5 (3×C), 152.5 (3×CH), 159.6 (3×C). MS (ESI): 966.4 [M + H]⁺. HR-MS (ESI): calcd for C₆₆H₆₄NO₆: 966.47336; found 966.47338.

16d: white solid. yield: 67%. Mp: 173-175 °C. IR (KBr) ν (cm⁻¹): 694, 733, 1154, 1211, 1364, 1453, 2229, 2859, 2913, 3032, 3066. ¹H-NMR: (250 MHz, CDCl₃) δ 2.37 (9H, s), 3.79 (6H, s), 4.30 (6H, s), 6.91 (6H, *dd*, *J* = 7.8, 1.8 Hz), 7.02 (3H, *d*, *J* = 1.8 Hz), 7.11- 7.20 (6H, *m*), 7.42 (3H, *t*, *J* = 7.8 Hz), 7.52 (3H, *t*, *J* = 2.3 Hz), 7.62 (3H, *t*, *J* = 7.8 Hz), 7.70- 7.85 (9H, *m*). ¹³C{¹H}-NMR: (62.9 MHz, CDCl₃) 21.0 (3×CH₃), 52.2 (3×CH₂), 75.6 (3×CH₂), 112.2 (3×C), 118.7 (3×C), 128.0 (6×CH), 128.2 (6×CH), 128.8 (3×CH), 129.7 (3×CH), 130.0 (3×CH), 130.5 (3×CH), 131.0 (3×CH), 131.3 (3×CH), 131.7 (3×CH), 132.7 (3×C), 133.1 (3×C), 133.8 (3×CH), 133.9 (3×C), 136.3 (3×C), 139.9 (3×C), 152.2 (3×C). MS (ESI): 951.2 [M + H]⁺. HR-MS (ESI): calcd for C₆₆H₅₅N₄O₃: 951.42742; found 951.42744.

16e: white solid. yield: 66%. Mp: 123-125 °C. IR (KBr) ν (cm⁻¹): 696, 752, 816, 867, 1082, 1111, 1264, 1366, 1436, 1454, 1723, 2859, 2920, 2948, 3030, 3062. ¹H-NMR: (250 MHz, CDCl₃) δ 2.38 (9H, s), 3.80 (6H, s), 3.89 (9H, s), 4.31 (6H, s), 6.94 (6H, *dd*, *J* = 7.7, 1.6 Hz), 7.08- 7.16 (12H, *m*), 7.41 (3H, *t*, *J* = 7.7 Hz), 7.53 (3H, *d*, *J* = 2.2 Hz), 7.79 (3H, *d*, *J* = 7.7 Hz), 8.00 (3H, *d*, *J* = 7.7 Hz), 8.24 (3H, s). ¹³C{¹H}-NMR: (62.9 MHz, CDCl₃) 21.3 (3×CH₃), 52.3 (3×CH₃), 52.6 (3×CH₂), 75.5 (3×CH₂), 128.0 (3×CH), 128.37 (3×CH), 128.40 (12×CH), 128.5 (12×CH), 130.2 (3×CH), 130.40 (3×C), 130.44 (3×CH), 130.6 (3×CH), 133.4 (3×C), 134.0 (3×C), 134.1 (3×C), 134.4 (3×CH), 137.0 (3×C), 139.3 (3×C), 152.5 (3×C), 167.3 (3×C=O). MS (ESI): 1050.2 [M + H]⁺. HR-MS (ESI): calcd for C₆₉H₆₄NO₉: 1050.45811; found 1050.45813.

16f: white solid. yield: 90%. Mp: 124- 126 °C. IR (KBr) ν (cm⁻¹): 696, 735, 780, 1155, 1206, 1368, 1454, 1698, 2859, 2919, 3030, 3062. ¹H-NMR: (250 MHz, CDCl₃) δ 2.39 (9H, s), 3.84 (6H, s), 4.31 (6H, s), 6.91 (6H, *dd*, *J* = 7.8, 1.5 Hz), 7.07- 7.17 (12H, *m*), 7.47- 7.56 (6H, *m*), 7.84 (6H, *dd*, *J* = 7.7, 1.8 Hz), 8.04 (3H, s), 9.93 (3H, s). ¹³C{¹H}-NMR: (62.9 MHz, CDCl₃) 21.3 (3×CH₃), 52.5 (3×CH₂), 75.6 (3×CH₂), 128.1 (6×CH), 128.36 (6×CH), 128.43 (6×CH), 129.0 (3×CH), 130.1 (3×CH), 130.9 (3×CH), 131.2 (3×CH), 133.3 (3×C), 133.7 (3×C), 134.1 (3×C), 135.7 (3×CH), 136.6 (3×C), 136.7 (3×C), 139.9 (3×C), 152.5 (3×C), 192.5 (3×CHO). MS (ESI): 960.6 [M + H]⁺. HR-MS (ESI): calcd for C₆₆H₅₈NO₆: 960.42641; found 960.42643.

Tris-(2-hydroxy-3-aryl-5-methyl-benzyl)amine (17)

Substrate **16** (2 mmol) was weighed in a double necked round bottom flask, AcOEt (100 mL) and 10% Pd/C were added under nitrogen. After three H₂/vacuum cycles, the suspension was let under H₂ (balloon pressure) and stirred at room temperature for 3 h. Then it was filtered over Celite and concentrated under vacuum. After a column chromatography on silica gel, **17** was isolated in high yields (82- 89%).

17a: white solid. yield: 89%. Mp: 148- 150 °C. IR (KBr) ν (cm⁻¹): 698, 785, 862, 1102, 1214, 1437, 1476, 1497, 2916, 2972, 3393. ¹H-NMR: (250 MHz, CDCl₃) δ 2.26 (9H, s), 3.83 (6H, s), 6.92 (3H, s), 6.94 (3H, s), 7.34- 7.43 (15H, *m*). ¹³C{¹H}-NMR: (62.9 MHz, CDCl₃) δ 20.7 (3×CH₃), 56.6 (3×CH₂), 123.2 (3×C), 127.5 (3×CH), 128.6 (3×C), 128.8 (6×CH), 129.0 (3×C), 129.5 (6×CH), 130.6 (3×CH), 131.0 (3×CH), 138.0 (3×C), 150.3 (3×C). MS (ESI): 606.2 [M + H]⁺. HR-MS (ESI): calcd for C₄₂H₄₀NO₃: 606.30082; found 606.30084.

17b: white solid. yield: 85%. Mp: 170- 172 °C. IR (NaCl) ν (cm⁻¹): 1063, 1090, 1133, 1244, 1265, 1450, 1464, 1617, 2990. ¹H-NMR: (250 MHz, CDCl₃) δ 2.26 (9H, s), 3.68 (9H, s), 3.84 (6H, s), 6.90- 7.10 (12H, m), 7.22- 7.38 (6H, m). MS (ESI): 696.3 [M + H]⁺. HR-MS (ESI): calcd for C₄₅H₄₆NO₆: 696.33251; found 696.33253.

17c: white solid. yield: 82%. Mp: 168-169 °C. IR (NaCl) ν (cm⁻¹): 1064, 1089, 1133, 1240, 1265, 1448, 1464, 1617, 2980. ¹H-NMR: (250 MHz, CDCl₃) δ 2.26 (9H, s), 3.68 (9H, s), 3.84 (6H, s), 6.90- 7.10 (12H, m), 7.22- 7.38 (6H, m). ¹³C{¹H}-NMR: (62.9 MHz, CDCl₃) 20.6, 55.3, 56.6, 113.5, 114.6, 121.7, 123.5, 128.6, 128.8, 129.2, 129.8, 131.0, 139.4, 150.2, 155.0, 159.9. MS (ESI): 696.3 [M + H]⁺. HR-MS (ESI): calcd for C₄₅H₄₆NO₆: 696.33251; found 696.33253

17d: white solid. yield: 85%. Mp: 197- 199 °C. IR (KBr) ν (cm⁻¹): 699, 728, 801, 1106, 1227, 1470, 1481, 2224, 2837, 2917, 3054, 3322. ¹H-NMR: (250 MHz, CDCl₃) δ 2.22 (9H, s), 3.73 (6H, s), 5.77 (3H, bs), 6.76 (6H, d, J = 5.8 Hz), 7.36- 7.41 (9H, m), 7.52 (3H, d, J = 6.6 Hz). ¹³C{¹H}-NMR: (62.9 MHz, CDCl₃) δ 20.4 (3×CH₃), 65.8 (3×CH₂), 112.3 (3×C), 118.8 (3×C), 124.1 (3×C), 126.5 (3×C), 129.1 (3×CH), 129.8 (3×C), 130.2 (3×CH), 130.5 (3×CH), 131.5 (3×CH), 132.7 (3×CH), 133.6 (3×CH), 138.7 (3×C), 149.5 (3×C). MS (ESI): 681.3 [M + H]⁺. HR-MS (ESI): calcd for C₄₅H₃₇N₄O₃: 681.28657; found 681.28655.

17e: white solid. yield: 82%. Mp: 106- 108 °C. IR (KBr) ν (cm⁻¹): 744, 748, 913, 1118, 1265, 1437, 1480 1722, 2841, 2919, 2951,3401. ¹H-NMR: (250 MHz, CDCl₃) δ 2.25 (9H, s), 3.81 (6H, s), 3.84 (9H, s), 5.59 (3H, bs), 6.90 (6H, d, J = 15.4, 1.6 Hz), 7.37 (3H, t, J = 7.8 Hz), 7.60 (3H, dd, J = 7.8, 1.4 Hz), 7.91 (3H, dd, J = 7.8, 1.4 Hz), 8.02 (3H, s). ¹³C{¹H}-NMR: (62.9 MHz, CDCl₃) δ 20.4 (3×CH₃), 52.1 (3×CH₃), 53.5 (3×CH₂), 123.5 (3×C), 127.6 (3×C), 128.2 (3×CH), 128.4 (3×CH), 129.1 (3×C), 130.3 (3×C), 130.4 (3×CH), 130.5 (3×CH), 131.2 (3×CH), 133.9 (3×CH), 138.1 (3×C), 150.0 (3×C), 167.0 (3×C=O). MS (ESI): 780.3 [M + H]⁺. HR-MS (ESI): calcd for C₄₈H₄₆NO₉: 780.31726; found 780.31728.

Boratrane complex (18)

Substrate **16f** (1 mmol, 960 mg) was weighed in a oven dried, double necked round bottom flask, pentamethylbenzene (30 mmol, 900 mg) and dry CH₂Cl₂ (150 mL) were added under nitrogen. The solution was cooled down to -78 °C and then BCl₃ (9.9 mmol, 9.9 mL, 1M in hexane) was slowly added in a period of 5 minutes. After 30 minutes, complete conversion was checked by ESI-MS analysis. The reaction was quenched with 5% methanol/chloroform (150 mL), vigorously stirring for 10 minutes, and then the solution was warmed to room temperature. It was washed with Na₂CO₃aq. sat (150 mL) and the aqueous phase was extracted with CH₂Cl₂ (3 × 100 mL). The combined organic phase were dried over Na₂SO₄ and concentrated. The residue was washed with hexane and filtered, affording product **18** as a white solid.

18: ¹H-NMR: (250 MHz, CDCl₃) δ 2.26 (9H, s), 4.22 (6H, s), 6.82 (3H, s), 7.16 (3H, s), 7.44 (3H, t, J = 7.8 Hz), 7.79 (3H, dd, J = 7.7, 1.1 Hz), 7.96 (3H, dd, J = 7.7, 1.1 Hz), 8.08 (3H, s), 9.83 (H, s). ¹³C{¹H}-NMR: (62.9 MHz, CDCl₃) δ 20.7 (3×CH₃), 57.4 (3×CH₂), 118.5 (3×C), 127.7

(3×CH), 128.2 (3×CH), 128.6 (3×CH), 130.1 (3×C), 130.3 (3×C), 131.1 (3×CH), 131.2 (3×C), 131.5 (3×CH), 136.2 (3×CH), 136.4 (3×C), 139.1 (3×C), 148.4 (3×C), 192.9 (3×CHO). ((MS (ESI): 720.3 [M + Na]⁺).

Synthesis of titanatrane mononuclear complexes (19)

Complexes **19a-e** were prepared in glovebox by mixing homogeneous solutions of the corresponding ligands **17a-e** (0.10 M) and Ti(O*i*-Pr)₄ (0.18 M) in dry CDCl₃ in a 1:1 ratio to a final concentration 0.01 M of the complex. Bright yellow solutions were obtained which were used without further purifications and without removing the three equivalents of *i*-PrOH released from the metal precursor. In all cases resonances relative to free *iso*-propanol released in the reaction were present in the NMR spectra: ¹H-NMR (300 MHz, CDCl₃): 1.22 (6H, *d*, *J* = 6.1 Hz), 4.04 (1H, *hept*, *J* = 6.1 Hz). ¹³C-NMR (75 MHz, CDCl₃): δ 25.1 (CH₃), 64.5 (CH).

Ti(IV)/17a Complex (19a): ¹H-NMR: (300 MHz, CDCl₃) δ 1.03 (6H, *d*, *J* = 6.0 Hz), 2.30 (9H, *s*) 3.62 (6H, *bs*), 4.64 (1H, *hept*, *J* = 6.0 Hz), 6.89 (3H, *s*), 7.11 (3H, *s*), 7.25– 7.39 (9H, *m*), 7.64– 7.66 (6H, *m*).

Ti(IV)/17b Complex (19b): ¹H-NMR: (300 MHz, CDCl₃) δ 1.20 (6H, *d*, *J* = 5.1 Hz), 2.29 (9H, *s*) 2.92 (3H, *s*), 3.52 (9H, *s*), 4.14 (3H, *s*), 6.78–6.96 (12H, *m*), 7.14– 7.26 (6H, *m*).

Ti(IV)/17c Complex (19c): ¹H-NMR: (300 MHz, CDCl₃) δ 1.20 (6H, *d*, *J* = 6.1 Hz), 2.29 (9H, *s*) 3.60 (6H, *bs*), 3.81 (9H, *s*), 4.64 (1H, *hept*, *J* = 6.1 Hz), 6.81 (3H, *d*, *J* = 7.1 Hz), 6.90 (3H, *s*), 7.10 (6H, *d*, *J* = 12.1 Hz), 7.17– 7.28 (6H, *m*). ¹³C{¹H}-NMR: (62.9 MHz, CDCl₃) δ 20.9 (3×CH₃), 25.01 (2×CH₃), 55.4 (3×CH₃), 59.0 (3×CH₂), 80.6 (CH), 112.5 (3×C), 115.4 (3×CH), 122.3 (3×CH), 125.0 (3×CH), 127.9 (3×C), 128.9 (3×CH), 129.6 (3×CH), 130.0 (3×CH), 130.6 (3×C), 140.1 (3×C), 158.5 (3×C), 159.3 (3×C).

Ti(IV)/17d Complex (19d): ¹H-NMR: (300 MHz, CDCl₃) δ 1.00 (6H, *d*, *J* = 6.0 Hz), 2.31 (9H, *s*), 3.57 (6H, *bs*), 4.67 (1H, *hept*, *J* = 6.0 Hz), 7.00 (6H, *d*, *J* = 7.1 Hz), 7.53 (6H, *m*), 7.88 (6H, *m*). ¹³C{¹H}-NMR: (62.9 MHz, CDCl₃) δ 20.6 (3×CH₃), 26.5 (2×CH₃), 58.7 (3×CH₂), 81.1 (CH), 112.1 (3×C), 119.1 (3×C), 124.8 (3×C), 125.5 (3×C), 128.8 (3×CH), 130.2 (3×C), 130.3 (3×CH), 130.4 (3×CH), 132.9 (3×CH), 134.15 (3×CH), 134.16 (3×CH), 139.8 (3×C), 157.9 (3×C).

Ti(IV)/17e Complex (19e): ¹H-NMR: (300 MHz, CDCl₃) δ 0.84 (6H, *d*, *J* = 6.0 Hz), 2.31 (9H, *s*), 3.57 (6H, *bs*), 3.88 (9H, *s*), 4.49 (1H, *hept*, *J* = 6.0 Hz), 6.91 (3H, *s*), 7. (3H, *s*), 7.41 (3H, *t*, *J* = 7.3 Hz), 7.95 (6H, *d*, *J* = 7.3 Hz), 8.14 (3H, *s*). ¹³C{¹H}-NMR: (62.9 MHz, CDCl₃) δ 20.6 (3×CH₃), 25.0 (2×CH₃), 52.0 (3×CH₃), 58.7 (3×CH₂), 80.2 (CH), 124.7 (3×C), 126.6 (3×C), 127.76 (3×CH), 127.79 (3×CH), 129.8 (3×CH), 129.89 (3×C), 129.94 (3×C), 130.3 (3×CH), 130.4 (3×CH), 134.6 (3×CH), 138.9 (3×C), 158.1 (3×C), 167.3 (3×C=O).

Synthesis of Ti(IV) μ -oxo complexes (20)

Addition of a mixture 5% THF/water to the solution of complex **19a/19c-e** allowed the complete formation of μ -oxo complex **20a, 20c-e**. The reaction mixture was evaporated under reduced pressure and the resulting solid was washed with hot Et₂O. The suspension was centrifuged, isolating the product **20** all as yellow solids.

20a: Mp > 300 °C. IR (KBr) ν (cm⁻¹): 750, 885, 1040, 1268, 1457, 1483, 1598, 2852, 2922. ¹H-NMR: (300 MHz, CDCl₃) δ 2.35 (18H, s), 3.14 (6H, *d*, *J* = 13.7 Hz), 4.29 (6H, *d*, *J* = 13.7 Hz), 6.25 (6H, *t*, *J* = 7.4 Hz), 6.57 (12H, *t*, *J* = 7.4 Hz), 6.68 (12H, *d*, *J* = 7.4 Hz), 6.97 (6H, s), 7.04 (6H, s). ¹³C{¹H}-NMR: (62.9 MHz, CDCl₃) δ 21.0 (6 \times CH₃), 59.0 (6 \times CH₂), 124.5 (6 \times C), 125.9 (6 \times CH), 127.6 (12 \times CH), 128.4 (6 \times C), 129.1 (6 \times CH), 129.7 (6 \times C), 129.8 (6 \times CH), 129.9 (12 \times CH), 137.5 (6 \times C), 158.4 (6 \times C). MS (ESI): 1317.3 [M+H]⁺, 1339.3 [M+Na]⁺, 1356.3 [M+K]⁺. HR-MS (ESI): C₈₄H₇₃N₂O₇Ti₂ calcd for 1317.43767; found 1317.43769.

20c: ¹H-NMR: (300 MHz, CDCl₃) δ 2.29 (18 H, s), 3.10 (6H, *d*, *J* = 14.0 Hz), 3.14 (18 H, s), 4.26 (6H, *d*, *J* = 14.0 Hz), 5.83 (6H, *d*, *J* = 7.9 Hz), 6.26 (6H, *d*, *J* = 7.9 Hz), 6.37 (6H, *t*, *J* = 7.9 Hz), 6.54 (6H, s), 6.94 (6H, s), 7.02 (6H, s).

20d: Mp > 300 °C. IR (KBr) ν (cm⁻¹): 742, 865, 913,1242, 1268, 1461, 2229, 2856, 2920. ¹H-NMR: (300 MHz, CDCl₃) δ 2.38 (18H, s), 3.14 (6H, *d*, *J* = 14.1 Hz), 4.46 (6H, *d*, *J* = 14.1 Hz), 6.56- 6.67 (12H, *m*), 6.94- 7.04 (24H, *m*). ¹³C{¹H}-NMR: (62.9 MHz, CDCl₃) δ 20.8 (6 \times CH₃) , 58.9 (6 \times CH₂), 111.4 (6 \times C), 118.5 (6 \times C), 124.9 (6 \times C), 125.6 (6 \times C), 128.1 (6 \times CH), 129.5 (6 \times CH), 129.7 (6 \times CH), 130.6 (6 \times CH), 130.8 (6 \times C), 132.4 (6 \times CH), 134.4 (6 \times CH), 139.4 (6 \times C), 157.6 (6 \times C). MS (ESI): 1467.1 [M+H]⁺, 1489.1 [M+Na]⁺.

20e: Mp: 205- 206 °C. IR (KBr) ν (cm⁻¹): 743, 816, 866, 914, 1178, 1256, 1437, 1468, 1722, 2853, 2922. ¹H-NMR: (300 MHz, CDCl₃) δ 2.39 (18H, s), 3.21 (6H, *d*, *J* = 13.9 Hz), 3.58 (18H, s), 4.32 (6H, *d*, *J* = 13.9 Hz), 6.37 (6H, *t*, *J* = 7.8 Hz), 6.71 (6H, *t*, *J* = 7.8 Hz), 6.90 (6H, *d*, *J* = 7.8 Hz), 7.04- 7.11 (12H, *m*), 7.71 (6H, s). ¹³C{¹H}-NMR: (62.9 MHz, CDCl₃) δ 20.8 (6 \times CH₃) , 51.6 (6 \times CH₃), 58.7 (6 \times CH₂), 124.1 (6 \times C), 124.4 (6 \times C), 127.6 (6 \times CH), 127.2 (6 \times CH), 129.1 (6 \times CH), 129.2 (6 \times C), 129.6 (6 \times CH), 129.9 (6 \times CH), 130.4 (6 \times C), 135.5 (6 \times CH), 137.5 (6 \times C), 157.8 (6 \times C), 166.8 (6 \times C=O).

Synthesis of the hexa-functionalized μ -oxo complex (21)

To a solution of pyrrolidine (0.576 mmol, 48 μ L) in anhydrous toluene (220 μ L), the catalyst Al Me₃ (288 μ L, 2M in heptane) was added dropwise. After stirring the reaction mixture for 1 h at room temperature, a suspension of **20e** (0.024 mmol, 40 mg) in toluene (150 μ L) was added and the mixture was thermostated at 70°C. After 48h, the reaction mixture was cooled down to room temperature, diluted with CH₂Cl₂ and washed with HCl 1M (3 mL) until reaching an acidic pH. Then the aqueous phase was extracted with CH₂Cl₂ (3 \times 3 mL) and the combined organic phases were dried over MgSO₄ and the solvent evaporated, obtaining an orange solid.

(21): MS (ESI): 1900.8 [M+H]⁺, 1923.8 [M+Na]⁺, 1939.7 [M+K]⁺.

(-)-(S)-2-[[1-(2-Benzyloxybipheny-3-yl)-meth-(E)-ylidene]-amino]-2-phenyl-ethanol ((-)-(S)-22)

A solution of (S)-(+)-2-amino-2-phenylethanol (2.21 mmol, 303 mg) and 2-hydroxybiphenyl-3-carbaldehyde (2.21 mmol, 637 mg) in ethanol (5 mL) was refluxed for 30 min in the presence of activated 4 Å molecular sieves. The hot reaction mixture was filtered over Celite and then cooled to room temperature. The product crystallized upon standing over night. The brownish crystals were filtered and dried *in vacuo* to give 798 mg of the imine **21** (1.95 mmol, 88%).

(-)-(S)-22: Mp: 97–99 °C. IR (KBr) ν (cm⁻¹): 698, 734, 761, 803, 865, 911, 981, 1026, 1072, 1156, 1173, 1201, 1256, 1307, 1375, 1429, 1453, 1497, 1581, 1601, 1663, 1808, 1876, 1950, 2868, 2927, 2961, 3030, 3061, 3339. ¹H-NMR: (500 MHz, CDCl₃) δ 3.90 (1H, *dd*, *J* = 11.1, 4.6 Hz), 3.96 (1H, *dd*, *J* = 11.1, 8.2 Hz), 4.38– 4.49 (3H, *m*), 6.97– 7.01 (2H, *m*), 7.23– 7.32 (3H, *m*), 7.36– 7.50 (10H, *m*), 7.62– 7.64 (2H, *m*), 8.11 (1H, *dd*, *J* = 7.75, 1.85 Hz); 8.74 (1H, *s*). ¹³C{¹H}-NMR: (125 MHz, CDCl₃) δ 67.7 (CH₂), 75.6 (CH), 76.1 (CH), 124.6 (CH), 126.88 (CH), 127.4 (CH), 127.48 (CH), 127.52 (2xCH), 128.2 (CH), 128.35 (2xCH), 128.42 (2xCH), 128.57 (2xCH), 128.63 (2xCH), 129.3 (2xCH), 130.0 (C), 133.8 (CH), 135.8 (C), 136.1 (C), 137.9 (C), 140.7 (C), 156.3 (C), 159.1 (CH). MS (ESI): 408.4 [M + H]⁺. HR-MS (ESI): calcd for C₂₈H₂₆NO₂: 408.1963; found 408.1965. [α]_D²⁰ : -55.6 (*c* = 0.4, CH₂Cl₂).

(+)-(S)-2-[(S)-1-(2-Benzyloxybiphenyl-3-yl)-ethylamino]-2-phenylethanol ((+)-(S,S)-23)

Methyl-lithium (6.4 mmol, 4.3 ml of 1.5 M in Et₂O) was added dropwise to a magnetically stirred solution of (S)-**22** (1.61 mmol, 637 mg) in dry, degassed THF (30 ml) at -78 °C under N₂. This mixture was stirred for 24 h at -78 °C. It was then brought to -30 °C over a 4 h period and stirring was continued for an additional 20 h. The reaction was quenched at -30 °C by the addition of sat. aq. NH₄Cl and was allowed to warm to 20 °C. The organic layer was separated. After evaporation of the solvent the residue was taken up in Et₂O (20 mL), and washed with sat. aq. NaHCO₃ (3 x 10 mL). The combined organic layers were dried over Na₂SO₄ and concentrated *in vacuo* to give an orange oil. Purification by flash chromatography (CH₂Cl₂/MeOH/Et₃N 98:1:1) gave amine (+)-(S,S)-**23** as a pale yellow oil. The other diastereoisomer could not be detected by ¹H NMR (*de* >95%).

(+)-(S,S)-23: IR (KBr) ν (cm⁻¹): 699, 734, 760, 803, 865, 914, 980, 1027, 1071, 1201, 1255, 1309, 1328, 1376, 1430, 1454, 1497, 1584, 1601, 1655, 1714, 1806, 1881, 1951, 2867, 2928, 2965, 3030, 3062, 3326, 3557. ¹H-NMR: (500 MHz, CDCl₃) δ 1.37 (3H, *d*, *J* = 6.5 Hz), 3.56 (1H, *dd*, *J* = 10.7, 7.9 Hz), 3.75 (1H, *dd*, *J* = 10.7, 4.7 Hz), 3.91 (1H, *dd*, *J* = 7.9, 4.7 Hz), 4.17 (1H, *d*, *J* = 10.4 Hz), 4.22 (1H, *d*, *J* = 10.4 Hz), 4.31 (1H, *q*, *J* = 6.6 Hz), 6.77– 6.80 (2H, *m*), 7.18– 7.44 (14H, *m*), 7.57– 7.60 (2H, *m*). ¹³C{¹H}-NMR: (125 MHz, CDCl₃) δ 22.3 (CH₃), 48.6 (CH), 61.6 (CH), 66.0 (CH₂), 75.0 (CH₂), 124.7 (CH), 126.4 (CH), 127.15 (2xCH), 127.23 (CH), 127.5 (CH), 127.8 (CH), 128.1 (2xCH), 128.2 (2xCH), 128.3 (2xCH), 128.6 (2xCH), 129.2 (2xCH), 129.9 (CH), 135.3 (C), 135.8 (C), 136.7 (C), 138.7 (C), 139.3 (C), 140.9 (C), 153.2 (CH). MS (ESI): 424.3 [M + H]⁺. HRMS: calcd for C₂₉H₃₀NO₂: 424.2276; found 424.2278. [α]_D²⁰ : +45.0 (*c* = 0.1, CH₂Cl₂).

(+)-(S)-1-(2-Benzyloxybiphenyl-3-yl)-ethylamine ((+)-(S)-24):

A 250 mL flask was charged with anhydrous K₂CO₃ (0.9 mmol, 124.5 mg) and methanol (0.3 mL). The resulting white suspension was cooled to 0 °C with an ice bath. A solution of (S,S)-**23** (0.15 mmol, 63 mg) in CH₂Cl₂ (0.6 mL) and a solution of Pb(OAc)₄ (0.18 mmol, 78.6 mg) in CH₂Cl₂ (0.6 mL) were simultaneously added dropwise over a 12 min period. After 10 min, the reaction was hydrolysed with sat. aq. Na₂CO₃ (0.5 mL). The mixture was filtered through Celite and washed with CH₂Cl₂ and sat. aq. Na₂CO₃. The combined aqueous phases were extracted with CH₂Cl₂. The combined organic layers were dried over K₂CO₃ and the solvents were removed *in vacuo*.

The crude imine was taken up in THF (1 mL) and hydrolysed with an AcOH_{aq} 30% (1 mL) for 20 h at 20 °C. The mixture was concentrated under vacuum and the aqueous layer was extracted with Et₂O. The combined organic layers were washed with an AcOH_{aq} 30%. The combined aqueous layers were cooled to 0 °C, brought to pH 14 by addition of NaOH 6 N and extracted with Et₂O. The combined organic layers were dried (K₂CO₃) and concentrated. The crude amine was dissolved in Et₂O and a commercial solution of HCl in Et₂O (0.5 M) was added until no more precipitation was observed. The precipitate was filtered and washed with cold hexane and dried to afford the ammonium salt **24·HCl** (30.6 mg, 0.10 mmol, 60%). A sample was crystallized from cyclohexane/ethyl acetate (4:1). The enantiomeric purity of the free amine was determined by chiral HPLC (Chiralcel OD-H, hexane/2-propanol 97:3, 1 ml/min: 10.0 min (minor, R), 13.2 min (major, S): ee 95%.

24·HCl: Mp: 118–121 °C. IR: 696, 757, 804, 865, 917, 973, 1070, 1112, 1202, 1266, 1367, 1432, 1455, 1520, 1598, 1603, 1803, 1881, 1943, 1981, 2873. ¹H-NMR: (300 MHz, CD₃OD) δ 1.47 (3H, *d*, J = 6.9 Hz), 4.41 (1H, *d*, J = 10.8 Hz), 4.54 (1H, *d*, J = 10.9 Hz), 4.70 (1H, *q*, J = 7.0 Hz), 7.1–7.2 (2H, *m*), 7.2–7.6 (9H, *m*), 7.66 (2H, *bd*, J = 6.8 Hz). ¹³C{¹H}-NMR: (100 MHz, CD₃OD) δ 19.7 (CH₃), 46.3 (CH), 76.5 (CH₂), 123.8 (CH), 126.3 (CH), 126.4 (CH), 129.0 (C and CH), 129.6 (C and CH), 129.7 (CH), 129.8 (4xCH), 130.2 (2xCH), 133.2 (C), 133.5 (CH), 139.5 (C), 154.8 (C). MS (ESI): 304.4 [M + H]⁺. HRMS (ESI): calculated for C₂₁H₂₂NO: 304.1701 found 304.1703. [α]_D²⁰: +22.7 (c = 1.9, CH₂Cl₂).

(S)-Bis-(2-Benzyloxy-3-phenyl-benzyl)-[1-(2-Benzyloxybiphenyl-3-yl)-ethyl]amine

A mixture of (S)-**24** (0.205 mmol, 70 mg), 1-(2-Benzyloxybiphenyl-3-yl)-methylbromide **7a** (0.453 mmol, 160 mg) and K₂CO₃ (1.03 mmol, 142 mg) in dry MeCN (4 mL) was refluxed for 24h. The mixture was filtered over Celite washing with AcOEt (5 mL), concentrated and purified by column chromatography on silica gel, using petroleum ether/AcOEt/Et₃N 50:5:1 as eluant, to give the *tri-O*-benzyl protected product as a colourless oil (90%).

IR (KBr) ν (cm⁻¹): 697, 735, 867, 909, 1172, 1211, 1243, 1271, 1382, 1452, 1469, 1495, 1592, 2861, 2921, 3030, 3060. ¹H-NMR: (300MHz, CDCl₃) δ 1.39 (3H, *d*, J = 7.0 Hz), 3.82 (2H, *d*, J = 15.6 Hz), 3.89 (2H, *d*, J = 15.6 Hz), 4.13 (2H, *s*), 4.15 (2H, *d*, J = 10.5 Hz), 4.27 (2H, *d*, J = 10.5 Hz), 4.54 (1H, *quintet*, J = 7.0 Hz), 6.58 (2H, *d*, J = 7.6 Hz), 6.90–6.94 (4H, *m*), 7.02–7.40 (24H, *m*), 7.47–7.68 (7H, *m*), 7.78–7.81 (2H, *m*). ¹³C{¹H}-NMR: (75 MHz, CDCl₃) δ 19.3 (CH₃), 49.0 (2xCH₂), 52.5 (CH), 74.2 (2xCH₂), 75.2 (CH₂), 123.8 (2xCH), 124.1 (2xCH), 125.1 (CH), 126.8 (2xCH), 127.5 (CH), 127.6 (4xCH), 127.8 (2xCH), 127.97 (4xCH), 128.03 (2xCH), 128.1 (2xCH),

128.2 (4xCH), 128.4 (2xCH), 128.8 (2xCH), 128.9 (2xCH), 129.2 (4xCH), 129.3 (2xCH), 129.4 (CH), 134.6 (2xC), 134.7 (2xC), 135.4 (C), 135.8 (C), 136.3 (C), 136.9 (2xC), 138.7 (2xC), 138.8 (C), 154.0 (C); 154.5 (2xC). MS (ESI): 848.7 [M + H]⁺. HR-MS (ESI): calcd for C₆₁H₅₄NO₃: 848.4098; found 848.4097. $[\alpha]_D^{20}$: +68.1 (c = 0.1, CH₂Cl₂).

(S)-Bis-(2-hydroxy-3-phenyl-benzyl)-[1-(2-hydroxybiphenyl-3-yl)-ethyl]amine (S)-1b

(S)-Bis-(2-Benzyloxy-3-phenyl-benzyl)-[1-(2-Benzyloxybiphenyl-3-yl)-ethyl]amine (0.2 mmol, 170 mg) was dissolved in ethyl acetate (15 mL) and 10% Pd/C (25 mg) was added. The mixture was stirred under H₂-atmosphere for 2h, then filtered through a pad of Celite and concentrated under vacuum. Purification by preparative TLC (petroleum ether/AcOEt 9:1) gave the pure ligand (S)-**1b** as a colourless oil (85 %).

(S)-**1b**: IR (KBr) ν (cm⁻¹): 699, 755, 827, 1082, 1222, 1382, 1431, 1460, 1497, 1590, 1608, 2926, 2972, 3033, 3056, 3422. ¹H-NMR: (300 MHz, CDCl₃) δ 7.52-7.46 (2H, *m*), 7.44- 7.30 (13H, *m*), 7.25- 7.15 (2H, *m*), 7.11- 7.05 (4H, *m*), 6.90 (1H, *t*, J = 7.6 Hz), 6.80 (2H, *t*, J = 7.6 Hz), 4.53 (1H, *q*, J = 6.7 Hz), 3.90 (6H, *s*), 1.62 (3H, *d*, J = 6.7 Hz). ¹³C{¹H}-NMR: (75 MHz, CDCl₃) δ 19.4 (CH₃), 50.2 (2xCH₂), 55.0 (CH), 120.1 (2xCH), 123.5 (C), 125.3 (2xC), 125.4 (CH), 127.1 (CH), 127.3 (2xCH), 128.2 (2xC), 128.5 (2xCH), 128.6 (2xCH), 128.7 (4xCH), 128.8 (C), 128.9 (CH), 129.0 (6xCH), 129.6 (CH), 130.3 (2xCH), 136.9 (2xC), 137.2 (C), 152.0 (C), 152.5 (2xC). MS (ESI): 578.1 [M + H]⁺. HR-MS (ESI): calcd for C₄₀H₃₆NO₃: 578.2690; found 578.2693. $[\alpha]_D^{20}$: -17.0 (c = 0.1, CH₂Cl₂).

Ti(IV)/(S)-1b Complex ((S)-2b)

Complex (S)-**2b** was prepared in glovebox by mixing homogeneous solutions of ligand (S)-**1b** (0.10 M) and Ti(O*i*-Pr)₄ (0.18 M) in dry CDCl₃ in a 1:1 ratio to a final concentration 0.01 M of the complex. A bright yellow solutions was obtained which was used without further purifications and without removing the three equivalents of *i*-PrOH released from the metal precursor. Resonances relative to free *iso*-propanol released in the reaction were present in the NMR spectra: ¹H-NMR (300 MHz, CDCl₃): 4.04 (1H, *hept*, J = 6.1 Hz), 1.22 (6H, *d*, J = 6.1 Hz). ¹³C-NMR (75 MHz, CDCl₃): δ 64.5 (CH), 25.1 (CH₃).

(S)-**2b**: ¹H NMR: (300 MHz, CDCl₃) δ 0.96 (3H, *d*, J = 6.0 Hz), 0.98 (3H, *d*, J = 6.0 Hz), 1.62 (3H, *d*, J = 6.6 Hz), 3.40 (2H, *m*), 3.75 (1H, *d*, J = 13.5 Hz), 3.90 (1H, *d*, J = 14.1 Hz), 4.17 (1H, *q*, J = 6.6 Hz), 4.58 (1H, *hept*, J = 6.0 Hz), 6.87- 7.00 (4H, *m*), 7.0- 7.17 (2H, *m*), 7.25- 7.41 (12H, *m*), 7.62-7.69 (6H, *m*).

Zr(IV)/1a Complex (26)

Zr(O*t*-Bu)₄ (98 μ L, 0.25 mmol) in dry CD₂Cl₂ (1 mL) was added dropwise by syringe, to a stirred solution of ligand **1a** (141.8 mg, 0.25 mmol) in dry CD₂Cl₂ (1 mL), leading to the formation of complex **26**.

26: ¹H NMR: (300 MHz, CD₂Cl₂) δ 0.99 (9H, s), 1.20 (27H, s, *t*-BuOH), 3.44 (6H, bs), 6.70 (3H, *t*, J = 7.5 Hz), 7.01 (3H, *d*, J = 7.3 Hz), 7.21- 7.24 (6H, *m*), 7.34 (6H, *t*, J = 7.3 Hz), 7.67 (6H, *dd*, J = 7.5, 1.4 Hz). ¹³C{¹H}-NMR: (75 MHz, CDCl₃) δ 31.2 (3xCH₂), 32.7 (3xCH₃), 61.4 (C), 118.2 (3xCH), 126.5 (3xCH), 128.3 (9xCH), 129.8 (3xC), 130.0 (3xCH), 130.1 (6xCH), 130.6 (3xCH), 140.2 (3xC), 158.4 (3xC). Signals of *tert*-butyl alcohol are presents: 31.4 (3xCH₃), 68.9 (C).

Zr(IV) complex (27)

Addition of water to the solution of complex **26** and successive removal of the solvent under reduced pressure afforded the formation of a new specie (Figure 22, c), which was also obtained through the following procedure: a solution of Zr(*Ot*-Bu)₄ (64.3 μL, 0.165 mmol, in 500 μL of dry toluene) was added dropwise to a stirred suspension of ligand **1a** (93 mg, 0.165 mmol) in dry toluene (200 mL) at 0° C. The reaction mixture was allowed to warm to room temperature, with stirring, in a period of 3 h, resulting in a white solution. After 15 minutes from water addition (10 μL), removal of solvent under reduced pressure permitted to obtain a white residue, which was washed in fresh toluene (1 mL) while heating and then washed with hexane repeatedly (3 x 1 mL). Compound **27** was obtained as a white solid (200 mg, 92%).

27: ¹H NMR: (300 MHz, CD₂Cl₂) δ 1.20 (27H, s, *t*-BuOH), 3.10 (6H, *d*, J = 13.5 Hz), 4.18 (6H, *d*, J = 13.5 Hz), 6.62-6.89 (24H, *m*), 7.10- 7.25 (24H, *m*).

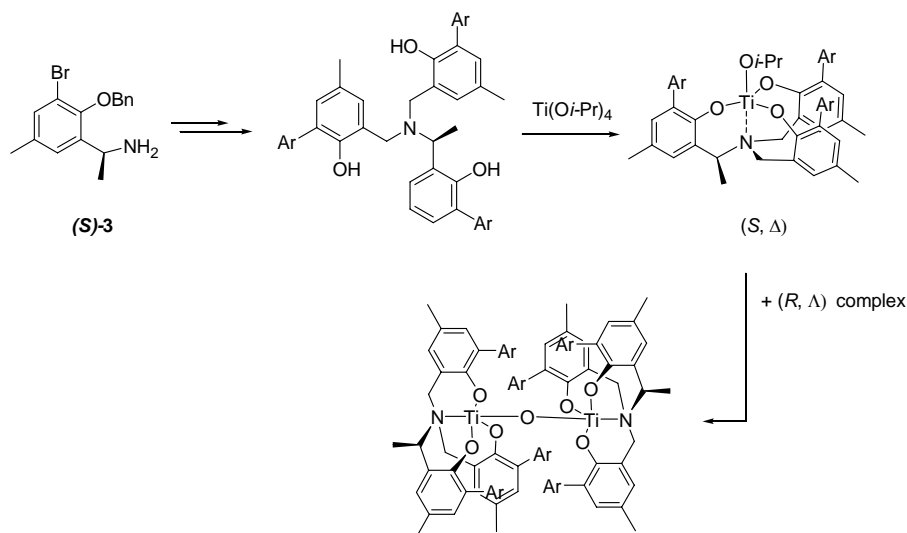
Hf(IV)/ **1a** Complex (28)

Hf(*Ot*-Bu)₄ (101 μL, 0.25 mmol) in dry CD₂Cl₂ (1 mL) was added dropwise by syringe, to a stirred solution of ligand **1a** (141.8 mg, 0.25 mmol) in dry CD₂Cl₂ (1 mL), leading to the formation of complex **25**.

28: ¹H NMR: (300 MHz, CD₂Cl₂) δ 0.99 (9H, s), 1.20 (27H, s, *t*-BuOH), 3.75 (6H, bs), 6.76 (3H, *t*, J = 7.5 Hz), 7.04 (3H, *d*, J = 7.2 Hz), 7.21- 7.28 (6H, *m*), 7.35 (6H, *t*, J = 7.5 Hz), 7.63 (6H, *d*, J = 7.5 Hz).

Chapter 4

Enantiopure pseudo- C_3 titanatranes



The preparation of enantiopure complexes with aryl peripheral substituents was achieved: the complete control of the helicity of the complex has been obtained introducing a single stereogenic centre at the benzylic position of one arm of the ligand. Enantiopure aminophenols **3** were obtained as building blocks, via stereoselective synthesis, classical resolution and enzymatic kinetic resolution.

Studies on the $Ti(IV)$ μ -oxo complexes formation evinced how at the basis of the self-assembly there is a process of heterochiral recognition.

4.1 Introduction

There are two principal ways to obtain enantio enriched or enantiopure compounds (e.e.>99%):

- Resolution of racemic mixtures
- Stereoselective synthesis

Separation of enantiomers through classical resolution is usually achieved by reacting the mixture with a chiral, enantiopure resolving agent. Because the two resulting products will be diastereoisomers, they can be in principle separated: by crystallization (classical resolution) or chromatography. A related method consists in preparative HPLC on chiral stationary phases: diastereotopic interactions between the chiral stationary phase and the racemic solute can result in a different elution order with subsequent separation of the two enantiomers. This approach can be used at a small-medium industrial scale (approximately 100 Kg) especially useful in the early phase of the product/drug development. Large amounts of solvents have to be handled in both cases and the enantiopure resolving agent or the chiral column must be readily accessible. Furthermore maximum yield, which can be achieved, corresponds to 50% and the undesired enantiomer must be recycled or discarded.

A related strategy is kinetic resolution in which the racemic mixture is reacted with a chiral, enantiopure reagent/catalyst. The two enantiomers will react with different rates, due to the fact that the two or more processes occur via diastereomeric transition states. Coupling the kinetic resolution with a faster racemization of the starting material (Dynamic Kinetic Resolution) could increase the total yield in the desired enantiomer, up to 100% in principle. Up today resolution is still the most commonly used methodology in industry for obtaining enantiopure compounds and a number of examples of efficient dynamic kinetic resolution processes, performed using both chemical or/and enzymatic processes, have been applied to industrial manufactures.

At the same time, a wide variety of synthetic methods have been developed over the time for obtaining directly enantiopure molecules via stereoselective synthesis, than can be performed:

- by the use of chiral auxiliaries/enantiopure stoichiometric reagents
- by the use of enzymes or chiral catalysts

The incorporation of chiral auxiliaries into a molecule represents a powerful method to transfer chiral information from an existing to a new stereogenic centre. The major drawback of this strategy is that a chiral auxiliary has to be installed and removed and this adds two steps to a synthetic sequence. On the contrary chiral catalysts (both artificial and enzymatic) have the big advantages of being used under sub-stoichiometric amounts and they do not require any substrate transformation before or after the process. Moreover, a catalyst continues to carry its task until it gets deactivated by a side reaction or until there is no more substrate to be transformed. In particular the catalysts of Nature, the enzymes, possess another powerful means: they are highly stereoselectively for the formation of specific new stereogenic centres, producing chiral molecules enantiomerically pure and reaching activities and selectivities actually higher and largely superior to the chiral transition metal or small

organic catalysts. On the contrary, due to their specific mechanism of action they are specific for a rather narrow type of substrata. Hence the creation of artificial enzymes and catalytically active antibodies has attracted attention for their potential capability to overcome this problem.

The more versatile way for stereoselective catalytic processes is to use synthetic chiral catalysts. Probably the first chiral organic catalyst reported was quinine, found in 1912 by Breiding and Fiske, which was found to give enantiomeric excess up to 10% in the formation of mandelonitril from benzaldehyde.^{1,2} Since then, many chiral organic molecules, often chiral natural products such as amino acids, carbohydrates and alkaloids, have found applications for stereoselective transformations. Organocatalysts, although providing spectacular results, exhibit low reactivity as major drawback and need to be added in large quantity (also 30%). Alternatively metal complexes with low molecular weight organic ligands can form chiral complexes accelerating and facilitating stereoselective processes. Metal catalyst is an important, viable alternative to bio catalysis, since metals can promote reactions not known to occur in nature; the choice of substrate and reaction type are not limited by enzymatic specificity and the performance of the catalyst and as consequence the stereochemical course of the reaction can be readily tuned by appropriate variations in the ligand, reaction conditions, presence of additives.

Over the past thirty years a number of different ligand classes has been synthesized and applied to a large variety of catalytic reactions. "Developing a new ligand is usually extremely time consuming; in addition there is no guarantee of success as there is no such thing as ligand design." - Johannes de Vries and Laurent Lefort.³

4.1.1 Chiral amine triphenolate ligands

The synthesis of enantiopure chiral complexes to be used in stereoselective catalysis requires a complete control of structures of the metal complexes in order to avoid the presence in solution of different diastereomeric species or multinuclear aggregates that can act as independent catalysts. In the case of the *tris*-phenolamines with bulky *ortho* substituents, due to the high symmetry of the system, a single, racemic mixture of mononuclear complexes are obtained. The presence of a single enantiomer with complete control of the helicity of the complex has been achieved introducing a single stereogenic centre at the benzylic position of one arm of the ligand,⁴ as already described and discussed in *Chapter 3*.

Even if the presence of a single stereogenic centre (Figure 3, A) has been shown by us and others to be capable to control the propeller-like chirality of the corresponding Ti(IV) complex, the preparation of C₃ *tris*-phenolamine ligands in their enantiopure form is still an unsolved problem. In fact, all the attempts to prepare ligands with three stereogenic centres

¹ Breiding, G.; Fiske, P. S. *Biochem. Z.* **1912**, 46, 7.

² Jacobsen, E. N.; Pfaltz, A.; Yamamoto, H.; Editors *Comprehensive Asymmetric Catalysis I-III, Volume I*, 1999.

³ de Vries, J. G.; Lefort, L. *Chem. Eur. J.* **2006**, 12, 4722.

⁴ (a) Bernardinelli, G.; Seidel, T. M., Kündig, E. P.; Prins, L. J.; Kolarovic, A.; Mba, M.; Pontini, M.; Licini, G. *J. Chem. Soc. Dalton Trans.* **2007**, 1573. (b) Axe, P.; Bull, S. D.; Davidson, M. G.; Gilfillan, C. J.; Jones, M. D.; Robinson, D. E. J. E.; Turner, L. E.; Mitchell, W. L. *Org. Lett.* **2007**, 9, 223.

have failed (Figure 3, B), because of the low stability of the ligand, also in its *O*-protected form.⁵ This lack of stability is most probably to ascribe to the steric crowding around the nitrogen atom and together with it to the introduction of three π -donor substituents, as methoxy groups, on the adjacent aromatic ring which can increase the basicity of the amine, favouring its degradation by destabilization of the three N-C benzylic bond or via retro-Mannich reaction.

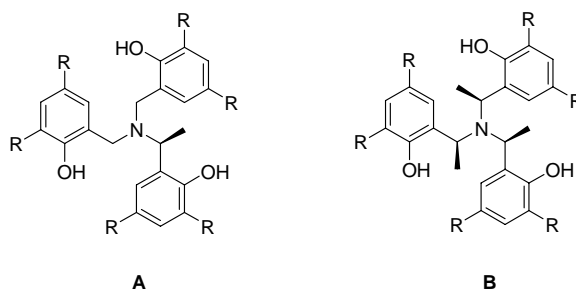


Figure 3

Consequently the study reported in this chapter deals with the synthesis of a chiral, enantiopure triphenolamines with only one stereogenic centre, like A, Figure 3.

Beside the possibility of using enantiopure complexes in stereoselective catalysis, we were attracted by the possibility to prepare single enantiomers of different complexes and explore their capability to assemble selectively, forming, in a complete controlled way, single, enantiopure μ -oxo complexes. In order to achieve this goal, suitable methods for obtaining enantiopure 1-(2-hydroxyphenyl)-ethylamine derivatives have been developed and will be described in the following part.

4.1.2 Chiral 1,3- Aminophenols

In the structural core of the building block 1-(2'-alkoxyaryl)alkyl-amine, two binding sites for building up more complex structures are provided by the amine and the phenol functional groups. At the same time a stereogenic benzylic carbon is present and the aromatic ring rigidifies a potential six-membered metallacycles (Figure 4).⁶

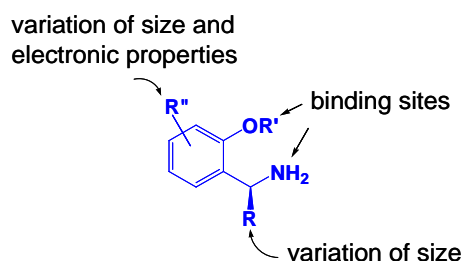


Figure 4

⁵ Thomas M. Siedel, PhD thesis, University of Geneva, 2007.

⁶ (a) Bernardinelli, G.; Fernandez, D.; Gosmini, R.; Meier, P.; Ripa, P. A.; Schupfer, P.; Treptow, B.; Kündig, E. P. *Chirality* **2000**, *12*, 529. (b) Kündig, E. P.; Botuha, C.; Lemercier, G.; Romanens, P.; Saudan, L.; Thibault, S. *Helv. Chim. Acta*, **2004**, *87*, 561.

Aminophenols belong to the class of aminoalcohols which are common and abundant structural elements in nature. 1,3-Aminoalcohols have been efficiently used as chiral auxiliaries or chiral ligands,⁷ but with scarce development because of the lack of natural sources of these compounds, even if they result important constituents of several antibiotics⁸ and other biologically active natural products.⁹

4.1.3 Synthesis of 1-(2'-alkoxyaryl)-alkylamine

Various methods for alkylation of imines or reductive amination of ketones have been reported, allowing a simple access to the racemic 1-(2'-alkoxyaryl)-ethylamines. The first optically active 1-(2'-methoxyphenyl)-ethylamine derivative was described in the 1970's, synthesized by Eschweiler Clark reductive amination and resolved by salt formation with tartaric or mandelic acid.^{10,11,12}

Many stereoselective synthetic strategies for these building blocks have been developed, but classical resolution remains so far the method of choice, especially for bulky substituents on the 1-(2'-alkoxyaryl)-ethylamine, like *tert*-butyl.⁶ However the effective and efficacious route for the preparation of these building block aminophenols is strongly influenced by the substituents on 1-(2'-alkoxyaryl)-ethylamine, with their size, steric hindrance and electronic properties.

Among the reported stereoselective synthesis, the chiral auxiliary phenyl ethylamine was used in the group VIII metal catalyzed hydrogenolysis (especially, Pd and Pt) to obtain chiral 1-(2'-methoxyphenyl)-ethylamine¹³ via stereoselective reduction of the corresponding ketimine and subsequent cleavage of the auxiliary in a one-pot reaction (Scheme 2, Eq. 1). High selectivity of up to 90 % ee was obtained in the Pd/H₂ reduction by Hogeveen and coworkers (Scheme 2, Eq. 2).¹⁴

⁷ Denmark, S. E.; Chatani, N.; Pansare, S. V. *Tetrahedron* **1992**, *48*, 2191.

⁸ (a) Weinreb, S. M.; Melnick, M. J. *Org. Chem.* **1988**, *53*, 850. (b) Ohno, M.; Wang, Y.; Izawa, T.; Kobayashi, S. *J. Am. Chem. Soc.* **1982**, *104*, 6465.

⁹ (a) Wovkulich, P.M.; Uskokovic, M. R. *J. Am. Chem. Soc.* **1981**, *103*, 3956. (b) Jäger, V.; Müller, I. *Tetrahedron Lett.* **1982**, *23*, 4777. (c) Shono, T.; Matsumura, Y.; Tsubata, K.; Uchida, K. *J. Org. Chem.* **1993**, *51*, 2590.

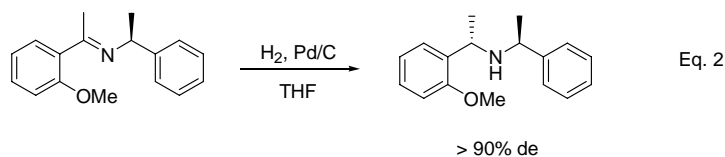
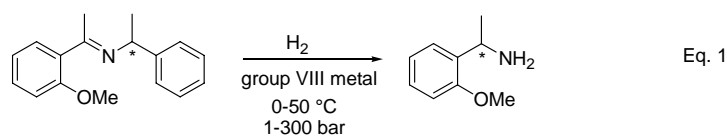
¹⁰ Rufer, C.; Ahrens, H.; Biere, H.; Schröder, E.; Gerhards, E.; Schillinger, E.; Losert, W. F.; Loge, O.; (Schering A.-G.). Application: DE, 1971, p32 pp.

¹¹ Wang, M.; Liu, J.; Hu, B. F. *J. Org. Chem.* **1995**, *60*, 7364.

¹² Mereyala, H. B.; Fatima, L.; Pola, P. *Tetrahedron: Asymmetry* **2004**, *15*, 585.

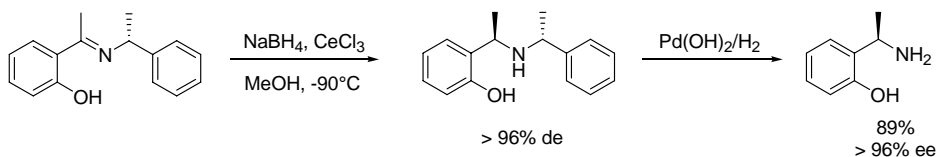
¹³ Bringmann, G.; Geisler, J.P.; Jansen, J.R.; (BASF A.-G., Fed. Rep. Ger.) Application: DE, 1989, p 5 pp.

¹⁴ Eleveld, M. B.; Hogeveen, H.; Shudde, E. P. *J. Org. Chem.* **1986**, *51*, 3635.



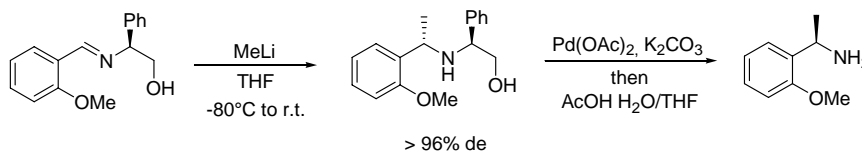
Scheme 2

Other chiral auxiliaries were used for this process. In particular, Palmieri reported the diastereoselective reduction of 2-imidoylphenols to *o*-hydroxybenzylamines with various α -substituents.¹⁵ Using cerium chloride, the reduction by sodium borohydride resulted faster and with higher diastereoselectivity, the latter being in the range of 78% to 95% de. Finally Kündig and coworkers reported a study on the reductive cleavage of chiral auxiliary phenylethylamine via hydrogenolysis: the enantiopure aminophenol was afforded in good yield, using Perlman's catalysts selective cleavage with Pd(OH)₂/C, (Scheme 3).^{6b}



Scheme 3

Phenylethylamine has also been used in the diastereoselective addition of alkyl lithium to imines, even if with lower diastereomeric excess (24% to 52%) for the synthesis of 1-(2'-alkoxyphenyl)-alkylamine.¹⁶ Chiral oxime ethers were also used as chiral auxiliaries for imines, but always with lower stereoselectivities (64% to 76% de).¹⁷ Phenylglycinol was recently proposed by Kündig and coworkers as the chiral auxiliary for diastereoselective addition of methyl lithium to arylidene imines, achieving selectivities up to 96% de (Scheme 4).^{6b}



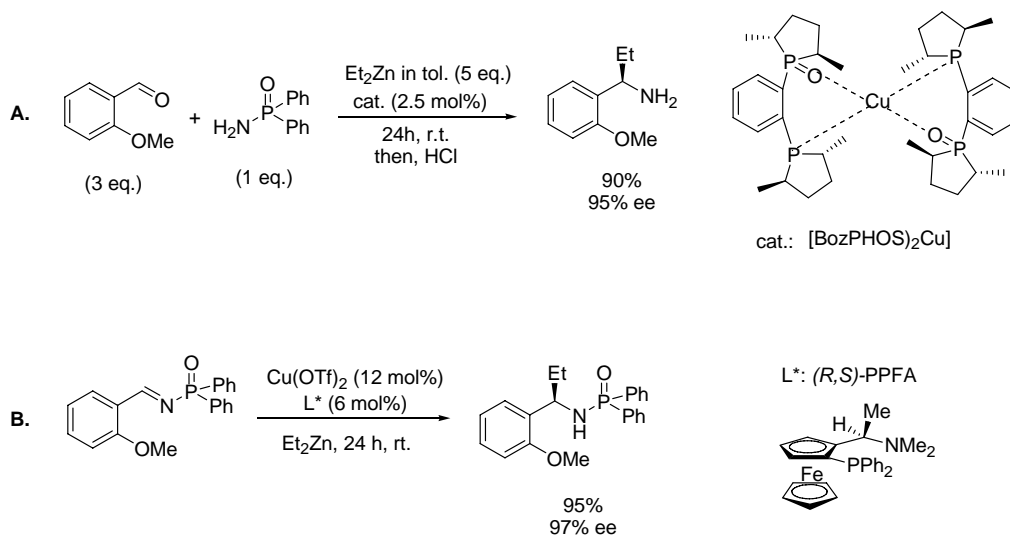
Scheme 4

¹⁵ Palmieri, G. *Eur. J. Org. Chem.* **1999**, 805.

¹⁶ Cimarelli, C.; Palmieri, G.; Volpini, E. *J. Org. Chem.* **2002**, *68*, 1200.

¹⁷ (a) Yamazaki, N.; Atobe, M.; Kibayashi, C. *Tetrahedron Lett.* **2001**, *42*, 5029. (b) Atobe, M.; Yamazaki, N.; Kibayashi, C. *J. Org. Chem.* **2004**, *69*, 5595.

Recently Charette and coworkers reported a multicomponent one-pot synthesis for obtaining free α -chiral amines from aldehydes, through copper-catalyzed dialkyl zinc addition to *N*-phosphinoylimines. In this way 1-(*o*-methoxyphenyl)-propylamine was obtained with e.e.=95% (Scheme 5, A).^{18,19} The same catalytic system using a different ligand, (*R,S*)-PPFA, and diethyl zinc furnished various α -arylpropylamines in high selectivity, in the range of 84% to 97% e.e., where 1-(*o*-methoxyphenyl)-propylamine gave the best selectivities (e.e.=97%) (Scheme 5, B).²⁰



Scheme 5

The effective methodology for obtaining these building blocks in high e.e.s strongly depends on size, steric hindrance and electronic properties of substituents of 1-(2'-alkoxyaryl)-ethylamine, as well evidenced by Kündig and coworkers.^{6b}

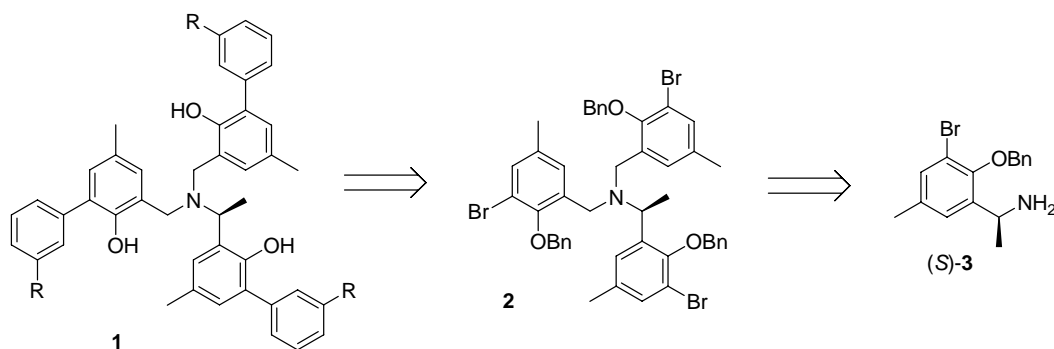
4.2 Synthetic strategy based on the aminophenol building block

In order to set up a general synthesis for obtaining enantiopure *tris*-phenolamine ligands **1** a synthetic procedure similar to the one described in *Chapter 3* for the achiral ligand was developed. In order to do this, enantiopure primary amine **2** possessing an *ortho*-bromo group was required (Scheme 6). In this way the *ad hoc* synthesis for each derivative could be avoided inserting the different aryl substituents at the very end of the synthetic process.

¹⁸ Cote, A.; Charette, A. B. *J. Org. Chem.* **2005**, *70*, 10864.

¹⁹ Boezio, A. A.; Pytkowicz, J.; Cote, A.; Charette, A. B. *J. Am. Chem. Soc.* **2003**, *125*, 14260.

²⁰ Wang, M. C.; Liu, L.T.; Hua, Y. Z.; Zhang, J. S.; Shi, Y. Y.; Wang, D. K. *Tetrahedron: Asymmetry* **2005**, *16*, 2531.

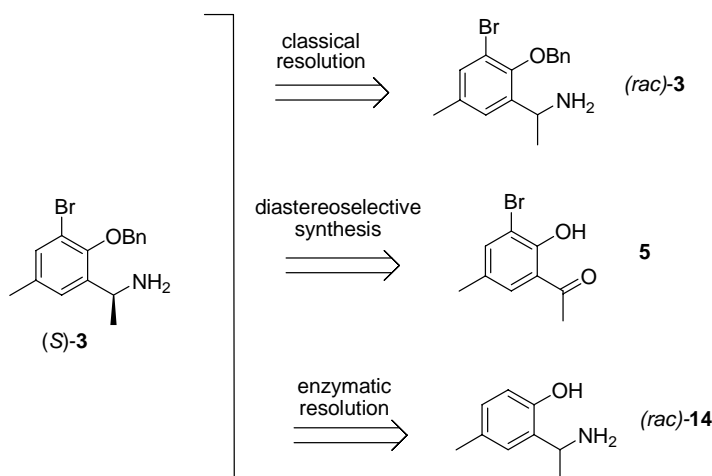


Scheme 6

4.2.1 1-(2-(benzyloxy)-3-bromo-5-methylphenyl)ethanamine: synthesis

In order to obtain enantiopure primary amines **3** in significant quantities three different strategies have been explored: (Scheme 7):

- Synthesis of the racemic mixture followed by classical resolution
- Stereoselective synthesis
- Enzymatic kinetic resolution



Scheme 7

4.2.1.1 Synthesis of the racemic aminoalcohol and classical resolution

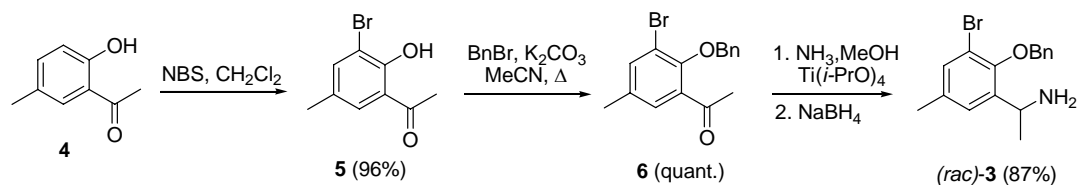
The racemic aminophenol *rac*-**3** was synthesized through a four-steps procedure starting from 1-(2-hydroxy-5-methyl-phenyl)ethanone **4** (Scheme 7). After the *ortho*-bromination²¹ of the phenol using *N*-bromosuccinimide (NBS) and successive protection of the phenolic function as benzyl ether, compound **6** was obtained in almost quantitative yields. A chemoselective alkylation of ammonia using the Ti(Oi-Pr)₄-NaBH₄ reagent system^{22,23}

²¹ Fujisaki, S.; Educhi, H.; Omura, A.; Okamoto, A.; Nishida, A. *Bull. Chem. Soc. Jpn.* **1993**, *66*, 1576.

²² Miriyala, B.; Bhattacharyya, S.; Williamson, J. S. *Tetrahedron* **2004**, *60*, 1463.

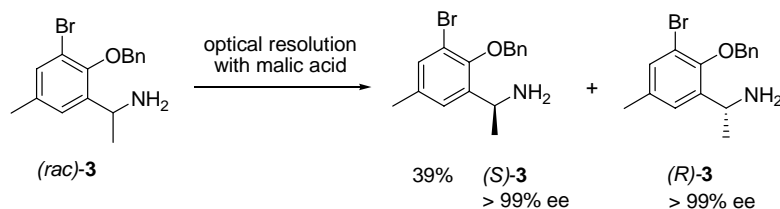
²³ Nugent, T. C.; Ghosh, A. K.; Wakchaure, V. N.; Mohanty, R. R. *Adv. Synth. Catal.* **2006**, *348*, 1289.

allowed to obtain 1-(2-(benzyloxy)-3-bromo-5-methylphenyl)ethanamine *rac*-**3** in 87% yield (Scheme 8).



Scheme 8

The resolution of *rac*-**3** was afforded by crystallization in the presence of (*S*)-malic acid as resolving agent, following the procedure, described by Saigo and coworkers, with mandelic acid²⁴ (Scheme 9).



Scheme 9

Two recrystallisations were required to obtain the product with an enantiomeric excess exceeding 99%. On the other hand attempts to use different acids like (*R*)-mandelic acid or (*R*)-tartaric acid were not successful (no crystalline compounds in the first case and low e.e. (35%) in the second one).²⁵

The enantiomeric purity could be estimated by HPLC on a chiral stationary phase (Figure 5) and also by ¹⁹F NMR, after formation of the Mosher amide with (*R*)-Mosher chloride²⁶.

²⁴ Kimbara, H.; Sakai, K.; Hashimoto, Y.; Nohira, H.; Saigo, K. *Tetrahedron: Asymmetry* **1996**, *7*, 1539.

²⁵ Yixia Jia, Marta Pontini, Peter E. Kündig, Giulia Licini unpublished results.

²⁶ Dale, J. A.; Mosher, H. S. *J. Am. Chem. Soc.* **1973**, *95*, 512.

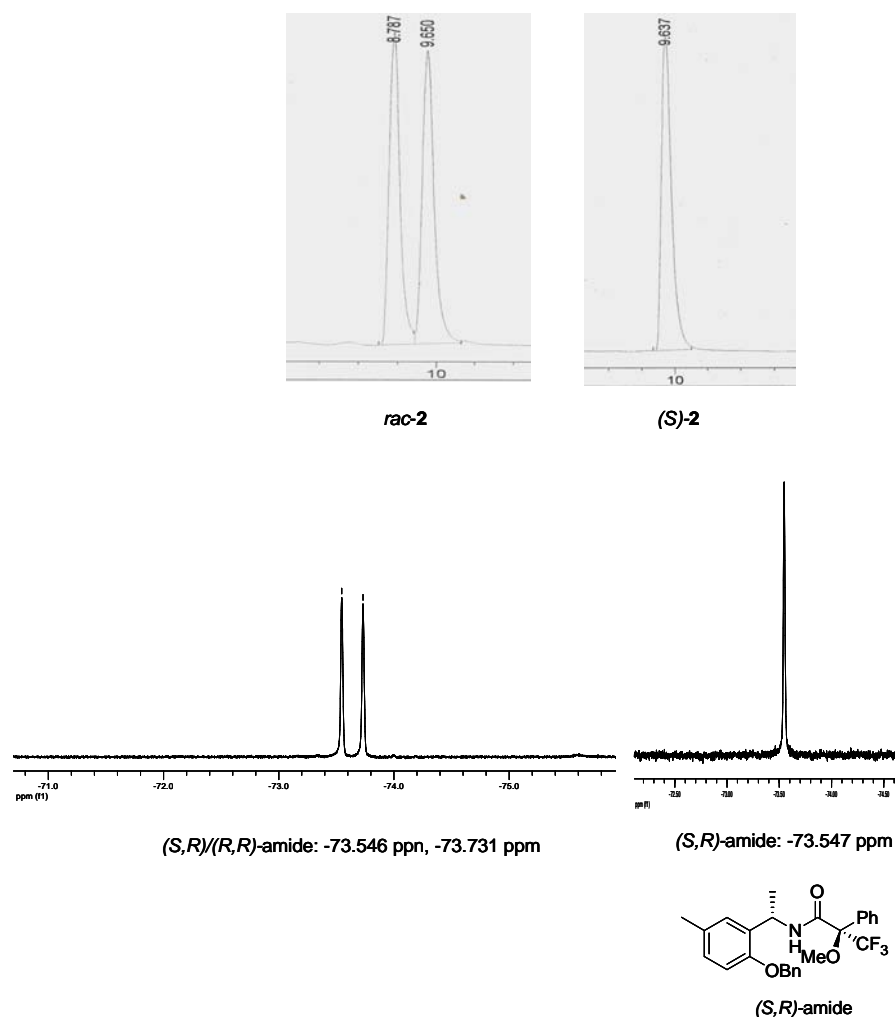


Figure 5. Chiral HPLC (Chiralcel AS-H column) of **3** and ^{19}F NMR (376 MHz, CDCl_3) of the Mosher's amide of **3**.

The absolute configuration was determined by the application of the salicylideneamine chirality rule,²⁷ which predicts the absolute stereochemistry of 1-phenyl-1-alkyl-methylimino-methylphenols and of analogues with substituted aromatic rings by CD spectroscopy. Condensation of **3** with salicylic aldehyde afforded the corresponding imine **7**, which CD spectrum showed positive bands, at nm 255 nm and 315 nm (Figure 6), consistent with an *S* absolute configuration.

²⁷ Smith, H.E. *Chem. Rev.* **1983**, 83, 359.

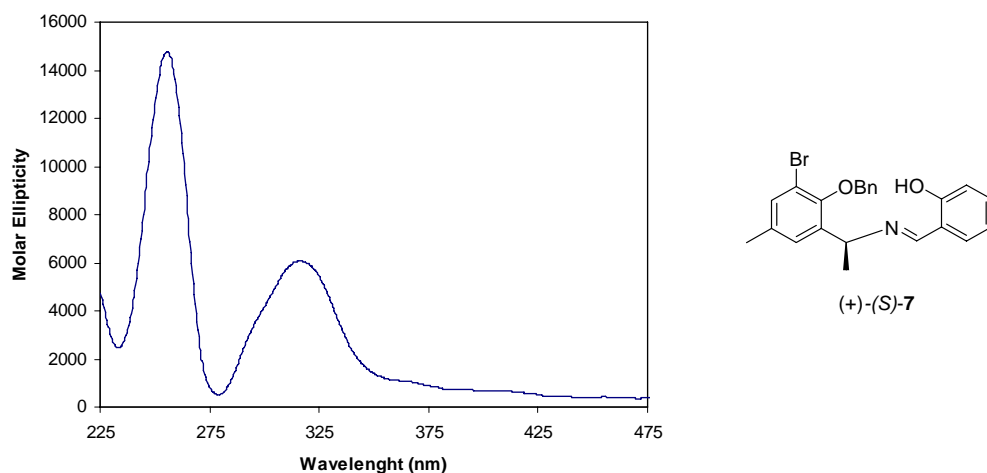


Figure 6. CD spectrum of (*S*)-7, CH₂Cl₂ C = 8.24 10⁻⁴ M

4.2.1.2 Stereoselective synthesis

An efficient stereoselective synthesis of 1-(2-benzyloxy-3-bromo-5-methyl-phenyl)-ethylaniline was set up as well. Two different synthetic approaches were explored dealing in one case with the stereoselective reduction^{6b} of the 1-(2-(benzyloxy)-3-bromo-5-methylphenyl)ethanone **6** by using an enantiopure oxazaborolidine (*R*)-**8** (Scheme 10) and in the second one the diastereoselective reduction of a chiral imine (*R*)-**12**,^{6b} synthesized using (*R*)-phenylethylamine as chiral auxiliary (Scheme 11).

The first approach let us to access to the enantiopure amine (*R*)-**3**, through the stereoselective reduction of an achiral ketone **6** by the Corey-Bakshi-Shibita method,^{28,29,30} (Scheme 10). The successive treatment with diphenyl phosphorazide (DPPA) and 1,8-diazabicyclo[5.4.0]undec-7-ene (DBU) in dry THF gave the azide (*R*)-**10**,³¹ which was reduced to the product (*R*)-**3**³² through the Staudinger protocol.³³ The use of a polymer bound triphenylphosphine allowed a much easier work up and purification of the polar amine (*R*)-**2** which was obtained with an e.e.=83%. Unfortunately this method suffers from three main drawbacks: low enantiomeric excess, due to the erosion of the e.e. in the stereospecific transformation of alcohol (*S*)-**9** into amine (*R*)-**3** (92% to 83% e.e.), which has to be ascribed to the activated benzylic centre in these compounds. The second disadvantage is related to the not high yield (29%) of the last step of the synthesis and to the difficult recover of the final

²⁸ Corey, E. J.; Helal, C. J. *Angew. Chem. Int. Ed.* **1998**, *37*, 1986.

²⁹ (a) Corey, E. J.; bakshi, R. K.; Shibita, S. *J. Am. Chem. Soc.* **1987**, *109*, 5551. (b) Corey, E. J.; Bakshi, R. K.; Shibita, S.; Chen, C.-P., Singh, V. K. *J. Am. Chem. Soc.* **1987**, *109*, 7925. (c) Corey, E. J.; Shibita, S.; Bakshi, R. K. *J. Org. Chem.* **1988**, *53*, 2861.

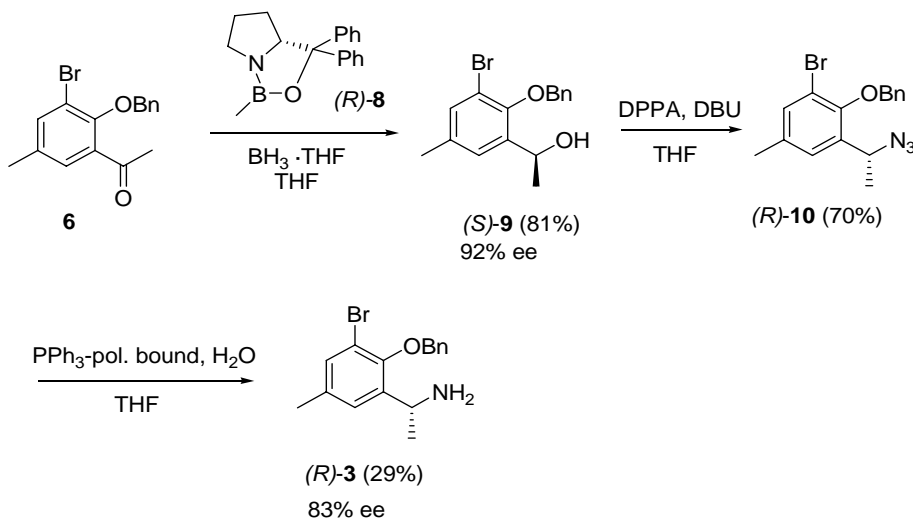
³⁰ The enantiomeric excess of (*S*)-**9** was determined by ¹H and ¹⁹F NMR after formation of the *Mosher* ester with (*R*)-*Mosher* chloride and its absolute configuration was determined by NMR correlation of the obtained ester derivative. See ref 6b and: Kelly, D. R. *Tetrahedron: Asymmetry* **1999**, *10*, 2927.

³¹ (a) Lal, B.; Pramanik, B. N.; Manhas, M. S.; Bose, A. K. *Tetrahedron Lett.* **1977**, 1977. (b) Thompson, A. S.; Humphrey, G. R.; DeMarco, A. M.; Mathre, D.; Grabowski, E. J. *J. Org. Chem.* **1993**, *58*, 5886.

³² The e.e. of (*R*)-**3** was determined by ¹H and ¹⁹F NMR after formation of the *Mosher* amide with (*R*)-*Mosher* chloride and its absolute configuration was determined by NMR correlation of the obtained amide as described for other chiral amines. See ref. 6b.

³³ Lindsley, C. W.; Zhao, Z.; newton, R. C., Leister, W. H.; Strauss, K. A. *Tetrahedron Lett.* **2002**, 4467.

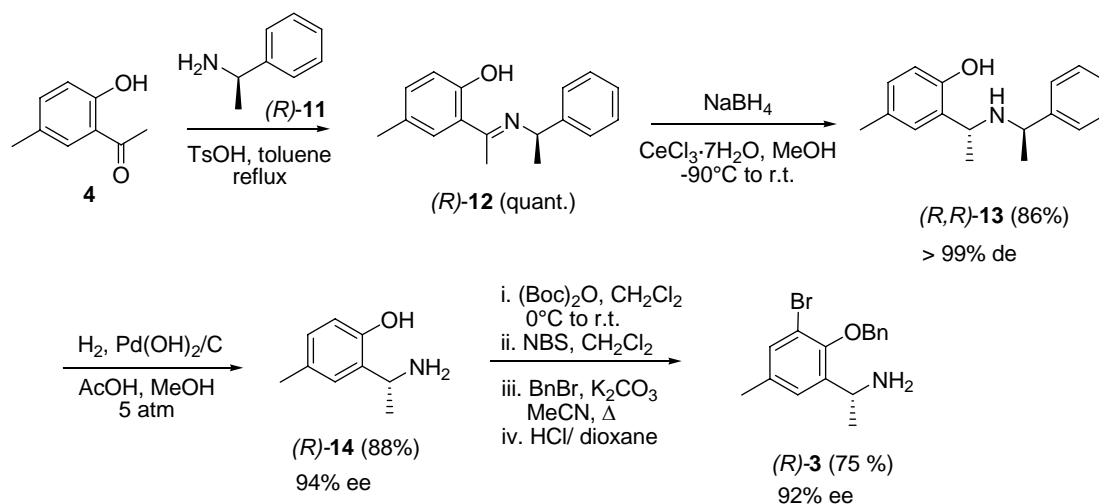
product. Finally, even if not so important at this preliminary stage of the research, the high cost of the enantiopure oxazaborolidine (*R*)-**8**.



Scheme 10

The second approach deals with stereoselective reduction of a chiral imine, as reported by Kündig and coworkers for a very similar aminophenol (Scheme 11).^{6b} Condensation of α -methylbenzylamine (*R*)-**11** with the 1-(2-hydroxy-5-methyl-phenyl)ethanone **4** furnished the corresponding imine derivative (*R*)-**12**. Addition of the reducing agent NaBH₄ to a suspension in methanol of (*R*)-**12** and catalyst CeCl₃ · 7 H₂O at -90° C provided a single diastereomeric amine (*R,R*)-**13** (>99% de), being completely stereoselective.¹⁵ Using Perlman's catalyst Pd(OH)₂/C under H₂ pressure (5 bar), the selective cleavage of the N-C benzylic bond, bearing the less substituted aromatic ring, was obtained, affording amine (*R*)-**14**. The final product (*R*)-**3** (92% e.e.) was achieved with good yields after a series of passages of protection of the amine, *ortho*-bromination of the phenol, successive protection of the phenolic moiety as benzyl ether and removal of the Boc-protective group from the amine. This last approach was also applied on 30 mmol-scale.³⁴

³⁴ The enantiomeric excesses of (*R*)-**3** and (*R*)-**14** were determined by ¹H NMR and ¹⁹F NMR after formation of the Mosher amide with (*R*)-Mosher chloride and their absolute configurations by NMR correlation of the obtained amides as described for other chiral amines. See ref. 6b.



4.2.1.3 Kinetic enzymatic resolution

Among the different methodologies developed for the production of enantiopure amines, kinetic enzymatic resolution³⁵ is increasing in significance at research and industrial level if compared with the other competitive procedures already described. It refers to the separation of enantiomers taking advantage of their different reaction rates when reacting with enantiomerically pure reagents/catalysts. Because the separation is based on the different rate constants (k_R/k_S), the degree of resolution that can be obtained depends on both the magnitude of the rate constants and the conversion of the reaction.

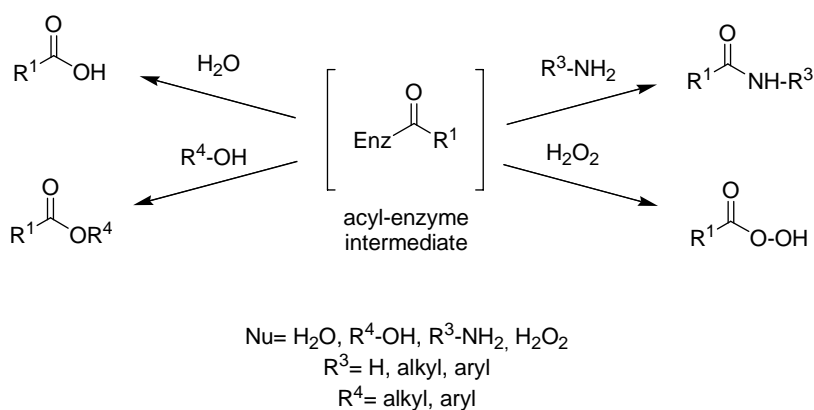
Generally enzymatic kinetic resolution is characterized by high Enantiomeric Ratios ($E > 100$) giving total conversion of one enantiomer into the product and leaving the other one as unreacted substrate (the other enantiomer).

Several enzymes are now commercially available and they can be also used in non-aqueous environment. Among them the hydrolases are the mainly used also due to their robustness. Hydrolases catalyze the hydrolysis of esters or amides in water, while operating in organic medium and replacing the natural nucleophile water, with a different one, such as an alcohol, hydroperoxide or amine, they are able to catalyze esterification, transesterification, aminolysis and perhydrolysis (Scheme 12).^{36,37}

³⁵ Faber, K. *Biotransformations in Organic Chemistry*, Springer-Verlag Berlin Heidelberg New York, 2005.

³⁶ van Rantwijk, F.; Sheldon, R. *Tetrahedron* **2004**, *60*, 501.

³⁷ Schmid, R. D.; Verger, R. *Angew. Chem. Int. Ed. Engl.* **1998**, *37*, 1608.



Scheme 12. Reactions catalyzed by hydrolases

In particular for the kinetic resolution of primary amines, good results were achieved with lipases from *Candida antarctica*. The number of chiral amines that has been resolved via lipase mediated stereoselective acylation has grown explosively over the last years and most of them have involved *Candida antarctica* lipase B.

Lipase B (CaLB) is one of the two variants of *Candida antarctica* lipases, the other being Lipase A (CaLA), produced by the alkaline yeast. They possess different properties at chemical and physical level. Both of them are relatively stable in a high pH range (pH 6-9 for CaLA and 7-10 for CaLB), while CaLB tolerates higher temperatures (until 70°C) especially if immobilized on a polymeric matrix. CaLB is a highly enantioselective and stable biocatalyst and because of this it tends to eclipse many other potentially useful lipases. The, hereto, little-used CaLA has shown unexpected strength in the enantioselective acylation of α - and β -amino esters. The stereoselection of the process very often depends on a suitable optimization of the reaction conditions that means chose the proper acylating agent, reaction medium, additives. The role of non-enzymatic background reactions in these phenomena is still obscure, but surely it is a major actor.

In particular CaLB retains its activity in anhydrous organic solvents, and this is why it has been efficiently used in aminolysis, esterification and transesterification reactions. Even traces of water in the reaction mixture will lead to undesirable hydrolysis of the acyl donor and the liberated acid may affect deactivation of lipase. Thus water, the natural reaction medium of the enzyme, is not a good solvent for aminolysis, because hydrolysis of the donor is bound to predominate. The consequent use of lipases in anhydrous organic solvents renders indispensable their immobilization on a support.

Within the collaboration with the group of Prof. Lucia Gardossi in University of Trieste, many efforts were directed to the resolution of (*rac*)-**14** using CaLB as catalyst, since this enzyme is characterized by a high stereoselectivity towards chiral amines and alcohols.^{37,38,39}

According the Kazlauskas model,⁴⁰ CaLB preferentially converts (*R*)-enantiomers of secondary alcohols and primary amines to the acylated product.⁴¹ This important feature is

³⁸ (a) Uppenberg, J.; Öhrner, N.; Norin, M.; Hult, K.; Kleywegt, G. J.; Patkar, S.; Waagen, V.; Anthonsen, T.; Jones, A. *Biochemistry* **1995**, *34*, 16838. (b) Uppenberg, J.; Patkar, S.; Bergforst, T.; Jones, A. *J. Mol. Biol.* **1994**, *235*, 790.

³⁹ (a) Inglesias, L. E.; Sanchez, V. M.; Rebolledo, F.; Gotor, V. *Tetrahedron Asymmetry* **1997**, *8*, 2675. (b) Gotor-Fernandez, V.; Busto, E.; Gotor, V. *Adv. Synth. Catal.* **2006**, *348*, 797.

due to the structure of the enzyme and to the conformation of the active site, which is characterized by two sub-sites, an acyclic one and an aminic/alcoholic one, and contains a serine residue that is activated by histidine and aspartate residues; these together form the catalytic triad (Figure 6), which discriminates the favoured enantiomer from the disfavoured one.

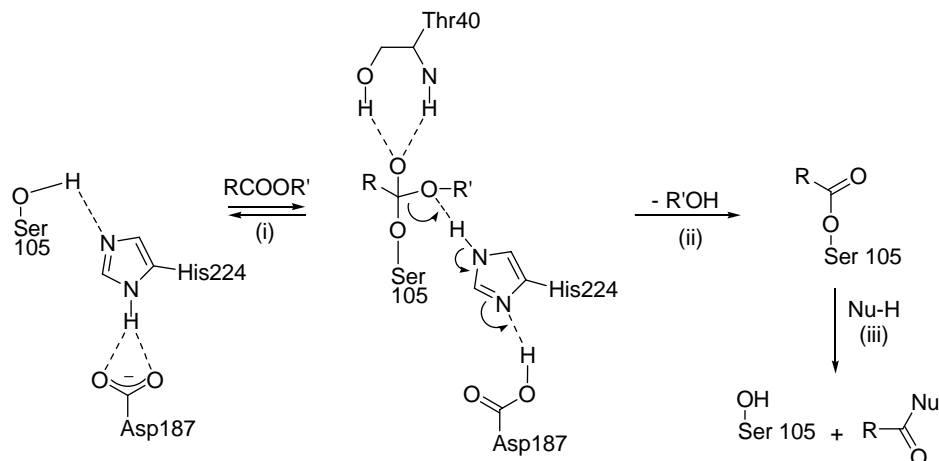


Figure 6. Reaction mechanism of lipase catalysis (numbering is for *Candida Antarctica* lipase B); - - - denotes a hydrogen bond. Step (iii) is the microscopic reversal of step (i) and (ii).

The reactant ester forms a tetrahedral acyl-enzyme intermediate by reaction with the OH group of the catalytic serine residue; the resulting excess of negative charge that develops on the carbonyl oxygen is stabilized by the oxyanion hole. Subsequently, the tetrahedral intermediate collapses to the serinate ester with elimination of the alcohol. Successive reaction of the acyl-enzyme intermediate with a nucleophile, the acyl acceptor, affords the product. Thus the reaction of the acyl-enzyme with an amine gives the corresponding carboxylic amide (Figure 6).

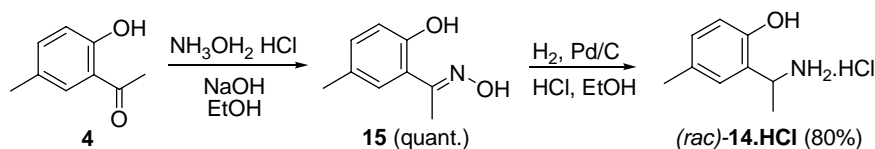
In this contest, the kinetic resolution catalyzed by the immobilized CaLB (Novozym 435®) was studied with (*rac*)-**14** as substrate, since this amine is less hindered than (*rac*)-**3** and thus more suitable for the entrance into the enzymatic pocket. Novozym 435®, commercialized by Novozym, is a CaLB preparation adsorbed on acrylic resin with a 2% in CaLB.⁴² On the basis of Kazlauskas model, the expected reacting enantiomer is (*R*)-**14**, and therefore (*S*)-**14** should be recovered as unreacted enantiomer, in an enriched form.

The synthesis of (*rac*)-**14** consisted in a two-steps procedure: the reaction of acetophenone derivative **4** with hydroxylamine afforded ketoxime **15**, which was converted to the racemic amine **14.HCl** via hydrogenolys Pd-catalyzed under acidic conditions (Scheme 13).

⁴⁰ (a) Kazlauskas, R. J.; Weissfloch, A. N. E.; Rappaport, A. T., Cuccia, L. A. *J. Org. Chem.* **1991**, *56*, 2656. (b) Kazlauskas, R. J. *Trends Biotechnol.* **1994**, *12*, 464. (c) Kazlauskas, R. J.; Weissfloch, A. N. E. *J. Mol. Catal. B: Enzym.* **1997**, *3*, 65.

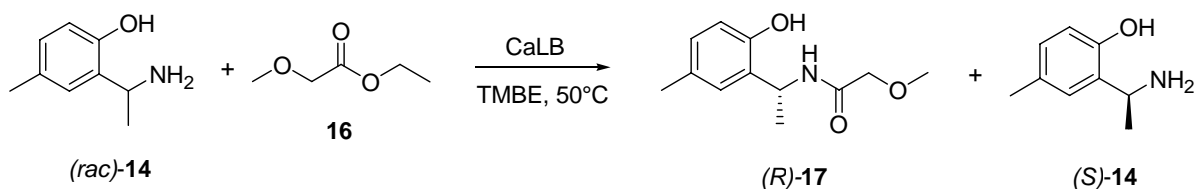
⁴¹ (a) Evans, D. A.; Johnson, J. S. *J. Am. Chem. Soc.* **1999**, *121*, 2617. (b) Evans, D. A.; Burgey, C. S.; Paras, N. A.; Vojkovsky, T.; Tregay, S. W. *J. Am. Chem. Soc.* **1998**, *120*, 5824.

⁴² Paetzld, J.; Backvall, J. E. *J. Am. Chem. Soc.* **2005**, *125*, 17620.



Scheme 13

The acylation reaction performed using ethyl-methoxyacetate⁴³ **16** as acyl donor, under mild reaction conditions, turned out to be the most effective as far as yields and enantioselectivities are concerned. In particular at 50°C in methyl-*tert*-butyl ether as solvent and using (*rac*)-**14**/ ethyl-methoxyacetate (1:1), product (*R*)-**17** was obtained after six days in 50% yield and e.e. of 98%, with the unreacted enantiomer (*S*)-**14** enriched with e.e. of 91%. These are the best reaction conditions found up to now (Scheme 14).



Scheme 14

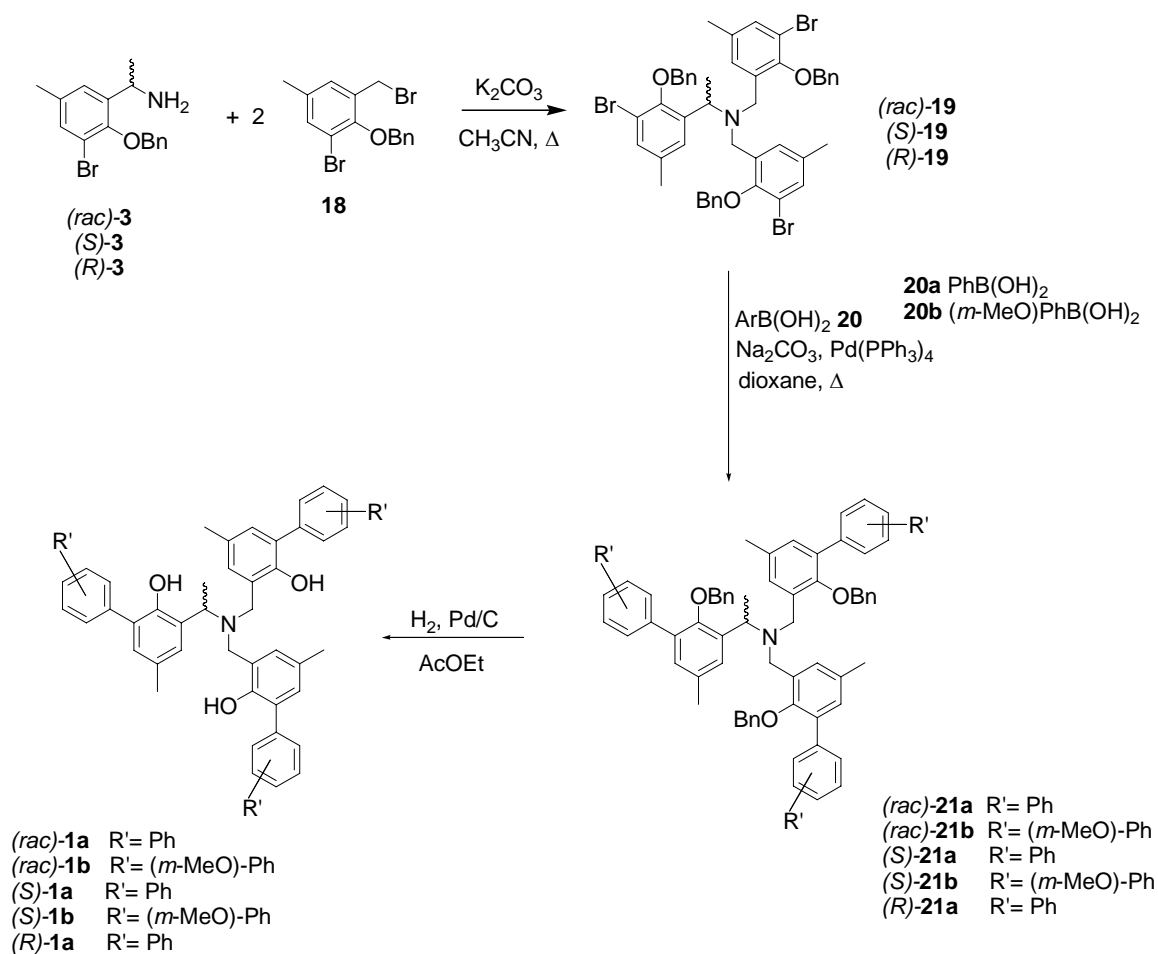
Despite the high stereoselectivity and the quantitative recovery of enantiomer (*R*), severe problems are still present for the unreacted reagent recover out of the reaction mixture: in fact there is a strong affinity between the polymeric matrix and the reagent, which makes the recovery of the unreacted enantiomer (*S*)-**14** very difficult. Future studies will deal with the use of different polymeric matrixes for CaLB and the set up of a Dynamic Kinetic Resolution process in order to obtain a single enantiomer out of the racemic mixture.

Even if all the three approaches resulted effective to obtain the enantiopure or enantioenriched form of amine **3** or of its precursor **14**, at the present the classical resolution seems to be the most valid route for this amine, thanks to the high yields, limited number of synthetic passages and easy scale up of the process.

4.3 Chiral amine tri-phenolate ligands: synthesis and coordination chemistry with Ti(IV)

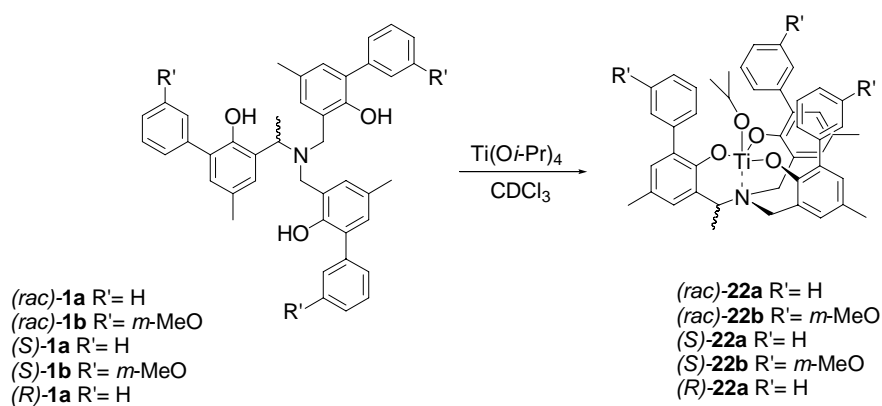
Chiral amine tris-phenolate ligands **1a-b** were obtained through a three-steps procedure involving bis-benylation of primary amine **3** with 2-(benzyloxy)-1-bromo-3-bromomethyl-5-methyl-benzene **18** under basic conditions, affording the *tris-O*-benzylated ligand, followed by Suzuki coupling reaction and Pd-catalyzed hydrogenolysis of the benzylic protecting groups (Scheme 15).

⁴³ (a) Balkenhohol, F.; Ditrich, K.; Hauer, B.; Ladner, W. J. *Prakt. Chem.* **1997**, 339, 381. (b) Cammenberg, M.; Hult, K.; Seongsoon, P. *ChemBioChem* **2006**, 7, 1745.



Scheme 15

The access to the enantiomerically pure ligand **1** permitted to obtain conformationally stable Ti(IV) phenolate complexes **22** with a controlled propeller-like chirality (Scheme 16). Furthermore, these complexes do not interconvert into the two propeller forms in solution, even at high temperatures, unlike the racemic complexes derived from achiral ligands.



Scheme 16

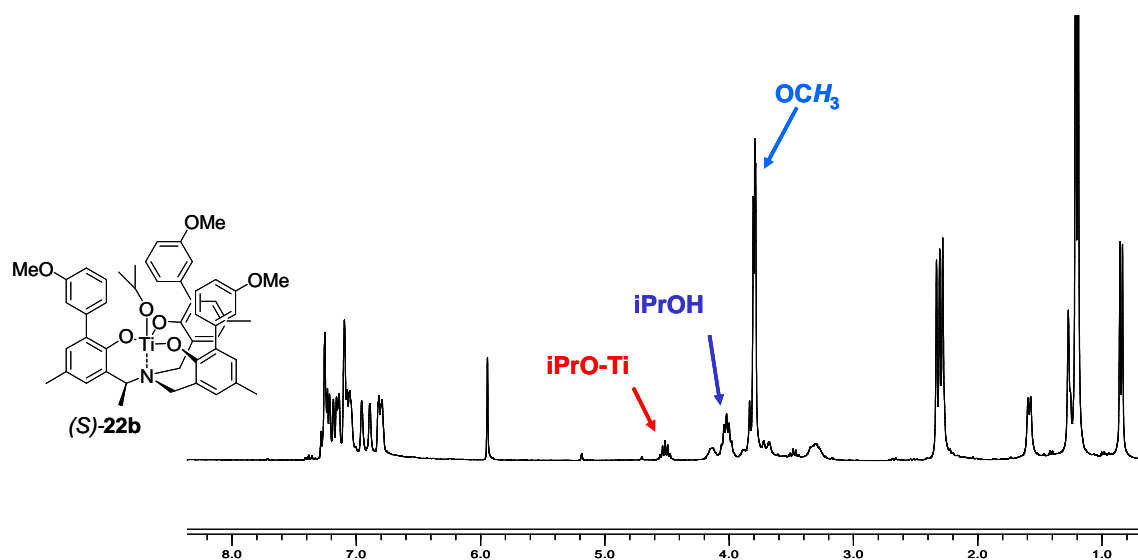


Figure 7. ^1H NMR (300 MHz, CDCl_3) spectrum of the enantiopure complex (*S*)-**22b**

As an example ^1H NMR spectrum of complex (*S*)-**22b** shows the presence of a single set of signals for each proton, the system is more complex due to the fact that now the complex is C_1 -symmetrical. The signals of the three arms are no longer identical and this is why, for example, the three methyls in the *para* position furnish three different singlet in the range 2.29-2.33 ppm (Figure 7).

Coordination of the amine triphenolate to the Ti(IV) metal centre, after reaction with one equivalent of $\text{Ti}(\text{O}i\text{-Pr})_4$, affords a chiral complex, whose helical chirality is controlled by its stereogenic α -methyl group adopting pseudoaxial conformation. In this way the formation of the diastereoisomer, bearing the methyl group in *anti* position with respect to the proximal phenyl moiety, is favoured by the absence of *syn*-pentane-like interactions. Thus, an *S* stereocenter would induce a Δ (right-handed) propeller-like twist, whereas a *R* one would induce the opposite one. This has also recently confirmed by the X-ray crystal structure of the enantiopure titanatrane chiral complex (*R*, Λ) obtained from (*R*)-bis-(2-hydroxy-3,5-di-*t*-butylbenzyl)-[1-(2-hydroxy-3,5-di-*t*-butylphenyl)ethyl]amine ligand reported by Bull, Davidson *et al.*⁴⁴: the introduction of an *R* stereocenter led to the formation of a left-handed propeller like twist (Figure 8).

⁴⁴ Axe, P.; Bull, S.D.; Davidosn, M. G.; Gilfillan, C. J.; Jones, M. D.; Robinson, D.E.J.E., Turner, L.E.; Mitchell, W.L. *Organic Lett.* **2007**, *9*, 223.

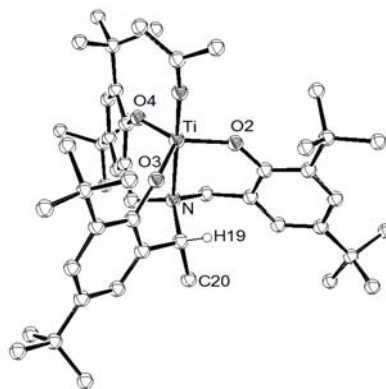
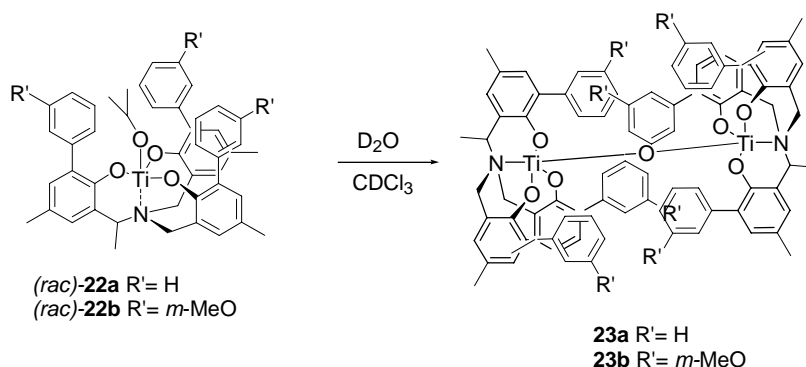


Figure 8. Molecular structure of the pentacoordinate TBP enantiopure Ti(IV) complex (*R*, Λ) with ligand (*R*)-*N,N*-bis-(2-hydroxy-3,5-di-*t*-butylbenzyl)-[1-(2-hydroxy-3,5-di-*t*-butylphenyl)ethyl]amine.⁴⁴

While enantiopure (*S*)-**22a**, (*S*)-**22b** and (*R*)-**22a** remained mononuclear in solution, the corresponding racemic complexes (*rac*)-**22a** and (*rac*)-**22b** evolve to the corresponding dinuclear μ -oxo complexes **23a** and **23b** (Scheme 17), in accordance with what we observed with the racemic complexes **2** in Chapter 3.



Scheme 17

If compared to the fast μ -oxo complex formation of achiral ligands, dimers **23a** and **23b** form much more slowly, probably due to the higher constrain of these systems. In particular the μ -oxo complex **23b**, with *meta*-methoxy groups in the peripheral aromatic rings, forms even more slowly in respect of **23a** (Figure 9) and complete formation is observed only after water addition. The ¹H NMR spectra of dinuclear complexes **23** are rather complicated, due to the C₁-symmetry of the chiral titanatranes. Furthermore they do not form as a single μ -oxo species: in fact, if we assume the reaction of two enantiomeric units, three different diastereomers are anyhow present in solution due to the three possible intercalation ways between the two enantiomeric chiral titanatranes.

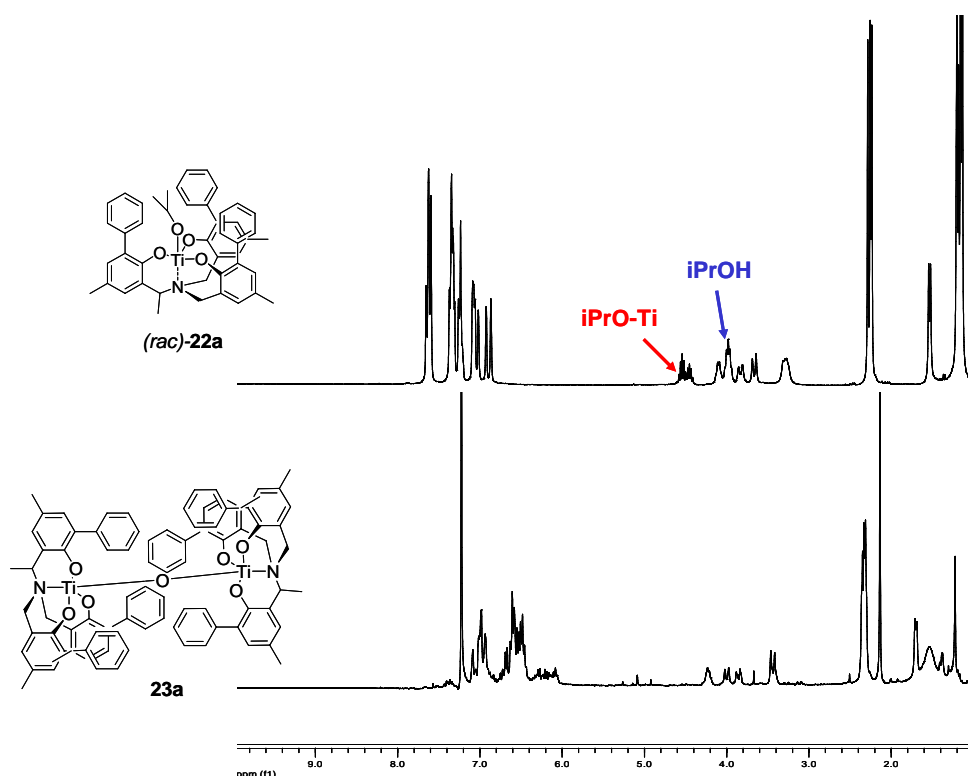


Figure 9

4.4 Selective synthesis of mixed μ -oxo complexes

In order to have a deeper understanding on the basis of the stereoselective recognition process occurring in the μ -oxo Ti(IV) dinuclear complex formation, the process have been studied with different complexes in opposite enantiomeric form. As we discussed in the previous chapter, the C_1 titanatranes forms the corresponding μ -oxo complexes more slowly and the addition of substituents on the peripheral aromatic groups (i.e. *m*-methoxy) slows down even more the μ -oxo complex formation. Therefore we mixed solutions of the racemic, mononuclear, *meta*-methoxy substituted complex **22b** with the enantioenriched monomeric complex (*R*)-**22a** (e.e. 83 %). In this way, the formation of the 'heterochiral' mixed dimer (*R*)-**22a**/*S*)-**22b** should be kinetically favoured in respect of the heterochiral one (*R*)-**22b**/*S*)-**22b**. Two different experiments were performed, in the first one a 1:1 mixture of (*R*)-**22a**/*(rac)*-**22b** (0.008M) was used with an excess of (*R*)-**22a** and in the second case 1:2 mixture of (*R*)-**22a**/*(rac)*-**22b** (0.008M) and in this case we are working with an excess of *(rac)*-**22b**. Due the the ^1H NMR complexity of these systems, the product distribution was monitored via ESI-MS (Figure 10).

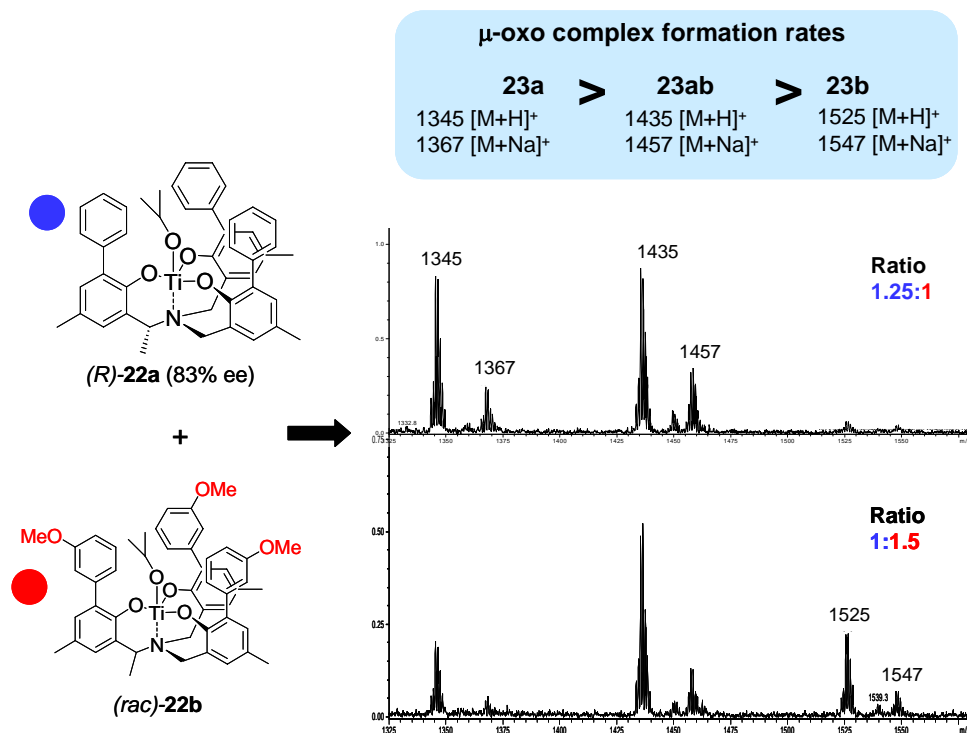


Figure 10. ESI-MS experiments, FIA positive analysis, solution 10⁻⁷M CH₃CN: solutions obtained from mixing excess of monomer (*R*)-**22a** (83% e.e., 0.002 mmol of solution 0.008243 M) and monomer (*rac*)-**22b** (0.002 mmol of solution 0.008243 M) and viceversa, that is (*R*)-**22a** (83% e.e., 0.0014 mmol of solution 0.008243 M) and monomer (*rac*)-**22b** (2 equivalents 0.0028 mmol of solution 0.008243 M).

The ESI-MS spectra of the two experiments are rather different (Figure 10). In the spectrum part relative to the μ-oxo complexes $m/z = 1300-1600$, three different species have been detected: the heterochiral μ-oxo **23a** from (*R*)-**22a**/*(S)*-**22a** ($m/z = 1345$ (M+H⁺); 1367 (M+Na⁺), the mixed 'heterochiral' μ-oxo **23ab** from (*R*)-**22a**/*(S)*-**22b** ($m/z = 1435$ (M+H⁺); 1457 (M+Na⁺) and the heterochiral μ-oxo **23b** from (*R*)-**22b**/*(S)*-**22b** ($m/z = 1525$ (M+H⁺); 1547 (M+Na⁺). In the first case we observe mainly the mixed 'heterochiral' μ-oxo **23ab**, together with the heterochiral μ-oxo **23a** origination from the poor enantiomeric excess of the starting complex. In the second case the mixed heterochiral μ-oxo **23ab** is the main compound, but the heterochiral μ-oxo **23b** is also present, even if in a much lower quantities. Even if the analysis is not quantitative (monomers **23a** and **23b** are not stable under ESIMS conditions), the results obtained clearly indicate that the heterochiral dimers are favored and that the different μ-oxo formation rates could be used for resolving a racemic mixture. Future studies will face the quantitative aspects of the process (kinetics of μ-oxo formation, quantification of the products via other spectroscopic methods like heteronuclear NMR, etc).

4.5 Conclusions

Efficient methods for the obtaining enantiopure aminophenols, building blocks for the construction of enantiopure amine triphenolate titanium(IV) complexes, have been set up. In particular, classical resolution with (*S*)-malic acid allowed to obtain (*S*)-**3**. The obtaining of the triphenolamines in enantiopure form allowed to explore more in detail the recognition

process between the titanatrane complexes: the experiments performed via ESI-MS techniques confirm the existence of a recognition process between titanatranes with opposite helices not only in the same complexes but also between systems with different aryl groups in the periphery. In particular, in this case the different reaction rates, which depend on the bulkiness of the aryl residues, could be used for controlling the dimerization process.

4.6 Experimental

General remarks

All reagents have been purchased from Aldrich or Fluka and used as received. Thin-layer chromatographies have been carried out on 0.2 mm Macherey-Nagel silica gel plates (G/UV 254) using UV light, ninhydrin or cerium molybdenum solution as the visualizing agent. Flash chromatographies have been performed with Macherey-Nagel silica gel 60 (0.04-0.063 mm, 230-400 mesh). The NMR spectra have been recorded on a Bruker AC 250 (^1H : 250.13 MHz; ^{13}C : 62.9 MHz) or a Bruker AV 300 (^1H : 300.13 MHz; ^{13}C : 75.5 MHz) spectrometer. Chemical shift (δ) have been reported in parts per million (ppm) relative to the residual undeuterated solvent as an internal reference (CDCl_3 : 7.26 ppm for ^1H NMR and 77.0 ppm for ^{13}C NMR; CD_3OD : 4.84 ppm for ^1H NMR and 49.05 ppm for ^{13}C NMR). The following abbreviations have been used to explain the multiplicities: s = singlet, d = doublet, t = triplet, dd = double doublet, m = multiplet, br = broad. ^{13}C NMR spectra have been recorded with complete proton decoupling.

ESI-MS spectra have been obtained on a LC/MS Agilent series 1100 spectrometer in positive mode, by flow injection analysis, with methanol/formic acid 0.1% as the solvent mixture, with electrospray ionization and ion trap mass detector. High-resolution mass spectra have been obtained with ESI-TOF MarinerTM BiospectrometryTM Workstation of Applied Biosystem by flow injection analysis; exact mass measurements have been obtained by external calibration with two appropriate lock mass compounds.

IR spectra have been recorded on a Nicolet 5700 FT-IR, with range 4000-400 cm^{-1} and resolution 4 cm^{-1} ; only the most important and relevant frequencies have been reported.

Optical rotations have been recorded on a Perkin-Elmer 241 polarimeter at 589 nm and values have been reported as follows: $[\alpha]_D^{25}$ (concentration c g/100 mL, solvent).

Melting points are uncorrected and have been determined with a Leitz-Laboroux 12.

All oxygen or moisture sensitive compounds have been handled under controlled atmosphere (nitrogen) in a glovebox Mbraun MB 200MOD, equipped with a MB 150 G-I recycling system.

1-(2-hydroxy-3-bromo-5-methyl-phenyl)ethanone (5)

A solution of N-bromosuccinimide (48.267 mmol, 8.59 g) in dry CH_2Cl_2 was added dropwise to a magnetically stirred solution of 1-(2-hydroxy-5-methyl-phenyl)ethanone **4** (40.22 mmol, 10.1 g) in dry CH_2Cl_2 (300 mL) at room temperature. The mixture was left under stirring overnight and then was washed with $\text{H}_2\text{SO}_{4\text{aq}}$ 10% (2×150 mL). The layers were separated and the aqueous one extracted with CH_2Cl_2 (3×150 mL). The combined organic phases were washed with NaCl_{aq} sat. (2×150 mL), dried over MgSO_4 and concentrated.

Compound **5** was recovered as a pale yellow solid (9.0 g, 98%), which was crystallized in petroleum ether (8.8 g, 96%).

(5): Mp: 57- 59°C. IR (KBr) ν (cm⁻¹): 554, 645, 773, 795, 1171, 1249, 1311, 1343, 1441, 1612, 1639, 1696, 2926, 2962, 3419. ¹H-NMR: (250 MHz, CDCl₃) δ 2.30 (3H, s), 2.63 (3H, s), 7.48 (3H, s), 7.55 (3H, s). ¹³C{¹H}-NMR: (62.9 MHz, CDCl₃) δ 20.5 (CH₃), 26.9 (CH₃), 111.8 (C), 120.3 (C), 129.3(C) , 130.1 (CH)140.5 (CH), 157.0 (C), 204.4 (C). Anal. Calcd. for C₉H₉BrO₂: C 47.19, H 3.96. Found: C 47.50, H 3.98.

1-(2-Benzyloxy-3-bromo-5-methyl-phenyl)-ethanone (6)

Substrate **5** (33.66 mmol, 7.71 g) was weighed in a double necked round bottom flask, then dry CH₃CN (70 mL), K₂CO₃ (134.6 mmol, 18.6 g) and benzyl bromide (38.7 mmol, 4.6 mL) were added under N₂. The reaction mixture was thermostated at 85 °C, left under reflux for 18 h and then cooled to room temperature. The mixture was filtered through Celite, washing with ethyl acetate, and the filtrate was concentrated under reduced pressure. The resulting pale yellow oil was dissolved in CHCl₃ (150 mL), treated with HCl 1M (3 x 150 mL) and brine (3 x 150 mL). The organic layer was dried over MgSO₄ and the solvents were removed under vacuum. The product was further purified by flash chromatography on silica gel, using petroleum ether/ethyl acetate 10:1 as eluant. Compound **6** was quantitatively isolated as a colourless oil.

(6): IR (KBr) ν (cm⁻¹): 596, 758, 865, 971, 1170, 1256, 1283, 1398, 1456, 1598, 1687, 2924, 3032. ¹H-NMR: (250 MHz, CDCl₃) δ 2.34 (3H, s), 2.54 (3H, s), 4.95 (2H, s), 7.32 (1H, s), 7.33- 7.48 (3H, m), 7.50- 7.55 (2H, m), 7.56 (1H, m). ¹³C{¹H}-NMR: (62.9 MHz, CDCl₃) δ 20.6 (CH₃), 30.9 (CH₃), 77.2 (CH₂), 118.5 (C), 128.7 (CH) , 128.7 (2×CH), 128.8 (2×CH), 129.4 (CH), 135.7 (C), 135.9 (C), 136.3 (C), 137.5 (CH), 152.2 (C), 200.3 (C). MS (ESI): 341.0 [M+Na]⁺.

Classical resolution

(±)-1-(2-Benzyloxy-3-bromo-5-methyl-phenyl)-ethylamine ((rac)-3)

Substrate **6** (18.89 mmol, 6.0 g) was weighed in a double necked round bottom flask, then a solution of NH₃ 2M in MeOH (94.4 mmol, 47.2 mL) and Ti(OⁱPr)₄ (37.77 mmol, 11.14 mL) were added under nitrogen. The mixture was left under stirring at room temperature for 12 h and then NaBH₄ (1.07 g, 28.3 mmol) was slowly added at 0 °C (ice bath). The mixture was warmed to room temperature and stirred for 3 h and then quenched with NH₄OH 2M (47 mL). The resulting inorganic precipitate was filtered off and washed with AcOEt (50 mL). The phases were separated and the aqueous one was extracted with AcOEt (2 x 50 mL). The combined organic layers were dried over MgSO₄ and concentrated under reduced pressure, affording compound (*rac*)-**3** as a yellow oil (5.3 g, 87%).

(*rac*)-**3**: IR (KBr) ν (cm⁻¹): 696, 732, 856, 977, 1215, 1270, 1376, 1453, 1601, 2964, 3373. ¹H-NMR: (250 MHz, CDCl₃) δ 1.33 (3H, d, J = 7.5 Hz), 2.31 (3H, s), 4.42 (1H, q, J = 7.5 Hz), 4.96 (1H, d, J = 11.0 Hz, part A, AB system), 5.01 (1H, d, J = 11.0 Hz, part B, AB system), 7.20 (1H, s),

7.30- 7.41 (4H, *m*), 7.51 (2H, *d*, *J* = 7.5 Hz). $^{13}\text{C}\{^1\text{H}\}$ -NMR: (62.9 MHz, CDCl_3) δ 20.95 (CH_3), 24.51 (CH_3), 45.35 (CH), 75.78 (CH_2), 117.32 (C), 126.32 (CH), 128.48 (2 \times CH), 128.51(CH), 128.77 (2 \times CH), 132.61(CH), 136.01 (C), 137.00 (C), 142.25 (C), 150.52 (C). MS (ESI): 320.1 $[\text{M}+\text{H}]^+$. HR-MS (ESI): calcd for $\text{C}_{16}\text{H}_{19}\text{BrNO}$: 320.0650; found 320.0653.

(-)-(S)-1-(2-Benzyloxy-3-bromo-5-methyl-phenyl)-ethylamine ((S)-3)

A 100 mL flask equipped with a condenser was charged with the (*rac*)-**3** amine (14.05 mmol, 4.5 g), (*L*)-malic acid (14.05 mmol, 1.88 g) and ethanol (50 mL). The mixture was manually shaken while heating to reflux until all the solid was completely dissolved. Meanwhile cooling to ambient temperature, the salt was precipitating. After 14 h at room temperature, the solid was filtered and washed with Et_2O and dried in vacuum to afford the enantiomerically enriched (*S,S*)-salt (4.965 g, 81%, ee of the free ammine 92%). Then the salt was crystallized again: a flask with a condenser was charged with the salt and ethanol (30 mL) and heated to reflux, until the salt was completely dissolved. The mixture was allowed to cool slowly down to room temperature and after 14 h the crystals were filtered from the mother liquor and dried under vacuum (4.84 g, 79%). The salt was treated with NaOH 2M (75 mL) and aqueous phase was extracted with Et_2O (3 \times 75 mL), affording the free amine (*S*)-**3** in (1.39 g, 39%) yield.

The enantiomeric purity of the free amine was determined by chiral HPLC (Chiralcel AS-H column, hexane/2-propanol 99:1, 1mL/min: 9.156 min (minor, *R*) 10.075 min (maior, *S*)) or by conversion to the Mosher amide: ee > 99 %.

(*S*)-**3**: $[\alpha]_D^{20}$: -2.85 (*c* = 0.85, CH_2Cl_2).

(+)-(R)-1-(2-Benzyloxy-3-bromo-5-methyl-phenyl)-ethylamine ((R)-3)

According to the procedure for (*S*)-**2**, (*rac*)-**2** amine (7.8 mmol, 2.5 g), (*D*)-malic acid (7.8 mmol, 1.047 g) and ethanol (40 mL) were used to obtain (*R*)-**2** (950 mg, 38%, ee > 99%), after two recrystallizations.

(*R*)-**3**: $[\alpha]_D^{20}$: + 2.85 (*c* = 0.85, CH_2Cl_2).

(S,R)-N-[1-(2-Benzyloxy-3-bromo-5-methyl-phenyl)-ethyl]-3,3,3-trifluoro-2-methoxy-2-phenyl-propionamide and (R,R)-N-[1-(2-Benzyloxy-3-bromo-5-methyl-phenyl)-ethyl]-3,3,3-trifluoro-2-methoxy-2-phenyl-propionamide ((S,R)-Mosher amide and (R,R)-Mosher amide)

Triethylamine (0.125 mmol, 17.6 μL) and (*R*)-methoxy-trifluoromethyl-phenyl acetyl chloride ((*R*)-Mosher acyl chloride, 0.124 μL , 0.5 M in dichloromethane) were added to (*S*)-**2** (or (*R*)-**2** or (*rac*)-**2**) (0.062 mmol, 20 mg) in CH_2Cl_2 (1 mL). The solution was stirred for 6 h at room temperature. Then it was washed with NaHCO_3 sat., HCl 1M and H_2O . The organic phase was dried over MgSO_4 and evaporated. The product (33.3 mg, 98%) was analyzed by ^1H NMR (300 MHz, CDCl_3) and ^{19}F NMR (376 MHz, CDCl_3).

^{19}F NMR (376 MHz, CDCl_3): δ -73.547 (*S,R*)-Mosher amide, -73.724 (*R,R*)-Mosher amide.

(+)-(S)-2-[[1-(2-Benzyloxy-3-bromo-5-methyl-phenyl)-ethylimino]-methyl]-phenol ((S)-7)

(S)-**3** (0.5 mmol, 160.1 mg) and salicylaldehyde (0.51 mmol, 62 mg) were dissolved in methanol (12 mL) and heated to 50° C for 40 min. The solvent was evaporated and the residue purified by column chromatography (ether/hexane 1:2) to afford (S)-**7** (160 mg, 75%) as a yellow oil.

(S)-**7**: IR (KBr) ν (cm⁻¹): 697, 733, 754, 753, 858, 884, 976, 1010, 1089, 1150, 1206, 1225, 1278, 1378, 1461, 1497, 152,, 1581, 1629, 1664, 2663, 2748, 2869, 2926, 2972, 3031, 3064. ¹H-NMR: (250 MHz, CDCl₃) δ 1.64 (3H, *d*, J = 6.9 Hz), 2.33 (3H, *s*), 2.33 (3H, *s*), 4.83 (1H, *q*, J = 6.9 Hz), 4.97 (1H, *d*, J = 6.9 Hz, part A, *AB system*), 5.07 (1H, *d*, J = 6.9 Hz, part B, *AB system*), 6.86 (1H, *d*, J = 7.3 Hz), 6.97- 7.02 (2H, *m*), 7.15- 7.18 (1H, *dd*, J = 7.8, 1.5 Hz), 7.25- 7.34 (3H, *m*), 7.38- 7.46 (2H, *m*), 7.49- 7.58 (2H, *m*), 8.13 (1H, *m*). ¹³C{¹H}-NMR: (62.8 MHz, CDCl₃) δ 20.8 (CH₃), 24.4 (CH₃), 61.9 (CH), 75.7 (CH₂), 116.9 (CH), 117.0 (C), 118.7 (CH), 118.8 (C), 127.3 (CH), 128.3 (CH \times 2), 128.4 (CH), 128.6 (CH \times 2), 131.5 (CH), 132.3 (CH), 132.9 (CH), 136.0 (C), 136.9 (C), 138.9 (C), 150.3 (C), 161.0 (C), 164.1 (CH). MS (ESI): 424.1 [M+H]⁺. $[\alpha]_D^{20}$: +30.22 (c = 0.87, in CH₂Cl₂).

Asymmetric synthesis: enantioselective reduction

(-)-(S)-1-(2-Benzyloxy-3-bromo-5-methyl-phenyl)-ethanol ((S)-9)

To a solution of oxazaborolidine (R)-**8** (2.87 mL, 1M in toluene) in dry THF (14 mL), BH₃·THF (8.61 mmol, 8.61 mL, 1M in THF) was added. Within 1 h, a solution in THF (18 mL) of compound **5** (7.17 mmol, 2.29 g) was added slowly. After 3 h, the reaction was stopped by addition of methanol (18 mL) and stirred vigorously for 30 minutes (T.l.c petroleum ether/AcOEt 7:3). The reaction mixture was concentrated and the residue taken up with Et₂O, washed with HCl 1M, Na₂CO₃aq. sat. and brine. After being dried over Na₂SO₄, the solvent was evaporated. Column chromatography of the crude product, using petroleum ether/AcOEt 9:1 as eluant, afforded compound (S)-**9** as a colourless oil (1.87 g (81%); ee 97%).

(S)-**9**: ¹H-NMR: (250 MHz, CDCl₃) δ 1.40 (3H, *d*, J = 6.2 Hz), 1.92 (1H, *d*, J = 3.7 Hz), 2.30 (3H, *s*), 5.00 (2H, *s*), 5.06 (1H, *dq*, J = 6.2, 3.7 Hz), 7.20 (1H, *d*, J = 1.5 Hz), 7.24- 7.39 (4H, *m*), 7.41- 7.49 (2H, *m*). ¹³C{¹H}-NMR: (62.9 MHz, CDCl₃) δ 20.9 (CH₃), 24.1 (CH₃), 65.2 (CH), 75.8 (CH₂), 117.1 (C), 126.5 (CH), 128.5 (2 \times CH), 128.6 (CH), 128.8 (2 \times CH), 133.2 (CH), 136.0 (C), 136.8 (C), 140.6 (C), 150.3 (C). MS (ESI): 343.2 [M+Na]⁺. $[\alpha]_D^{20}$: -33.0 (c = 1.50, in CH₂Cl₂).

(+)-(R)-1-(1-Azido-ethyl)-2-benzyloxy-3-bromo-5-methyl-benzene ((R)-10)

Compound (S)-**9** (5.6 mmol, 1.80 g) was weighed in a double necked round bottom flask, dissolved in dry THF (28 mL) and stirred at room temperature. Diphenylphosphorylazide (DPPA, 7.0 mmol, 1.926 g), followed by 1,8-diazabicyclo[5.4.0]undec-7-ene (DBU, 7.0 mmol, 1.046 mL) were added dropwise. The reaction mixture was stirred for 48 h and then concentrated under vacuum. Water was added to the residue and the solution was extracted with Et₂O (3 \times 20 mL). The combined organic phase was dried over Na₂SO₄ and evaporated.

Purification of the residue by column chromatography, using petroleum ether/AcOEt 8:2 as eluant, afforded azide (*R*)-**10** as a colourless oil (1.36 g, 70%).

(*R*)-**10**: IR (KBr) ν (cm⁻¹): 743, 882, 1206, 1373, 1457, 1584, 2098, 2926, 2966, 2982. ¹H-NMR: (250 MHz, CDCl₃) δ 1.44 (3H, *d*, *J* = 6.9 Hz), 2.36 (3H, *s*), 4.91– 4.99 (2H, *m*), 4.94 (1H, *m*), 4.99 (1H, *d*, *J* = 10.6 Hz, part A, *AB system*), 5.10 (1H, *d*, *J* = 10.6 Hz, part B, *AB system*), 7.16 (1H, *s*), 7.36– 7.44 (4H, *m*), 7.46– 7.52 (2H, *m*). ¹³C{¹H}-NMR: (62.9 MHz, CDCl₃) δ 20.9 (CH₃), 21.2 (CH₃), 55.3 (CH), 76.1 (CH₂), 117.5 (C), 126.9 (CH), 128.4 (2×CH), 128.6 (CH), 128.8 (2×CH), 133.9 (CH), 136.2 (C), 136.7 (C), 140.6 (C), 150.8 (C). MS (ESI): 368.3 [M+Na]⁺. [α]_D²⁰: + 29.1 (*c* = 0.67, in CH₂Cl₂).

(+)-(R)-1-(2-Benzyloxy-3-bromo-5-methyl-phenyl)-ethylamine ((R)-3)

To a suspension of polymer bound-PPh₃ (3.073 mmol, 1.024 g) in dry THF (6 mL), the substrate (*R*)-**9** (1.538, 532 mg) was added, followed by water (4.61 mmol). The reaction was stirred at room temperature for 5 days. Then the reaction mixture was filtered through a pad of Celite, washing with Et₂O, dried over MgSO₄ and concentrated. Purification of the crude product by column chromatography, using petroleum ether/AcOEt/Et₃N 6:4:0.001 as eluant, afforded the amine (*R*)-**2** as a yellow oil (143 mg (29%); ee 83%, obtained from ¹H NMR and ¹⁹F NMR of the corresponding (*R,R*)-Mosher amide).

Asymmetric synthesis: diastereoselective reduction of a chiral imine

(-)-(R)-Methyl-2-[1-(1-phenyl-ethylimino)-ethyl]-phenol ((R)-12)

A mixture of 1-(2-hydroxy-5-methyl-phenyl)ethanone **4** (20.97 mmol, 3.15 g), (+)-(α R)- α -methylbenzylamine (*R*)-**11** (20.97 mmol, 2.55 g, > 99% ee), TsOH (2.097 mmol, 0.399 g) and 4 Å activated molecular sieves (16 g) in dry toluene (28 mL) was heated to reflux for 17 h. The solution was filtered through a pad Celite, and the filtrate was evaporated. (*R*)-**12** was recovered in quantitative yield as a yellow oil (5.33 g, quant.).

(*R*)-**12**: IR (KBr) ν (cm⁻¹): 552, 700, 782, 823, 1023, 1085, 1233, 1295, 1323, 1399, 1450, 1493, 1585, 1619, 2866, 2924, 2971, 3028, 3059. ¹H-NMR: (250 MHz, CDCl₃) δ 1.64 (3H, *d*, *J* = 6.4 Hz), 2.30 (3H, *s*), 2.33 (3H, *s*), 4.94 (1H, *q*, *J* = 6.4 Hz), 6.89 (1H, *d*, *J* = 8.7 Hz), 7.10– 7.37 (7H, *m*). ¹³C{¹H}-NMR: (62.9 MHz, CDCl₃) δ 14.7 (CH₃), 20.8 (CH₃), 25.5 (CH₃), 58.6 (C), 118.5 (CH), 119.1 (C), 126.0 (C), 126.4 (CH×2), 127.2 (CH×2), 128.2 (CH), 128.3 (CH), 128.9 (CH×2), 133.5 (CH), 144.5 (C), 161.8 (C), 170.5 (C). MS (ESI): 255.4 [M+H]⁺. [α]_D²⁰: -215.15 (*c* = 1.03, in CHCl₃).

(+)-(R,R)-4-Methyl-2-[1-(1-phenyl-ethylamino)-ethyl]-phenol ((R,R)-13)

A mixture of (*R*)-**12** (20.47 mmol, 5.20 g), CeCl₃·7 H₂O (10.23 mmol, 3.81 g) in MeOH (72 mL) was thermostated at -90°C. NaBH₄ (40.94 mmol, 1.55 g) was added in one portion. The temperature was allowed to rise slowly to room temperature (16 h) and CH₂Cl₂ (290 mL) was added, followed by sat aq. NH₄Cl (290 mL). The solution was extracted with CH₂Cl₂ and the

combined organic layers were dried over MgSO₄ and the solvents were removed under reduced pressure. The crude product was obtained as a pale yellow oil, which was diluted in Et₂O and the hydrochloride salt precipitated by adding HCl 1.5M in Et₂O (1 equiv.). The precipitate was washed in water and dried. (86%, de > 99%, no detection of the other diastereoisomer). Treatment with NaOH 1M afforded the free amine (*R,R*)-**13** (4.70 g, 90%) as a pale yellow oil. The absolute configuration was assigned by comparison with literature data.^{6b,15}

(*R,R*)-13: IR (KBr) ν (cm⁻¹): 501, 701, 767, 818, 961, 1036, 1108, 1124, 1136, 1249, 1261, 1374, 1394, 1450, 1500, 1599, 2867, 2924, 2965, 3026, 3303. ¹H-NMR: (300 MHz, CDCl₃) δ 1.35 (3H, *d*, *J* = 6.8 Hz), 1.43 (3H, *d*, *J* = 6.8 Hz), 2.25 (3H, *s*) 3.62 (1H, *q*, *J* = 6.8 Hz), 3.95 (1H, *q*, *J* = 6.8 Hz), 6.60 (1H, *s*), 6.76– 6.80 (1H, *d*, *J* = 8.4 Hz), 6.96– 6.70 (1H, *d*, *J* = 8.4 Hz), 7.17– 7.20 (1H, *d*, *J* = 8.4 Hz), 7.28– 7.43 (4H, *m*). ¹³C{¹H}-NMR: (62.9 MHz, CDCl₃) δ 20.7(CH₃), 23.3 (CH₃), 23.8 (CH₃), 55.6 (CH), 56.4 (CH), 116.7 (CH), 126.3 (C), 126.4 (2×CH), 127.6 (CH), 128.3 (C), 128.90 (CH), 128.94 (CH), 129.0 (2×CH), 143.9(C), 155.3 (C). MS (ESI): 256.0 [M+H]⁺. HR-MS (ESI): calcd for C₁₇H₂₂NO: 256.1701; found 256.1704. $[\alpha]_D^{20}$: + 56.86 (c = 1.18, CHCl₃).

(-)-(*R*)-2-(1-Amino-ethyl)-4-methyl-phenol (*R*)-14

An autoclave was charged by a mixture of (*R,R*)-**13** (17.62 mmol, 4.50 g), MeOH (176 mL), AcOH (4.031 mL), and PdOH₂/C (20 wt%, 900 mg) and then purged with H₂. The reaction mixture was stirred under H₂ (5 atm) at room temperature for 54 h and then filtered over Celite. The solution was concentrated, treated with HCl 1M (90 mL) and extracted with Et₂O (2× 90 mL). The aqueous layer was basified with NaOH 2M and extracted with Et₂O (2× 90 mL). The combined organic phase (pH 9) was dried over Na₂SO₄ and concentrated under vacuum. The amine (*R*)-**14** was recovered as a white solid (2.34 g, 88%).

(*R*)-14: Mp: 82– 83 °C. IR (KBr) ν (cm⁻¹): 792, 821, 1008, 1092, 1110, 1216, 1265, 1288, 1381, 1479, 1528, 1612, 1652, 2189, 2490, 2899, 2980, 3407. ¹H-NMR: (250 MHz, CDCl₃) δ 1.49 (3H, *d*, *J* = 6.6 Hz), 2.28 (3H, *s*), 4.28 (1H, *q*, *J* = 6.6 Hz), 6.75– 6.80 (2H, *m*), 6.95– 7.00 (1H, *d*, *J* = 8.3 Hz). ¹³C{¹H}-NMR: (62.9 MHz, CDCl₃) δ 20.7 (CH₃), 24.0 (CH₃), 51.9 (CH), 117.1 (CH), 127.9 (CH), 128.0 (C), 128.2 (CH), 129.0 (CH), 155.3 (C). MS (ESI): 152.1 [M+H]⁺. HR-MS (ESI): calcd for C₉H₁₃NO: 152.1075; found 152.1071. $[\alpha]_D^{20}$: -3.8 (c = 1.0, CHCl₃).

(+)- (*R*)-[1-(2-Hydroxy-5-methyl-phenyl)-ethyl]-carbamic acid tert-butyl ester

Di-*tert*-butyl dicarbonate (Boc₂O, 15.7 mmol, 3.43 g) was added in one portion to a solution of (*R*)-**14** (14.5 mmol, 2.19 g) in CH₂Cl₂ (75 mL) cooled at 0°C with an ice/water bath. The reaction mixture was stirred for 12 h in an open flask and the temperature of the reaction mixture was allowed to warm up to room temperature. The solvent was evaporated and the residue was taken up in Et₂O, washed with sat. aq. NaHCO₃ (75 mL), HCl 1M (75 mL) and brine (75 mL), dried over Na₂SO₄ and concentrated under vacuum, to obtain the protected amine as a white solid (3.65 g, quant.).

Mp: 68–70 °C. IR (KBr) ν (cm⁻¹): 825, 1028, 1068, 1083, 1176, 1232, 1342, 1367, 1496, 1540, 1660, 2934, 3321. ¹H-NMR: (250 MHz, CDCl₃) δ 1.42 (9H, *s*), 1.54 (3H, *d*, *J* = 7.3 Hz), 2.27 (3 H,

s), 4.99 (2H, *m*), 6.83 (1H, *d*, $J = 8.8$ Hz), 6.98 (2H, *m*), 8.33 (1H, *bs*). $^{13}\text{C}\{^1\text{H}\}$ -NMR: (62.9 MHz, CDCl_3) δ 20.1 (CH_3), 20.9 (CH_3), 27.6 (CH), 28.5 ($3\times\text{CH}_3$), 81.1 (C), 118.0 (CH), 126.4 (CH), 129.2 (C), 129.5 (C), 152.8(C), 157.4 (C). MS (ESI): 274.1 $[\text{M}+\text{Na}]^+$. $[\alpha]_D^{20}$: +78.9 ($c = 1.09$, CHCl_3).

(+)-(R)- [1-(3-Bromo-2-hydroxy-5-methyl-phenyl)-ethyl]-carbamic acid tert-butyl ester

N-bromosuccinimide (11.0 mmol, 1.96 g) was added to a solution of the protected amine [1-(2-Hydroxy-5-methyl-phenyl)-ethyl]-carbamic acid tert-butyl ester (9.16 mmol, 2.30 g) in dry CH_2Cl_2 (37 mL) under nitrogen. The reaction mixture was stirred at room temperature for 5 h and then washed with H_2SO_4 10% (2×40 mL). The layers were separated and the aqueous one extracted with CH_2Cl_2 (2×20 mL). The combined organic phases were washed with brine (40 mL), dried over MgSO_4 and concentrated under reduced pressure. The crude product was washed with CH_3CN to give a white solid (3.0 g, 99%).

Mp: 78-80 °C. ^1H -NMR: (250 MHz, CDCl_3) δ 1.42 (9H, *s*), 1.48 (3H, *d*, $J = 7.0$ Hz), 1.55 (3H, *s*), 2.25 (3H, *s*), 4.95 (1H, *dq*, $J = 7.0$ Hz), 5.09 (1H, *m*), 6.94 (1H, *s*), 7.22 (1H, *s*). $^{13}\text{C}\{^1\text{H}\}$ -NMR: (62.9 MHz, CDCl_3) δ 20.5 (CH_3), 21.0 (CH_3), 28.6 ($3\times\text{CH}_3$), 46.9 (CH_2), 85.4 (C), 109.6 (C), 111.6 (C), 127.1(CH), 130.9 (C), 131.1 (C), 131.7 (CH), 132.6 (CH), 156.4 (C). MS (ESI): 352.1 $[\text{M}+\text{Na}]^+$. $[\alpha]_D^{20}$: + 22.06 ($c = 1.0$, CHCl_3).

(-)-(R)- [1-(2-Benzyloxy-3-bromo-5-methyl-phenyl)-ethyl]-carbamic acid tert-butyl ester

A mixture of [1-(3-Bromo-2-hydroxy-5-methyl-phenyl)-ethyl]-carbamic acid tert-butyl ester (3.816 mmol, 1.26g), K_2CO_3 (15.26 mmol, 2.11 g) and benzyl bromide (4.39 mmol, 522 μL) in dry CH_3CN (7.7 mL) was refluxed for 18 h under N_2 . The mixture was filtered through a pad of Celite, washed with ethyl acetate and the filtrate was concentrated under reduce pressure. The resulting pale yellow oil was taken up with CHCl_3 and washed with HCl 1M and brine. The organic layer was dried over MgSO_4 and the solvent was removed under vacuum. Column chromatography on aluminium oxide, using petroleum ether/ethyl acetate/ Et_3N 8:2:0.005 as eluant, afforded the product as a light-yellow solid (1.53 g, 96%).

Mp: 67-69 °C. IR (KBr) ν (cm^{-1}): 822, 850, 1040, 1059, 1136, 1191, 1296, 1374, 1662, 1690, 1734, 1740, 1773, 2956, 3079, 3157. ^1H -NMR: (250 MHz, CDCl_3) δ 1.36 (3H, *d*, $J = 6.9$ Hz), 1.42 (9H, *s*), 2.30 (3H, *s*), 4.92 (1H, *m*), 5.1 (2H, *s*), 7.04 (1H, *s*), 7.30-7.59 (4H, *m*), 7.62 (2H, *d*, $J = 6.9$ Hz). $^{13}\text{C}\{^1\text{H}\}$ -NMR: (62.8 MHz, CDCl_3) δ 21.0(CH_3) , 23.0 (CH_3), 28.6 ($3\times\text{CH}_3$), 46.7(C), 75.3 (CH_2), 79.7 (C), 117.7 (C), 126.5 (C), 128.4($2\times\text{CH}$) , 128.5(C), 128.7 ($2\times\text{CH}$), 132.9 (CH), 135.9 (CH), 137.2 (CH), 139.6(C), 150.7 (C), 155.0 (C). MS (ESI): 442.1 $[\text{M}+\text{Na}]^+$. $[\alpha]_D^{20}$: - 15.98 ($c = 0.97$, CHCl_3).

(-)-(R)-1-(2-Benzyloxy-3-bromo-5-methyl-phenyl)-ethylamine ((R)-3)

(-)- [1-(2-Benzyloxy-3-bromo-5-methyl-phenyl)-ethyl]-carbamic acid tert-butyl ester (3.57 mmol, 1.50 g) was dissolved in 4M HCl/dioxane (64 mL) and the mixture was stirred for 10 minutes at room temperature. The residue was dissolved in water (110 mL) and extracted with AcOEt (3×50 mL). The organic phase was dried over Na_2SO_4 and then evaporated under reduced pressure, affording compound **3** as a yellow oil.

*Kinetic enzymatic resolution***1-(2-Hydroxy-5-methyl-phenyl)-ethanone oxime (15)**

1-(2-hydroxy-5-methyl-phenyl)ethanone **4** (33.5 mmol, 5.02 g) was weighed in a round bottom flask and dissolved in ethanol (17 mL). Hydroxylamine hydrochloride (38.5 mmol, 2.67 g) and NaOH aq. soln. (38.5 mmol) were added. The reaction mixture was stirred for 48 h at room temperature and then concentrated under vacuum. The residue was taken up with CH₂Cl₂ (30 mL) and washed with water (30 mL). The aqueous phase was extracted with CH₂Cl₂ (2 × 30 mL) and the combined organic phases were dried over Na₂SO₄ and evaporated, yielding a pale-yellow solid (5.36 g, 97%).

15: Mp: 157- 159° C. IR (KBr) ν (cm⁻¹): 696, 760, 958, 1087, 1236, 1373, 1454, 2870, 2923, 3208. ¹H-NMR: (250 MHz, CDCl₃) δ 2.31, 2.35, 6.88 (1H, *d*, J = 7.5 Hz), 7.08 (1H, *d*, J = 7.5 Hz), 7.22 (1H, *s*). ¹³C{¹H}-NMR: (62.8 MHz, CDCl₃) δ 11.0 (CH₃), 20.9 (CH₃), 117.3 (CH), 118.3 (C), 128.1 (CH), 128.3 (C), 131.7 (CH), 155.6 (C), 159.9 (C). MS (ESI): 165.2 [M + H]⁺.

2-(1-Amino-ethyl)-4-methyl-phenol ((rac)-14)

HCl (69.6 mmol, 5.8 mL, 12 M) and Pd/C (20 wt%, 950 mg) were added to a solution in ethanol (290 mL) of **15** (29.1 mmol, 4.74 g). After three H₂/vacuum cycles, the suspension was let under H₂ (balloon pressure) and stirred at room temperature for 15 h. Then the reaction mixture was filtered over Celite and concentrated under vacuum. After washing the residue with Et₂O, *rac*-**14.HCl** was afforded as a white solid (4.38 g, 99%). The free amine was obtained after washing with Na₂CO₃aq. Sat and extracting with CH₂Cl₂.

rac-**14.HCl**: Mp: 170- 172° C. IR (KBr) ν (cm⁻¹): 668, 826, 1079, 1152, 1253, 1359, 1379, 1500, 1516, 1585, 2574, 3052, 3220. ¹H-NMR: (250 MHz, CDCl₃) δ 1.63 (3H, *d*, J = 7.5 Hz), 2.27 (3H, *s*), 4.56 (1H, *q*, J = 7.5 Hz), 6.79 (1H, *d*, J = 7.5 Hz), 7.04 (1H, *d*, J = 7.5 Hz), 7.08 (1H, *s*). ¹³C{¹H}-NMR: (62.8 MHz, CDCl₃) δ 19.2 (CH₃), 20.7 (CH₃), 49.1 (CH), 116.7 (CH), 125.0 (C), 129.1 (CH), 130.5 (C), 131.7 (CH), 154.1 (C). MS (ESI): 152.1 [M + H]⁺. HR-MS (ESI): calcd for C₉H₁₃NO: 152.1075; found 152.1071.

N-[1-(2-Hydroxy-5-methyl-phenyl)-ethyl]-2-methoxy-acetamide ((rac)-17)

To a solution of methoxy-acetic acid (1.32 mmol, 119 mg) in dry CH₂Cl₂ (25 mL) and DME (0.5 mL), *rac*-**14.HCl**, N-ethyl-N'-(3-dimethylaminopropyl)carbodiimide (EDC, 1.39 mmol, 266 mg) and 1-hydroxybenzotriazole (Hobt, 1.39 mmol, 187.8 mg) were added. After 5 min, Et₃N (2.64 mmol, 360 μ L) was added and the reaction mixture was stirred at room temperature for 20 h (T.l.c. petroleum ether/EtOAc 1:1). Then the mixture was washed with water (10 mL) and then the aqueous phase was extracted with EtOAc (3 × 10 mL). The combined organic phase was dried over Na₂SO₄ and evaporated under vacuum. Purification by column chromatography (petroleum ether/EtOAc 1:1 as eluant) afforded product **17** as a pale-yellow oil (240 mg, 82%).

rac-**17**: ¹H-NMR: (250 MHz, CDCl₃) δ 1.57 (3H, *d*, J = 7.3 Hz), 2.23 (3H, *s*), 3.34 (3H, *s*), 3.83 (2H, *q*, J = 14.4 Hz), 5.24 (1H, *quint.*, J = 7.3 Hz), 6.80 (1H, *d*, J = 7.3 Hz), 6.93- 6.98 (2H, *m*),

8.75 (1H, s). $^{13}\text{C}\{^1\text{H}\}$ -NMR: (62.8 MHz, CDCl_3) δ 19.5 (CH_3), 20.8 (CH_3), 42.8 (CH), 59.3 (CH_3), 71.4 (CH_2), 118.3 (CH), 126.6 (CH), 128.3 (C), 129.6 (C), 129.8 (CH), 152.8 (C), 170.8 (C). MS (ESI): 224.1 $[\text{M} + \text{H}]^+$.

General procedure for enzymatic reactions catalyzed by CalB (Novozym 435)

The acylating agent (1.98 mmol) was added to a solution of (*rac*)-**15** (1.98 mmol, 300 mg) in the desired solvent (2.6 mL). After taking apart an aliquot (20 μL) diluted in acetonitrile (3 mL) for t_0 , Novozyme 435 (30%) was added. The reaction was thermostated at 50° C and stirred at 200 rpm. Aliquots (20 μL) were taken and analysed by HPLC. After 6 days, methanol (3.5 mL) was added to the reaction mixture and then it was filtered and the catalyst washed with methanol (3.5 mL), CH_2Cl_2 (3.5 mL), toluene (2 mL) and acetone (2 mL). The organic phase was concentrated and the residue dissolved in CH_2Cl_2 . The solution was washed with HCl 1N (3 \times 5 mL), dried over Na_2SO_4 and then evaporated, affording amide **17**. The aqueous phase was basified till pH= 12 using NaOH 3M and then was extracted with CH_2Cl_2 . The organic phase was dried over Na_2SO_4 and then evaporated to give amine **14**.

The obtained product were analyzed via and quantitative HPLC (Aqua C18 column (Phenomenex), water/acetonitrile 1:1, 1 mL/min, UV 220 nm: 5.3 min (**17**), 8.65 min (**14**)). chiral HPLC (IB Chiralpak column (Daicel Chemical Industries), hexane/2-propanol/ Et_3N 95:5:0.0005, 1 mL/min, UV 215 nm: 12.00 min (*R*)-**17**, 18.00 min (*S*)- **17**): for the study of the ee, a double acylation resulted necessary: the sample was dissolved in CH_2Cl_2 and a drop of anhydride acetic 10^{-6} M and one of a solution of Et_3N were added. The it was concentrated and diluted in hexane/2-propanol 95:5 solution.

(2-Benzyloxy-3-bromo-5-methyl-phenyl)-methanol

3-bromo-2-hydroxy-5-methylbenzaldehyde⁴⁵ (37.26 mmol, 10g) was dissolved in ethanol (200 ml) and NaBH_4 (44.7 mmol, 1.69 g) was added in one portion. The resulting suspension was stirred for 4 h at room temperature (TLC AcOEt/petroleum ether 1:9). The mixture was concentrated and the residue was taken up with a mixture of Et_2O (200 ml) and NaOH 1M (100 ml). The layers were separated and the aqueous phase was extracted with Et_2O (3 \times 100 ml). The combined organic phases were washed with brine (50 ml), dried over Na_2SO_4 and concentrated to give a white solid (11.21 g, 98%).

Mp: 56– 58 °C. ^1H -NMR: (250 MHz, CDCl_3) δ 1.84 (1H, *t*, $J = 6.05$ Hz), 2.32 (3H, *s*), 4.58 (2H, *d*, $J = 6.05$ Hz), 5.02 (2H, *s*), 7.12 (1H, *s*), 7.36– 7.43 (4H, *m*), 7.48– 7.51 (2H, *m*). $^{13}\text{C}\{^1\text{H}\}$ -NMR: (62.9 MHz, CDCl_3) δ 20.7 (CH_3), 61.3 (CH_2), 75.8 (CH_2), 117.1 (C), 128.6 (2 \times CH), 128.7 (2 \times CH), 128.8 (C), 129.2 (CH), 133.4 (CH), 135.9 (CH), 136.0 (C), 136.8 (C), 151.3 (C). MS (ESI): 329.2 $[\text{M} + \text{Na}]^+$. Anal. Calcd. for $\text{C}_{15}\text{H}_{15}\text{BrO}_2$: C 58.65, H 4.92. Found: C 58.86, H 4.91.

2-Benzyloxy-1-bromo-3-bromomethyl-5-methyl-benzene (18)

2-Benzyloxy-3-bromo-5-methyl-phenyl)-methanol (37.26 mmol, 11.21 g) was dissolved in dry toluene (170 mL) and placed on ice bath for ~10 min, under N_2 -atmosphere. PBr_3 (40.99

⁴⁵ For the synthesis of the substrate 3-bromo-2-hydroxy-5-methylbenzaldehyde, see compound (13) in Chapter 3.

mmol, 4 mL) was dissolved in dry toluene (35 mL) and added to the solution of alcohol in 2 min. The mixture was stirred on ice bath for 20 min, later for further 30 min at room temperature. The solution was diluted with cold water (50 mL) and stirred vigorously for 2 min. The organic phase was separated, washed with saturated aqueous NaHCO₃ (100 mL) and NaCl_{aq} sat (70 mL), dried over MgSO₄ and concentrated. Column chromatography of the crude product on silica gel, using petroleum ether/ethyl acetate 20:1 as eluant, afforded compound **18** (11.58 g, 84%) as a yellow oil.

18: IR (KBr) ν (cm⁻¹): 96, 731, 776, 761, 860, 915, 974, 1004, 1029, 1098, 1144, 1210, 1230, 1272, 1377, 1454, 1473, 1498, 2874, 2922, 2975, 3031, 3064. ¹H-NMR: (250 MHz, CDCl₃) δ 2.32 (3H, s), 4.50 (2H, s), 5.14 (2H, s), 7.17 (1H, s), 7.38– 7.48 (4H, m), 7.57– 7.60 (2H, m). ¹³C{¹H}-NMR: (62.9 MHz, CDCl₃) δ 20.7 (CH₃), 28.2 (CH₂), 75.3 (CH₂), 117.6 (C), 128.5 (2×CH), 128.6(CH) , 128.8 (2×CH) , 131.4(CH), 133.3 (C), 134.8 (CH), 136.0 (C), 136.9 (C), 151.9 (C).

[(2-benzyloxy-3-bromo-5-methyl-benzyl)-(1-(2-benzyloxy-3-bromo-5-methyl-phenyl)ethyl)amine (19)

Compounds **2** (6.25 mmol, 2 g) and **18** (13.31 mmol, 4.93 g), together with K₂CO₃ (31.25, 4.32 g) were suspended in dry CH₃CN (125 mL), in a double necked round bottom flask, under nitrogen. The reaction mixture was refluxed for 24 h (TLC petroleum ether/ ethyl acetate 10:1), then cooled to room temperature, filtered over Celite washing with ethyl acetate and the solvents were evaporated under vacuum. The residue was taken up with Et₂O (100 mL), washed with NaOH 1M (2 x 100 mL) and brine (2 x 100 mL) . The organic layers were dried over MgSO₄ and concentrated under vacuum. After column chromatography on silica gel, using hexane/ethyl acetate/Et₃N 20:1:0.005 as eluant, (*rac*)-**19** (4.82 g, 86%), (*S*)- **19** (4.32 g, 77%), (*R*)- **19** (4.55 g, 81%) were recovered as white solids.

(*rac*)-**19**: Mp 156-158 °C. IR (KBr) ν (cm⁻¹): 860, 892, 1127, 1224, 1278, 1370, 1450, 1499, 2870, 2928, 3032, 3065. ¹H-NMR: (250 MHz, CDCl₃) δ 1.34 (3H, d, *J* = 7.0 Hz), 2.26 (6H, s), 2.27 (3H, s), 3.49 (2H, d, *J* = 15.7 Hz, part B, AB system), 3.63 (2H, d, *J* = 15.7 Hz, part A, AB system), 4.42 (1H, q, *J* = 7.0 Hz), 4.58 (1H, d, *J* = 10.6 Hz, part B, AB system), 4.72 (4H, s), 4.81 (1H, d, *J* = 10.6 Hz, part A, AB system), 7.08- 7.12 (3H, m), 7.21- 7.84 (18H, m). ¹³C{¹H}-NMR: (62.9 MHz, CDCl₃) δ 19.4 (CH₃), 21.0 (2×CH₃), 21.1 (CH₃), 49.2 (2×CH₂), 53.0 (CH), 74.6 (2×CH₂), 75.9 (CH₂), 117.1 (2×C), 117.7 (C), 128.1 (2×CH), 128.28 (4×CH), 128.33 (2×CH), 128.4 (CH), 128.5 (6×CH), 128.6 (2×CH), 129.1 (CH), 132.0 (2×CH), 132.9 (CH), 135.1 (2×C), 135.2 (C), 135.6 (2×C), 136.5 (C), 136.9 (C), 137.3 (2×C), 151.4 (2×C), 151.5 (C). MS (ESI): 898.2 [M+H]⁺ . HR-MS (ESI): calcd for C₄₆H₄₅Br₃NO₃: 898.0929; found 898.0925.

(*S*)-**18**: [α]_D²⁰: + 39.09 (c = 0.665, CH₂Cl₂).

[(2-benzyloxy-3-phenyl-benzyl)-(1-(2-benzyloxy-3-phenyl-5-methyl-phenyl)ethyl)amine (20a)

Substrate **18** (3.50 mmol, 3.145 g) and the boronic acid **19a** (21 mmol, 2.56 g) were added to a Schlenk tube under nitrogen. The Schlenk tube was evacuated and then refilled with nitrogen. Degassed dioxane (25 mL), degassed Na₂CO_{3aq} 2M (16 mL) and finally the

palladium source Pd(PPh₃)₄ (0.35 mmol, 404 mg) were added to the Schlenk tube. The reaction was stirred at 110° C for 18 h. At the end of the reaction, which was checked by ESI-MS, the mixture was cooled down to room temperature, filtered over Celite and then concentrated under vacuum. The residue was diluted with CH₂Cl₂, washed with NaOH 1M and NaCl_{aq} sat., concentrated and purified by column chromatography on silica gel, using hexane/Et₂O/Et₃N 2:1:0.005 as eluant. Product **20a** was recovered as a white solid (2.87 g, 92%).

20a: Mp 165-167 °C. IR (KBr) ν (cm⁻¹): 694, 755, 820, 1228, 1368, 1382, 1431, 1490, 1599, 1609, 2932, 2980, 3035, 3057, 3422. ¹H-NMR: (250 MHz, CDCl₃) δ 1.50 (3H, *d*, *J* = 6.9 Hz), 2.44 (3H, *s*), 2.46 (6H, *s*), 3.97 (4H, *bs*), 4.22- 4.39 (6H, *m*), 4.65 (1H, *q*, *J* = 6.9 Hz), 6.73 (2H, *d*, *J* = 6.6 Hz), 6.99- 7.03 (4H, *m*), 7.10 (1H, *s*), 7.14- 7.28 (10H, *m*), 7.34- 7.46 (11H, *m*), 7.60-7.66 (8H, *m*). ¹³C{¹H}-NMR: (62.9 MHz, CDCl₃) δ 20.0 (CH₃), 21.4 (CH₃), 21.5 (2×CH₃), 49.2 (2×CH₂), 52.9 (CH), 74.7 (2×CH₂), 75.5 (CH₂), 127.1(2×CH), 127.8 (CH), 127.9 (2×CH), 128.2 (2×CH), 128.25 (4×CH), 128.31 (4×CH), 128.35 (C), 128.39 (CH), 128.5 (4×CH), 128.6 (CH), 128.8 (2×CH), 129.46 (2×CH), 129.53 (4×CH), 129.6 (2×CH), 129.7 (2×CH), 130.5 (CH), 133.3 (C), 133.4 (2×CH), 134.6 (2×C), 134.8 (2×C), 135.3 (C), 136.2 (C), 136.9 (2×C), 137.4 (2×C), 139.2 (2×C), 139.3 (2×C), 152.5 (2×C). MS (ESI): 890.5 [M+H]⁺. HR-MS (ESI): calcd for C₆₄H₆₀NO₃: 890.4573; found 890.4575.

(S)-**20a**: $[\alpha]_D^{20}$: + 31.31 (*c* = 0.313, CH₂Cl₂).

((2-benzyloxy-3-(3'-methoxyphenyl)-5-methyl-benzyl)-(1-(2-benzyloxy-3-(3'-methoxyphenyl)-5methyl-phenyl)ethyl)amine (20b)

According with the procedure for **20a**, substrate **18** (3.50 mmol, 3.145 g) boronic acid **19b** (21 mmol, 3.19 g), degassed dioxane (25 mL), degassed Na₂CO_{3aq} 2M (16 mL) and palladium source Pd(PPh₃)₄ (0.35 mmol, 404 mg) were used to obtain product **20b** as a white solid (3.05 g, 89%).

20b: Mp 118-120 °C. IR (KBr) ν (cm⁻¹): 760, 888, 1041, 1084, 1154, 1210, 1225, 1268, 1286, 1360, 1456, 1508, 1630, 3025, 3044. ¹H-NMR: (250 MHz, CDCl₃) δ 1.40 (3H, *d*, *J* = 6.9 Hz), 2.35 (9H, *s*), 3.58 (3H, *bs*), 3.69 (6H, *s*), 3.88 (4H, *s*), 4.17 (2H, *s*), 4.19 (2H, *d*, *J* = 10.2 Hz, part A, AB system), 4.26 (2H, *d*, *J* = 10.2 Hz, part B, AB system), 4.56 (1H, *q*, *J* = 6.9 Hz), 6.68 (2H, *d*, *J* = 6.8 Hz), 6.77- 6.87 (3H, *m*), 6.95 (3H, *m*), 7.02 (2H, *s*), 7.08- 7.18 (18H, *m*), 7.25 (2H, *m*), 7.33 (1H, *s*), 7.56 (2H, *s*). ¹³C{¹H}-NMR: (62.9 MHz, CDCl₃) δ 20.1 (CH₃), 21.47 (2×CH₃), 21.54 (CH₃), 49.3 (2×CH₂), 53.2 (CH), 55.4 (CH₃), 55.3 (2×CH₃), 74.8 (2×CH₂), 75.4 (CH₂), 113.4 (2×CH), 114.5 (CH), 114.6 (2×CH), 122.1 (2×CH), 122.2 (CH), 127.9 (CH), 128.0 (2×CH), 128.3 (2×CH), 128.4 (4×CH), 128.6 (4×CH), 128.8 (2×CH), 129.3 (2×CH), 129.4 (CH), 129.6 (2×CH), 129.7 (2×CH), 130.5 (CH), 133.3 (C), 133.5 (2×C), 134.5 (C), 134.7 (2×C), 135.0 (C), 136.5 (2×C), 137.0 (C), 137.4 (2×C), 140.5 (2×C), 140.7 (C), 152.1 (2×C), 152.2 (C), 159.5 (2×C), 159.6 (C). MS (ESI): 980.2 [M+H]⁺.

(S)-**20b**: $[\alpha]_D^{20}$: + 5.50 (*c* = 0.2, CH₂Cl₂).

[(2-hydroxy-3-phenyl-5-methyl-benzyl)-(1-(2-hydroxy-3-phenyl-5-methyl-phenyl)ethyl)]amine (21a)

The catalyst Pd/C (10 wt%, 287 mg) was added to a solution of **20a** (3.22 mmol, 2.87 g) in AcOEt (180 mL) under nitrogen. After three H₂/vacuum cycles, the suspension was let under H₂ (1 atm) and stirred at room temperature for 3 h. The mixture was filtered over Celite and concentrated under vacuum. After column chromatography on silica gel, using hexane/Et₂O/Et₃N 2:1:0.005 as eluant, product **21a** was recovered as a white solid (1.84 g, 92%).

21a: Mp: 119-121 °C. ¹H-NMR: (300 MHz, CDCl₃) δ 1.60 (3H, *d*, *J* = 6.8 Hz), 2.19 (3H, *s*), 2.27 (6H, *s*), 3.83 (4H, *s*), 4.40 (1H, *q*, *J* = 6.8 Hz), 6.85 (4H, *d*, *J* = 6.6 Hz), 6.96 (2H, *d*, *J* = 6.9 Hz), 7.25- 7.47 (15H, *m*). ¹³C{¹H}-NMR: (62.9 MHz, CDCl₃) δ 20.7 (3×CH₃), 21.0 (CH₃), 52.7 (2×CH₂), 55.8 (CH), 124.1 (3×C), 127.3 (2×CH), 127.39 (CH), 127.44 (C), 128.1 (CH), 128.4 (2×C), 128.7 (4×CH), 128.77 (2×CH), 128.79 (2×C), 129.0 (C), 129.6 (4×CH), 129.7 (2×CH), 130.3 (2×CH), 130.4 (CH), 130.9 (2×CH), 138.1 (2×C), 138.2 (C), 150.0 (C), 150.3 (2×C). MS (ESI): 620.3 [M+H]⁺.

(*S*)-**21a**: [α]_D²⁰: -17.96 (*c* = 0.167, CH₂Cl₂).

[(2-hydroxy-3-(3'-methoxyphenyl)-5-methyl-benzyl)-(1-(2-hydroxy-3-(3'-methoxyphenyl)-5-methyl-phenyl)ethyl)]amine (21b)

The catalyst Pd/C (10 wt%, 305 mg) was added to a solution of **20b** (3.11 mmol, 3.05 g) in AcOEt (175 mL) under nitrogen. After three H₂/vacuum cycles, the suspension was let under H₂ (1 atm) and stirred at room temperature for 3 h. The mixture was filtered over Celite and concentrated under vacuum. After column chromatography on silica gel, using hexane/Et₂O/Et₃N 2:1:0.005 as eluant, product **21b** was recovered as a white solid (2.029 g, 92%).

21b: Mp: 110-112 °C. IR (KBr) ν (cm⁻¹): 783, 844, 1048, 1084, 1156, 1230, 1465, 1576, 1590, 2949, 2980. ¹H-NMR: (250 MHz, CDCl₃) δ 1.41 (3H, *d*, *J* = 7.3 Hz), 2.14 (6H, *s*), 2.20 (3H, *s*), 3.60 (3H, *s*), 3.63 (6H, *s*), 3.77 (4H, *bs*), 4.42 (1H, *q*, *J* = 7.3 Hz), 6.78-7.00 (14H, *m*), 7.20- 7.35 (4H, *m*). ¹³C{¹H}-NMR: (62.9 MHz, CDCl₃) δ 20.6 (2×CH₃), 20.9 (CH₃), 21.2 (CH₃), 52.5 (2×CH₂), 55.5 (2×CH₃), 55.7 (CH₃), 60.6 (CH), 113.4 (2×CH), 113.6 (CH), 114.6 (2×C), 114.7 (C), 116.9 (2×CH), 122.0 (2×CH), 122.1 (CH), 124.0 (2×C), 127.4 (C), 128.1 (C), 128.5 (2×C), 128.6 (CH), 128.8 (2×CH), 128.9 (2×CH), 129.6(CH), 130.3 (CH), 130.5(CH), 131.0 (2×CH), 139.8 (2×C), 140.1 (C), 150.3(C), 150.6 (2×C). MS (ESI): 710.3 [M+H]⁺.

(*S*)-**21b**: [α]_D²⁰: -11.68 (*c* = 0.95, CH₂Cl₂).

Synthesis of mononuclear titanatranes (22)

Titanatrane complexes **22a,22b** were prepared in glovebox by mixing homogeneous solutions of the corresponding ligands **21a,22b** (0.10 M) and Ti(O*i*-Pr)₄ (0.18 M) in dry CDCl₃ in a 1:1 ratio to a final concentration 0.01 M of the complex. Bright yellow solutions were obtained which were used without further purifications and without removing the three

equivalents of *i*-PrOH released from the metal precursor. In all cases resonances relative to free *iso*-propanol released in the reaction were present in the NMR spectra: $^1\text{H-NMR}$ (300 MHz, CDCl_3): 1.22 (6H, *d*, $J = 6.1$ Hz), 4.04 (1H, *hept*, $J = 6.1$ Hz). $^{13}\text{C-NMR}$ (75 MHz, CDCl_3): δ 25.1 (CH_3), 64.5 (CH).

22a: $^1\text{H-NMR}$: (300 MHz, CDCl_3) δ 0.87 (6H, *d*, $J = 6.0$ Hz), 1.59 (3H, *d*, $J = 6.6$ Hz), 2.28 (3H, *s*), 2.31 (3H, *s*), 2.34 (3H, *s*), 3.32- 3.36 (2H, *m*), 3.70 (1H, *d*, $J = 13.5$ Hz), 3.87 (1H, *d*, $J = 13.5$ Hz), 4.13- 4.15 (1H, *m*), 4.60 (1H, *q*, $J = 6.0$ Hz), 6.89 (1H, *s*), 6.95 (1H, *s*), 7.04- 7.11 (4H, *m*), 7.25- 7.27 (4H, *m*), 7.32- 7.39 (5H, *m*), 7.60- 7.68 (6H, *m*). MS (ESI): 696.3 [LTiOMe+H] $^+$, 682.3 3 [LTiOH+H] $^+$

22b: $^1\text{H-NMR}$: (300 MHz, CDCl_3) δ 0.87 (6H, *d*, $J = 6.0$ Hz), 1.58 (3H, *d*, $J = 6.6$ Hz), 2.28 (3H, *s*), 2.31 (3H, *s*), 2.33 (3H, *s*), 3.30 (2H, *m*), 3.70 (1H, *d*, $J = 13.5$ Hz), 3.79- 3.84 (10H, *m*), 4.10- 4.13 (1H, *m*), 4.52 (1H, *q*, $J = 6.0$ Hz), 6.79- 6.82 (3H, *m*), 6.89 (1H, *s*), 6.96 (1H, *s*), 7.05- 7.28 (16H, *m*).

Synthesis of titanatrane μ -oxo complex (23)

A chloroform solution of complex (*rac*)-**22a**, **22b** in presence of a mixture methanol/water slowly and quantitatively evolves into μ -xo complexes **23a**, **23b** respectively.

23a: $^1\text{H-NMR}$: (300 MHz, CDCl_3) δ 1.71-1.74 (3H, *m*), 2.32- 2.38 (27H, *m*), 3.46 (4H, *d*, $J = 13.5$ Hz), 3.89 (2H, *d*, $J = 13.5$ Hz), 4.02 (2H, *d*, $J = 14.0$ Hz), 4.21- 4.27 (2H, *m*), 6.02- 6.35 (6H, *m*), 6.40- 6.75 (22H, *m*), 6.96- 7.26 (14H, *m*). MS (ESI): 1345.3 [M+H] $^+$, 1367.3 [M+Na] $^+$, 1382.3 [M+K] $^+$.

23b: complex $^1\text{H-NMR}$ spectrum. MS (ESI): 1525.3 [M+H] $^+$, 1547.3 [M+Na] $^+$, 1563.3 [M+K] $^+$.

Synthesis of μ -oxo complex with mixed titanatrane complexes (*R*)-**22a** + (*rac*)-**22b**

In a first experiment 0.002 mmol of (*R*)-**22a** (83% ee, 0.008243 M) and 0.002 mmol (*rac*)-**22b** (0.008243 M) were mixed in acetonitrile and in a second one 0.0014 mmol of (*R*)-**22a** (83% ee, 0.008243 M) 0.0028 mmol of (*rac*)-**22b** (0.008243 M). The solutions were leaved in contact with air for one our then analyzed via ESI-MS, FIA positive analysis, 10^{-7}M , mobile phase acetonitrile.

Results are reported in Figure 10.

Summary

This Ph.D. thesis describes the synthesis of Ti(IV) and V(V) complexes with tetradentate C_3 -symmetric amine triphenolate ligands, their application in catalysis and for building up functional structures with controlled geometries.

A general introduction on tripodal C_3 -symmetric amine triphenolate complexes is outlined in *Chapter 1*: the high modular nature of the phenol moieties, associated to the three-fold symmetry and tetradentate nature of the system, allows to obtain a large family of ligands where steric and electronic factors play an important role. Even if a large number of examples dealing with the synthesis and coordination chemistry of amine tri-phenolate ligands are available, studies regarding their catalytic activities have been only recently reported. These reports are related to their behaviour as Lewis Acid and consequently, to the capability of the tetradentate amine tri-phenolate ligands to stabilize the active species under turnover conditions, in particular in polymerization and oxygen transfer processes. In this contest, the study described in *Chapter 2* pertains to V(V)-oxo amine triphenolate complexes as functional and structural models of vanadium haloperoxidases: their trigonal bipyramidal geometry emulates the one found in the enzymes and their ability to catalyse efficiently sulfoxidations as well as chlorination and bromination of trimethoxybenzene reflects the properties of the enzyme. In particular, sulfoxidations using hydrogen peroxide as terminal oxidant are performed in quantitative yields and high selectivities (catalyst loading down to 0.01%, TONs up to 9900, TOF up to 8000 h⁻¹), while in the second case TONs up to 1260 and TOF up to 220 h⁻¹ are achieved with a catalyst loading down to 0.05%.

Regarding the titanatrane complexes, their thermodynamic stability in solution strongly depends on the steric size of the peripheral substituents. The particular coordination behaviour of *tris*-(2-hydroxy-3-phenylbenzyl)amine with Ti(IV) is elucidated in *Chapter 3*: a highly stable, inert, heterochiral, dinuclear S_6 -symmetric μ -oxo complex forms through a stereoselective self-assembly process. To exploit this particular feature, a new efficient method for the synthesis of *ortho*-aryl functionalized *tris*-arylphenol amines has been developed, using a Suzuki coupling reaction as the main strategic step: the study of their coordination chemistry with Ti(IV) showed that the dimerization process is still possible and thus μ -oxo derivatives with methoxy, cyano and methyl esters have been obtained. In the latter case the μ -oxo complex could be further functionalized to a hexa amide. This study confirms that it is possible to achieve the construction of stable and spatially ordered new materials.

Furthermore, the preparation of enantiopure complexes let us to synthesize mixed μ -oxo complexes and to demonstrate that at the origin of the μ -oxo complex formation there is a

stereo-self-discrimination process between two enantiomeric structures. *Chapter 4* deals in fact with the synthesis of chiral, enantiopure *tris*-(*o*-aryl-phenol)amines ligands and with the study of their properties in the coordination chemistry with Ti(IV).

Riassunto

Questa tesi di dottorato descrive la sintesi di complessi con ioni metallici in massimo stato di ossidazione, quali Ti(IV) e V(V), con leganti tetradentati a simmetria C_3 , il loro utilizzo come catalizzatori omogenei e per la costruzione di strutture funzionali a geometria controllata.

Nel *Capitolo 1* è riportata un'introduzione generale riguardante le caratteristiche principali dei complessi ammino tri-fenolati. La natura modulare di tali leganti, capaci di fornire tre siti anionici di legame e un donatore neutro azotato in posizione assiale, partecipante alla coordinazione, permette, in associazione all'alta simmetria di tali sistemi, di ottenere una famiglia di leganti particolarmente versatili. Variando, infatti, i sostituenti periferici in posizione *orto* al gruppo ossidrilico dell'unità fenolica è possibile modulare le caratteristiche strutturali ed elettroniche dei leganti e dei rispettivi complessi.

Sebbene in letteratura siano riportati svariati esempi sulla chimica di coordinazione di tali sistemi, il loro utilizzo come acidi di Lewis, in particolare come catalizzatori in reazioni di polimerizzazione e di trasferimento di ossigeno, è più recente.

A questo riguardo, nel *Capitolo 2* vengono descritti i complessi ammino tri-fenolati di ossovanadio(V) come modelli funzionali e strutturali di aloperossidasi, grazie alla loro geometria trigonale bipyramidale e alla loro abilità nel catalizzare efficacemente sia le solfossidazioni così come la clorurazione e bromurazione del trimetossibenzene. In particolare, nell'ossidazione di solfuri, usando perossido d'idrogeno come ossidante primario, sono state ottenute rese quantitative in prodotto con alte chemoselettività, anche in presenza dello 0.01% di catalizzatore, con TON fino a 9900 e TOF fino a 8000 h⁻¹. Nel caso della bromurazione si sono ottenuti TON pari a 1260 e TOF fino a 220 h⁻¹ usando fino allo 0.05% di catalizzatore.

Per quanto concerne i complessi titanatranici, si è visto che la loro stabilità termodinamica in soluzione è fortemente influenzata dall'ingombro sterico dei sostituenti periferici, che determinano l'accesso allo ione metallico. Il comportamento particolare della *tris*-(2-idrossi-3-fenilbenzil)ammina nella coordinazione con il Ti(IV) è esposto nel *Capitolo 3*: un complesso μ -osso altamente stabile, inerte e a simmetria S_6 viene a formarsi, grazie a un processo stereoselettivo di autoassemblaggio. Al fine di sfruttare quest'ultima caratteristica per l'utilizzo di tale specie di-nucleare come piattaforma, è stata sviluppata una nuova strategia sintetica, via reazione di Suzuki coupling, al fine di ottenere delle *tris*-fenolammine *orto*-sostituite con gruppi arili. Lo studio della chimica di coordinazione di tali leganti ha evidenziato come il processo di dimerizzazione sia ancora possibile: si sono ottenuti complessi dimerici aventi gruppi periferici ciano, metossi e metil esterei e in quest'ultimo

caso il complesso μ -osso è stato ulteriormente funzionalizzato portando alla pirrolidin-esamamide. Tutto ciò conferma come questi complessi μ -osso possano essere utilizzati come piattaforme polifunzionalizzate a geometria controllata per la costruzione di materiali funzionali o catalizzatori.

Infine, la messa a punto di metodologie efficaci per la sintesi di *tris*-(*o*-aril-fenol)ammine enantiopure e dei relativi complessi metallici di Ti(IV) ha permesso di studiare più approfonditamente il processo di formazione dei complessi μ -osso e di prepararne di misti, dimostrando come all'origine della formazione di tali specie di-nucleari ci sia un processo di stereo-discriminazione fra due strutture enantiomeriche (*Capitolo 4*).

Ringraziamenti

Desidero ringraziare la Prof.ssa Giulia Licini per avermi permesso di svolgere il mio dottorato in un ambiente di lavoro così vivo.

Un ringraziamento speciale alla Dott.ssa Miriam Mba, che ha seguito gran parte del lavoro con entusiasmo e a cui va gran parte del merito di molti dei risultati raggiunti, per avermi insegnato a fare ricerca.

Thanks to Prof. Peter E. Kündig and to all the people of his group, particularly: Yia, Laetitia, Séverine, Audrey, Andrei, Sirinporn for their help during the month that I spent in Geneve.

Grazie a mamma, papà e a Paolo, per aver sempre creduto in me e per aver avermi sempre sostenuto.

Grazie di cuore a tutte le persone del laboratorio 108 e della stanzina dottorandi 110, con le quali ho trascorso bellissime giornate, in particolare: Silvia, Cristiano B., Gianni, Francesco R., Cristian G., Cristian G., Miriam, Eszter, Cristiano Z., Mariella, Flavio, Serena, Martino, Andrea M., Massimo, Filippo, Giulio, Giovanni, Leonard, Mauro, Ester e Andrea, Andrej, Paola, Lucia, Milko, Luca, Francesco S.

*Grazie a tutti di cuore,
Marta*